VOL. 19 NO. 3 NOVEMBER 1968
PUBLISHED MONTHLY

JOURNAL OF

ELECTROANALYTICAL CHEMISTRY

AND INTERFACIAL ELECTROCHEMISTRY

International Journal devoted to all Aspects of Electroanalytical Chemistry, Double Layer Studies, Electrokinetics, Colloid Stability, and Electrode Kinetics.

ELSEVIER

GENERAL INFORMATION

Types of contributions

(a) Original research work not previously published in other periodicals.
(b) Reviews on recent developments in various fields.
(c) Short communications.
(d) Bibliographical notes and book reviews.

Languages

Papers will be published in English, French or German.

Submission of papers

Papers should be sent to one of the following Editors:
Professor J. O'M. BOCKRIS, John Harrison Laboratory of Chemistry, University of Pennsylvania, Philadelphia 4, Pa. 19104, U.S.A.
Dr. R. H. OTTEWILL, Department of Chemistry, The University, Bristol 8, England.
Dr. R. PARSONS, Department of Chemistry, The University, Bristol 8, England.
Professor C. N. REILLEY, Department of Chemistry, University of North Carolina, Chapel Hill, N.C. 27515, U.S.A.

Authors should preferably submit two copies in double-spaced typing on pages of uniform size. Legends for figures should be typed on a separate page. The figures should be in a form suitable for reproduction, drawn in Indian ink on drawing paper or tracing paper, with lettering etc. in thin pencil. The sheets of drawing or tracing paper should preferably be of the same dimensions as those on which the article is typed. Photographs should be submitted as clear black and white prints on glossy paper. Standard symbols should be used in line drawings, the following are available to the printers:

All references should be given at the end of the paper. They should be numbered and the numbers should appear in the text at the appropriate places.
A summary of 50 to 200 words should be included.

Reprints

Fifty reprints will be supplied free of charge. Additional reprints (minimum 100) can be ordered at quoted prices. They must be ordered on order forms which are sent together with the proofs.

Publication

The *Journal of Electroanalytical Chemistry and Interfacial Electrochemistry* appears monthly and four volumes will appear in 1968.
Subscription price: $ 70.00 or Sfr. 304.00 per year; $ 17.50 or Sfr. 76.00 per volume; plus postage. Additional cost for copies by air mail available on request. For advertising rates apply to the publishers.

Subscriptions

Subscriptions should be sent to:

ELSEVIER SEQUOIA S.A., P.O. Box 851, 1001 Lausanne 1, Switzerland

THE MASS SPECTRA OF ORGANIC MOLECULES

by J. H. Beynon, R. A. Saunders and A. E. Williams, Research Department,
Imperial Chemical Industries Ltd., Manchester, Great Britain

7 x 10″, ix + 510 pages, 20 tables, 181 illus., 547 lit. refs., 1968, Dfl. 97.50

Contents: 1. The principles and methods of mass spectrometry. 2. Types of ions in the mass spectra of organic compounds. 3. The mass spectra of hydrocarbons. 4. The mass spectra of oxygenated compounds. 5. The mass spectra of nitrogen compounds. 6. The mass spectra of sulphur compounds. 7. The mass spectra of halogenated compounds. 8. The mass spectra of boron compounds. 9. The mass spectra of phosphorus compounds. 10. The mass spectra of silicon compounds. 11. Examples of structure determination from mass spectra. Appendix 1. Peaks commonly encountered in the mass spectra of organic compounds. Appendix 2. The masses and abundances of nuclides commonly encountered in the mass spectra of organic compounds. References. Indexes.

MASS SPECTROMETRIC ANALYSIS OF SOLIDS

edited by A. J. Ahearn, Member of Technical Staff, Bell Telephone Laboratories, Inc.,
Murray Hill, New Jersey, U.S.A.

5½ x 8½″, viii + 175 pages, 13 tables, 46 illus., 242 lit. refs., 1966, Dfl. 30.00

Contents: 1. Introductory survey. 2. The production of ions from solids. 3. Photographic emulsions as ion detectors in quantitative mass spectrography. 4. Analysis of special samples. 5. Mass spectrographic microprobe analysis. Indexes.

ATOMIC-ABSORPTION SPECTROSCOPY

and Analysis by Atomic-Absorption Flame Photometry

by J. Ramírez-Muñoz, Principal Applications Chemist at Beckman Instruments Inc. and Scientific Research Collaborator of the C.S.I.C., Spain

6 x 9″, xii + 493 pages, 23 tables, 156 illus., 950 lit. refs., 1968, Dfl. 80.00

Contents: *Part I: Fundamentals.* 1. Origins of the method and nomenclature. 2. General principles and characteristics. 3. Absorption and emission. 4. The literature of atomic-absorption spectroscopy. 5. Theory. *Part II: Instrumental Systems.* 6. Instrumental systems. 7. Emission systems. 8. Absorption system. 9. Selection system. 10. Photometric system. 11. Instruments. *Part III: Range and Limitations of Atomic Absorption Methods.* 12. Determinable elements. Choice of lines. 13. Sensitivity. 14. Limitations in atomic absorption. *Part IV: Experimental Methods.* 15. Experimental process. 16. Standard solutions. 17. Preparation of the sample. 18. Experimental measurements and calibration. *Part V: Applications.* 19. Applications. Appendix. Bibliography.

Still available:

MASS SPECTROMETRY AND ITS APPLICATIONS TO ORGANIC CHEMISTRY

by J. H. Beynon

7 x 10″, xii + 640 pages, 11 tables, 185 illus., 2213 lit. refs., 1960, reprinted 1964 and 1967, Dfl. 85.00

TABLE OF META-STABLE TRANSITIONS FOR USE IN MASS SPECTROMETRY

by J. H. Beynon, R. A. Saunders and A. E. Williams

10 x 7″, xix + 392 pages, 1965, Dfl. 50.00

MASS AND ABUNDANCE TABLES FOR USE IN MASS SPECTROMETRY

by J. H. Beynon and A. E. Williams

10 x 7″, xxi + 570 pages, 1963, Dfl. 60.00

Elsevier Publishing Company Amsterdam London New York

408 E

technological forecasting

AN INTERNATIONAL JOURNAL

...devoted to the methodology of exploratory and normative forecasting to encourage applications to planning in an environment of technological and social change

Volume 1, Number 1, early 1969

Technological Forecasting selects for publication articles which deal directly with the methodology and practice of technological forecasting as a planning tool, including the interrelationship of social, environmental, and physical factors affecting such forecasts. Readability and good writing style are important criteria for publication. Content and presentation will meet the normal standards for scientific credibility and will be of scholarly caliber.

Although the majority of papers are specifically confined to the field of technological forecasting, the journal will occasionally carry articles on topics which have potential implications for technological forecasting (e.g., environmental analysis).

Elsevier Sequoia S.A., Lausanne – Printed in The Netherlands

A SELF-TIMING BRIDGE EMPLOYING PHASE DETECTION FOR DIFFERENTIAL CAPACITANCE MEASUREMENT

JOHN B. HAYTER
Department of Physical Chemistry, University of Sydney, Sydney, N.S.W., 2006 (Australia)
(Received April 24th, 1968)

INTRODUCTION

Since the pioneer work of GRAHAME[1,2], much of the tedium has been removed from the evaluation of double-layer parameters at a dropping mercury electrode by the use of semi-automatic measurement techniques. With the high-speed computing facilities currently available, a knowledge of drop-time *versus* applied potential allows highly accurate determination of the electrocapillary maximum, by the method of isotension potentials[3], and the concurrent measurement of electrode capacitance at a known time in its life provides, in principle, all that is required to establish such values as the charge density, surface tension, and hence surface excesses in the system under study.

One of the most successful methods for obtaining such information is the NANCOLLAS AND VINCENT self-timing bridge[4,5], and its various modifications (see, for example, ref. 6). In this device, the electrode is coupled to an impedance-sensitive oscillator which starts an electronic timer at the instant of detachment of a fully grown drop, *i.e.*, at the birth of the next drop. The electrode is then switched to a transformer bridge, the output of which is fed to an amplitude sensitive detector which stops the timer at balance.

Such a system has two basic disadvantages: the need for a separate drop-birth detector, and the use of signal amplitude to determine balance, both of which add considerably to the complexity of operation. The latter, in particular, requires special skill on the part of the operator to obtain maximum accuracy, since the bridge output at balance falls, in general, not to zero, but to a minimum which cannot always be detected with accuracy.

The self-timing bridge to be described here detects the phase, rather than the amplitude, of the bridge output, and so eliminates these difficulties. It also provides two further major advantages. The first of these is the elimination of spurious "balance" points. When the bridge is correctly balanced at one point in drop life, the phase of the output signal in the birth-balance period differs from that in the balance-birth period by π radians, and the transition from one value to the other is instantaneous. In some measurements made in this laboratory on quaternary ammonium compounds, however, pseudo-balance points (with respect to amplitude) have occurred. These apparent balance points are thought to occur when the double-layer formation is strongly diffusion-controlled, and the measurements are on a non-equilibrium system. In these cases, the output amplitude may fall to a local minimum which appears to

represent bridge balance, but the phase shifts in only a random manner, which is easily detected.

The second advantage is that the detector output now carries unambiguously the information that the electrode is in either the post-birth/pre-balance state, or the pre-birth/post-balance state, and hence allows the use of binary logic circuitry to automate the entire timing procedure. The resulting gains in operational simplicity and speed of data collection have more than justified the minor increases in circuit complexity required to achieve them.

GENERAL PRINCIPLES

The basic form of the self-timing bridge is depicted in Fig. 1.

It is similar to that developed by NANCOLLAS AND VINCENT[4], differing mainly in the replacement of their separate birth and balance detectors by a phase comparator and digital pulse selector (DPS), the latter being responsible for the automation of the timing procedure.

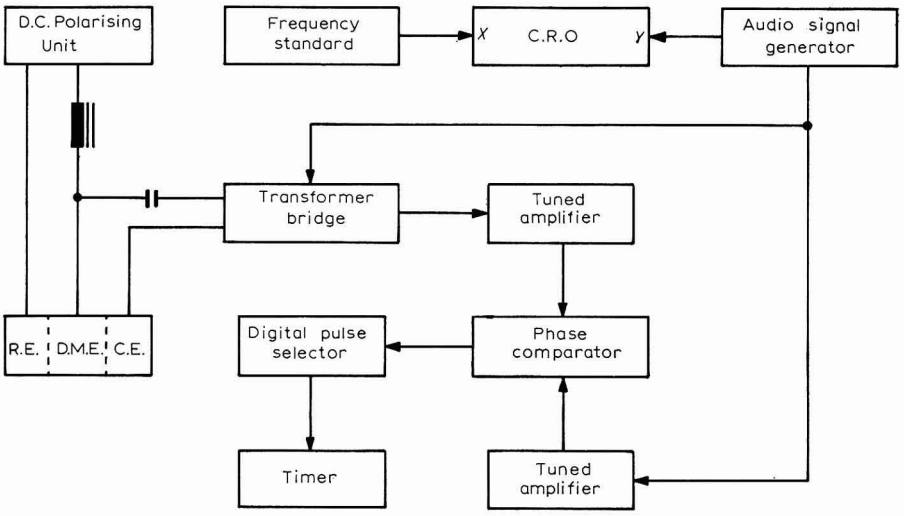

Fig. 1. Block diagram of the semi-automatic self-timing bridge. (RE), reference electrode; (DME), dropping mercury electrode; (C.E.), counter electrode.

The bridge operates in the following manner: An (ideally) polarized dropping mercury electrode containing the solution under study is set up in the usual way (see, for example, ref. 2) and a transformer bridge is connected across the dropping mercury electrode (DME) and a counter electrode, *via* a d.c. isolating capacitor having low impedance at the frequency of measurement. A.c. is supplied to the bridge by an audio signal generator, the frequency normally being monitored by a Lissajous method. The bridge output is amplified and its phase compared with that of the input signal, the phase comparator giving a d.c. output the level of which is proportional to phase difference.

As the electrode passes through successive birth and balance states, the output from the phase comparator is thus a train of square pulses carrying unambiguous information on the state of the electrode. In the present equipment, where the phase comparator output varies from -1 V at 0° to $+1$ V at 180°, the pulse train will have the form shown in Fig. 2.

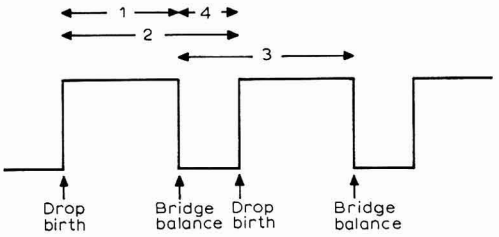

Fig. 2. Phase comparator output. Intervals correspond to positions of switch S1 in Fig. 3.

The digital pulse selector then selects for timing any one of the four distinct intervals marked, having been "instructed" by the operator which particular one to choose, and switches the timer on and off at the appropriate moments.

LOGICAL DESIGN OF DIGITAL PULSE SELECTOR

A consideration of the manner of operation, together with the foregoing, leads to three criteria for the DPS:

(i) it must ignore the first pulse to allow for switching on at any point in drop life;
(ii) it must then hold the timer on for any chosen one of the four possible intervals in Fig. 2, and
(iii) it must ignore all further pulses until intentionally reset, to allow for logging of the data.

Figure 3 shows in schematic form how this has been achieved.

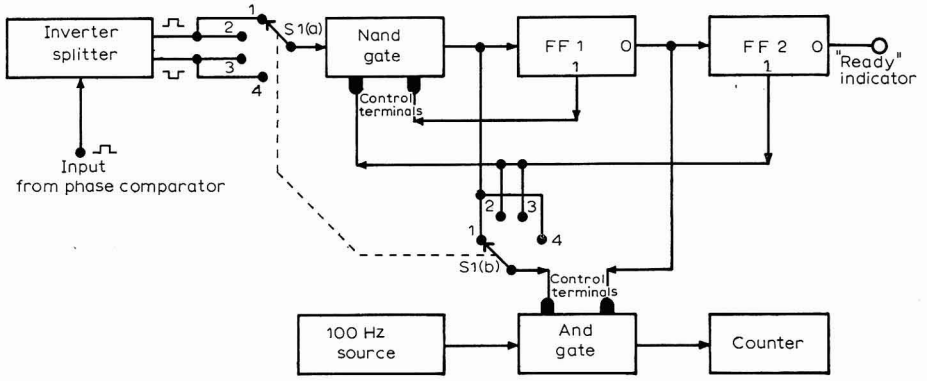

Fig. 3. Block diagram of the digital pulse selector and timer.

For the purpose of this discussion, we will assume logic circuits which respond only to negative-going pulses. Thus a NAND = NOT AND gate will pass a signal *except* when both control terminals are negative, and hence an AND gate will pass a signal *only* when both of these terminals are negative.

A flip-flop will be in the "0" state if its "0" level is negative, and in the "1" state if its "1" level is negative. Reset will set it to the "0" state, and only negative input pulses will alter it from one state to the other.

With these conventions in mind it is evident from Fig. 2 that the logic circuits will be affected only at balance-points. To start the timer at balance, the signal may therefore be used as it is, but to start at drop-birth, it requires inversion. The inverter-splitter is used to make either form of the signal available through switch S1 (a). In positions 1 and 2, pulses are negative-going at drop-birth, and in positions 3 and 4 are negative-going at bridge balance.

Whichever form of the signal is chosen is sent to a NAND gate, the gate being controlled by the "1" level outputs of the two flip-flops (FF1 and FF2). Since these are initially both in the "0" state (*i.e.*, both "0" levels are negative), the signal is passed and the first negative-going pulse switches FF1 to the "1" state. Nothing further happens, and this pulse has therefore been ignored by the timer, which is on only when both AND gate control levels are negative.

Let us now suppose that S1 is in position 1. When the next negative-going pulse arrives, it switches FF1 to "0", and this in turn switches FF1 to the "1" state, at the same time turning off the "READY" indicator. Furthermore, for as long as the incoming pulse is negative, both AND control levels are negative, and 100 Hz pulses reach the counter. When the input reverts to the positive level, the AND gate no longer passes pulses to the counter, and interval "1" in Fig. 2 has been timed.

The arrival of the next pulse switches FF1 back to the "1" level, and the NAND gate closes, preventing any further pulses from reaching the flip-flops and hence leaving the time displayed until the system is reset, at which point the "READY" indicator lights up again.

With S1 in position 2, the sequence of events is identical except that the AND gate is open for as long as the flip-flops are in the 01 state, and the time recorded is the time between two negative-going pulses, *i.e.*, that interval marked 2 in Fig. 2.

In a similar manner, S1 positions 3 and 4 time the intervals marked 3 and 4 in Fig. 2.

CIRCUIT DETAILS

The electronic circuitry of the bridge, while somewhat extensive, is straightforward, and it is felt that a full description would be out of place in a non-constructional article. A few points may be worth discussing, however, in order to emphasize the advantages that are realisable with this bridge.

Primarily, control is by a single three-position toggle switch, normally centred in a "WAIT" position. The operator presses this down to "RESET" the timer and flip-flops, balances the bridge while it is in the natural "WAIT" position, and then switches it to "TIME", to permit the phase comparator output to pass to the DPS. The interval timed is chosen by switch S1, which will usually remain fixed during a single experimental run.

Since the gates are required to pass the signal unchanged, these are fast response, low gain gated amplifiers, rather than gates in the normal (pulse generating) sense.

The phase comparator is a standard half-cycle integrator, and therefore has an output centred about zero at quadrature. This output is also used to drive a drop counter, and is monitored on a CRO screen, normally with a Lissajous figure superimposed to allow simultaneous frequency comparison.

The amplitude of the bridge output is also monitored as an aid to finding bridge balance, in conjunction with the phase shift display.

CONCLUSION

The bridge described here has now been operating reliably for some eighteen months, and in this time has been found to increase both the speed and the reliability of data collection in the field of differential capacity studies.

The general concept has been presented only as a basis for the possible design of an instrument to suit the needs of a particular laboratory. While details of the original hybrid valve and transistor circuitry are available from the author, it is felt that the availability of micro-integrated circuits now makes it a worthwhile proposition to design from first principles a bridge for any specific installation.

ACKNOWLEDGEMENT

The author wishes to express his thanks to Dr. R. J. HUNTER, of this department, for many helpful discussions.

SUMMARY

The use of phase, rather than amplitude detection in a self-timing bridge allows one signal to carry full information on the state of a dropping mercury electrode. The manner in which this may be used to automate the timing procedures in differential capacitance measurements is discussed. Details are given of the design concepts in the logic circuitry, which remembers the states of the electrode during the timing cycle, and can thus choose for timing any pre-selected interval in the life of a drop.

REFERENCES

1 D. C. GRAHAME, *Phys. Rev.*, 72 (1947) 522.
2 D. C. GRAHAME, *J. Am. Chem. Soc.*, 71 (1949) 2975.
3 D. C. GRAHAME, R. P. LARSEN AND M. A. POTH, *J. Am. Chem. Soc.*, 71 (1949) 2978.
4 G. H. NANCOLLAS AND C. A. VINCENT, *J. Sci. Instr.*, 40 (1963) 306.
5 G. H. NANCOLLAS AND C. A. VINCENT, *Electrochim. Acta*, 10 (1965) 97.
6 R. G. BARRADAS AND F. M. KIMMERLE, *Can. J. Chem.*, 45 (1967) 109.

ELECTROANALYTICAL CHEMISTRY AND INTERFACIAL ELECTROCHEMISTRY
Elsevier Sequoia S.A., Lausanne – Printed in The Netherlands

GESETZMÄSSIGKEIT FÜR DEN DIFFUSIONSGRENZSTROM AN TEILWEISE BLOCKIERTEN MODELLELEKTRODEN

F. SCHELLER, S. MÜLLER, R. LANDSBERG, H.-J. SPITZER
Physikalisch-Chemisches Institut der Humboldt-Universität, 108 Berlin, (DDR)
(Received February 12th, 1968)

THEORETISCHE GRUNDLAGEN

Die Mehrzahl der elektrochemischen Prozesse in der Technik wird an Festelektroden durchgeführt, bei denen man die Heterogenität der Oberfläche berücksichtigen muss. Die Durchtrittsreaktion läuft nur an den aktiven Stellen ab, bzw. ist die Austauschstromdichte an den inaktiven Bereichen viel kleiner[1]. Die Klärung des Einflusses der Heterogenität der Oberfläche auf die Elektrodenprozesse ist deshalb für die Untersuchung technischer elektrochemischer Prozesse äusserst wichtig.

Fliesst durch eine teilweise blockierte Elektrode ein Strom, so erfolgt der Stoffumsatz nur an den aktiven Stellen, während der Stofftransport aus dem gesamten Raum über der Elektrode stattfindet. Neben der linearen Diffusion zu den aktiven Stellen muss hier auch die nichtlineare Diffusion am Stofftransport zur Elektrode beteiligt sein[1,2].

Mit rotierenden Scheibenelektroden lassen sich Diffusionsprozesse bequem untersuchen, da nach Lewitsch mit einer einheitlichen Diffusionsschichtdicke δ, gerechnet werden kann. Die Heterogenität der Oberfläche wird hier zu Abweichungen von der LEWITSCH-Beziehung[3] führen, die für homogene Oberflächen abgeleitet wurde, wenn die Zahl der aktiven Oberflächenbereiche nicht sehr gross und ihre Ausmasse mit der Grösse von δ vergleichbar sind.

Die Wirkung inaktiver Stellen auf den Grenzstrom an einer rotierenden Scheibenelektrode ist bereits mehrfach beobachtet worden, u.a. von NAGY[4] und Mitarbeitern bei der Wasserstoffentwicklung an inaktiven Pt-Elektroden und von uns bei der Reduktion von H_2O_2 und O_2 an paraffiniertem Graphit[5–7] sowie bei der Untersuchung der Redoxsysteme $[Fe(CN)_6]^{3+}/[Fe(CN)_6]^{4+}$, I_2/I^- und MnO_4^-/MnO_4^{2-} an Graphitelektroden[8].

Um den Diffusionsgrenzstrom an einer teilweise blockierten (inhomogenen) rotierenden Scheibenelektrode zu berechnen, übertrugen NAGY u.a.[4] die Analogie von Diffusionsgrenzstrom und Konzentrationsgradient einerseits und elektrischem Strom und Potentialgradient andererseits auf die rotierende Scheibenelektrode. Sie bestimmten experimentell den elektrischen Widerstand eines Zylinders der Länge, δ, dessen eine Stirnfläche mit dem Radius, r_2, elektrisch leitend ist, während die andere Stirnfläche eine kleinere, runde, leitende Scheibe mit dem Radius, r_1, im Zentrum besitzt. Abb. 1.

SMYTHE[9] hat das Grenzwertproblem des Widerstandes eines solchen Zylinders rechnerisch näherungsweise gelöst. Bei der Übertragung des Modellzylinders auf den

Diffusionsgrenzstrom an der rotierenden Scheibenelektrode entspricht die Diffusionsschichtdicke, δ, der Länge des Zylinders bei der jeweiligen Umdrehungszahl, während r_1 der Radius der kreisförmig angenommenen aktiven Stelle ist und $2\,r_2$ den Durchmesser des Diffusionszylinders darstellt. An den inaktiven Bereichen wird die Austauschstromdichte Null gesetzt. Für b aktive Stellen auf der Elektrodenoberfläche

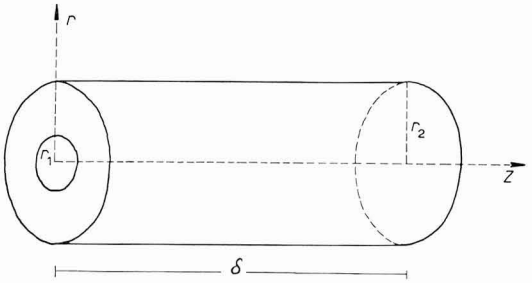

Abb. 1 Modell für den Diffusionszylinder über einem aktiven Bereich. (r_1), Radius des aktiven Bereiches; (r_2), Radius des Zylinders; (δ), Diffusionsschichtdicke.

müssen wir b Diffusionszylinder parallel schalten. Zu den azentrischen Stellen kann ein erhöhter Stofftransport durch die Zentrifugalströmung des Elektrolyten auf Grund der Rotation der Elektrode erfolgen[6]. Da auf der Lösungsseite der Diffusionsschicht die gesamte geometrische Fläche, q_{geo}, vom Diffusionsstrom durchflossen wird, kann man für r_2 setzen

$$N\pi r_2^2 = 1 \qquad N = b/q_{geo} \tag{1}$$

und damit

$$r_1^2/r_2^2 = 1 - \psi \quad (\psi, \text{ Blockierungsgrad}) \tag{2}$$

Hierbei wird vorausgesetzt, dass die Flächen, die zwischen den Diffusionszylindern frei bleiben, gleich der Summe der Flächenanteile sind, die zwei Zylindern angehören.

Nach LANDSBERG UND THIELE[8] gilt für die Rührabhängigkeit des Diffusionsgrenzstromes an einer teilweise blockierten Scheibenelektrode:

$$1/I_{gr} = (1.61\,\nu^{\frac{1}{6}}/nFD^{\frac{2}{3}}c_L(2\pi)^{\frac{1}{2}}\,q_{geo})\;u^{-\frac{1}{2}} + |\Sigma A_n \operatorname{tgh}(x_n\delta/r_2)|/nFDc_L\,q_{geo} \tag{3}$$

ν, kinematische Viskosität
n, Zahl der ausgetauschten Elektronen
F, Faradaykonstante
D, Diffusionskoeffizient
c_L, Konzentration in der Lösung
x_n, Nullstelle der Besselfunktion 1. Ordnung
A_n, Koeffizienten nach Gl. (7)
q_{geo}, geometrische Elektrodenfläche
u, Umdrehungszahl (1/sec)

Abbildung 2 zeigt den prinzipiellen Verlauf des Grenzstromes als Funktion der Umdrehungszahl entsprechend Gl. (3): Für kleine Umdrehungszahlen bzw. grosse Werte von δ, verglichen mit r_2, vereinfacht sich Gl. (3), da der tgh x für grosse x gegen 1 geht, und man erhält:

$$1/I_{gr} = (1.61\nu^{\frac{1}{6}}/nFD^{\frac{2}{3}}c_L(2\pi)^{\frac{1}{2}}q_{geo})u^{-\frac{1}{2}} + |\Sigma A_n|/nFDc_L q_{geo} \quad (4)$$

Das entspricht in der Auftragung I_{gr}^{-1} gegen $u^{-\frac{1}{2}}$ einer Parallelen zur Lewitsch-Geraden (Bereich a, Abb. 2), die Extrapolation auf $u^{-\frac{1}{2}}=0$ liefert den Ordinatenabschnitt (I_b^{-1}):

$$1/I_b = |\Sigma A_n|/nFDc_L q_{geo} \quad (5)$$

Dieser Zusammenhang ist demjenigen analog, der für die Überlagerung von Diffusions- und Reaktionsüberspannung für eine homogene oder heterogene Reaktion

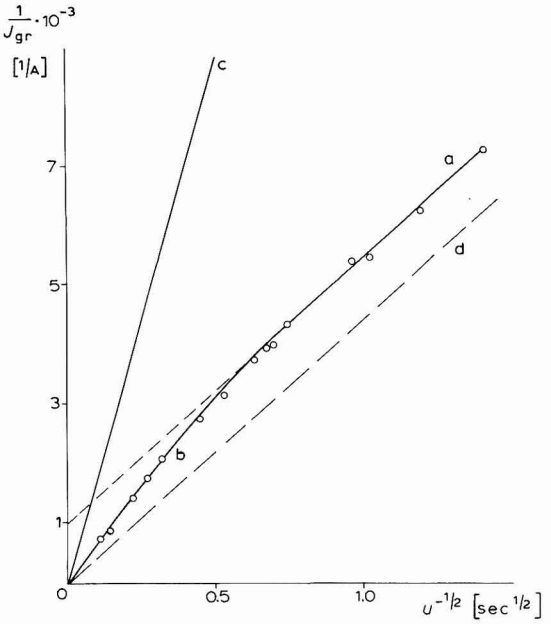

Abb. 2 Abhängigkeit des reziproken Grenzstromes der Reduktion von $K_3[Fe(CN)_6]$ an einer teilweise blockierten Pt-Elektrode von der Umdrehungszahl der Elektrode. $t = 20°$; $1M$ KCl; $c_L = 1\cdot10^{-2}$ M $K_3[Fe(CN)_6]$ $\psi = 70.5\%$; $r_1 = 1.25\cdot10^{-3}$ cm. (a), Frumkin-Gebiet; (b), Quasi-Lewitsch-Gebiet; (c), Lewitsch-Beziehung mit $q_{akt}(b\pi r_1^2)$; (d), Lewitsch-Beziehung mit q_{geo}.

1. Ordnung gilt[10,11]. Die entsprechende Extrapolation ergibt hier den Ordinatenabschnitt (I_r^{-1}):

$$1/nFkc_L q_{geo} = 1/I_r \quad (6)$$

Wir nennen deshalb den Bereich a in Abb. 2 "Frumkin-Gebiet". Für kleine Werte des Arguments (kleine $u^{-\frac{1}{2}}$) kann tgh x durch das Argument selbst ersetzt werden, und dieses ist δ proportional, man sollte eine Gerade erhalten, die durch den Koordinatenursprung verläuft. Die Neigung dieser Geraden ist in der Auftragung I_{gr} über $u^{\frac{1}{2}}$ kleiner als dem Produkt aus Diffusionskoeffizient und geometrischer Fläche entspricht. Wir bezeichnen diesen Zusammenhang (Bereich b Abb. 2) als "Quasi-Lewitsch-Gebiet".

Bei relativ wenigen und grossen aktiven Stellen führt auch die Strömung an den azentrischen Stellen zu einem derartigen Zusammenhang, worüber wir an ande-

rer Stelle berichten. Zwischen dem "Frumkin-" und "Quasi-Lewitsch-Gebiet" erfolgt ein allmählicher Übergang. Merkliche Abweichungen von der "Frumkin-Beziehung" sollten nach Gl. (3) bei $\delta/r_2 = 1$ auftreten. Es hängt also nur von der Zahl der aktiven Stellen ab, bei welchen Rührgeschwindigkeiten das Übergangsgebiet beginnt. Trägt man den Grenzstrom über $u^{\frac{1}{2}}$ auf, so kann unter Umständen eine Gerade vorgetäuscht werden[12-14], die nicht durch Null verläuft, wenn der Messbereich im Übergangsgebiet liegt.*

Die durch Gl. (3) gegebene Beziehung stimmt qualitativ gut mit den von NAGY und uns gemessenen Kurven überein, beide theoretisch ableitbaren Gebiete wurden experimentell gefunden[4-8]. Für eine quantitative Anwendung von Gl. (3) und (4) in einem weiten Bereich des Blockierungsgrades und des Verhältnisses, δ/r_2 (d.h. der Rührgeschwindigkeit) war es notwendig $|\Sigma A_n \mathrm{tgh}(x_n \delta/r_2)|$ als Funktion von r_1/r_2 und δ/r_2 zu berechnen.

Die Bestimmungsgleichung von SMYTHE für A_n

$$-\frac{A_n}{r_2} = \frac{1}{x_n^2 J_0^2(x_n)} \left\{ \left[\frac{r_2}{r_1} - \left(\frac{r_1}{r_2}\right)^{2.5} \right] \sin\left(x_n \frac{r_1}{r_2}\right) + 2\left(\frac{r_1}{r_2}\right)^{2.5} J_1\left(\frac{x_n\, r_1}{r_2}\right) \right\} \qquad (7)$$

J_n, Besselfunktion n. Ordnung 1. Gattung

x_n, Nullstellen von $J_1(x)$

wurde programmiert und $|\Sigma A_n/r_2|$ unter Berücksichtigung der ersten 80 Glieder für $r_1/r_2 = 0.05$; 0.10 ... ... 1.0 mit dem ZRA1 berechnet. Dazu benutzten wir die von DAVIS[15] angegebenen Werte für x_n und $J_0(x_n)$. Die Ergebnisse sind in Tabelle 1 und Abb. 3 dargestellt:

TABELLE 1

r_1/r_2	$\lvert\Sigma A_n\rvert/r_2$	r_1/r_2	$\lvert\Sigma A_n\rvert/r_2$
0.05	14.570	0.55	0.410
0.10	6.853	0.60	0.310
0.15	4.150	0.65	0.229
0.20	2.805	0.70	0.166
0.25	2.040	0.75	0.116
0.30	1.535	0.80	0.077
0.35	1.170	0.85	0.047
0.40	0.900	0.90	0.025
0.45	0.692	0.95	0.010
0.50	0.535	1.00	0.000

Abbildung 4 zeigt die Partialsummen, S_1, S_2 ... S_{150}, von $1/r_2 |\Sigma A_n|$ für das Radienverhältnis $r_1/r_2 = 0.3$. Die Konvergenz der Reihe gestattet es, gute Aussagen über die Genauigkeit der Werte zu machen. Wegen der schwachen Konvergenz der Reihe berechneten wir die Partialsummen, S_1 ... S_{80}, und ermittelten $1/r_2 |\Sigma A_n|$ durch Mittelwertbildung aus den letzten Partialsummen. Die Genauigkeit der berechneten Werte sollte für die Praxis ausreichend sein.

* Auch eine Nebenreaktion kann zu diesem Resultat führen[17,18].

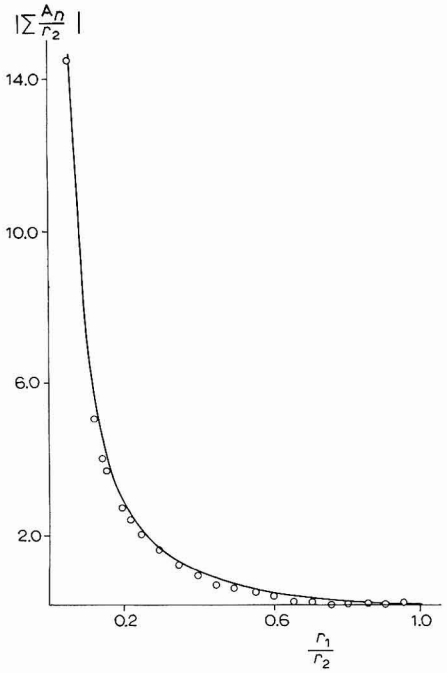

Abb. 3 Die Koeffizienten $|\Sigma A_n/r_2|$ als Funktion von r_1/r_2.

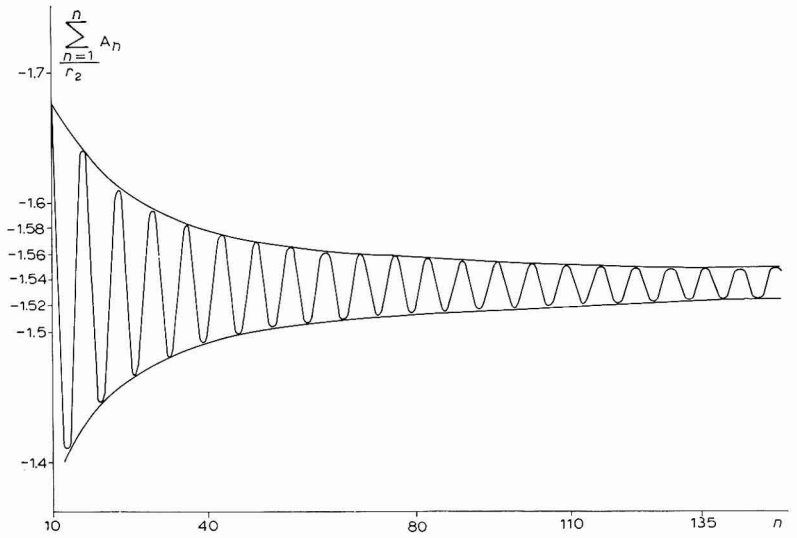

Abb. 4 Die Partialsummen der Funktion $1/r_2 \Sigma A_n$ in Abhängigkeit von der Zahl der Glieder $r_1/r_2=0.3$

EXPERIMENTELLER TEIL

Zur Prüfung von Gl. (3) und (4) führten wir Messungen mit Modellelektroden durch, die einen bekannten Blockierungsgrad und eine bekannte Grösse der aktiven Stellen besitzen. Zur Erzeugung der Modelle wurde die Platinelektrode von 5 mm ⌀ mit Photoresist beschichtet und die inaktiven Stellen mittels Belichtung mit UV-Licht durch Schablonen erzeugt, wie sie zur Herstellung von Halbleiterbauelementen verwendet werden. Die aktiven Stellen entstehen durch Herauslösen des unbelichteten Resist, sie sind kreisförmig und auf einem Kreuzgitter angeordnet. Bleibt die gesamte Elektrode unbelichtet, wie sonst die aktiven Stellen, und wird der Resist danach wieder abgelöst, so verhält sich die Elektrode nach der gleichen Vorbehandlung (alternierendes Vorpolarisieren—bis zur beginnenden Wasserstoff—und Sauerstoffentwicklung) wie eine unvergiftete, d.h. die Lewitsch-Beziehung wird beobachtet.

Wir stellten Modellelektroden mit 100–160,000 aktiven Stellen/cm² und Radien von $5 \cdot 10^{-2}$–$6 \cdot 10^{-4}$ cm her. Die Grösse der aktiven Stellen wurde mit dem Okularmikrometer nachgemessen, nachdem die freie Platinfläche zur Kontrasterhöhung platiniert worden war.

Als geeignetes System benutzten wir $K_4[Fe(CN)_6]/K_3[Fe(CN)_6]$ in 1 *M* KCl, die Austauschstromdichte, i_0, beträgt 5 A/cm² [16]. Es wurde die Reduktion von Ferricyanid bei 20° untersucht. Dabei wurden die Lösungen aus bidestilliertem Wasser hergestellt und das KCl und das Ferricyanid umkristallisiert. Zur Entfernung des Sauerstoffs wurde gereinigter Stickstoff durch die Lösung geleitet.

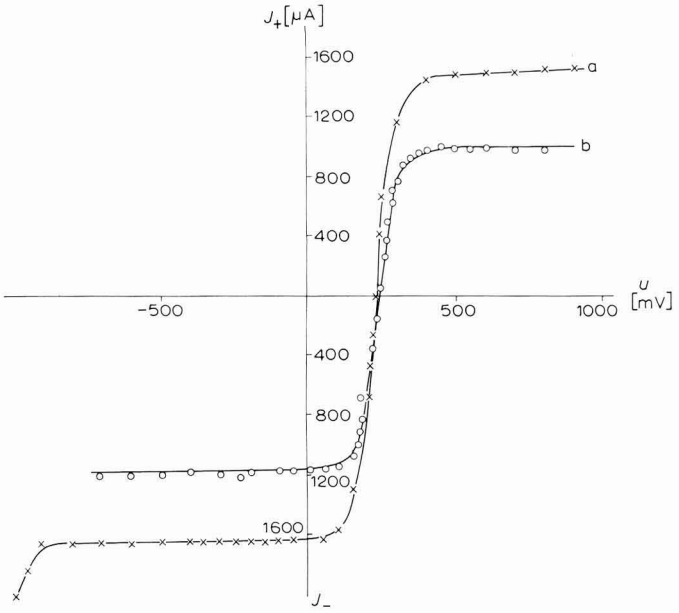

Abb. 5 Stromspannungskurve. $t = 20°$; 1 *M* KCl; $1 \cdot 10^{-2}$*M* $K_3[Fe(CN)_6]$; $1 \cdot 10^{-2}$ *M* $K_4[Fe(CN)_6]$. (U) Potential gegen ges. Kalomel; (a) unblockierte Pt-Elektrode 5 mm ⌀; (b) teilweise blockierte Pt-Elektrode 5 mm ⌀; $\psi = 61.8\%$; $r_1 = 2.5 \cdot 10^{-3}$cm.

MESSERGEBNISSE UND DISKUSSION

Abbildung 5 zeigt die Stromspannungskurve dieses Systems an einer unblockierten Platinelektrode (Kurve a) und an einer teilweise blockierten Elektrode (Kurve b).

Die Rührabhängigkeit des Diffusionsgrenzstromes für eine Modellelektrode ist in Abb. 6 und 2 dargestellt.

Abbildung 7 zeigt den nach Gl. (4) erwarteten Ordinatenabschnitt für Modellelektroden mit unterschiedlichen Blockierungsgraden. Eine Gegenüberstellung der nach Gl. (7) und (4) berechneten und der durch Extrapolation der Messkurven erhaltenen Werte für $1/I_b$ gibt Tabelle 2:

TABELLE 2

ψ (%)	r_r/r_2	$r_1 \cdot 10^3$ (cm)	$1/I_b \cdot 10^{-3}$ (Messwert) (1/A)	$1/I_b \cdot 10^{-3}$ (Theorie) (1/A)
94.0	0.248	1.40	10.00	9.6
84.0	0.400	1.25	2.25	2.3
80.5	0.440	1.25	1.70	1.6
72.5	0.520	1.35	1.00	1.0
70.5	0.530	1.25	0.85	0.85
61.8	0.620	2.50	1.00	0.9
45.5	0.740	2.60	0.35	0.36

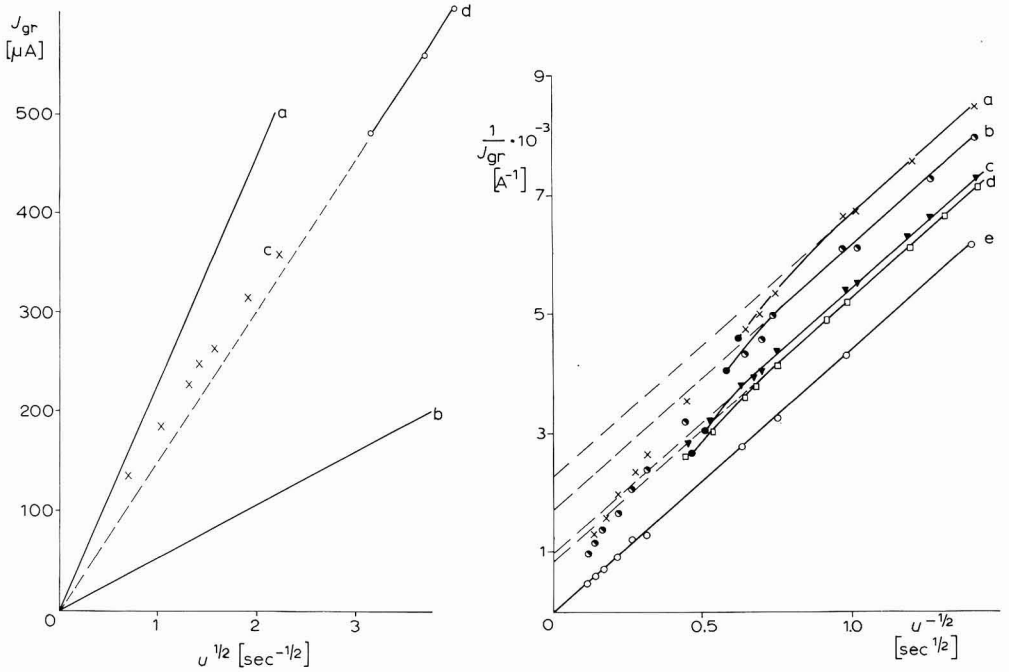

Abb. 6 Rührabhängigkeit des Grenzstromes. $t = 20°$; 1 M KCl; $c_L = 1 \cdot 10^{-2}$ M $K_3[Fe(CN)_6]$; $\psi = 70.5\%$; $r_1 = 1.25 \cdot 10^{-3}$ cm. (a), Lewitsch-Beziehung mit q_{geo}; (b), Lewitsch-Beziehung mit q_{akt}; (c) Frumkin-Gebiet; (d), Quasi-Lewitsch-Gebiet.

Abb. 7 Rührabhängigkeit des Grenzstromes bei verschiedenen Blockierungsgraden der Elektroden. $t = 20°$; 1M KCl; $c_L = 1 \cdot 10^{-2}$ M $K_3[Fe(CN)_6]$. (a), $\psi = 84.0\%$, $r_1 = 1.25 \cdot 10^{-3}$cm; (b), $\psi = 80.5\%$, $r_1 = 1.25 \cdot 10^{-3}$cm; (c), $\psi = 72.5\%$, $r_1 = 1.35 \cdot 10^{-3}$cm; (d), $\psi = 70.5\%$ $r_1 = 1.25 \cdot 10^{-3}$cm; (e), Lewitsch-Beziehung mit q_{geo}. Bei den vollausgefüllten Punkten gilt $\delta = r_2$.

Die Übereinstimmung liegt innerhalb der Messgenauigkeit. Damit wurde bewiesen, dass Gl. (4) die Rührabhängigkeit des Diffusionsgrenzstromes teilweise blockierter rotierender Scheibenelektroden im Frumkin-Gebiet richtig wiedergibt. Gleichzeitig ergibt sich daraus, dass die Annahme nach Gl. (1) berechtigt ist, die Diffusion also aus dem gesamten Volumen über der Elektrode erfolgt. Die azentrische Anordnung der aktiven Stellen verursacht für grosse δ/r_2 (Frumkin-Gebiet) keine Stromüberhöhung durch zusätzliche Konvektion.

Abbildung 8 zeigt, dass die Abhängigkeit des reziproken Ordinatenabschnitts vom Blockierungsgrad nicht linear ist. Einen solchen Zusammenhang ergaben frühere Experimente[7,8], was jedoch Gl. (7) widerspricht.

Für Elektroden mit sehr vielen kleinen, aktiven Stellen wird selbst bei hohen Blockierungsgraden das Korrekturglied in Gl. (4) so klein, dass dann die Lewitsch-Beziehung innerhalb der Messgenauigkeit erfüllt ist.

Die Abhängigkeit des Ordinatenabschnitts von der Konzentration, c_L, und der Ionenstärke μ unterstreicht noch einmal die Gültigkeit von Gl. (4) im Frumkin-Gebiet (Abb. 9, 10 und 11).

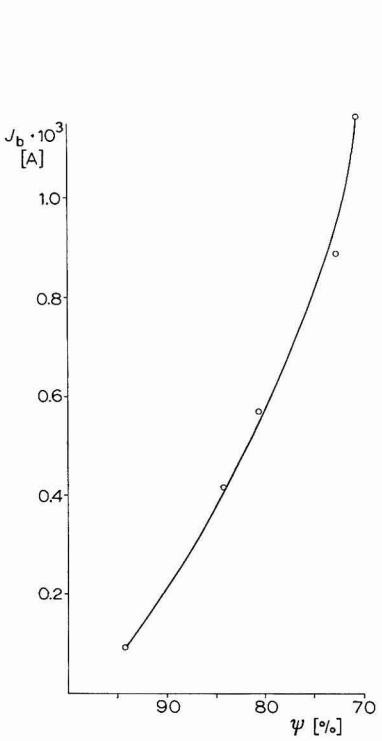

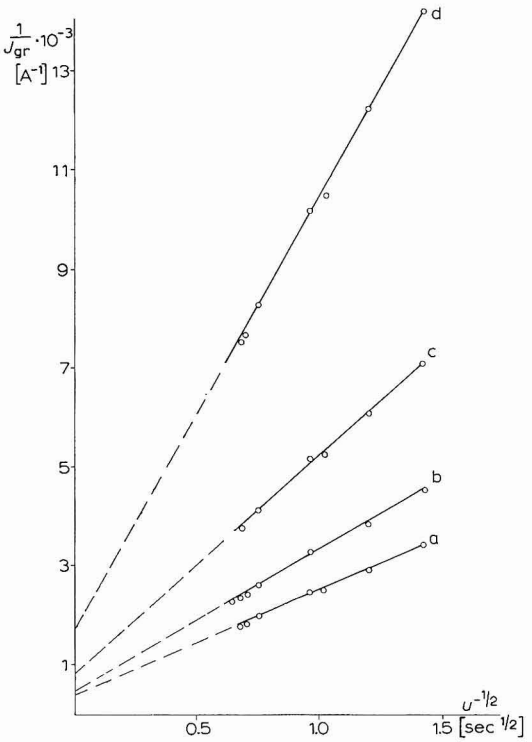

Abb. 8 Die Grösse I_b in Abhängigkeit vom Blockierungsgrad. $t = 20°$; 1 M KCl; $c_L = 1 \cdot 10^{-2}$ M $K_3[Fe(CN)_6]$; $q_{geo} = 0.2$ cm^2; $r_1 = 1.25 \cdot 10^{-3}$cm.

Abb. 9 Abhängigkeit des reziproken Grenzstromes von der Umdrehungszahl der Elektrode bei verschiedenen Konzentrationen. $t = 20°$; 1 M KCl; $\psi = 70.5\%$; $r_1 = 1.25 \cdot 10^{-3}$ cm. (a) 2×, (b) 1.5×, (c) 1×, (d) 0.5× $10^{-2}M$.

Die Messungen haben gezeigt, dass der Beginn der Abweichungen vom Frumkin-Gebiet unabhängig vom Blockierungsgrad bei einem Wert von δ liegt, der etwas grösser als r_2 ist (Abb. 7). Abbildung 12 zeigt die Ergebnisse an zwei verschiedenen Elektroden mit gleichem r_2, aber unterschiedlichen Blockierungsgraden. Man

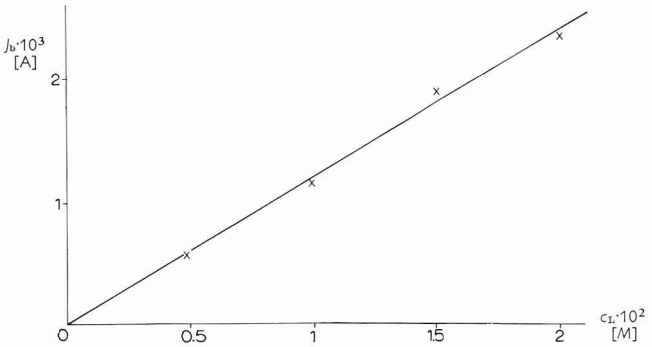

Abb. 10 Abhängigkeit der Grösse I_b von der Ferricyanidkonzentration. $t = 20°$; 1 M KCl; $\psi = 70.5\%$; $r_1 = 1.25 \cdot 10^{-3}$ cm.

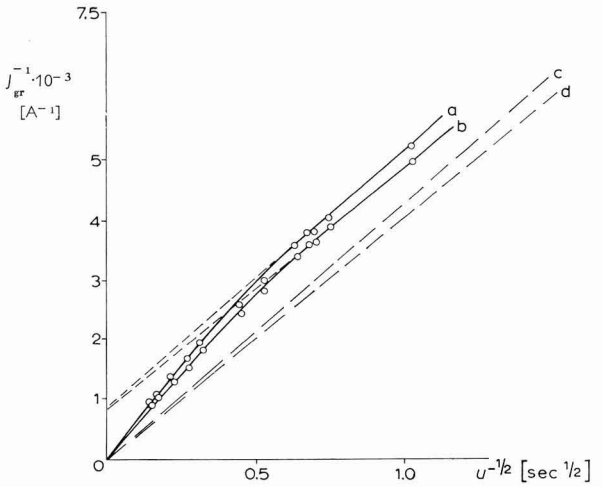

Abb. 11 Einfluss der Ionenstärke auf die Rührabhängigkeit des Grenzstromes. $t = 20°$; $c_L = 1 \cdot 10^{-2}$ M $K_3[Fe(CN)_6]$. (a), 4 M KCl, $\psi = 70.5\%$, $r_1 = 1.25 \cdot 10^{-3}$cm; (b), 1 M KCl, $\psi = 70.5\%$; $r_1 = 1.25 \cdot 10^{-3}$cm; (c), Lewitsch-Beziehung mit q_{geo}, 4 M KCl; (d) Lewitsch-Beziehung mit q_{geo}, 1 M KCl.

kann aus der Kurvenform also r_2 abschätzen, aus dem extrapolierten Abschnitt ist $|\Sigma A_n|$ zugänglich, während $1/r_2|\Sigma A_n| = f(r_1/r_2) = f(\psi)$ tabelliert ist. Es besteht damit die Möglichkeit, auch den Blockierungsgrad und r_1 angenähert zu bestimmen. Diese Methode muss aber noch verfeinert werden.

Im ansteigenden Teil der Stromspannungskurve gilt für den Diffusionsstrom an einer teilweise blockierten Elektrode analog zu Gl. (4):

$$I = nFDq_{geo}(c_L - c_0)/(\delta + |\Sigma A_n|) \qquad \text{für } (\delta > r_2) \tag{8}$$

c_0, Konzentration an der Elektrodenoberfläche. Aus der Nernstschen Gleichung erhält man:

$$c_0 = c_L \exp(nF\eta/RT) \tag{9}$$

Damit ergibt sich unter Berücksichtigung der Lewitsch-Beziehung[3] für die Abhängigkeit der Diffusionsüberspannung, η, vom Strom an einer teilweise blockierten rotierenden Scheibenelektrode:

$$\frac{1}{I} = \frac{1.61\nu^{\frac{1}{6}}u^{-\frac{1}{2}}}{nFD^{\frac{2}{3}}q_{geo}c_L(2\pi)^{\frac{1}{2}}\{1-\exp(nF\eta/RT)\}} + \frac{|\Sigma A_n|}{nFDq_{geo}c_L\{1-\exp(nF\eta/RT)\}} \tag{10}$$

Variiert man die Überspannung im ansteigenden Teil der Stromspannungskurve, so ändern sich in der Auftragung $1/I$ gegen $u^{-\frac{1}{2}}$ der extrapolierte Ordinatenabschnitt

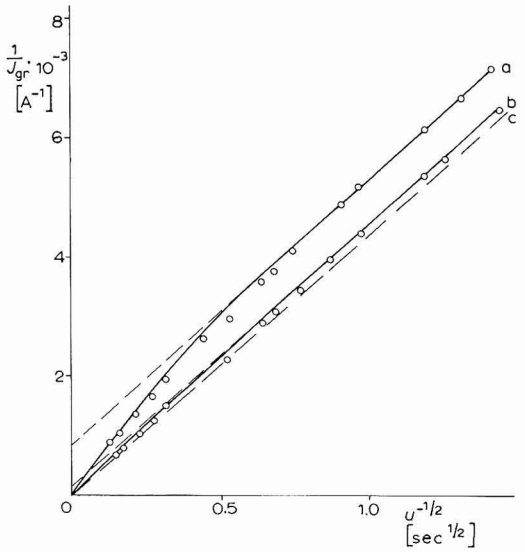

Abb. 12 Rührabhängigkeit des Grenzstromes bei Elektroden mit gleicher Anzahl aktiver Stellen, aber unterschiedlicher Stellengrösse, d.h. unterschiedlichem Blockierungsgrad. $t = 20°$; 1 M KCl; $c_L = 1 \cdot 10^{-2}$ M $K_3[Fe(CN)_6]$. (a), $\psi = 70.5\%$, $r_2 = 2.34 \cdot 10^{-3}$ cm; (b), $\psi = 29.5\%$, $r_2 = 2.34 \cdot 10^{-3}$ cm; (c), Lewitsch-Beziehung mit q_{geo}.

$1/I_b$ und der Anstieg m der Frumkin-Geraden in gleicher Weise. Bei zwei verschiedenen Überspannungen gilt dann für die charakteristischen Grössen der beiden Frumkin-Geraden:

$$I_{b1}/I_{b2} = m_2/m_1 \tag{11}$$

Abbildung 13 zeigt, dass diese Beziehung gut erfüllt ist; es gilt hier:

$$I_{b1}/I_{b2} = 1.4; \qquad m_2/m_1 = 1.35 \tag{11a}$$

Die Gerade b in Abb. 13 beweist, dass bei dem obigen Redoxsystem unter den

vorliegenden Bedingungen keine nennenswerte Durchtrittsüberspannung im untersuchten Teil der Stromspannungskurve auftritt.

Über die Messergebnisse im Quasi-Lewitsch-Gebiet und Untersuchungen über die Unterscheidung von Reaktionshemmungen und Blockierungseffekten werden wir später berichten.

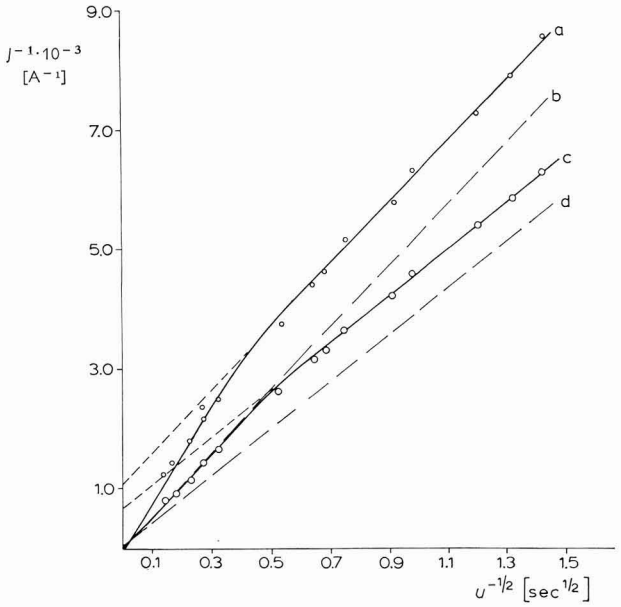

Abb. 13 Abhängigkeit des extrapolierten Abschnittes von der Überspannung. $t = 20°$; 1 M KCl; $c_L = 1\cdot 10^{-2}$ M $K_3[Fe(CN)_6]$; $\psi = 70.5\%$; $r_1 = 1.25\cdot 10^{-3}$ cm. (a), $\eta = -50$ mV; (b), unblokkierte Elektrode, $\eta = -50$ mV; (c), $\eta = -500$ mV; (d), unblockierte Elektrode, $\eta = -500$ mV.

ZUSAMMENFASSUNG

Die Rührabhängigkeit des Grenzstromes an einer rotierenden teilweise blokkierten Scheibenelektrode lässt sich unter vereinfachenden Voraussetzungen mit Hilfe des elektrischen Analogons als Näherungslösung angeben. Diese Theorie wurde an Platin-Modellelektroden für die Reduktion des Ferricyanids überprüft. Der Radius der kreisförmigen aktiven Stellen variierte von $5\cdot 10^{-2}$–$6\cdot 10^{-4}$ cm, wobei bis zu 10^5 aktive Bereiche/cm² modellmässig erzeugt wurden. Im sogenannten "Frumkin-Gebiet", d.h. bei nicht allzu grossen Rührgeschwindigkeiten, konnte die vorgeschlagene Theorie voll und ganz bestätigt werden. Die Rührgeschwindigkeiten, bei denen Abweichungen von der Frumkin-Geraden auftreten, geben einen Anhaltspunkt für den Abstand zwischen den aktiven Bereichen.

Die Theorie wurde auch im ansteigenden Teil der Strom–Spannungs-Kurve bei reiner Diffusionsüberspannung bestätigt.

SUMMARY

The use of the electrical analogy as well as the simplification of assumptions

enables an approximate solution for the dependence of the limiting current on the rate of rotation at a rotating, partially covered disk electrode, to be given.

The reduction of ferricyanide ions at a platinum model electrode was used as a test for the given relationship. The radius of the active circular sites lay between $5 \cdot 10^{-2}$ and $6 \cdot 10^{-4}$ cm, and up to 10^5 active sites/cm^2 were produced on the model electrodes. The relationship was fully confirmed within the so-called "Frumkin region", that is, if the rate of rotation is not too large. The rates of rotation for which deviations from the linear "Frumkin-dependence" arise are an indication of the distance between the active sites. The theory was also fully confirmed for the rising part in the current–potential relationship, provided the polarisation is due purely to diffusion.

LITERATUR

1 K. J. VETTER, *Z. Phys. Chem.*, 199 (1952) 300.
2 D. M. TODES UND A. P. SHAPIRO, *Kinetika i Kataliz*, 2 (1960) 324.
3 W. G. LEWITSCH, *Phys.-Chem. Hydrodynamik*, Moskau, Verlag der Akad. Nauk, 1959.
4 F. NAGY, G. HORANYI UND G. VERTES, *Acta Chim. Acad. Sci. Hung.*, 34 (1962) 35.
5 S. MÜLLER UND R. LANDSBERG, *Ber. Bunsenges. Phys. Chem.*, 70 (1966) 586.
6 R. LANDSBERG, S. MÜLLER UND F. SCHELLER, im Druck.
7 R. LANDSBERG, S. MÜLLER UND R. THIELE, *Acta Chim. Acad. Sci. Hung.*, 51 (1967) 85.
8 R. LANDSBERG UND R. THIELE, *Electrochim. Acta*, 11 (1966) 1243.
9 W. R. SMYTHE, *J. Appl. Phys.*, 24 (1953) 70.
10 A. N. FRUMKIN UND G. TEDORADSE, *Z. Elektrochem.*, 62 (1958) 251.
11 J. KOUTECKÝ UND W. G. LEWITSCH, *Zh. Fiz. Khim.*, 34 (1958) 1565.
12 S. V. GORBATSCHOW UND W. A. BELJAEWA, *Zh. Fiz. Khim.*, 35 (1961) 2158.
13 G. BUTLER UND S. C. SHOME, Zitiert bei A. C. RIDDIFORD, *Advan. Electrochem. Eng.*, 4 (1966) 97.
14 Z. GALUS, C. OLSON, H. J. LEE UND R. N. ADAMS, *Anal. Chem.*, 34 (1964) 164.
15 H. T. DAVIS UND W. J. KIRKHAM, *Bull. Am. Math. Soc.*, 33 (1927) 760.
16 W. VIELSTICH UND D. JAHN, *J. Electrochem. Soc.*, 109 (1962) 849.
17 J. W. PLESKOW, *Zh. Fiz. Khim.*, 34 (1960) 296.
18 R. R. JOHNSTON UND M. SPIRO, *J. Phys. Chem.*, 71 (1967) 3784.

ELECTROANALYTICAL CHEMISTRY AND INTERFACIAL ELECTROCHEMISTRY
Elsevier Sequoia S.A., Lausanne – Printed in The Netherlands

THE BOOTH THEORY OF ELECTROPHORESIS OF LIQUID DROPS

M. SENGUPTA
Department of Chemistry, Science College, Calcutta-9 (India)
(Received April 18th, 1968)

The electrophoresis equation for liquid droplets has been derived by BOOTH[1] to the first approximation in ζ (the potential fall at the drop–solution interface), for some particular types of charge and potential distribution inside the liquid drop. The two important assumptions underlying this derivation (in addition to the usual ones) are that (to the approximation considered), (i) the externally applied field is, in both the inner liquid and the outer solution, linearly superimposed on the spherically symmetrical internal fields due to the ionic charges, *i.e.*, the relaxational asymmetry of charge distribution[2] in both fluids may be neglected as in the corresponding case of solid particles; and (ii) any asymmetry in surface charge distribution produced, for example, by the motion of the surface layer does not affect the final result, again as in the case of solid spheres[3]. Under these assumptions, the Booth equations for the electrophoretic velocity, U, of drops of radius, a, under an applied field, E, are:

(a) When the charge in the inner fluid is all located in a thin layer adjacent to the interface, producing a constant potential, ζ, inside the drop,

$$U = \{E\varepsilon_1\zeta/6\pi\eta_1(3\eta_2+2\eta_1)\}[3\eta_2(1+\lambda F_1)+2\eta_1(1-\lambda F_2)] \quad (1)$$

where $F_1(b)$ and $F_2(b)$ are functions of HENRY[4] and BOOTH[1], respectively, of the ratio $b=\varkappa a$ ($1/\varkappa$ = the Debye–Hückel thickness of the outer solution electrical double layer), $\lambda = (\sigma_1-\sigma_2)/(2\sigma_1+\sigma_2)$ and $\eta_1, \varepsilon_1, \sigma_1$ and $\eta_2, \varepsilon_2, \sigma_2$ are the viscosity coefficients, dielectric constants and specific conductivities of the outer solution and the inner fluid, respectively;

(b) When the charge distribution in the fluid of the drop is of the diffuse double-layer type[5],

$$U = \frac{E\varepsilon_1\zeta}{6\pi\eta_1(3\eta_2+2\eta_1)}\left[3\eta_2(1+\lambda F_1)+2\eta_1(1-\lambda F_2)+5\eta_1(1+\lambda)F_3F_4\frac{(1+b)}{b'^2}\right] \quad (2)$$

where $F_3(b')$ and $F_4(b')$ are Booth functions[1] of the ratio $b'=\varkappa' a$ ($1/\varkappa'$ = thickness of the diffuse double layer within the drop).

Two aspects of the above formulae: the effects of particle conductivity and size, are of interest and have been considered in detail[1,6]. In the first case for example, when $\sigma_1=\sigma_2$; the Hückel equation, *viz.*, $U=E\varepsilon_1\zeta/6\pi\eta_1=U'$ (say), holds, irrespective not only of particle size but also of the magnitude of particle viscosity. When $\sigma_1\neq\sigma_2$, the limiting forms of eqn. (1) for large ($b>1$) and small ($b<1$) non-conducting ($\lambda=\frac{1}{2}$) drops are respectively:

$$U = U' \cdot 4.5\, \eta_2/(3\eta_2 + 2\eta_1)$$

and

$$U = U'(3\eta_2 + 1.5\, \eta_1)/(3\eta_2 + 2\eta_1)$$

while the same for highly conducting ($\lambda = -1$) drops are, respectively:

$$U = U' \cdot 6\, \eta_1/(3\eta_2 + 2\eta_1)$$

and

$$U = U'(3\eta_2 + 3\eta_1)/(3\eta_2 + 3\eta_1)$$

The last two formulae hold, naturally, irrespective of the precise nature of charge distribution within the drop (*i.e.* equally well for both the types of charge distribution considered) or of the presence or absence of any highly conducting surface shell (surface conductivity).

In the case of the other type of charge distribution in the drop, the corresponding equation (2) again reduces, for b' very large (very thin, internal double layer, confined to near the interface) and b' very small (very thick, internal double layer) respectively to eqn. (1) and yet another equation of Booth for the case when the charge in the drop is uniformly distributed throughout. Again, the general equations, or their limiting forms for $b < 1$, and $b > 1$, when the particle is poorly conducting or equi-conducting with respect to the solution, can easily be written down from eqn. (2).

GRAPHICAL REPRESENTATION OF THE RESULTS

It must be remembered when considering the effect of conductivity or charge distribution in the particle, that not all the three conductivity types considered may actually be realized physically; also, a clear cut separation between the two charge distribution types may not always be feasible. Further, even minute traces of impurity tend to be preferentially adsorbed at the interface and disastrously affect the conditions of motion there. Therefore, pending the accumulation of the results of experiments designed specifically to test the theory, a discussion of the different Booth equations or their various particular forms must necessarily remain somewhat formal in nature. Nevertheless, it is of interest to consider the implication of these results in quantitative terms, *i.e.*, by actual numerical calculation in some specific cases.

The viscosity of the fluid of the drop being a variable parameter, we consider three well-defined limiting cases: (1) when the fluid viscosity and the solution viscosity are identical (the *equi-viscous* case); (2) when the fluid has a very low viscosity in comparison with that of the solution, *e.g.*, in the case of gas bubbles (*highly fluid* case, $\eta_2 \sim 0$); and finally (3) when the fluid is very viscous compared to the solution, *e.g.*, in the case of solid particles (*highly viscous* case, $\eta_2 \sim \infty$). Further, the value of the conductance parameter, λ, may vary from $\frac{1}{2}$ to -1, as σ_2 changes from 0 to ∞. The following results are generally given for the following values of λ: $\frac{1}{2}, 0, -\frac{1}{4}, -\frac{1}{2}$ and -1.

Figure 1 shows graphically the results for the *interfacial layer charge distribution* type (for the infinite fluid viscosity case, the results are identical with those already given by HENRY and shown, for example, in ref. 7). The results show the interesting spread (to different degrees) of the different $6\pi\eta_1 U/E\varepsilon_1\zeta$ *vs.* log $\varkappa a$* curves as the viscosity of the fluid either increases or decreases from that of the solution. At

* The values of the functions $F_1(\varkappa a)$ and $F_2(\varkappa a)$, for different values of $\varkappa a$, necessary for the present calculations, were obtained from a suitably photo-magnified copy of the figure given in ref. 1.

constant electrolyte concentration, say, this would mean that the difference in size-dependence of the quantity, $6\pi\eta_1 U/E\varepsilon_1\zeta$, increases as the viscosity difference between the fluid and the solution increases. In the equi-viscous case, the $6\pi\eta_1 U/E\varepsilon_1\zeta$ curves show a mild extremum at moderate values of $\varkappa a$, which disappears as the viscosity difference increases. Also, whereas for solid particles, the $6\pi\eta_1 U/E\varepsilon_1\zeta$ curves for different conductivities all tend to the Hückel curve as size decreases, this is no longer so for viscous drops, and for very fluid drops the relative magnitudes of the quantity $6\pi\eta_1 U/E\varepsilon_1\zeta$ for different conductivities are quite different even for small particle size.

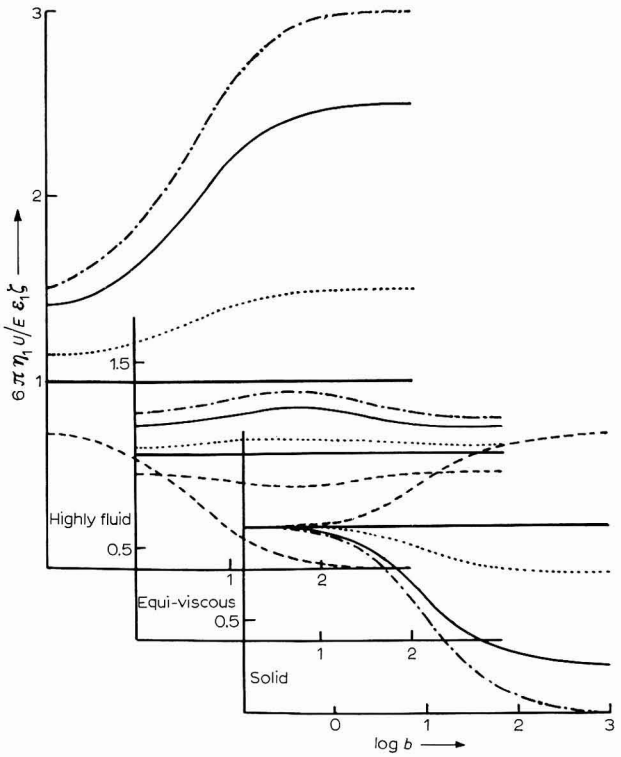

Fig. 1. Plot of $6\pi\eta_1 U/E\varepsilon_1\zeta$ as function of b for different values of conductance parameter, λ, according to Booth liquid droplet electrophoresis equation (interfacial layer charge distribution) for solid, equi-viscous and highly fluid drops. λ-values: (– – – –), $\frac{1}{2}$; (————), 0; (. . . . . .), $-\frac{1}{4}$; (————), $-\frac{3}{4}$; (–·–·–·–), -1.

All this is in keeping with the theoretical equations and is clear from the above discussion for the interfacial layer charge distribution type.

The most significant effect of particle viscosity is related to variations in conductivity. For infinitely viscous (*i.e.*, solid) particles the quantity, $6\pi\eta_1 U/E\varepsilon_1\zeta$, is known to increase with particle size (at constant $\varkappa$) only in the case that it is non-conducting; with increase in conductivity, the increase with size diminishes, and for better conducting (with respect to the solution) particles, $6\pi\eta_1 U/E\varepsilon_1\zeta$ decreases with increase in size. For less viscous particles, the situation is reversed, and in the case of very fluid drops, $6\pi\eta_1 U/E\varepsilon_1\zeta$ decreases with increase in size in the case that it is non-conducting, but increases with size as its conductivity increases.

For calculations in the case of the *diffuse double-layer of charge distribution* in the inner fluid, the thickness of this double layer, $1/\varkappa'$, becomes a new parameter. In any actual case, its magnitude will be determined by the electrolyte solubility in the inner fluid. For the general considerations given here, three definite cases have been considered; (1) when the inner double-layer thickness is much less than that of the outer solution ($b=0.1\,b'$); (2) when the two are equal in magnitude ($b=b'$); and finally (3) when the inner double layer is thick compared to that of the outer solution ($b=10\,b'$). Since in neither of the limiting cases of solid particles or gas bubbles would the diffuse double-layer type of charge distribution under consideration obtain within the particle, the effect of viscosity of the fluid of the drop is therefore more properly shown here by considering (besides the above equiviscous case) the case of a highly viscous ($\eta_2=10\eta_1$) and a highly fluid ($\eta_2=0.1\eta_1$) drop. With electrolytes dissolved in it, the inner fluid can hardly be a total non-conductor, or happen to be an infinitely good conductor, so the limiting cases then considered are, $\lambda=\frac{3}{8}$, and $\lambda=-\frac{1}{4}$.

The values of $F_3F_4/(\varkappa'a)^2$ for different values of $\varkappa'a$, necessary for the present calculations, were obtained from the graphical plot of this quantity as a function of $\varkappa'a$ [8]. Consequently it has been necessary to restrict the calculations in every case from $b'=0.25$ to $b'=10$; this means that the calculated values of $6\pi\eta_1U/E\varepsilon_1\zeta$ range over $b=0.025$–1 for a value of the ratio $b/b'=0.1$, over values of $b=0.25$–10 for $b/b'=1$, and over values of $b=2.5$–100 for $b/b'=10$.

The results for the three viscosity types are shown graphically in Fig. 2. For a thinner (with respect to that in the solution) inner double layer, the conductivity of the fluid is seen to be unimportant, and the curves for the three different values of the

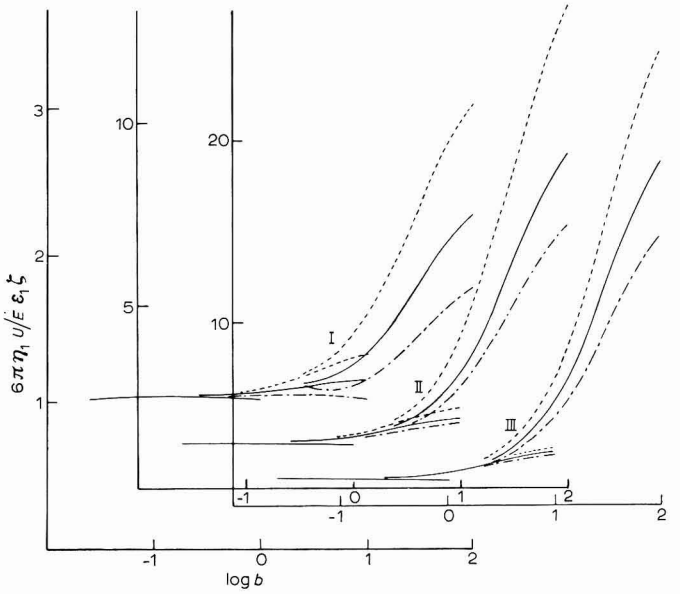

Fig. 2. Plot of $6\pi\eta_1U/E\varepsilon_1\zeta$ as function of b for different values of conductance parameter, λ, according to Booth liquid droplet electrophoresis equation (inner diffuse double layer charge distribution) for the cases: (I) *highly viscous*; (II) *equi-viscous*; (III), *highly fluid* drops. The three sets of curves in each case are, from left to right: (1), $b = 0.1b'$; (2), $b = b'$; (3), $b = 10b'$. λ values: (---), $\frac{3}{8}$; (—), 0; (—·—·), $-\frac{1}{4}$.

conductance parameter nearly coincide. As the inner double layer becomes comparatively thicker, the effect of particle conductivity increases and for $b = 10\ b'$ the $6\pi\eta_1 U/E\varepsilon_1\zeta$ *vs.* log $\varkappa a$ curves for the three values of the conductance parameter, λ, are well separated from one another. The effect of viscosity is seen to be important; as the particle viscosity decreases, the calculated value of $6\pi\eta_1 U/E\varepsilon_1\zeta$ becomes comparatively high, and for $\eta_2 = 0.1\ \eta_1$, the value may even exceed 20 for poorly conducting particles (for the equi-viscous case, see also ref. 8).

APPLICATION OF BOOTH ELECTROPHORESIS EQUATION TO EXPERIMENTAL RESULTS

It is of interest to see how far the Booth equations agree with experimental observations. Among the experimental results recorded in the literature, MOONEY's data[9] appear to be the most suitable for comparison with theory because of the absence of any type of contaminants, which is an essential condition in order that the tiny fluid motion within the drop is not affected. Calculations have been made* for those

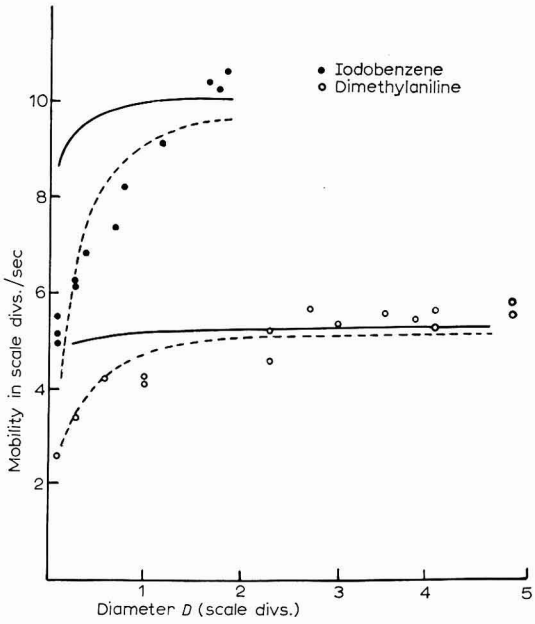

Fig. 3. Calculation of electrophoretic mobility of non-conducting fluid drops according to Booth theory, applied to the mobility data of MOONEY for (●) iodobenzene, (○) dimethylaniline. (———), Interfacial layer charge distribution: dimethylaniline ζ = 110 mV, iodobenzene ζ = 20 mV; (-------) diffuse double-layer charge distribution: dimethylaniline ζ = 14 mV, $b/b' = 6$; iodobenzene ζ = 30 mV, $b/b' = 6$.

oils (dimethylaniline and iodobenzene), for which viscosity data were available[10]. The viscosities at 25° were obtained by interpolation from the values at neighbouring temperatures, and are: $\eta_{\text{Dimethylaniline}} = 0.013$ P, $\eta_{\text{Iodobenzene}} = 0.0156$ P (also $\eta_{\text{water}} = 0.00895$ P). Calculations have been made for both possible types of charge distribution in the

* Details regarding the method for obtaining the data from the published figures, and the calculations, are given in refs. 12 and 6 respectively.

inner fluid; (1) interfacial layer distribution, and (2) diffuse double layer distribution (eqns. (1) and (2), respectively). For the latter type, the double-layer thickness ratio, b/b', is a parameter for which two different suitable values were obtained by trial (result shown for only one value, in each case). Finally, the ζ-potential, the value of which under the experimental conditions is a constant for each particular system investigated, can be considered to be another adjustable parameter for fitting the theoretical curve with the experimental points.

The results are shown graphically in Fig. 3 and show that: (1) an appropriate Booth equation for liquid drop electrophoresis more or less correctly reproduces the general nature of the mobility–particle size curve, for a proper choise of the parameters, b/b' and ζ, and (2) the equation for the interfacial layer type of charge distribution is, surprisingly, less successful than that for the diffuse double layer type of charge distribution. Similar conclusions have also been obtained[11] in respect of MOONEY's data for the electrophoretic mobility of Stanolind droplets. The successful equation (2) is, however, seen to require almost unacceptably small values of ζ; however the equations have been derived under the condition, $e\zeta/kT < 1$.

ACKNOWLEDGEMENTS

The author would like to express his thanks to Professors B. N. GHOSH and S. K. MUKHERJEE and Dr. T. C. ROY for their kind encouragement. The award of a senior fellowship of the C.S.I.R., Government of India, during the tenure of which this work was begun, is gratefully acknowledged.

SUMMARY

The Booth electrophoresis equation for liquid drops has been considered in detail. Illustrative numerical calculations of the mobility function, $6\pi\eta_1 U/E\varepsilon_1\zeta$, for different values of $\varkappa a$ have been made for two different types of charge distribution in the fluid of the drop (*viz.*, the interfacial layer and the diffuse double layer types for certain limiting values of fluid viscosity, and different values of the conductance parameter, λ. The mobility equations for these two types of charge distribution have also been applied to some experimental data of MOONEY.

REFERENCES

1 F. BOOTH, *J. Chem. Phys.*, 19 (1951) 1331.
2 F. BOOTH, *Proc. Roy. Soc. London*, A. 203, (1950) 514.
3 F. BOOTH, *J. Colloid Sci.*, 6 (1951) 549.
4 D. C. HENRY, *Proc. Roy. Soc. London*, A 133, (1931) 106.
5 E. J. W. VERWEY AND K. F. NIESSEN, *Phil. Mag.*, (7) 28 (1939) 435.
6 M. SENGUPTA, D.Phil.(Sc.) Thesis, Calcutta University, 1966, unpublished.
7 F. BOOTH, *Trans. Faraday Soc.*, 44 (1948) 955.
8 M. SENGUPTA, *Indian J. Chem.*, 5 (1967) 648.
9 M. MOONEY, *Phys. Rev.*, 23 (1924) 396.
10 *International Critical Tables*, Vol. VII, McGraw Hill Book Co. Inc., New York, 1930, p. 217.
11 D. N. BISWAS AND M. SENGUPTA, *J. Indian Chem. Soc.*, 44 (1967) 1042.
12 M. SENGUPTA, *J. Electroanal. Chem.*, 18 (1968) 21.

ELECTROANALYTICAL CHEMISTRY AND INTERFACIAL ELECTROCHEMISTRY
Elsevier Sequoia S.A., Lausanne – Printed in The Netherlands

REDOX EQUILIBRIA

PART VI. A COMPLETELY GENERAL TITRATION CURVE EQUATION FOR HOMOGENEOUS AND SYMMETRICAL REDOX REACTIONS

JAMES A. GOLDMAN
Department of Chemistry, Polytechnic Institute of Brooklyn, Brooklyn, New York (U.S.A.)
(Received February 19th, 1968)

INTRODUCTION

Part IV[1] of this series presented the results of extending the development of an idealized[2] titration curve equation, for homogeneous and symmetrical redox reactions, to more realistic situations where the limitation of the presence of only one form of each redox couple in each solution was removed.

Two cases were considered. The first is very common in almost any ordinary titration, *viz.*, the original solution to be titrated initially contains not only the reduced form of the couple—which is to be oxidized by the titrant—but also a finite, rather than zero, concentration of the oxidized form of this couple. The titrant is idealized in that it is assumed to contain only the oxidized form of the corresponding couple. The conclusion was that this causes the potential to be *always more positive throughout* the titration than it would be at corresponding locations in the absence of some initially present oxidized form of the couple to be titrated.

The other case for which results were presented was that occurring often in coulometric titrations where the original solution to be titrated initially contains not only the reduced form which is to be oxidized, but also initially contains some concentration of the reduced form of the *titrant*. The titrant itself is idealized in that it is assumed to contain only the oxidized form of the corresponding couple. The result is that the potential always is *more negative throughout* the titration than it would be at corresponding locations in the absence of some initially present reduced form of the titrant. In this part of the series of papers on redox equilibria (see ref. 1 for listing of earlier parts), the results of an investigation into two more cases will be presented. The first is the case where the solution to be titrated is treated as ideal, *i.e.*, containing only the reduced form of the couple to be oxidized, but the *titrant* is considered to contain not only the oxidized form of the titrant but also the reduced form of this couple. In the coulometric titration situation[1], the reduced form of the couple was assumed to be *in the solution to be titrated*; now, it is to be assumed to be *in the titrant*.

The other case to be considered is the *most general* one where the titrant is assumed to contain both forms of the titrant couple, and the solution to be titrated is assumed to contain both forms of the other couple.

Furthermore, it is found possible to represent readily, by explicit expressions,

the variation with respect to potential during the titration of the equilibrium concentrations of all species represented in the titration equation.

GENERAL RELATIONSHIPS

The general relationships that are applicable for all situations were carefully delineated in Part IV[1] and will be only briefly repeated here.

For homogeneous and symmetrical redox reactions, two reversible redox couples are considered, for which the respective Nernst expressions are

$$E = E_1^{0\prime} - (RT/n_1F) \ln [\mathrm{Red_1}]/[\mathrm{Ox_1}] \quad (1)$$

$$E = E_2^{0\prime} - (RT/n_2F) \ln [\mathrm{Red_2}]/[\mathrm{Ox_2}] \quad (2)$$

where $E^{0\prime}$ represents the formal potential of the indicated couple; R, T, and F have their customary significance, and the concentrations of all species are expressed as molarity.

In the titration of $\mathrm{Red_2}$ *with* $\mathrm{Ox_1}$ as the titrant, the redox titration equation is:

$$n_2\mathrm{Ox_1} + n_1\mathrm{Red_2} = n_2\mathrm{Red_1} + n_1\mathrm{Ox_2} \quad (3)$$

The relationship between the equilibrium constant for this reaction and the formal potentials of the two redox couples is:

$$\Delta E^{0\prime} = E_1^{0\prime} - E_2^{0\prime} = (RT/n_1n_2F) \ln K \quad (4)$$

The progress of the titration is conveniently expressed in terms of the fraction titrated, f, as

$$f = n_1C_1^0V/n_2C_2^0V^0 \quad (5)$$

where C_1^0 represents the molar concentration of $\mathrm{Ox_1}$ in the titrant solution, C_2^0 the initial molar concentration of V^0 ml of solution containing $\mathrm{Red_2}$, and V, the ml of titrant added at any point during the titration. It is also convenient to define additionally the following quantities:

$$\beta = V/(V^0 + V), \quad \beta^0 = V^0/(V^0 + V) \quad (6)$$

so that eqn. (5) may be rewritten as

$$f = n_1C_1^0\beta/n_2C_2^0\beta^0 \quad (6a)$$

CLASSIFICATION OF TITRATION SITUATIONS

Table 1 presents a general classification of the various different titration situations.

Case A is the idealized situation whereas the equations for cases B and D may be expected to resemble each other and be special cases of E.

Case D

The solution to be titrated is considered to contain initially only the reduced form of the redox couple, $\mathrm{Red_2}$, at a concentration C_2^0. The titrant is assumed to contain not only the oxidized form of the other couple, $\mathrm{Ox_1}$, at concentration C_1^0, but also some of the reduced form, $\mathrm{Red_1}$, at a concentration of $C_{\mathrm{Red_1}}^0$.

TABLE 1

CLASSIFICATION OF TITRATION SITUATIONS

Case	$[Red_1]$	$[Ox_2]$	$[Red_2]$	$[Ox_1]$	*at* $f=o$
A	o	o	C_2^0	C_1^0	
B	o	$C_{Ox_2}{}^0$	C_2^0	C_1^0	
C	$C_{Red_1}{}^{0a}$	o	C_2^0	C_1^0	
D	$C_{Red_1}{}^0$	o	C_2^0	C_1^0	
E	$C_{Red_1}{}^0$	$C_{Ox_2}{}^0$	C_2^0	C_1^0	

The representation of the concns. is that previously employed[1,2]. A is the idealized case[2]; cases B and C were previously discussed in Part IV[1].

[a]Normally, at $f=o$, Ox_1 and Red_1 can only be in the titrant, and Ox_2 and Red_2 can only be in the solution to be titrated, but case C is the special case of coulometric titrations where the *reduced* form of the titrant is initially present in *the solution to be titrated* and therefore differs from case D where the reduced form is present in the titrant.

For each couple, the material balance relationships may then be expressed as

$$\beta^0 C_2^0 = [Ox_2] + [Red_2] \tag{7}$$

$$\beta C_1^0 + \beta C_{Red_1}{}^0 = [Ox_1] + [Red_1] \tag{8}$$

Furthermore, it is now stoichiometrically required that throughout the titration

$$[Red_1] - \beta C_{Red_1}{}^0 = (n_2/n_1)[Ox_2] \tag{9}$$

The left-hand side of eqn. (9) represents the concentration of Red_1 produced *via* the titration reaction.

At the normal† equivalence point

$$[Ox_1]^* = (n_2/n_1)[Red_2]^* \tag{10}$$

Division of eqn. (8) by eqn. (7) and substitution of eqns. (1) and (2), and eqn. (6a), into the resulting expression yields after some rearrangement

$$(1+\alpha_1^0)(n_2/n_1)f = \{[Red_1]/[Ox_2]\}\ \{1+k\exp(n_1\psi)/\{1+k\exp(-n_2\psi\} \tag{11}$$

where $\alpha_1^0 = C_{Red_1}{}^0/C_1^0$ and $\psi = (F/RT)(E-E^*)$.

To find an expression for the ratio, $[Red_1]\ /\ [Ox_2]$, during the entire course of the titration, we follow the procedure previously used, by defining Q as

$$Q = [Red_1]/[Ox_1] \tag{12}$$

so that eqn. (8) may be rewritten as

$$[Ox_1] = C_1^0\beta/(1+Q) + C_{Red_1}{}^0\beta/(1+Q) \tag{13}$$

and therefore, by use of eqn. (12)

$$[Red_1] = [Q/(1+Q)]C_1^0\beta + [Q/(1+Q)]C_{Red_1}{}^0\beta \tag{14}$$

Combination of eqn. (14) with eqn. (9) then yields

$$[Ox_2] = (n_1/n_2)[Q/(1+Q)]C_1^0\beta - [(n_1/n_2)/(1+Q)]C_{Red_1}{}^0\beta \tag{15}$$

In eqn. (15), the first term on the right hand side represents the concentration of Ox_2 that is *normally* produced during the titration *via* oxidation of Red_2 according to eqn. (3). This first term has always appeared in equations developed for $[Ox_2]$ in the other categories of titration situations previously discussed[1].

†The normal equivalence point is the point where $E^* = (n_1E_1{}^{0\prime} + n_2E_2{}^{0\prime})/(n_1+n_2)$.

Substitution of eqns. (14) and (15) into eqn. (11), after some rearrangement, results in

$$f=[\{1+k\exp(n_1\psi\}/\{1+k\exp(-n_2\psi\}]\ Q/(Q-\alpha_1{}^0)$$

or

$$f=[\{1+k\exp(n_1\psi\}/\{1+k\exp(-n_2\psi\}]\ 1/\{1-\alpha_1{}^0k\exp(n_1\psi)\} \tag{16}$$

where use has been made of $Q^{-1}=k\exp(n_1\psi)$. When $\alpha_1{}^0=0$, we obtain the familiar idealized form[1,2].

The value of f at which $\psi=0$ is not unity but instead

$$f\ (\text{at}\ \psi=0)=1/(1-\alpha_1{}^0k) \tag{17}$$

so that the potential calculated from $E^*=(n_1E_1{}^{0\prime}+n_2E_2{}^{0\prime})/(n_1+n_2)$, *i.e.*, the normal equivalence potential, always occurs after the equivalence point and the value of f at which it occurs depends not only on the value of $C_{\mathrm{Red}_1}{}^0$, in the titrant, but also on the value of k. Also, when $k\to 0$, $f(\text{at}\psi=0)\to 1$. For any practical titration where $p\Delta E^{0\prime}\geq 300$ mV (and thus $k\leq 2.91\cdot 10^{-3}$), the value of $\alpha_1{}^0$ must exceed 0.344 (for $n_1=n_2=p$) in order for the value of f at $E=E^*$ to differ from unity by more than 0.1%. Furthermore, comparison of eqn. (17) with a similar equation presented[1] for the situation where it is the solution to be titrated that contains both forms of the corresponding couple, shows not unexpected similarities. For example, at $\psi=0, f\to 1$ as $k\to 0$.

Because the value of f is greater than unity at $E=E^*$, the value of E at which $f=1$ will occur at a point where $E-E^*<0$, *i.e.*, the potential at the equivalence point ($f=1$) will be less positive than that obtained from E^*. This conclusion is verified, restricting ourselves to symmetrical reactions, by evaluating eqn. (16) at $f=1$

$$\exp(-p\psi)-\alpha_1{}^0\exp(p\psi)-k\alpha_1{}^0=\exp(p\psi)$$

which may be rearranged to yield

$$(1+\alpha_1{}^0)\exp(2p\psi)+k\alpha_1{}^0\exp(p\psi)-1=0$$

so that

$$p\psi=\ln\left\{\frac{-k\alpha_1{}^0+[(k\alpha_1{}^0)^2+4(1+\alpha_1{}^0)]^{\frac{1}{2}}}{2(1+\alpha_1{}^0)}\right\} \tag{18}$$

from which it is seen that if $\alpha_1{}^0=0$, then $\psi=0$, as expected. When $k=10^{-3}$ and $\alpha_1{}^0=10^{-1}$, $p(E-E^*)=-1.224$ mV at $f=1$ whereas when $k=10^{-3}$ but $\alpha_1{}^0=10^{-2}$, $p(E-E^*)=-0.1278$ mV at $f=1$. For the values of $\alpha_1{}^0$ and k commonly encountered, eqn. (18) may be approximated by $p\psi\simeq -1/2\ \ln\ (1+\alpha_1{}^0)$ when $k\alpha_1{}^0\ll 1$, and therefore it is again seen that $p\psi\to 0$ as $\alpha_1{}^0\to 0$.

Restricting ourselves to symmetrical redox reactions, eqn. (16) may be rearranged to

$$f\,k\exp(-2p\psi)+[f(1-k\alpha_1{}^{0^2})-1]\exp(-p\psi)-k(1+\alpha_1{}^0f)$$

so that

$$p\psi=-\ln\left\{\frac{1-f(1-\alpha_1{}^{0^2}k)+\{[1-f(1-\alpha_1{}^{0^2}k)]^2+4k^2f(1+\alpha_1{}^0f)\}^{\frac{1}{2}}}{2fk}\right\} \tag{19}$$

and when $\alpha_1{}^0 = 0$, eqn. (19) reduces to

$$p\psi = -\ln\left\{\frac{(1-f)+[(1-f)^2+4k^2f]^{\frac{1}{2}}}{2fk}\right\} \tag{20}$$

which is the expression previously[1] derived for the idealized titration curve. Comparison of the arguments of the logarithmic functions in eqns. (19) and (20), respectively, lead to the general conclusion that in the presence of Red_1 in the titrant, the *potential at any point is always more negative* than when the titrant contains only Ox_1.

We now consider the values of f at which $E = E_2{}^{0\prime}$ and $E = E_1{}^{0\prime}$ respectively. From eqn. (16), we obtain

$$f = \tfrac{1}{2}\{1+\exp(-n_1\delta)\}/\{1-\alpha_1{}^0\exp(-n_1\delta)\} \quad \text{at } E = E_2{}^{0\prime}$$

and

$$f = \{2/(1-\alpha_1{}^0)\}/\{1+\exp(-n_2\delta)\} \quad \text{at } E = E_1{}^{0\prime}$$

which may be transformed[1] into

$$f = \tfrac{1}{2}(1+k^{(n_1+n_2)/n_2})/(1-\alpha_1{}^0 k^{(n_1+n_2)/n_2}) \quad \text{at } E = E_2{}^{0\prime}$$

and

$$f = \{2/(1-\alpha_1{}^0)\}/\{1+k^{(n_1+n_2)/n_1}\} \quad \text{at } E = E_1{}^{0\prime}$$

For symmetrical reactions, these equations assume the particularly simple forms

$$f = \tfrac{1}{2}(1+k^2)/(1-\alpha_1{}^0 k^2) \quad \text{at } E = E_2{}^{0\prime}$$

and

$$f = \{2/(1-\alpha_1{}^0)\}/(1+k^2) \quad \text{at } E = E_1{}^{0\prime}$$

demonstrating that the value of f can never be exactly equal to $\frac{1}{2}$ at $E = E_2{}^{0\prime}$, but is always greater than $\frac{1}{2}$, whereas the value of f at $E = E_1{}^{0\prime}$ can be exactly equal to 2 only if $\alpha_1{}^0 = k^2/(1+k^2)$.

Case E. The completely general case

This is the situation in which the titrant contains Red_1 as well as Ox_1, and the solution to be titrated contains Ox_2 as well as Red_2.

The appropriate material balance relationships are

$$\beta^0 C_2{}^0 + \beta^0 C_{Ox_2}{}^0 = [Red_2] + [Ox_2] \tag{21}$$

and

$$\beta C_1{}^0 + \beta C_{Red_1}{}^0 = [Ox_1] + [Red_1] \tag{8}$$

Furthermore, it is now stoichiometrically required that thoughout the titration

$$\{[Red_1] - \beta C_{Red_1}{}^0\} = (n_2/n_1)\ \{[Ox_2] - \beta^0 C_{Ox_2}{}^0\} \tag{22}$$

The left-hand side of eqn. (22) represents the concentration of Red_1 *produced via* the titration reaction, and the right-hand side of the equation represents the concentration of Ox_2 *produced via* the reaction.

At the normal equivalence point

$$[Ox_1]^* = (n_2/n_1)[Red_2]^* \tag{10}$$

Division of eqn. (8) by eqn. (21), and substitution of eqns. (1) and (2), and eqn. (6) into the resulting expression yields after some rearrangement

$$\frac{1+\alpha_1^0}{1+\alpha_2^0}(n_2/n_1)f = \frac{[\mathrm{Red_1}]}{[\mathrm{Ox_2}]}\frac{1+k\exp(n_1\psi)}{1+k\exp(-n_2\psi)} \tag{23}$$

where $\alpha_2^0 = C_{\mathrm{Ox_2}}^0/C_2^0$.

Combination of eqns. (21), (8), and (22) results in

$$\beta C_1^0 - [\mathrm{Ox_1}] = (n_2/n_1)\{\beta^0 C_2^0 - [\mathrm{Red_2}]\} \tag{24}$$

and substitution of $[\mathrm{Ox_1}]$ from eqn. (8) into eqn. (12), yields as before, after some rearrangement

$$[\mathrm{Red_1}] = [Q/(1+Q)]C_1^0\beta + [Q/(1+Q)]C_{\mathrm{Red_1}}^0\beta \tag{14}$$

which may then be substituted into eqn. (22) to obtain

$$[\mathrm{Ox_2}] = (n_1/n_2)[Q/(1+Q)]C_1^0\beta - [(n_1/n_2)/(1+Q)]C_{\mathrm{Red_1}}^0\beta + C_{\mathrm{Ox_2}}^0\beta^0 \tag{25}$$

Since $(1+Q)/Q = 1+k\exp(n_1\psi)$, eqns. (14) and (25) may be rewritten as

$$[\mathrm{Red_1}] = C_1^0\beta/[1+k\exp(n_1\psi)] + C_{\mathrm{Red_1}}^0\beta/[1+k\exp(n_1\psi)] \tag{26}$$

and

$$[\mathrm{Ox_2}] = (n_1/n_2)(C_1^0\beta)/[1+k\exp(n_1\psi)] - [(n_1/n_2)(C_{\mathrm{Red_1}}^0\beta)k\exp(n_1\psi)]/[1+k\exp(n_1\psi)] + C_{\mathrm{Ox_2}}^0\beta^0 \tag{27}$$

Substitution of eqns. (26) and (27) into eqn. (23), yields after considerable rearrangement

$$f = \frac{1+k\exp(n_1\psi)}{1+k\exp(-n_2\psi)}\frac{1+\alpha_2^0}{1-\alpha_1^0 k\exp(n_1\psi)} - \frac{\alpha_2^0[1+k\exp(n_1\psi)]}{1-\alpha_1^0 k\exp(n_1\psi)} \tag{28}$$

Equation (28) is a completely general equation. When $\alpha_1^0 = 0$, eqn. (28) reduces to eqn. (16), *i.e.*, that for case D of Table 1; and when $\alpha_2^0 = 0$, eqn. (28) reduces to the one previously[1] presented for case B of Table I.

It is interesting to evaluate eqn. (28) at $\psi = 0$,

$$f = (1-\alpha_2^0 k)/(1-\alpha_1^0 k) \quad \text{at } \psi = 0. \tag{29}$$

demonstrating that the point at which $\psi = 0$ can occur at $f = 1$ *only* when $\alpha_1^0 = \alpha_2^0$. In other words, the normal equivalence point potential, calculated from $E^* = (n_1 E_1^{0\prime} + n_2 E_2^{0\prime})/(n_1+n_2)$, can occur at $f = 1$ only when the titrant contains a ratio, α_1^0, of $\mathrm{Red_1}$ to $\mathrm{Ox_1}$ which is numerically equal to the *initial* ratio, α_2^0, of $\mathrm{Ox_2}$ to $\mathrm{Red_2}$ in the solution to be titrated. When $\alpha_1^0 < \alpha_2^0$, the value of f at which $\psi = 0$ will be less than unity; and when $\alpha_1^0 > \alpha_2^0$, the value of f at which $\psi = 0$ will be greater than unity. Cases B and D of Table 1 are examples, respectively, of situations where these conditions are somewhat trivially satisfied because then α_1^0 and α_2^0, respectively, are equal to zero.

It is significant to observe from eqn. (29) that as $k \to 0$ (and $\Delta E^{0\prime}$ becomes larger) the value of f at $\psi = 0$ approaches unity regardless of the values of α_1^0 and α_2^0. In other words, for sufficient small values of k (and large values of $\Delta E^{0\prime}$), the value of f can be, with negligible error, equal to unity at $\psi = 0$. For the value of f at

$E=E^*$ to differ from unity by $\pm 0.1\%$, or less, it is necessary that

$$k \leq 10^{-3}/|(\alpha_2^0-\alpha_1^0+10^{-3}\alpha_1^0)|=10^{-3}/|(\alpha_2^0-0.999\,\alpha_1^0)| \simeq 10^{-3}/|(\alpha_2^0-\alpha_1^0)|$$

In any practical titration where $p\Delta E^{0\prime} \geq 300$ mV (and thus $k \leqslant 2.91 \cdot 10^{-3}$), it would be necessary that $|\alpha_2^0-\alpha_1^0| \leqslant 0.344$ in order for the deviation of f from unity to be equal to, or less, than 0.1%.

Because the value of f at which $\psi=0$ is less than unity when $\alpha_1^0<\alpha_2^0$, the value of ψ at which $f=1$ will occur at $\psi>0$. Therefore, in general, when $\alpha_1^0<\alpha_2^0$, the titration curve at each value of f is shifted towards more *positive*—relative to the idealized curve—potential values. When $\alpha_1^0>\alpha_2^0$, the shift is towards more negative values. This conclusion may be verified by investigating the value of ψ at which $f=1$.

For symmetrical reactions, eqn. (28), evaluated at $f=1$ yields after rearrangement

$$(1+\alpha_1^0)\exp(2p\psi)+k(\alpha_1^0-\alpha_2^0)\exp(p\psi)-(1+\alpha_2^0)=0$$

so that

$$p\psi=\ln\left\{\frac{-k(\alpha_1^0-\alpha_2^0)+[k^2(\alpha_1^0-\alpha_2^0)^2+4(1+\alpha_2^0)(1+\alpha_1^0)]^{\frac{1}{2}}}{2(1+\alpha_1^0)}\right\}$$

from which it is easily verfied that $\psi=0$ at $f=1$ only when $\alpha_1^0=\alpha_2^0$. When $\alpha_2^0=0$, eqn. (30) reduces to eqn. (18) and when α_1^0 and α_2^0 are each considerably smaller than unity, eqn. (30) may be approximated by $p\psi \simeq \frac{1}{2}\ln(1+\alpha_2^0)/(1+\alpha_1^0)$ from which it is evident that when $\alpha_1^0<\alpha_2^0$, $p\psi>0$ at $f=1$, whereas when $\alpha_1^0>\alpha_2^0$, then $p\psi<0$ at $f=1$.

Concluding our investigation of the properties of eqn. (28) we consider the values of f at which $E=E_2^{0\prime}$ and $E=E_1^{0\prime}$, respectively. For symmetrical reactions

$$f=\tfrac{1}{2}(1-\alpha_2^0)(1+k^2)/(1-\alpha_1^0k^2) \quad \text{at } E=E_2^{0\prime} \tag{31}$$

and

$$f=2(1-\alpha_2^0k^2)/(1+k^2)(1-\alpha_1^0) \quad \text{at } E=E_1^{0\prime} \tag{32}$$

so that at $E=E_2^{0\prime}$, it is required that $\alpha_1^0=\alpha_2^0(1+k^2)/k^2-1$ in order for f to be equal to $1/2$, whereas at $E=E_1^{0\prime}$, it is necessary that $\alpha_2^0=\alpha_1^0(1+k^2)/k^2-1$ be satisfied in order for f to be equal to 2. The reason why when $\alpha_2^0=0$, f can never equal $1/2$ at $E=E_2^{0\prime}$, is now readily evident, because in order for this to be so, the value of α_1^0 would have to be -1. However, f can easily be equal to 2 at $E=E_1^{0\prime}$; it is only necessary that $\alpha_1^0=k^2/(1+k^2)$, as was concluded earlier. For the case where $\alpha_1^0=0$, *i.e.*, case B, it was concluded[1] (as is immediately evident from the above relationship between α_1^0 and α_2^0) that f could equal $1/2$ at $E=E_2^{0\prime}$ only when $\alpha_2^0=k^2/(1+k^2)$. It is easy to see that f could never equal 2 at $E=E_1^{0\prime}$, because this would require that $\alpha_2^0=-1$. It is interesting to note that the requirement $\alpha_1^0=\alpha_2^0$ which was earlier found sufficient to cause ψ to be equal to 0 at $f=1$ is not sufficient to cause coincidence in the situations now being considered unless $\alpha_1^0=\alpha_2^0=1$!

EQUATIONS EXPRESSING THE CONCENTRATION VARIATION THROUGHOUT THE TITRATION

During the derivation of many of the above equations, expressions have been obtained for the variation during the titration of the equilibrium concentrations of some of the species, for example, eqns. (26) and (27). Substitution of eqns. (26) and

(27) into eqns. (8) and (21), respectively, readily yield equations for $[Ox_1]$ and $[Red]_2$ so that

$$[Red_2]=C_2{}^0\beta^0-(n_1/n_2)C_1{}^0\beta/[1+k\exp(n_1\psi)]+(n_1/n_2)C_{Red_1}{}^0\beta k\exp(n_1\psi)/[1+k\exp(n_1\psi)] \quad (33)$$

$$[Ox_2]=C_{Ox_2}{}^0\beta^0+(n_1/n_2)C_1{}^0\beta/[1+k\exp(n_1\psi)]-[(n_1/n_2)(C_{Red_1}{}^0\beta)k\exp(n_1\psi)]/[1+k\exp(n_1\psi)] \quad (27)$$

$$[Red_1]=C_1{}^0\beta/[1+k\exp(n_1\psi)]+C_{Red_1}{}^0\beta/[1+k\exp(n_1\psi)] \quad (26)$$

$$[Ox_1]=C_1{}^0\beta k\exp(n_1\psi)/[1+k\exp(n_1\psi)]+C_{Red_1}{}^0\beta k\exp(n_1\psi)/[1+k\exp(n_1\psi)] \quad (34)$$

In order to calculate the values of each of these species, generally a value of ψ is selected first and the corresponding value of f is then calculated from eqn. (28); then eqn. (6a) is used to find the value of β corresponding to the selected values of $C_1{}^0$, $C_2{}^0$, V^0, n_1 and n_2. For symmetrical reactions, a value of ψ could be directly calculated for any particular f, and then one could proceed to calculate the concentration values.

The first term on the left-hand side of eqns. (33) and (27) represents the initial concentrations of Red_2 and Ox_2, respectively, corrected for dilution occurring during the titration. The second term on the right-hand side of eqns. (33) and (27) represents the concentration of Ox_2 that is normally produced during the titration *via* oxidation of Red_2, according to the redox reaction, eqn. (3). In eqns. (26) and (34), the first term on the right-hand side of each, represents the concentration, in the solution *being* titrated, of Red_1 and Ox_1, respectively. In the *solution* being titrated, the ratio $[Ox_1]/[Red_1]$ is continually increasing and some of the Red_1 initially present in the titrant is being transformed in the solution into Ox_1. This is represented by the contributions of the second terms on the right-hand side of eqns. (26) and (34).

Equations (33), (27), (26) and (34) are explicit expressions for the equilibrium concentrations throughout the titration of the four species of interest. Especially in the idealized situation where $C_{Red_1}{}^0=0=C_{Ox_2}{}^0$ it is particularly easy to calculate the values of the equilibrium concentrations at any point during the titration. The method presented here may be contrasted with that developed by BISHOP[3,4].

At $\psi=0$, eqns. (33), (27), (26), and (34) reduce to

$$[Red_2]=C_2{}^0\beta^0-(n_1/n_2)C_1{}^0\beta/(1+k)+(n_1/n_2)C_{Red_1}{}^0\beta k/(1+k) \quad (33a)$$

$$[Ox_2]=C_{Ox_2}{}^0\beta^0+(n_1/n_2)C_1{}^0\beta/(1+k)-(n_1/n_2)C_{Red_1}{}^0\beta k/(1+k) \quad (27a)$$

$$[Red_1]=C_1{}^0\beta/(1+k)+C_{Red_1}{}^0\beta/(1+k) \quad (26a)$$

$$[Ox_1]=C_1{}^0\beta k/(1+k)+C_{Red_1}{}^0\beta k/(1+k) \quad (34a)$$

where β and β^0 are to be evaluated at $\psi=0$. From what has been discussed earlier, it is evident that these would be the concentration values at $f=1$ only when $C_{Red_1}{}^0=C_{Ox_2}{}^0$.

Let us continue further and consider the *idealized* titration situation, $C_{Red_1}{}^0=0=C_{Ox_2}{}^0$, then

$$[Red_2]^*=C_2{}^0\beta^0-(n_1/n_2)C_1{}^0\beta/(1+k) \quad (33b)$$

$$[Ox_2]^*=(n_1/n_2)C_1{}^0\beta/(1+k) \quad (27b)$$

$$[Red_1]^*=C_1{}^0\beta/(1+k) \quad (26b)$$

$$[Ox_1]^*=C_1{}^0\beta k/(1+k) \quad (34b)$$

which are the concentrations at the equivalence point. Rewriting eqn. (6a) as $(n_1/n_2)\,C_1{}^0\beta=\beta^0C_2{}^0f$ and using it in these above four equations results in

$$[\mathrm{Red}_2]^*=C_2{}^0\beta^0[1-f/(1+k)]=C_2{}^0\beta^0k/(1+k)$$

$$[\mathrm{Ox}_2]^*=C_2{}^0\beta^0f/(1+k)=C_2{}^0\beta^0/(1+k)$$

because $\psi=0$ at $f=1$ for the idealized titration curve.

The quantitativeness[5,6] of reaction, P^*, is defined as the value of $[\mathrm{Ox}_2]/[\mathrm{Red}_2]$ at the equivalence point so that

$$P^*=[\mathrm{Ox}_2]^*/[\mathrm{Red}_2]^*=1/k \tag{35}$$

and $P^* \to \infty$ as $k \to 0$.

If the relative reaction deficiency (*cf.* ref. 4) is generally defined as $d=[\mathrm{Red}_2]/C_2{}^0\beta^0$, then $d^*=[\mathrm{Red}_2]^*/C_2{}^0\beta^0$ where β^0 is evaluated at the equivalence point. Using eqn. (35) and the definition of d^*, one can verify that $d^*=k/(1+k)$ so that as $k \to 0$ (and $\Delta E^{0\prime}$ becomes larger), $P^* \to \infty$ and $d^* \to 0$, as is to be expected. From eqn. (33) with $C_{\mathrm{Red}_1}{}^0=0$, we obtain

$$d=[\mathrm{Red}_2]/C_2{}^0\beta^0=k\exp(-n_2\psi)/[1+k\exp(-n_2\psi)]$$

so that as the titration proceeds and ψ becomes less negative as the value of ψ approaches zero, $d \to k/(1+k)=d^*$. It is also seen that $d^*<d$ when $\psi \leqslant 0$. However, d^* is not the minimum value of d during the titration because as the equivalence point is passed, ψ becomes positive and therefore, the value of d continues to decrease. The relationship between d^* and P^* can be shown to be $P^*=(1-d^*)/d^*$ so that small values of d^* correspond to large values of P^*.

Let us now investigate the value of P, in general, at $\psi=0$. From eqns. (33a) and (27a) evaluated at $\psi=0$, we obtain

$$P\ (\text{at } \psi=0)=\frac{C_{\mathrm{Ox}_2}{}^0\beta^0(1+k)+(n_1/n_2)C_1{}^0\beta-(n_1/n_2)C_{\mathrm{Red}_1}{}^0\beta k}{C_2{}^0\beta^0(1+k)-(n_1/n_2)C_1{}^0\beta+(n_1/n_2)C_{\mathrm{Red}_1}{}^0\beta k}$$

which may be rewritten as

$$P\ (\text{at } \psi=0)=\frac{C_{\mathrm{Ox}_2}{}^0\beta^0(1+k)+C_2{}^0\beta^0f-C_2{}^0\beta^0f\alpha_1{}^0k}{C_2{}^0\beta^0(1+k)-C_2{}^0\beta^0f+C_2{}^0\beta^0f\alpha_1{}^0k}$$

and into which eqn. (29) is substituted in order to obtain

$$P\ (\text{at } \psi=0)=1/k$$

which is identical with the result, eqn. (35), obtained for the situation where $C_{\mathrm{Ox}_2}{}^0=0=C_{\mathrm{Red}_1}{}^0$. In other words, the value of P at $\psi=0$ depends in general only on the value of k.

Combination of eqn. (33a) with $d\ (\text{at } \psi=0)=([\mathrm{Red}_2]/C_2{}^0\beta^0)_{\psi=0}$ yields

$$d\ (\text{at } \psi=0)=\{1+k-f(1-\alpha_1{}^0k)\}/(1+k)$$

and into which eqn. (29) is substituted to give

$$d\ (\text{at } \psi=0)=k(1+\alpha_2{}^0)/(1+k)$$

which demonstrates that at $\psi=0$ the value of d is dependent upon the value of $\alpha_2{}^0$

whereas the value of P is not. When $\alpha_2{}^0 \rightarrow 0$, then $d \rightarrow k/(1+k)$. Of course, the essential reason why d is dependent upon the value of $\alpha_2{}^0$ is that the normal definition of d was used which does not take into account the presence initially of Ox_2. If d is redefined as $[Red_2]/(C_2{}^0\beta^0+C_{Ox_2}{}^0\beta^0)$, then it will be simply equal to $k/(1+k)$ at $\psi=0$.

In conclusion, the value of $[Ox_1]/[Red_2]$ at $\psi=0$ may be easily derived using eqns. (34a) and (33a) to yield

$$([Ox_1]/[Red_2])_{\psi=0}=C_1{}^0\beta k(1+\alpha_1{}^0)/C_2{}^0\beta^0[1+k-f(1-\alpha_1{}^0k)]$$

where use has been made of eqn. (6a). Substituting the value of f at $\psi=0$ from eqn. (29) leads to

$$([Ox_1]/[Red_2])_{\psi=0}=(n_2/n_1)[(1-\alpha_2{}^0k)/(1-\alpha_1{}^0k)][(1+\alpha_1{}^0)/(1+\alpha_2{}^0)]$$

which demonstrates that the left-hand ratio can never be equal to n_2/n_1 even if $k \rightarrow 0$ unless $\alpha_1{}^0=\alpha_2{}^0$ (*cf.*, eqn. (10)).

SUMMARY

An equation expressing the dependence of f upon E for the redox titration of Red_2 *with* Ox_1 has been presented for the completely general case where the titrant contains the reduced form as well as the oxidized form of the titrant couple, and the solution to be titrated contains the oxidized as well as the reduced form of the other couple. The potential, in general, is shifted toward more *positive* potentials—relative to the idealized titration curve—when the titrant contains a $[Red_1]/[Ox_1]$ ratio that is numerically *less* than the *initial* $[Ox_2]/[Red_2]$ ratio in the solution to be titrated. The potential is shifted toward more *negative* potentials when the titrant contains a $[Red_1]/[Ox_1]$ ratio that is numerically *greater* then the initial $[Ox_2]/[Red_2]$ ratio in the solution to be titrated.

Also presented are equations for the equilibrium concentrations throughout the entire course of the titration of all species comprising the two redox couples. From these, numerical values are readily calculated at any point.

REFERENCES

1 J. A. GOLDMAN, *J. Electroanal. Chem.*, 16 (1968) 47.
2 J. A. GOLDMAN, *J. Electroanal. Chem.*, 11 (1966) 255.
3 E. BISHOP, *Anal. Chim. Acta*, 26 (1962) 397.
4 E. BISHOP, *Anal. Chim. Acta*, 27 (1962) 253.
5 E. BISHOP, *Theory and Principles of Titrimetric Analysis*, in *Comprehensive Analytical Chemistry*, Vol. 1B, edited by C. L. WILSON AND D. W. WILSON, Elsevier, Amsterdam, 1960.
6 I. M. KOLTHOFF AND N. H. FURMAN, *Potentiometric Titrations*, Wiley, New York, 1931, chap. III.

ELECTROANALYTICAL CHEMISTRY AND INTERFACIAL ELECTROCHEMISTRY
Elsevier Sequoia S.A., Lausanne – Printed in The Netherlands

POLAROGRAPHIC WAVE SHAPE OF THE DIMER–MONOMER REDUCTION WITH STRONG ADSORPTION

ROBERT I. GELB
Department of Chemistry, The University of Massachusetts at Boston, Boston, Massachusetts (U.S.A.)
(Received May 1st, 1968)

A treatment of the polarographic characteristics of a dimer–monomer cleavage where specific adsorption was important has recently been discussed[1,2].

$$O = O_{ads} \qquad \text{Ia}$$

$$O_{ads} + ne = 2\,R_{ads} \qquad \text{Ib}$$

The significance of adsorption processes in electrochemistry in general and in the important application discussed by JORDAN AND BEDNARSKI seem to warrant a more detailed analysis than previously reported.

I. THE DIFFUSION, ADSORPTION PROBLEM

1. Assumptions

It will be assumed that both materials, O and R, are strongly adsorbed to the electrode surface and that a Henry's Law isotherm accurately describes the adsorption process.

$$C_O|_{x=0} = \alpha_O \Gamma_O \qquad (1)$$

$$C_R|_{x=0} = \alpha_R \Gamma_R \qquad (2)$$

In addition, the usual assumptions of rapid adsorption and reversible electron transfer processes will be made.

The assumptions place certain restrictions on the value of the Henry's Law constant governing the adsorption and, assuming a *maximum of monolayer coverage*, on the concentration of the electroactive material in the solution bulk.

2. The boundary value problem

The Fick's Law equations which describe diffusion and reaction at the "expanding-plane electrode" that is normally employed to approximate the dropping mercury electrode are listed below.

$$\partial C_O/\partial t = D\partial^2 C_O/\partial x^2 + (2x/3t)\partial C_O/\partial x \qquad (3)$$

$$\partial C_R/\partial t = D\partial^2 C_R/\partial x^2 + (2x/3t)\partial C_R/\partial x \qquad (4)$$

$$D(\partial C_O/\partial x)_{x=0} + D(\partial C_R/\partial x)_{x=0} = \Gamma_O + \Gamma_R \qquad (5)$$

$$C_O = C_O^* \quad \text{as } x \to \infty \qquad (6)$$

$$C_R = O \quad \text{as } x \to \infty \qquad (7)$$

where D is the common value of the diffusion coefficients of O and R and the concentration of material R is expressed in mole-equivalents of O. The other terms have their usual significance.

Because material O is strongly adsorbed to the electrode surface,

$$C_O)_{x=0} < 0.01\, C_O^* \simeq O \tag{8}$$

Equation (3) may be solved by straightforward application of the Laplace transform technique.

$$D(\partial C_O/\partial x)_{x=0} = (7D/3\pi t)^{\frac{1}{2}} C_O^* \tag{9}$$

This is the usual result for diffusion-controlled mass transport to the dropping mercury electrode. Equations (8) and (9) may be combined to allow estimation of α_O in eqn. (1).

The maximum value of Γ_O is that obtained when the potential is situated at the foot of the polarographic wave so that none of material O is lost in electrolysis.

$$\Gamma_{O\,max.} = \int_0^t (7D/3\pi\tau)^{\frac{1}{2}} A(\tau) C_O^* \,d\tau / A(t) \tag{10}$$

where $A(t)$ denotes the area of the electrode.

$$A(t) = kt^{\frac{2}{3}} \tag{11}$$

so that

$$\Gamma_{O\,max.} = (7Dt/3\pi)^{\frac{1}{2}} \cdot (6/7) C_O^* \tag{12}$$

and

$$\alpha_O < 0.01/(7Dt/3\pi)^{\frac{1}{2}} \cdot (6/7) \tag{13}$$

Typically, $D = 5 \cdot 10^{-6}$ cm^{2}sec^{-1}, $t = 3$ sec and $\alpha_O < 0.3$ cm^{-1}. A similar argument shows that a negligible fraction of material R escapes into the bulk of solution if $\alpha_R < 0.3$ cm^{-1}.

Equation (12) allows estimation of the electrode surface coverage. Assuming an effective molecular area of 10 Å^2, complete surface coverage is obtained when the bulk concentration of material O is approximately 0.5 mF.

II. THE WAVE SHAPE

1. The average current

The Nernst equation for the electron transfer process, Ib, takes the form

$$\Gamma_O = \theta \Gamma_R^2 \tag{14}$$

where

$$\theta = \exp[(nF/RT)(E - E^\circ)] \tag{15}$$

and Γ_R is defined in mole-equivalents of O, as before.

Implicit in eqn. (15) is the assumption that α_O/α_R is invariant with the electrode potential. That is, the adsorption of both materials, O and R, are similarly affected by varying the potential of the electrode. The present treatment might be

extended to include potential-dependent adsorption by suitably altering the form of eqn. (15).

The polarographic wave shape may be determined through eqns. (14) and (15) by noting that the total quantity of material adsorbed at the electrode surface at any time during the drop-life (assuming that $\alpha_O < 0.3$ cm^{-1} and $\alpha_R < 0.3$ cm^{-1}) is the same as $\Gamma_{O\,max}$, since the transport of O to the electrode surface is diffusion-controlled and R is so strongly adsorbed that a negligible portion escapes into the bulk of the solution.

$$\Gamma_O + \Gamma_R = \Gamma_{total} = \Gamma_{O\,max} \tag{16}$$

By combining eqns. (9), (12) and (16) and defining

$$\left(\frac{7D}{3\pi}\right)^{\frac{1}{2}} \cdot \tfrac{6}{7} C_O^* = a \tag{17}$$

one obtains:

$$\theta\Gamma_R^2 + \Gamma_R = at^{\frac{1}{2}} \tag{18}$$

Since R is formed only by electrolysis,

$$\Gamma_R = \int_0^t i\,d\tau / A\,(t) \tag{19}$$

The average current during the drop-life is:

$$i = \frac{1}{t}\int_0^t i\,d\tau \tag{20}$$

The result of combining eqns. (18), (19) and (20) is:

$$E = E^0 - (2.303\,RT/nF)\,at^{\frac{1}{2}} - (2.303\,RT/nF)\,\log\{(i/i_d)^2/[1-(i/i_d)]\} \tag{21}$$

where i_d is the diffusion current averaged over the drop-life.

Equation (21) indicates that a plot of $\log [i^2/(i_d - i)]$ *vs.* the potential is linear and displays the Nernstian slope.

2. The instantaneous current

Equation (18) may be solved for the instantaneous current by, solution of the quadratic, differentiation, and subsequent simplification. The result is:

$$i/i_d = \tfrac{6}{7}\{1-(1+4Z)^{\frac{1}{2}} + (11/2)Z\}/\{3Z(1+4Z)^{\frac{1}{2}}\} \tag{22}$$

where $Z = a\theta t^{\frac{1}{2}}$ (23)

Analysis of eqn. (22) is given in Table 1.

TABLE 1

Z	i/i_d	$(i/i_d)^2/[1-(i/i_d)]$	Z	i/i_d	$(i/i_d)^2/[1-(i/i_d)]$
0.1	0.8857	6.862	4.0	0.3270	0.1589
0.2	0.8075	3.387	6.0	0.2762	0.1054
0.4	0.7032	1.667	10.0	0.2213	0.06289
0.6	0.6343	1.100	20.0	0.1619	0.03128
1.0	0.5448	0.6521	40.0	0.1173	0.01558
2.0	0.4286	0.3214			

III. DISCUSSION

Further analysis of the values in Table 1 shows that a plot of log $\{(i/i_d)^2/[1-(i/i_d)]\}$ *vs.* E is not strictly linear; but the plot deviates only slightly from linearity and may be accurately fitted with a straight line. The result of a least-square treatment for $0.1 < i_d < 0.9$ is given by eqns. (19) and (20).

$$E = E^1 - (0.05915/1.019n) \log \{(i/i_d)^2/[1-(i/i_d)]\} \quad (24)$$

where

$$E^1 = E^0 - (0.05915/n)\,(0.1804 + \log at^{\frac{1}{2}}) \quad (25)$$

The rigorous result here is at variance with the results of BEDNARSKI AND JORDAN but does not differ significantly from the Nernstian slope of $0.05915/n$ V/decade derived by them. The present derivation confirms their conclusions about the nature of the dimer-to-monomer reduction mechanism.

ACKNOWLEDGEMENTS

The author wishes to express his thanks to Professor JOSEPH JORDAN of The Pennsylvania State University.

SUMMARY

The theory for the polarographic current–voltage curve for the reversible dimer-to-monomer electrochemical reaction is developed for the case of strong Henry's Law adsorption of both monomer and dimer. The treatment is restricted to partial surface coverage. The limitations of the treatment are evaluated and the results indicate that the plot of log $\{(i/i_d)^2/[1-(i/i_d)]\}$ (where i is the instantaneous current) *vs.* E is not strictly linear. A least-square working equation is developed.

REFERENCES

1 J. JORDAN AND T. M. BEDNARSKI, *J. Am. Chem. Soc.*, 86 (1964) 5690.
2 T. M. BEDNARSKI AND J. JORDAN, *J. Am. Chem. Soc.*, 89 (1967) 1552.

Elsevier Sequoia S.A., Lausanne – Printed in The Netherlands

EQUATIONS OF THE POLAROGRAPHIC WAVES OF SIMPLE OR COMPLEXED METAL IONS

III. THE METAL ION IS REDUCED WITH AMALGAM FORMATION IN THE PRESENCE OF A HYDROLYSABLE LIGAND IN A NON-BUFFERED MEDIUM

MIHAIL E. MACOVSCHI
Institute of Physical Chemistry of Roumanian Academy of Sciences, Bucharest 13 (Roumania)
(Received April 8th, 1968)

This paper deals with the case of a hydrolysable ligand in a non-buffered medium under the same conditions as in the case of a hydrolysable ligand in buffered medium[1], that is:

— the metal ion is reduced with amalgam formation,
— there is a single complex, MX_q, in the solution,
— the ligand is a weak monobasic acid.

The last two conditions simplify the calculation without modifying the interpretation of phenomena. The ligand is assumed to be an acid; for the case of a basic ligand it is sufficient to replace pH by pOH and to make the corresponding changes in the notations in the results obtained.

In contrast with the case of the buffered medium, the condition:

$$C_H^\circ = C_H \tag{1}$$

is not fulfilled; instead we have:

$$C_H^\circ \neq C_H \tag{2}$$

The notations used are:

C_M° — concentration of metal ions at the electrode surface,
C_X° — concentration of free ligand at the electrode surface,
$C_{MX_q}^\circ$ — concentration of complex at the electrode surface,
C_{HX}° — concentration of non-dissociated acid at the electrode surface,
C_H° — concentration of H ions at the electrode surface,
C_{am}° — concentration of amalgam at the drop surface,
C_M — concentration of metal ions in solution,
C_X — concentration of ligand in solution,
C_{MX_q} — concentration of complex in solution,
C_{HX} — concentration of non-dissociated acid in solution,
C_H — concentration of H ions in solution,
C_M^{tot} — total concentration (analytical) of metal in solution,
C_X^{tot} — total concentration of ligand in solution,
$f...$ — corresponding activity coefficients,
$j...$ — corresponding mass currents,
$h...$ — corresponding mass currents constants,
n_M or n — the metallic ion charge.

The concept of "mass current" which has been introduced in a former paper[1] is also used.

The dissociation constants, β_q and α, of the complex and of the acid HX, which are the same in the bulk solution and at the electrode surface are:

$$\beta_q = (c_X f_X)^q \cdot C_M f_M / C_{MX_q} f_{MX_q} = (C_X^\circ f_X)^q \cdot C_M^\circ f_M / C_{MX_q}^\circ f_{MX_q} \quad (3)$$

$$\alpha = C_X f_X \cdot C_H f_H / C_{HX} f_{HX} = C_X^\circ f_X \cdot C_H^\circ f_H / C_{HX}^\circ f_{HX} \quad (4)$$

1. DEDUCTION OF THE POLAROGRAPHIC WAVE EQUATION

If there is no current passing through the solution, the concentrations at the electrode surface and in the bulk solution are the same. In the other case (current passing) some transport phenomena (illustrated in Fig. 1) take place.

The discharge of M ions leads to the appearance of concentration variations, ΔC_M and ΔC_{MX_q}, at the electrode surface. Hence:

$$C_M^\circ = C_M - \Delta C_M \quad (5)$$

$$C_{MX_q}^\circ = C_{MX_q} - \Delta C_{MX_q} \quad (6)$$

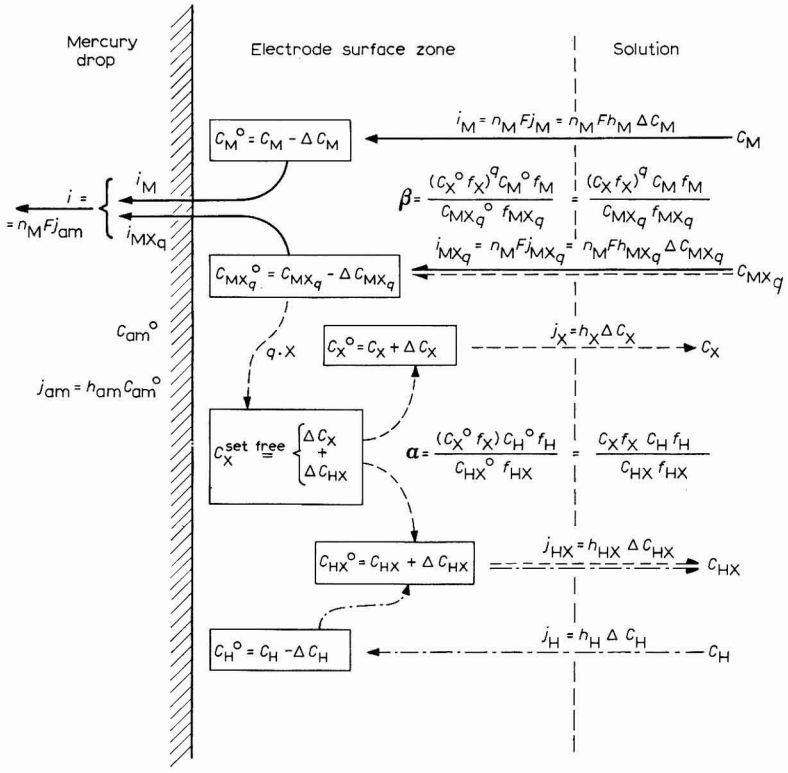

Fig. 1. Distribution of concns., diffusion and ionic equilibrium near the dropping electrode and in the bulk soln. (———) mass circuit of species M; (– – –) mass circuit of species X; (—.—) mass circuit of species H.

Concentrations, C_M° and $C_{MX_q}^\circ$, become greater than C_M and C_{MX_q}, and ions M and MX_q will diffuse out of the solution to the dropping electrode surface. Of the total current, i, passing through the solution, M ions carry the fraction i_M, and the complex MX_q the fraction i_{MX_q}, that is:

$$i = i_M + i_{MX_q} \tag{7}$$

If the concentration gradient is assumed constant and using the concept of "mass current", currents i_M and i_{MX_q} may be written as:

$$i_M = n_M F j_M = n_M F h_M (C_M - C_M^\circ) = k_M (C_M - C_M^\circ) \tag{8}$$

$$i_{MX_q} = n_M F j_{MX_q} = n_M F h_{MX_q} (C_{MX_q} - C_{MX_q}^\circ) \tag{9}$$

Inside the mercury drop, the diffusion of M atoms is described by the relation:

$$j_{am} = h_{am} C_{am}^\circ \tag{10}$$

The complex MX_q is broken by discharge of the metal ions and at the dropping electrode surface excess ligand appears; part of this remains as it is and the rest undergoes the equilibrium:

$$H + X \rightleftharpoons HX \tag{11}$$

to give the non-dissociated acid. In this way the concentration variations, ΔC_X and ΔC_{HX}, appear. Therefore:

$$C_X^\circ = C_X + \Delta C_X \tag{12}$$

$$C_{HX}^\circ = C_{HX} + \Delta C_{HX} \tag{13}$$

Since concentrations C_X° and C_{HX}° are greater than C_X and C_{HX}, X ions and HX molecules will diffuse to the solution:

$$j_X = h_X \Delta C_X \tag{14}$$

$$j_{HX} = h_{HX} \Delta C_{HX} \tag{15}$$

Because of the appearance of the non-dissociated acid, part of the H ions at the electrode surface enter into the HX molecules and therefore:

$$C_H^\circ = C_H - \Delta C_H \tag{16}$$

Therefore, H ions will diffuse from the bulk solution towards the dropping electrode surface:

$$j_H = h_H \Delta C_H \tag{17}$$

It can be seen in Fig. 1 that each of the ionic species, M, X and H, has its own "mass circuit":

(a) M ions, simple or complexed, diffuse from the solution to the dropping electrode, where they are reduced; the metal formed in this way dissolves into the mercury and then diffuses into the drop as amalgam. Obviously, the mass circuit of species M is open. The electric current carried by the metal ions (M or MX_q) is measured by the polarograph, the electric circuit being closed externally;

(b) X ions are carried to the dropping electrode surface as MX_q and return into the solution as X and HX;

(c) H ions are carried from the electrode surface into the solution as HX and return from the solution as H.

For quasi-stationary conditions, the following relations are valid:

$$j_{am} = j_M + j_{MX_q} \qquad q j_{MX_q} = j_X + j_{HX} \qquad j_{HX} = j_H \tag{18}$$

The potential of the dropping electrode, is given by the thermodynamic relation:

$$E = \varepsilon - (RT/n_M F) \ln (C_{am}^{\circ} f_{am} / C_M^{\circ} f_M) \tag{19}$$

The polarographic wave equation, $E = E_{(i)}$, can be obtained if the concentrations are expressed in terms of current. As

$$i = i_M + i_{MX_q} = n_M F (j_M + j_{MX_q}) = n_M F j_{am} = n_M F h_{am} C_{am}^{\circ} \tag{20}$$

E will be given by:

$$E = \varepsilon - (RT/n_M F) \ln (i f_{am} / n_M F h_{am} f_M C_M^{\circ}) \tag{21}$$

Equations (3), (7), (8), (9) and (12) give:

$$i_d - i = n_M F [h_M C_M^{\circ} + h_{MX_q} C_M^{\circ} (C_X + \Delta C_X)^q f_M f_X^q / \beta_q f_{MX_q}] \tag{22}$$

where i_d is the limiting diffusion current:

$$i_d = n_M F (h_M C_M + h_{MX_q} C_{MX_q}) \tag{23}$$

Expressing ΔC_X in terms of current and C_M°, and replacing the value obtained in eqn. (22) results in a relation which allows C_M° to be expressed in terms of current. Combining the expression obtained with eqn. (21) we find the desired polarographic wave equation.

Relations (4), (12), (13) and (16) result in:

$$\alpha = \frac{(C_X^{\circ} C_H^{\circ} - C_X C_H) f_H f_X}{(C_{HX}^{\circ} - C_{HX}) f_{HX}} = \frac{(\Delta C_X C_H - C_X \Delta C_H - \Delta C_X \Delta C_H) f_H f_X}{\Delta C_{HX} f_{HX}} \tag{24}$$

But from eqns. (14), (15), (17) and (18) we have:

$$\Delta C_H = (h_{HX}/h_H) \cdot \Delta C_{HX} \tag{25}$$

$$h_{HX} \Delta C_{HX} = q j_{MX_q} - h_X \Delta C_X \tag{26}$$

Introducing (25) and (26) into (24) and arranging the terms, gives:

$$(h_X \Delta C_X)^2 - (q j_{MX_q} - h_H C_H - h_X C_X - \alpha f_{HX} h_H h_X / f_H f_X h_{HX}) h_X \Delta C_X - q j_{MX_q} (h_X C_X + \alpha f_{HX} h_H h_X / f_H f_X h_{HX}) = 0 \tag{27}$$

It can be seen that in the eqn. (27) coefficients system there is a single change of sign (independent the sign of the ΔC_X coefficient term); consequently, according to Descartes' theorem[2], eqn. (27) has a single, real and positive solution (only the positive value obtained for ΔC_X will have a real physico-chemical significance). This positive solution is:

$$\Delta C_X = \frac{q j_{MX_q}}{h_X} - \tfrac{1}{2} \left(\frac{q j_{MX_q}}{h_X} + C_X + \frac{h_H}{h_X} C_H + \frac{\alpha f_{HX} h_H}{h_{HX} f_H f_X} \right) \times \left[1 - \left| \sqrt{1 - \frac{4 q j_{MX_q} h_H C_H}{h_X^2 (q j_{MX_q}/h_X + C_X + (h_H/h_X) C_H + \alpha f_{HX} h_H / h_{HX} f_H f_X)^2}} \right| \right] \tag{28}$$

Introducing (28) into (22) and taking into account that:

$$j_{MX_q} = i_{MX_q}/n_M F = (i-i_M)/n_M F = \{i-k_M(C_M-C_M^\circ)\}/n_M F \tag{29}$$

results in:

$$\begin{aligned} i_d - i = {} & n_M F h_M C_M^\circ + \frac{h_{MX_q} f_M}{f_q f_{MX_q} h_M} \left(\frac{q f_X}{h_X}\right)^q \\ & \times \left\{ \frac{h_X}{q} C_X + \frac{i-k_M(C_M-C_M^\circ)}{n_M F} - \right. \\ & -\tfrac{1}{2}\left[\frac{i-k_M(C_M-C_M^\circ)}{n_M F} + \frac{h_X}{q} C_X + \frac{h_H}{q} C_H + \frac{\alpha f_{HX} h_H h_X}{q f_H f_X h_{HX}}\right] \\ & \times \left[1 - \left| \left(1 - \frac{4[\{i-k_M(C_M-C_M^\circ)\}/n_M F]\, h_H C_H}{q\left(\frac{i-k_M(C_M-C_M^\circ)}{nF_M} + \frac{h_X}{q} C_X + \frac{h_H}{q} C_H + \frac{\alpha f_{HX} h_H h_X}{q f_H f_X h_{HX}}\right)^2} \right)^{\frac{1}{2}} \right| \right] \Bigg\}^q \\ & \times n_M F h_M C_M^\circ \end{aligned} \tag{30}$$

an equation that relates C_M° to the current. Considering the solution pH (experimentally determined), the concentrations C_M, C_X, C_{HX}, C_H and C_{MX_q} will be calculated by means of the system:

$$\begin{cases} C_X^{tot} = C_X + qC_{MX_q} + C_{HX} \\ C_M^{tot} = C_M + C_{MX_q} \\ \beta_q = (C_X f_X)^q \cdot C_M f_M / C_{MX_q} f_{MX_q} \\ \alpha = C_H f_H C_X f_X / C_{HX} f_{HX} \\ C_H = 10^{-pH} \end{cases} \tag{31}$$

Noting:

$$k_M C_M^\circ = y \tag{32}$$

$$(h_{MX_q} f_M / f_{MX_q} h_M)\,(q f_X / h_X)^q = Q \tag{33}$$

$$f_{HX} h_H h_X / q f_H f_X h_{HX} = Q_a \tag{34}$$

Equation (30) may be written as a function of y:

$$\begin{aligned} \Phi_{(y)} = {} & y \frac{Q}{\beta_q} \left\{ \frac{h_X}{q} C_X + \frac{i+y-k_M C_M}{n_M F} \right. \\ & -\tfrac{1}{2}\left(\frac{i+y-k_M C_M}{n_M F} + \frac{h_X}{q} C_X + \frac{h_H}{q} C_H + \alpha Q_a\right) \\ & \times \left[1 - \left| \left(1 - \frac{4[(i+y-k_M C_M)/n_M F] \cdot h_H C_H}{q\left(\frac{i+y-k_M C_M}{n_M F} + \frac{h_X}{q} C_X + \frac{h_H}{q} C_H + \alpha Q_a\right)^2} \right)^{\frac{1}{2}} \right| \right] \Bigg\}^q \\ & + y + i - i_d = 0 \end{aligned} \tag{35}$$

or in another form:

$$\Phi_{(y)} = y\,\frac{Q}{\beta_q}\left[\frac{h_X}{q}C_X + \tfrac{1}{2}\left(\frac{i+y-k_MC_M}{n_MF} - \frac{h_X}{q}C_X - \frac{h_H}{q}C_H - \alpha Q_a\right)\right.$$
$$+\tfrac{1}{2}\left|\left\{\left(\frac{i+y-k_MC_M}{n_MF} - \frac{h_X}{q}C_X - \frac{h_H}{q}C_H - \alpha Q_a\right)^2\right.\right.$$
$$\left.\left.\left. + \frac{i+y-k_MC_M}{n_MF}\left(\frac{h_X}{q}C_X + \alpha Q_a\right)\right\}^{\frac{1}{2}}\right|\right]^q + y + i - i_d = 0 \qquad (36)$$

It follows that:

$$C_M^\circ = \varphi(C_M^{tot}, C_X^{tot}, \mathrm{pH}, \alpha, \beta_q, f, \ldots, h, \ldots, n_M)/k_M \qquad (37)$$

where φ is the solution of equation (35–36)*. Introducing C_M° obtained in this way into (21) and using the expression of the simple metal ion half-wave potential (written as a function of h):

$$E_{\frac{1}{2}}^M = \varepsilon - (RT/nF)\ln(f_{am}h_M/f_Mh_{am}) \qquad (38)$$

the equation of the polarographic wave is obtained:

$$E = E_{\frac{1}{2}}^M - (RT/nF)\ln(i/\varphi) \qquad (39)$$

2. THE $\Phi_{(y)}$ EQUATIONS DEDUCED IN PREVIOUS PAPERS[1,3] ARE OBTAINED UNDER CORRESPONDING LIMITING CONDITIONS

A. The metal ion is reduced with amalgam formation in the presence of a hydrolysable ligand in buffered medium[1]

The supplementary limiting condition is:

$$h_H \to \infty \qquad (40)$$

In eqn. (35) there appears an indeterminate of "$\infty \cdot 0$" form, which is avoided using L'Hopital's rule**, giving:

$$\Phi_{(y)} = y\,\frac{Q}{\beta_q}\left(\frac{h_X}{q}C_X + \frac{i+y-k_MC_M}{nF}\cdot\frac{\alpha f_{HX}}{\alpha f_{HX} + (h_{HX}/h_X)C_Hf_Hf_X}\right)^q + y + i - i_d = 0 \qquad (41)$$

which is eqn. (38) from ref. 1.

B. The metal ion is reduced with amalgam formation and the ligand is a non-hydrolysable substance[3]

The supplementary limiting condition is:

$$\alpha \to \infty \qquad (42)$$

In eqn. (35) there is again an indeterminate of "$\infty \cdot 0$" form. Using L'Hopital's rule**, eqn. (35) becomes:

$$\Phi_{(y)} = y\ \ (Q/\beta_q)\{(h_X/q)C_X + (i+y-k_MC_M)/nF\}^q + y + i - i_d = 0 \qquad (43)$$

which is identical with relation (27) from ref. 3.

* The demonstration that the real solution, φ, is unique is given in Appendix 1.
** See Appendix 2.

C. The metal ion is reduced with amalgam formation and no complex is formed

The condition that any of the ionic species present in the solution should not form complexes with the metal ion considered, may be expressed in two ways:

$$\beta_q \to \infty \qquad \text{or} \qquad C_X^{tot} = 0 \,. \tag{44}$$

In both cases

$$\Phi_{(y)} = y + i - i_d = 0 \tag{45}$$

The solution to eqn. (45), $\varphi = i_d - i$, introduced into (39), leads to the well-known polarographic wave equation of the simple metal ion[4]:

$$E = E_{\frac{1}{2}}^{M} - (RT/nF) \ln \{i/i_d - i)\} \tag{46}$$

3. DISCUSSION OF THE EQUATION, $\Phi_{(y)} = 0$; EQUATION (35–36)

Discussion of eqn. (35–36) is rather difficult because of its irrational form.

In the previous paragraph it was shown how the equations corresponding to (A) the hydrolysable ligand in buffered medium; (B) the non-hydrolysable ligand; and (C) the simple metal ion, can be obtained from eqn. (35–36). We shall now try to find some other specific aspects of eqn. (35–36).

A. The Lingane-type approximation

The Lingane-type[5] approximation, assumes that the ligand concentration is so high in comparison with the metal ion concentration that the variation of the ligand concentration due to the formation of the complex is negligible, that is:

$$C_X^{tot} \gg q C_M^{tot} \tag{47}$$

This is valid for a non-hydrolysable ligand. If the ligand is involved in equilibrium (11) (the form HX is not active as a ligand), the condition of the Lingane-type approximation will be:

$$C_X \gg q C_M^{tot} \tag{48}$$

But C_X depends on α and C_H. Using the notation:

$$S' = \alpha f_{HX}/(\alpha f_{HX} + C_H f_H f_X) \tag{49}$$

introduced in a previous work[1] and taking into account (31):

$$C_X = C_X^{tot} S' \tag{50}$$

The Lingane approximation assumes also that practically all the metal ion is found in the complex. The above conditions may be expressed mathematically by the following approximate relations:

$$\begin{cases} C_{MX_q} = C_M^{tot} \\ i = i_{MX_q} \gg |y - k_M C_M| \\ C_X^{tot} = C_X + C_{HX} \\ (i/nF) \ll C_X = C_X^{tot} S' \end{cases} \tag{51}$$

In such conditions $\Phi_{(y)}$ becomes:*

$$\Phi_{(y)} = y(Q/\beta_q)\{(h_X/q)C_X{}^{tot}S'\}^q + i - i_d = 0 \tag{52}$$

But relation (52) is identical with relation (53) from ref. 1, in which the case of a hydrolysable ligand in buffered medium is discussed; it follows that under the conditions of the Lingane approximation, the polarographic behaviour of the complex is not influenced by the buffering of the solution (consequently, the discussion from §3b ref. 1 is entirely valid also in the present case).

But the S'-value has a lower limit imposed by the condition:

$$(i/nF) \ll C_X = C_X{}^{tot}S' \tag{53}$$

For S' which is lower than required by relation (53), the limits for which eqn. (52) has been deduced are exceeded and it no longer has a real physical significance.

B. The Buck-type approximation

The conditions for the Buck-type approximation[6] adapted for the present case are:

$$\begin{cases} C_X{}^{tot} \gg qC_M{}^{tot} \\ (i/nF) \ll C_X = C_X{}^{tot}S' \\ |y - k_M C_M|/nF \ll C_X = C_X{}^{tot}S' \end{cases} \tag{54}$$

For $\Phi_{(y)}$, it is found that:**

$$\Phi_{(y)} = y(Q/\beta_q)\{(h_X/q)C_X{}^{tot}S'\}^q + y + i - i_d = 0 \tag{55}$$

a relation that is identical with eqn. (58) of ref. 1. It follows that also in this case the buffering or non-buffering of the solution has no effect on the polarographic behaviour of the complex (discussion of eqn. (55) as a function of S' will be as that from §3c, ref. 1). In this case too, there is a lower limit for S' (relation (53)).

C. The Butler and Kaye-type approximation

This type of approximation involves[6]:

— the concentration of free ligand is practically equal to zero,

— the stability of the complex, MX_q, is great enough for the whole of the metal ion to be in the complex, that is:

$$C_X \approx 0 \qquad i \gg |y - k_M C_M| \tag{56}$$

(α and C_X have corresponding values to satisfy relation (56)). Therefore:

$$\Phi_{(y)} = y\frac{Q}{\beta_q}\left[\tfrac{1}{2}\left(\frac{i}{nF} - \frac{h_H}{q}C_H - \alpha Q_a\right) + \right.$$

$$\left. + \tfrac{1}{2}\left|\left\{\left(\frac{i}{nF} - \frac{h_H}{q}C_H - \alpha Q_a\right)^2 + 4\,\frac{i}{nF}\alpha Q_a\right\}^{\frac{1}{2}}\right|\right]^q + i - i_d = 0 \tag{57}$$

As in eqn. (57) the terms α and C_H appear unrelated to each other (through S'), they will be discussed as separate parameters.

* See Appendix 3.

** The calculation is carried out as for the Lingane-type approximation (see also Appendix 3).

(i) $i/nF \gg \alpha \gg C_H$ — equilibrium (11) is shifted to the left; consequently the phenomena are described by the Butler and Kaye equation for a non-hydrolysable ligand[3]:

$$E = E_{\frac{1}{2}}^{M} + \frac{RT}{nF} \ln \frac{\beta_q f_{MX_q} h_M}{h_{MX_q} f_M} - q \frac{RT}{nF} \ln \frac{q f_X}{h_X} - \frac{RT}{nF} \ln \frac{i^{q+1}}{i_d - i} \tag{58}$$

(ii) $i/nF \gg C_H \gg \alpha$ — from relations (9), (12), (18) and (56) it follows that:

$$i/nF = i_{MX_q}/nF = j_{MX_q} = (j_X + j_{HX})/q = (h_X \Delta C_X + h_{HX} \Delta C_{HX})/q$$
$$= (h_X C_X^\circ + h_{HX} \Delta C_{HX})/q \gg (h_H/q) C_H = (h_H C_H^\circ + h_H \Delta C_H)/q \tag{59}$$

from which:

$$h_X C_X^\circ + h_{HX} \Delta C_{HX} \gg h_H C_H^\circ + h_H \Delta C_H \tag{60}$$

but as:

$$h_X \Delta C_{HX} = h_H \Delta C_H \tag{61}$$

it follows that:

$$h_X C_X^\circ \gg h_H C_H^\circ \tag{62}$$

This means that the quantity of H ions at the electrode surface is very small in comparison with the quantity of ligand liberated from the complex as a consequence of the electrode reaction; therefore the quantity of the non-dissociated acid HX forming is far too small to affect significantly the processes at the electrode surface; the processes develop as if the ligand were a non-hydrolysable substance (relation (58)).

In both cases, (i) and (ii), for $i/nF \gg C_H$, to have meaning, the condition, $i > 0$, must be realised.

(iii) $C_H \gg \alpha \qquad C_H \gg i/nF$

— independently the value of the relation between α and i/nF, i/nF cannot be neglected in comparison with C_H because it results in:

$$\Phi_{(y)} = i - i_d = 0 \ (!) \tag{63}$$

a relation without physico-chemical meaning.

(iv) $\alpha \gg i/nF \qquad \alpha \gg C_H$

— in this situation too, i/nF cannot be neglected; see (iii).

(v) $\alpha \gg i/nF \qquad C_H \gg i/nF$

— see (iii).

(vi) $i/nF \gg C_H \qquad \alpha \gg C_H$

— independent of the relation between i/nF and α (comparable values) the phenomena do not depend upon the solution pH and are described by relation (58).

(vii) $i/nF \gg \alpha \qquad C_H \gg \alpha$

— neglecting α, $\Phi_{(y)}$ becomes:

$$\Phi_{(y)} = y\frac{Q}{\beta_q}\left[\tfrac{1}{2}\left(\frac{i}{nF} - \frac{h_H}{q}C_H\right) + \tfrac{1}{2}\left|\frac{i}{nF} - \frac{h_H}{q}C_H\right|\right]^q + i - i_d = 0 \quad (64)$$

If $(h_H/q)C_H \geqslant i/nF$, $\Phi_{(y)} = i - i_d$; this means that no matter how small α is, it cannot be neglected because the term, $4(i/nF)\alpha Q_a$, is one that ensures the existence of the non-equality:

$$\left|\left\{\left(\frac{i}{nF} - \frac{h_H}{q}C_H - \alpha Q_a\right)^2 + 4\frac{i}{nF}\alpha Q_a\right\}^{\frac{1}{2}}\right| > \left|\frac{i}{nF} - \frac{h_H}{q}C_H - \alpha Q_a\right| \quad (65)$$

If $(h_H/q)C_H < i/nF$, then:

$$\varphi = (i_d - i)\beta_q/Q\{(i/nF) - (h_H/q)C_H\}^q \quad (66)$$

$$E = E_{\frac{1}{2}}^M + \frac{RT}{nF}\ln\frac{\beta_q h_M f_{MX_q}}{f_M h_{MX_q}} - q\cdot\frac{RT}{nF}\ln\frac{qf_X}{h_X} - \frac{RT}{nF}\ln\frac{i\{i - (nFh_H/q)C_H\}^q}{i_d - i} \quad (67)$$

As long as the quantity of released ligand at the electrode is smaller than, or equal to, the quantity of the H ions able to reach the electrode by diffusion from the solution, $(h_H C_H \gg qi/nF)$, the phenomenon is described by relation (57); as soon as the quantity liberated at the electrode exceeds the quantity of the H ions able to reach the electrode surface by diffusion from inside the solution, the phenomenon can be described by not only relation (57), but also by the simpler relation (67); if qi/nF increases so much in comparison with $h_H C_H$ that $i \gg nFh_H C_H/q$, then case (ii) $(i/nF \gg C_H \gg \alpha)$ applies and the phenomenon is described by the Butler and Kaye relation for a non-hydrolysable ligand (relation (58)). In short, relation (67) is intermediate between relations (57) and (58).

4. CONCLUSIONS

The following conclusions can now be drawn. If the ligand is in great excess (Lingane or Buck-type approximation), the buffering or non-buffering of the solution has no effect upon the electrode phenomena, with the condition that α and C_H have such values that relation (53) is realised;

If relation (53) is not realised (the excess of ligand is insufficient, or α and C_H have corresponding values) the buffering of the solution plays a very important role;

For a non-buffered medium, when relation (53) is not satisfied, the equations that describe the phenomena are rather complicated and can only be solved in definite cases;

A simpler form of the equation, $\Phi_{(y)} = 0$, is obtained in the case of Butler and Kaye's approximation; the discussion of the equation obtained in this case shows the effect on the electrode phenomena of the relation between the quantity of ligand liberated at the electrode and the concentration and the diffusion of the H ions.

APPENDIX I

Function $\Phi_{(y)} = 0$ has a single real solution

(a) $\Phi_{(y)}$ has at most only a single real solution.

Function $\Phi_{(y)}$ is defined in the domain $y = 0$, $y = k_M C_M$. $\Phi_{(y)}$'s derivative (the form $\Phi_{(y)}$ from (36) is used) is:

$$\frac{\mathrm{d}\Phi_{(y)}}{\mathrm{d}y} = \frac{Q}{\beta_q}\left[\frac{h_X}{q}C_X+\tfrac{1}{2}(\ldots)+\tfrac{1}{2}|\gamma(\ldots)|\right]^{q-1}$$

$$\times\left\{\frac{h_X}{q}C_X+\tfrac{1}{2}(\ldots)+\tfrac{1}{2}|\gamma(\ldots)|\right.$$

$$\left.+\frac{qy[|\gamma(\ldots)|+(\ldots)+2\{(h_X/q)C_X+\alpha Q_a\}]}{2nF|\gamma(\ldots)|}\right\}+1 \qquad \text{(i)}$$

As:

$$i+y \geqslant |k_M C_M| \qquad \text{(ii)}$$

it follows that:

$$\left|\left\{\left(\frac{i+y-k_MC_M}{nF}-\frac{h_X}{q}C_X-\frac{h_H}{q}C_H-\alpha Q_a\right)^2+4\frac{i+y-k_MC_M}{nF}\left(\frac{h_X}{q}C_X+\alpha Q_a\right)\right\}^{\frac{1}{2}}\right|$$

$$\geq \left|\frac{i+y-k_MC_M}{nF}-\frac{h_X}{q}C_X-\frac{h_H}{q}C_H-\alpha Q_a\right| . \qquad \text{(iii)}$$

As C_X, C_H, C_M, Q, Q_a, β_q and α cannot be negative, relations (ii) and (iii) show that independent y value (on the definition domain):

$$\mathrm{d}\Phi_{(y)}/\mathrm{d}y > 0 \qquad \text{(iv)}$$

Therefore, function $\Phi_{(y)}$ may have, at most, one real solution.

(b) The real solution, φ, does exist.

The function $\Phi_{(y)}$-values at the ends of the interval are:

$$\Phi_{(0)} = i-i_d \leqslant 0 \qquad \text{(v)}$$

$$\Phi_{(k_MC_M)} = k_MC_M\frac{Q}{\beta_q}$$

$$\times\left[\frac{h_X}{q}C_X+\tfrac{1}{2}\left(\frac{i}{nF}-\frac{h_X}{q}C_X-\frac{h_H}{q}C_H-\alpha Q_a\right)\right.$$

$$\left.+\tfrac{1}{2}\left|\left\{\left(\frac{i}{nF}-\frac{h_X}{q}C_X-\frac{h_H}{q}C_H-\alpha Q_a\right)^2+\frac{4i}{nF}\left(\frac{h_X}{q}C_X+\alpha Q_a\right)\right\}^{\frac{1}{2}}\right|\right]^q$$

$$+k_MC_M+i-i_d . \qquad \text{(vi)}$$

Writing:

$$\left[\frac{h_X}{q}C_X+\tfrac{1}{2}\left(\frac{i}{nF}-\frac{h_X}{q}C_X-\frac{h_H}{q}C_H-\alpha Q_a\right)\right.$$

$$\left.+\tfrac{1}{2}\left|\left\{\left(\frac{i}{nF}-\frac{h_X}{q}C_X-\frac{h_H}{q}C_H-\alpha Q_a\right)^2+\frac{4i}{nF}\left(\frac{h_X}{q}C_X+\alpha Q_a\right)\right\}^{\frac{1}{2}}\right|\right]^q =$$

$$=\left(\frac{h_X}{q}C_X\right)^q+\left[\frac{i}{nF}-\frac{h_X}{q}C_X-\frac{h_H}{q}C_H-\alpha Q_a\right.$$

$$\left.-\left|\left\{\left(\frac{i}{nF}-\frac{h_X}{q}C_X-\frac{h_H}{q}C_H-\alpha Q_a\right)^2+\frac{4i}{nF}\left(\frac{h_X}{q}C_X+\alpha Q_a\right)\right\}^{\frac{1}{2}}\right|\right]\cdot P_{q-1} \qquad \text{(vii)}$$

relation (vi) becomes:

$$\Phi_{(k_M C_M)} = k_M C_M \frac{Q}{\beta_q}\left[\frac{i}{nF} - \frac{h_X}{q}C_X - \frac{h_H}{q}C_H - \alpha Q_a - \left|\left\{\left(\frac{i}{nF} - \frac{h_X}{q}C_X - \frac{h_H}{q}C_H - \alpha Q_a\right)^2 + \frac{4i}{nF}\left(\frac{h_X}{q}C_X + \alpha Q_a\right)\right\}^{\frac{1}{2}}\right|\right] \times P_{q-1} + i \geq 0 \quad \text{(viii)}$$

As a function of a parameter i, the $\Phi_{(y)}$'s sign at the ends of the interval vary as following:

$$i = 0 \qquad \Phi_{(0)} < 0 \quad \Phi_{(k_M C_M)} = k_M C_M \frac{Q}{\beta_q}\left[-\frac{h_X}{q}C_X - \frac{h_H}{q}C_H - \alpha Q_a + \left|\left\{\left(-\frac{h_X}{q}C_X - \frac{h_H}{q}C_H - \alpha Q_a\right)^2\right\}^{\frac{1}{2}}\right|\right] P_{q-1} = 0$$

$$0 < i < i_d \qquad \Phi_{(0)} < 0 \quad \Phi_{(k_M C_M)} > 0$$

$$i = i_d \qquad \Phi_{(0)} = 0 \quad \Phi_{(k_M C_M)} > 0 \quad \text{(ix)}$$

It is obvious that on the definition domain, the function $\Phi_{(y)}$ changes its sign, that is, the real solution, φ, does exist.

APPENDIX 2

Taking into account (34), we have from (35):

$$P = \left(\frac{i+y-k_M C_M}{nF} + \frac{h_X}{q}C_X + \frac{h_H}{q}C_H + \frac{\alpha f_{HX} h_H h_X}{q f_H f_X h_{HX}}\right) \times \left[1 - \left|\left(1 - \frac{4\{(i+y-k_M C_M)/nF\}(h_H/q)C_H}{\left(\frac{i+y-k_M C_M}{nF} + \frac{h_X}{q}C_X + \frac{h_H}{q}C_H + \frac{\alpha f_{HX} h_H h_X}{q f_H f_X h_{HX}}\right)^2}\right)^{\frac{1}{2}}\right|\right] = \frac{1 - |\sqrt{(\ldots)}|}{1/(\ldots)}$$

The application of L'Hopital's rule gives:

Case A

$$\lim_{h_H \to \infty} P = \lim_{h_H \to \infty} \frac{-2\,\dfrac{i+y-k_M C_M}{nF} \cdot \dfrac{C_H}{q}}{\left|\left\{\left(\dfrac{i+y-k_M C_M}{nF} + \dfrac{h_X}{q}C_H + \dfrac{h_H}{q}C_H + \dfrac{\alpha f_{HX} h_H h_X}{q f_H f_X h_{HX}}\right)^2 - 4\,\dfrac{i+y-k_M C_M}{nF}\,\dfrac{h_H}{q}C_H\right\}^{\frac{1}{2}}\right|}$$

$$\times \frac{\left(\frac{i+y-k_M C_M}{nF} + \frac{h_X}{q} C_X - \frac{h_H}{q} C_H - \frac{\alpha f_{HX} h_H h_X}{q f_H f_X h_{HX}}\right)}{\left(\frac{C_H}{q} + \frac{\alpha f_{HX} h_X}{q f_H f_X h_{HX}}\right)}$$

$$= +2 \frac{i+y-k_M C_M}{nF} \cdot \frac{C_H}{C_H + (\alpha f_{HX} h_X)/f_H f_X h_{HX}}$$

Consequently:

$$\lim_{h_H \to \infty} \Phi_{(y)} = y \frac{Q}{\beta_q} \left(\frac{h_X}{q} C_X + \frac{i+y-k_M C_M}{nF} - \frac{1}{2} \frac{2 \frac{i+y-k_M C_M}{nF} C_H}{C_H + \alpha \frac{f_{HX} h_X}{f_H f_X h_{HX}}} \right)^q + y + i - i_d$$

$$= y \frac{Q}{\beta_q} \left(\frac{h_X}{q} C_X + \frac{i+y-k_M C_M}{nF} \cdot \frac{\alpha f_{HX}}{\alpha f_{HX} + \frac{h_{HX}}{h_X} C_H f_H f_X} \right)^q + y + i - i_d = 0$$

Case B

$$\lim_{\alpha \to \infty} P =$$

$$\lim_{\alpha \to \infty} \frac{4 \frac{i+y-k_M C_M}{nF} \cdot \frac{h_H}{q} C_H}{\left| \left\{ \left(\frac{i+y-k_M C_M}{nF} + \frac{h_X}{q} C_X + \frac{h_H}{q} C_H + \frac{\alpha f_{HX} h_H h_X}{q f_H f_X h_{HX}} \right)^2 - 4 \frac{i+y-k_M C_M}{nF} \cdot \frac{h_H}{q} C_H \right\}^{\frac{1}{2}} \right|}$$

$$\frac{4 \{(i+y-k_M C_M)/nF\} \; (h_H/q) C_H}{\infty} = 0$$

Consequently:

$$\lim_{\alpha \to \infty} \Phi_{(y)} = y \frac{Q}{\beta_q} \left(\frac{h_X}{q} C_X + \frac{i+y-k_M C_M}{nF} \right)^q + y + i - i_d = 0$$

APPENDIX 3

The radical of expression (36) may be written as:

$$|\psi(\ldots)| = \left| \left\{ \left(\frac{i}{nF} \right)^2 + \left(\frac{h_X}{q} C_X{}^{tot} S' \right)^2 + \left(\frac{h_H}{q} C_H \right)^2 + (\alpha Q_a)^2 + 2 \frac{i}{nF} \frac{h_X}{q} C_X{}^{tot} S' - \right.$$

$$\left. - 2 \frac{i}{nF} \frac{h_H}{q} C_H + 2 \frac{i}{nF} \alpha Q_a + 2 \frac{h_X}{q} C_X{}^{tot} S' \frac{h_H}{q} C_H + 2 \frac{h_X}{q} C_X{}^{tot} S' \alpha Q_a + 2 \frac{h_H}{q} C_H \alpha Q_a \right\}^{\frac{1}{2}} \Bigg| \qquad \text{(i)}$$

The following approximations are then made with eqn. (51) in view:

$$\begin{cases} \{(h_X/q) C_X{}^{tot} S'\}^2 \gg (i/nF)^2 \\ \{(h_X/q) C_X{}^{tot} S'\}^2 \gg |-2 (i/nF) (h_X/q) C_X{}^{tot} S'| \\ 2 (h_X/q) C_X{}^{tot} S' (h_H/q) C_H \gg |-2 (i/nF) (h_H/q) C_H| \\ 2 (h_X/q) C_X{}^{tot} S' \alpha Q_a \gg 2 (i/nF) \alpha Q_a \, . \end{cases} \qquad \text{(ii)}$$

and therefore:

$$|/(...)| = \left|\left\{\left(\frac{h_X}{q}C_X{}^{tot}S'\right)^2 + \left(\frac{h_H}{q}C_H\right)^2 + (\alpha Q_a)^2 + 2\frac{h_X}{q}C_X{}^{tot}S'\frac{h_H}{q}C_H + \right.\right.$$
$$\left.\left. + 2\frac{h_X}{q}C_X{}^{tot}S'\alpha Q_a + 2\frac{h_H}{q}C_H\alpha Q_a\right\}^{\frac{1}{2}}\right| = \frac{h_X}{q}C_X{}^{tot}S' + \frac{h_H}{q}C_H + \alpha Q_a \qquad \text{(iii)}$$

SUMMARY

The investigation of the polarographic wave equations is continued for the case when the metal ion is reduced with amalgam formation in the presence of a hydrolysable ligand in a non-buffered medium. As shown in former papers, the polarographic waves equation of the complex, MX_q, (HX being an weak acid) has the form:

$$E = E_{\frac{1}{2}}{}^M - (RT/nF)\ln(i/\varphi)$$

φ is the solution of a function, $\Phi_{(y)}$, which in the present case has the form:

$$\Phi_{(y)} = y\frac{Q}{\beta_q}\left\{\frac{h_X}{q}C_X + \frac{i+y-k_MC_M}{nF} - \tfrac{1}{2}\left(\frac{i+y-k_MC_M}{nF} + \frac{h_X}{q}C_X + \frac{h_H}{q}C_H + \alpha Q_a\right)\right.$$
$$\left.\times\left[1 - \left|\left(1 - \frac{4\{(i+y-k_MC_M)/nF\}\ h_HC_H}{q\left(\frac{i+y-k_MC_M}{nF} + \frac{h_X}{q}C_X + \frac{h_H}{q}C_H + \alpha Q_a\right)^2}\right)^{\frac{1}{2}}\right|\right]\right\}^q + y + i - i_d = 0$$

where the concentrations refer to the bulk solution and h are the mass-current constants (concept introduced in a former paper). It is shown also how, under corresponding conditions, the equation, $\Phi_{(y)}$, takes the form corresponding to the cases: hydrolysable ligand in buffered medium; non-hydrolysable ligand; or the simple metal ion. The forms of equation $\Phi_{(y)}$ in the case of the Lingane-, Buck- and Butler- and Kaye-type approximation are studied. The effect of the solution buffering on the electrode phenomena is discussed.

REFERENCES

1 M. MACOVSCHI, *J. Electroanal. Chem.*, 18 (1968) 47.
2 A. G. KUROSH, *Kurs vîşei algebrî*, Izd. Nauka, Moskva, 1965, p. 255.
3 M. MACOVSCHI, *J. Electroanal. Chem.*, 16 (1968) 457.
4 J. HEYROVSKÝ AND J. KŮTA, *Tratat de polarografie*, Ed. Acad. R.P.R., p. 118.
5 J. J. LINGANE, *Chem. Rev.*, 29 (1941) 1.
6 R. P. BUCK, *J. Electroanal. Chem.*, 5 (1963) 295.
7 C. G. BUTLER AND R. C. KAYE, *J. Electroanal. Chem.*, 8 (1964) 463.

ELECTROANALYTICAL CHEMISTRY AND INTERFACIAL ELECTROCHEMISTRY
Elsevier Sequoia S.A., Lausanne – Printed in The Netherlands

THE STRUCTURE OF THE DOUBLE LAYER AT ANODICALLY POLARISED MERCURY ELECTRODES IN HYDROXIDE SOLUTIONS

R. D. ARMSTRONG, W. P. RACE AND H. R. THIRSK
School of Chemistry, University of Newcastle upon Tyne, Newcastle upon Tyne, NE1 7RU (England)
(Received February 10th, 1968)

INTRODUCTION

Recent impedance measurements[1,2] have shown that mercury, on anodic polarisation in 1 *M* NaOH solution, dissolves as $Hg(OH)_2$ at such a rate that the exchange current (i_0) for the reaction

$$Hg + 2\ OH^- = Hg(OH)_2 + 2\ e \qquad (1)$$

is too high to be determined. Simultaneously, the double layer capacity (C_{dl}) increases rapidly as the reversible mercuric oxide potential (E_r) is approached. The anodic rise of capacity is of similar magnitude to that observed by SLUYTERS[3–5] in his investigations of mercury in perchloric acid solutions. Potentiostatic measurements[2] in 1 *M* NaOH solution have indicated that at potentials more anodic than +15 mV (E_r), a monomolecular layer of mercuric oxide is formed by the nucleation and subsequent growth of two-dimensional centres. This monolayer is stable on the surface for a small potential region (~8 mV). On further anodic polarisation, a thick layer of mercuric oxide is formed.

The purpose of the present investigation was to examine the properties of this oxide monolayer and to draw comparisons between this system and the extensive work on the platinum/platinum "oxide" system[6–8]. In the present work, the monolayer has also been examined in 10 *M* NaOH, where it was anticipated that the interfacial impedance would be determinable with greater accuracy as a result of the increased conductivity of the solution. In addition to the impedance measurements, the effect of the monolayer on polarographic measurements has also been examined. Finally, the influence of the monolayer on the currents due to redox systems added to 1 *M* NaOH was investigated.

EXPERIMENTAL

Solutions were prepared in triply-distilled water using AnalaR NaOH pellets as received. Mercury was purified by prolonged agitation with nitric acid and then distilled twice *in vacuo*. All glassware was cleaned in chromic–sulphuric acid, and thoroughly rinsed with triply-distilled water. Measurements were made at 25.5°.

The reference electrodes used throughout this work were Hg/HgO electrodes made up in the solution under investigation. The electrodes were prepared in batches of four, and were periodically checked to be within 0.25 mV relative to each other. All potentials quoted are relative to this electrode.

(i) Impedance measurements

Details of the hanging mercury drop electrode (HMDE) and the audio-frequency Wien bridge on which the impedance measurements were made are given elsewhere[9], the cell impedance being measured as a series combination of resistance (R_s) and capacitance (C_s). There are two major difficulties in making measurements accurately on a system of this type.

(a) The very high values of the interfacial capacity (C_s, 2,000 μF cm^{-2}) render important the effects of circuit inductance.

(b) The strong potential-dependence of C_s necessitates very strict and accurate control of the d.c. polarisation.

The former problem is most readily solved by using very small drop areas for the HMDE; a minimum area of 0.005 cm^2 was employed. This necessitated hanging the drop from very finely drawn capillaries to reduce the effects of shielding and electrolyte penetration (the capillary resistance did not affect the results, since this was automatically subtracted out with the solution resistance (R_{so}), before the interfacial impedance was obtained). When such small drops were used, in order to eliminate "thermometer" effects: (a) the temperature was controlled accurately to $\pm 0.05°$ for any individual set of measurements on the same drop and (b) the volume of the mercury reservoir in the syringe was kept to a minimum (less than 1 ml). The areas of the drops were determined to better than 1% by calibration at negative potentials (*e.g.*, -900 mV).

Accurate potential control (± 0.5 mV over several minutes) of the HMDE was achieved by connecting the platinum cylinder counter electrode[9] to a second Hg/HgO reference electrode. Without this procedure the drift in d.c. potential was prohibitive.

The cell impedance was measured at 25 kHz, and at frequencies between 2.5 kHz and 300 Hz at potentials between 0 and 18 mV in 1 *M* NaOH, and -5 and 21 mV in 10 *M* NaOH. The potential region under investigation was always approached from more cathodic potentials because of the irreversibility of the formation of a thick layer of mercuric oxide[2].

An attempt was made to study the impedance of the systems at frequencies between 30 and 100 kHz using the parallel circuit transformer ratio arm bridge described elsewhere[9]. The potential-dependence of the capacitance was found to be similar to that observed using the Wien bridge at 25 kHz. The following experimental difficulties, peculiar to the system, were found to limit severely the accuracy of such radio frequency measurements.

(a) Since the series capacity is very high, a very large blocking capacitor (1,000 μF) was necessary to isolate the polarised cell from the bridge without effectively contributing to the cell impedance. The time taken to charge this capacitor through the necessarily resistive polarising circuit resulted in the overall potential control being slow and unstable.

(b) As in the series circuit measurements, drop areas had to be reduced to

limit the effects of circuit inductance. The increased resistance of the finer capillaries is a serious source of error in parallel circuit measurements, since it cannot be subtracted out with R_{so} as in the series circuit measurements.

It was found practicable to obtain an estimate of the C_{dl}–E relationship in 10 M NaOH by measuring the C_s–E curve on the audio frequency bridge at 25 kHz, using very small drops. This curve was determined at potentials between $-1{,}000$ and $+26$ mV.

(ii) Polarographic measurements

The experimental apparatus described earlier[10] was used with the addition of a sensitive, damped galvanometer in the circuit. Polarograms were recorded at potentials between -20 and $+34$ mV in both solutions. The drop-time was simultaneously recorded and the mercury flow rates were determined. The fact that the monolayer was being formed at about 16 mV was checked by applying a 5-mV a.c. signal (about 1 kHz) to the potentiostat, and displaying the resultant current–voltage ellipse on an oscilloscope. When the potential was swept slowly anodically through that corresponding to monolayer formation, a small sudden change in the dimensions of the ellipse was observed, due to the change in the interfacial impedance. The reverse change was observed if the potential was moved cathodically, as the monolayer was reduced. The monolayer could be formed and reduced in this way several times during the lifetime of a drop, the hysteresis between formation and reduction did not exceed 1 mV.

(iii) Current–voltage curves involving redox systems

The redox systems investigated were

$$O_2 + 2\,H^+ + 2\,e = H_2O_2 \qquad (2)$$

$$S_2O_8^{2-} + 2\,e = 2\,SO_4^{2-} \qquad (3)$$

For these measurements, the cell used contained an upturned mercury drop and a platinum spiral counter electrode; details are given elsewhere[11]. Rapid circulation of the solution past the electrodes was achieved by bubbling presaturated nitrogen through the cell; this gave a diffusion layer thickness of $\sim 10^{-3}$ cm. The d.c. polarisation was applied by means of a potentiostat[10]. The current due to the anodic oxidation of H_2O_2 was studied at potentials from -150 to $+25$ mV when multilayer growth prevented the reaction. The peroxide concentration was estimated (by titration with $KMnO_4$) to be 4.5 mM. The current due to the reduction of 5 mM $K_2S_2O_8$ was observed between -600 and $+25$ mV.

In these investigations, the current due to the dissolution of mercury by reaction (1) was always at least an order of magnitude less than the current arising from the redox process. The reason for not using the polarographic method in making these measurements was to avoid any possible effects due to the time-dependent formation of the monolayer phase on an expanding interphase.

During the course of these measurements, monolayer formation was verified by observing a current–voltage ellipse, as in the polarographic measurements. Also, on multilayer formation, the dimensions of the ellipse became time-dependent as the interfacial impedance increased.

RESULTS

(i) Impedance measurements

To obtain the interfacial impedance, the solution resistance, R_{so}, measured at -900 mV at 25 kHz (where the resistance was frequency-, and potential-independent) was subtracted from the measured R_s-values. The quantities $(R_s - R_{so})$ and C_s were then transformed into their equivalent parallel circuit values, R_p and C_p. The data were analysed assuming that a "Randles circuit"[12] with a negligible charge transfer resistance (R_{ct}) was the appropriate analogue. In this case where $c_0 \ll c_r$

$$R_p = 2\sigma/\omega^{\frac{1}{2}} c_0$$

$$C_p = C_{dl} + c_0/2\sigma\omega^{\frac{1}{2}}$$

where the symbols are defined in the notation section. Thus, for a diffusion controlled electrode process, R_p and C_p are themselves linear functions of $\omega^{-\frac{1}{2}}$ and extrapolate at infinite frequency through the origin and C_{dl}, respectively.

To obtain estimates of the potential-dependence of C_{dl}, and of "c_0", the pseudo-bulk concentration of the dissolving species ($Hg(OH)_2$), the dependences of C_p and R_p on $\omega^{-\frac{1}{2}}$ were examined. In the case of the 1 M solution, the results have also been examined after the method of DE LEVIE[13] by plotting C_p *vs.* $1/\omega R_p$. In the case of 10 M NaOH, however, there was a noticeable time-dependent increase of the observed capacity, which was suspected to arise from the specific adsorption of traces of chloride ion impurity. Since this led mainly to an increasing error in the

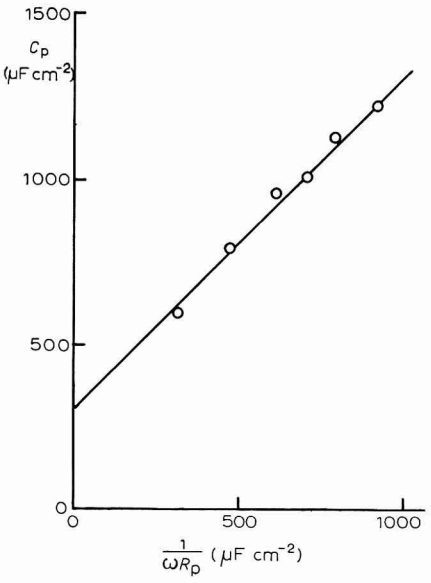

Fig. 1. 1 M NaOH, +18 mV; the dependence of C_p on $1/\omega R_p$; line drawn with unit slope.

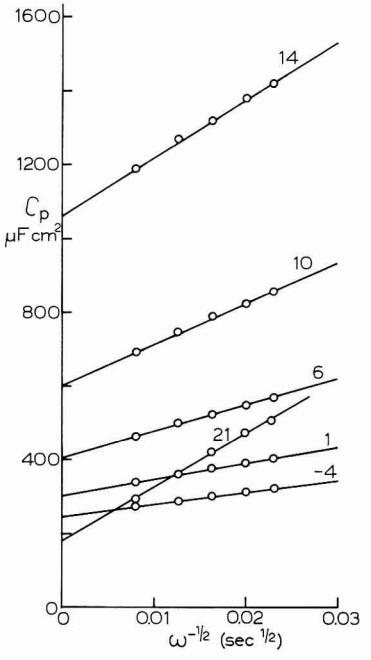

Fig. 2. 10 M NaOH, the dependence of C_p on $\omega^{-\frac{1}{2}}$; numbers above lines denote potentials.

value of C_p, it was considered justifiable to analyse the dependence of R_p on $\omega^{-\frac{1}{2}}$ alone for this solution in the determination of c_0.

Figure 1 shows the dependence of C_p on $1/\omega R_p$ for 1 M NaOH, in the presence of the monolayer. The line drawn through the points has unit slope. Figure 2 shows the dependence of C_p on $\omega^{-\frac{1}{2}}$ for the 10 M solution. The intercepts at infinite frequency of these lines were used as estimates of C_{dl}. Figure 3 shows the dependence on $\omega^{-\frac{1}{2}}$ of R_p for 1 M solution. The extrapolations of the low-frequency data to infinite frequency pass through the origin, as is required for the applicability of this analysis in the determination of c_0. Figure 4 shows the potential-dependence of the concentration of $Hg(OH)_2$ assuming that the diffusion coefficient, D_0, for this species in the 1 M solution is 10^{-5} cm^2 sec^{-1}. The line drawn through the points has a slope of 1 decade/30 mV, confirming that the electrode process involves two electrons. The concentration at the reversible potential is about $2.9 \cdot 10^{-4}$ M, in fair agreement with that predicted from stability constant data[14]. Figure 5 shows the same treat-

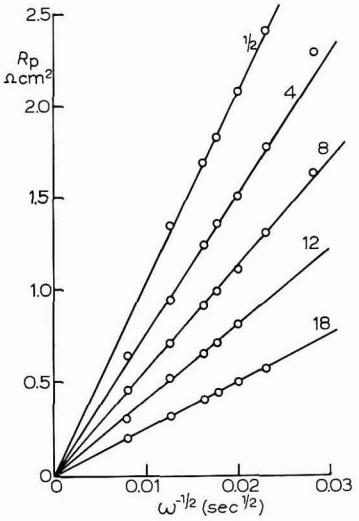

Fig. 3. 1 M NaOH, the dependence of R_p on $\omega^{-\frac{1}{2}}$; numbers above lines denote potentials.

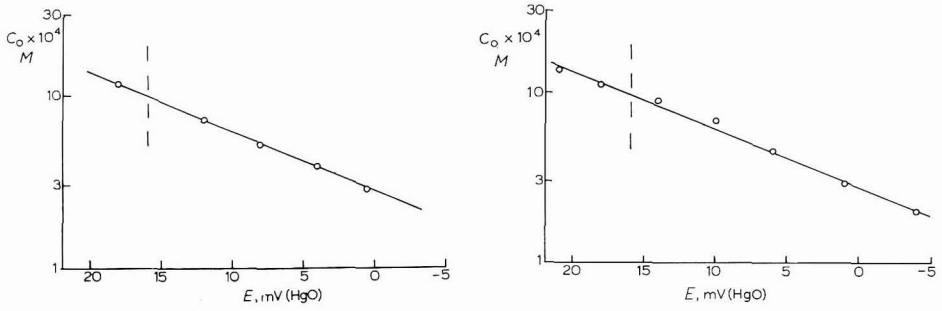

Figs. 4–5. The potential-dependence of the concentration of $Hg(OH)_2$; broken line indicates monolayer formation potential: line drawn through points with slope, 1 decade/30 mV. (4) 1 M, (5) 10 M NaOH.

ment for the 10 M solution, assuming that the value of c_0 at E_r is the same as that for the 1 M solution. This is tantamount to the assumption that D_0 in 10 M NaOH is $8 \cdot 10^{-7}$ cm^2 sec^{-1}. In both Figs. 4 and 5, the monolayer formation potential is shown by a broken line. It may be seen that the concentrations in the presence of the monolayer lie on the same lines as those before the monolayer was present. Also for the 10 M solution it appears that the potential-dependence of c_0 in the monolayer region itself, is identical with that at more cathodic potentials.

The close agreement of the observed potential-dependence of c_0 with the 1 decade/30 mV slope expected for a reversible process confirms that the simple Randles' circuit with a frequency-independent C_{dl} and a negligible R_{et} is a suitable analogue of the impedance of the interface over the frequency range studied. In addition, Figs. 6a and 6b show the classical Randles' treatment of some of the 1 M

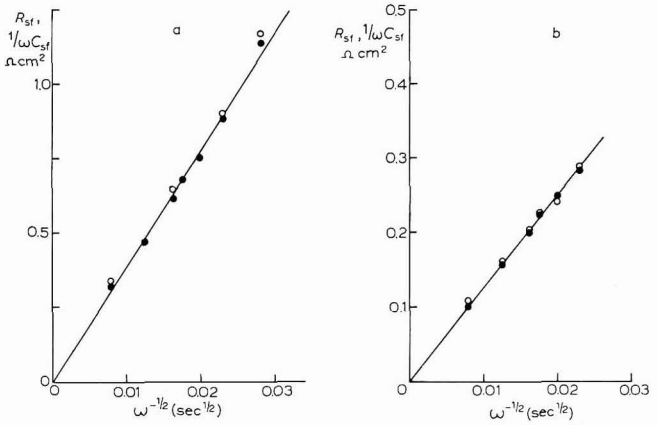

Fig. 6. 1 M NaOH, the dependence of R_{sf} and $1/\omega C_{sf}$ on $\omega^{-\frac{1}{2}}$ (a), +4; (b), +18 mV.

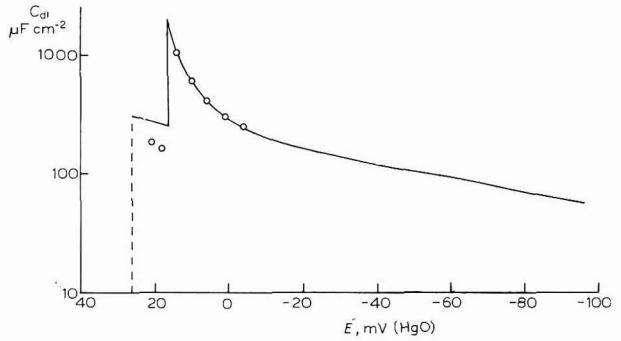

Fig. 7. 10 M NaOH, the potential-dependence of the interfacial capacity (log scale); (o), C_{dl}-values; (—) 25 kHz, C_s-values.

NaOH data. Since within experimental error, R_{sf} lies on the same line as $1/\omega C_{sf}$ *vs.* $\omega^{-\frac{1}{2}}$, it is apparent that both before and after the formation of the monolayer, the contribution from the charge transfer process is negligible, with i_0 greater than 1 A cm^{-2} at 18 mV.

The open circles of Fig. 7 represent the values obtained for C_{dl} from the infinite frequency intercepts of Fig. 2, plotted on a logarithmic scale against potential. The solid curve drawn through the points shows the experimental values of C_s at 25 kHz. A similar result was obtained for the 1 M solution, but owing to the reduced conductivity, the precision of the 25-kHz values in the region of strong anionic specific adsorption was reduced. It is apparent in both solutions that:

(a) before the monolayer is present, the 25-kHz value of C_s is very nearly equal to C_{dl};

(b) when the monolayer forms, the capacity falls by nearly an order of magnitude;

(c) the monolayer capacity is almost two orders of magnitude higher than that associated with previously reported monolayers of mercury salts[15,16].

The highest observed value of C_s at 25 kHz in the 10 M solution was 1900 ± 50 μF cm^{-2}. The actual value of the capacity in the monolayer region was observed to be rather dependent on the potential at which the monolayer was formed. Time-dependence of the capacitance was generally insignificant at potentials up to +20 mV. At potentials greater than +20 mV, both components of the electrode impedance became markedly time-dependent as a result of the formation of the multilayer. The interfacial impedance increased, and C_s approached a low value (less than 4 μF cm^{-2}). This capacity could still be observed to be potential-dependent, probably due to the effect of variations in the field strength on the thickness of the film. The resistive component of the interfacial impedance at 25 kHz was of the order of 0.05 Ω cm^2 in the presence of the multilayer.

The discontinuity of the interfacial impedance on forming the monolayer was clearly observable at frequencies up to 500 kHz, but the accuracy of such measurements was considerably reduced , due mainly to the high value of C_{dl}.

It may be concluded that the presence of a HgO monolayer does not measurably retard reaction (1), which is inhibited only when a thick layer of the oxide is formed. Thus it appears that the monolayer can behave as an ionic conductor.

(ii) Polarographic measurements

Figure 8 shows the polarograms for the two solutions in the potential range −10 to +34 mV. The comparatively large current steps rising at about +24 mV correspond to the formation of a multilayer of HgO. The small step due to monolayer formation in 1 M NaOH is barely discernible on this scale, whereas for the 10 M solution, where the dissolution current is much lower, the monolayer step is quite clear. Figure 9 shows a sensitive representation of the monolayer formation steps. A line of slope, 1 decade/30 mV, is drawn through the points cathodic to monolayer formation, where the current $\bar{\imath}$ corresponds solely to dissolution by reaction (1). The concentration of $Hg(OH)_2$ calculated from such current values using the Ilkovič expression,

$$\bar{\imath} = 6.07\, nm^{\frac{2}{3}} t_1^{\frac{1}{6}} D_0^{\frac{1}{2}} c_0$$

agrees well with the concentrations estimated from the impedance data, using the same assumptions about the respective values of D_0 for the two solutions.

Values of the monolayer charge were calculated using the differences of the current on the monolayer "step" from the extrapolated line of slope, 1 decade/30

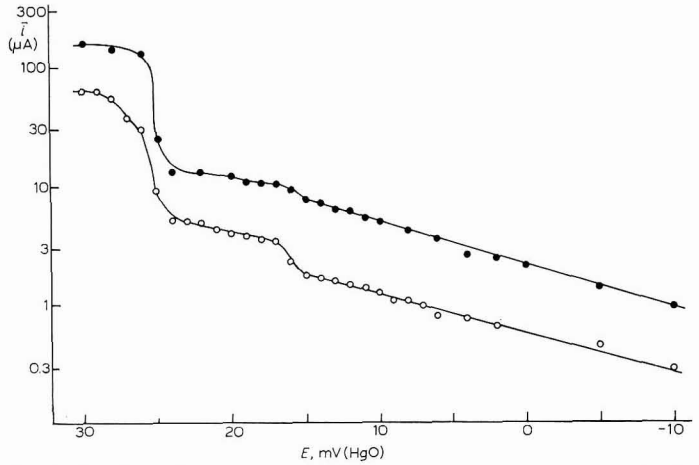

Fig. 8. Anodic polarograms covering potential range from onset of dissolution to multilayer formation. (●), 1 *M* NaOH, flow rate = 0.00181 g sec^{-1}, t_1 = 4.531 sec at +17 mV; (○) 10 *M* NaOH, flow rate = 0.00161 g sec^{-1}, t_1 = 5.330 sec at +17 mV. Straight lines at potentials cathodic to +15 mV drawn with slope, 1 decade/30 mV.

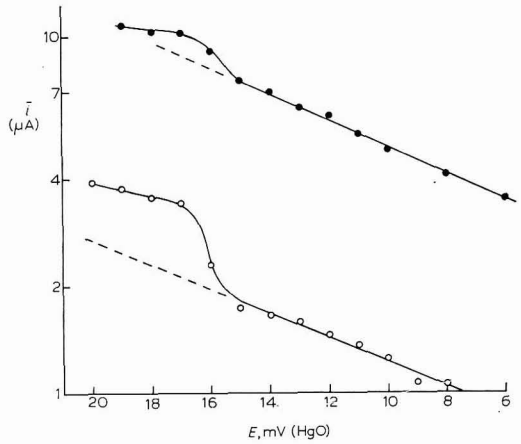

Fig. 9. Anodic polarograms in monolayer potential region. Details as for Fig. 8.

mV; employing the expression[16]

$$\Delta\bar{i} = (4\pi)^{\frac{1}{3}}(3/d)^{\frac{2}{3}} q_{\mathrm{mon}} m^{\frac{2}{3}} t_1^{-\frac{1}{3}}$$

q_{mon} was found to be 200±20 μC cm^{-2} in 1 *M* NaOH, and 193±6 μC cm^{-2} in 10 *M* NaOH, values which are not very different from estimates made previously from potentiostatic current–time transients[2]. The formation charge for the multilayer depends on the conditions of formation, *e.g.*, the time. The multilayer steps of Fig. 8 correspond to about 8 mC cm^{-2} for the 10 *M* solution, and 16 mC cm^{-2} for the 1 *M* solution.

The polarographic data also confirm the conclusion from the impedance data that the monolayer formation appears to have no effect on the dissolution reaction.

Otherwise, a decrease in the mean anodic current at potentials positive to monolayer formation would have been anticipated. In the (more accurate) case of 10 M solution, the current in the presence of the monolayer differs from the line of slope, 1 decade/30 mV, by an amount, $\Delta\bar{\imath}$,which is constant within experimental error throughout the monolayer region.

(iii) Current–voltage curves involving redox systems

Figure 10 shows the potential-dependence of the reduction current of 5 mM $K_2S_2O_8$. The current appeared to be slightly reduced in the monolayer region, but since the fall of current was seen to commence a few millivolts cathodic to monolayer formation, it is unlikely that it reflects any specific effect of the anodic phase.

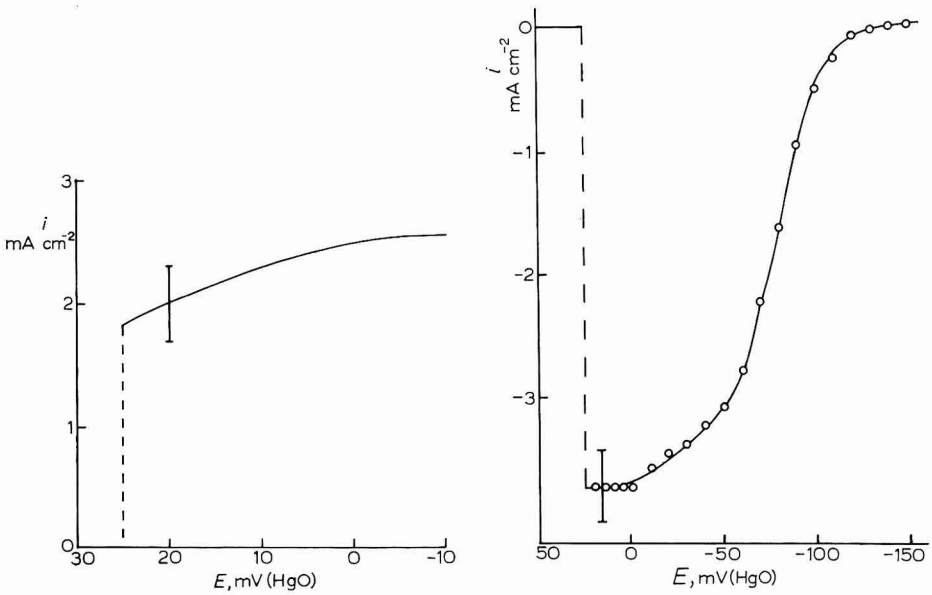

Figs. 10–11. The potential-dependence of the current due to the reduction in 1 M NaOH at a stationary mercury drop of: (10) 5 mM $K_2S_2O_8$, (11) 4.5 mM H_2O_2.

The error bar shows the limits within experimental error that the reduction current could take in the monolayer region; it may be concluded that the monolayer has no drastic effect on the reduction. On approaching the multilayer formation potential, the current became time-dependent, falling through zero. An anodic current was then observed for a time as the thick layer of HgO formed, eventually decreasing again to zero as the layer thickened (simultaneously, the impedance change due to multilayer formation was observed from the current–voltage ellipse, as described earlier).

Figure 11 shows the potential-dependence of the oxidation current of 4.5 mM H_2O_2 in 1 M NaOH. In this case, no change was observed on monolayer formation. On multilayer formation, the anodic current was increased for a while, before falling to zero. Figure 12 shows the potential-dependence of log $(i/(i_d-i))$ for points on the

peroxide oxidation wave, where i_d is the diffusion limited current. The slope of 1 decade/30 mV confirms the reversible behaviour of reaction (2).

The fact that the monolayer has little effect on reactions (2) and (3) shows that its electronic conduction properties are very different from those of monolayers of the mercury salts of some of the barbituric acids[17]. Monolayers of these compounds reduced the currents due to such redox systems to indeterminable levels.

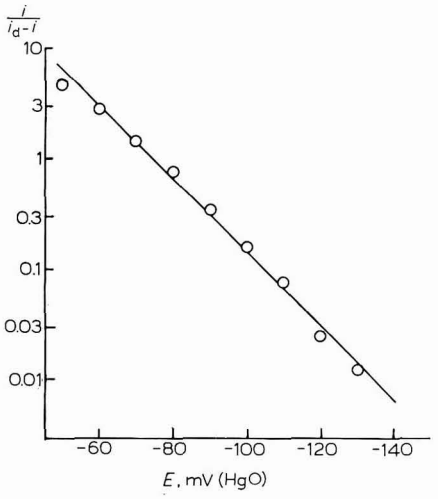

Fig. 12. Analysis of the peroxide oxidation wave shown in Fig. 15. Line drawn with slope, 1 decade/30 mV.

DISCUSSION

(i) The structure of the double layer cathodic to monolayer formation

The values of C_{dl} shown in Fig. 7 must be considered in the light of the recent work of SLUYTERS[18] and DELAHAY[19] concerning the charging of the double layer by "charge separation and recombination" as well as by ionic migration. Since the dissolution reaction (1) is equivalent to a reversible metal–metal ion reaction the modified Lippmann equation which is appropriate is

$$d\gamma + \Gamma_0 d\mu_0 + q_m dE = 0$$

Thus, the slope of the electrocapillary curve

$$-\left(\frac{\partial\gamma}{\partial E}\right) = q_m + 2F\Gamma_0 = q_m'$$

and also

$$C_{dl} = -\left(\frac{\partial^2\gamma}{\partial E^2}\right) = \frac{dq_m}{dE} + \frac{2F d\Gamma_0}{dE}$$

Thus, because of the dissolution reaction, C_{dl} differs from its value "in the absence of the reaction" by the term, $2F d\Gamma_0/dE$. As $Hg(OH)_2$ is uncharged, its adsorption in the diffuse layer will be negligible. It is possible that it is specifically absorbed,

but physically this is probably equivalent to the adsorption of hydroxyl ions. Also, since similar C_{dl} *vs.* E curves occur in the absence of dissolution reactions[20,21], we shall regard $C_{dl}=dq_m/dE$, and account for the variation of C_{dl} with E by assuming the specific adsorption of hydroxyl ions.

Then

$$\frac{dq_m}{dE}=\left(\frac{\partial q_m}{\partial E}\right)_{q_1}+\left(\frac{\partial q_m}{\partial q_1}\right)_E\frac{dq_1}{dE}$$

where q_1 is the charge due to specifically adsorbed hydroxyl ions. Taking x_1 and x_2 as the distances from the metal to the I.H.P. and O.H.P. respectively, and if it is assumed that the infinite imaging model of the double layer[22,23] is appropriate, then

$$\frac{dq_m}{dE}=\left(\frac{\partial q_m}{\partial E}\right)_{q_1}+\frac{x_2-x_1}{x_2}\frac{dq_1}{dE}$$

This is an exact relationship since only macropotentials are involved. It is physically incorrect inasmuch as it ignores the diffuseness of charge in the solution (in ref. 23 it was erroneously stated that the relationship

$$\left(\frac{\partial q_1}{\partial q_m}\right)_{\phi_m}=\frac{x_2}{x_2-x_1}$$

incurs the neglect of the discrete ion potential).

Thus

$$q_1=\frac{x_2}{x_2-x_1}\int_{-\infty}^{E}\left[\frac{dq_m}{dE}-\left(\frac{\partial q_m}{\partial E}\right)_{q_1}\right]dE$$

$$\text{If } \frac{d}{dq_1}\left(\frac{\partial q_m}{\partial E}\right)_{q_1}=0 \quad \text{and} \quad \left(\frac{\partial q_m}{\partial E}\right)_{q_1} \text{ is written } C_b$$

$$q_1=\frac{x_2}{x_2-x_1}\int_{-\infty}^{E}(C_{dl}-C_b)dE$$

For the present system, the following values have been assumed: $x_1=1.5$Å, $x_2=4$Å, $C_b=17$ μF cm^{-2}. Figure 3 shows the potential-dependence of

$$\int_{-\infty}^{E}(C_{dl}-C_b)\,dE$$

It may be seen that the charge, q_1, immediately before the monolayer is formed is 36.8 μC cm^{-2}.

This quantity is fairly insensitive to the value assumed for C_b but very sensitive to the value of the thickness ratio. The value chosen for the latter can be justified in that

(a) experimentally determined values of

$$\left(\frac{\partial q_1}{\partial q_m}\right)_{\phi_m}$$

for other ions are similar[23] and

(b) if half-coverage of the electrode by adsorbed anions was achieved ($q_1>$ 100 μC cm^{-2}) we should expect a peak in the C–E curve, which is not observed.

If hexagonal close packing of singly-charged ions of radius 1.5Å is considered, the charge, q_1, for complete monolayer coverage would be 206 μC cm^{-2}. Therefore, it is seen that in this case the array of adsorbed anions becomes unstable with respect to monolayer phase formation at a coverage of about 18%. This can be compared with the adsorption of S^{2-} on mercury[23] where, within experimental error, unity coverage is found before a monolayer of HgS is formed.

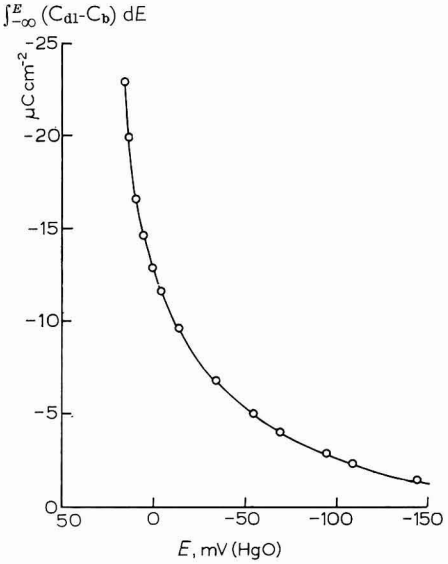

Fig. 13. 10 M NaOH, the potential-dependence of $\int_{-\infty}^{E}(C_{dl}-C_b)\,dE$, determined from integration of the capacity data.

(ii) The structure of the double layer in the presence of the monolayer

The modified Lippmann equation is also appropriate in this potential region, since in the frequency range investigated, reaction (1) proceeds reversibly, (Fig. 1). If $d\Gamma_0/dE$ is also unimportant in this case, then we might expect $C_{dl}=dq_m/dE$ to be near to that anticipated for a parallel plate capacitor one atomic spacing thick. If $\varepsilon_m=5$, and the monolayer thickness is taken as the "b"-spacing of the orthorhombic

TABLE 1

MONOLAYER CAPACITIES FOR THE Hg SALTS OF THE BARBITURIC ACIDS[17]

Compound	*Measured capacity ($\mu F\ cm^{-2}$)*	*No. of C atoms in the 5-position*
Barbituric acid	18	0
Veronal	7	4
Butobarbitone	3.5	6
Amylobarbitone	2.4	7
Rutonal	4.4	7
Phenobarbitone	4.3	8

unit cell of HgO, $=5.52$Å[24], then C_{dl} would be 8.02 μF cm^{-2}. Such agreement between observed and predicted monolayer capacities has indeed been found[17] for the mercury salts of some of the 5-5 substituted barbituric acids (see Table 1). However, in the present system, C_{dl} is found experimentally to be almost two orders of magnitude greater than the predicted value, and it therefore seems necessary to suppose that there are either electronic, or ionic surface states within the monolayer and that the number of these states is a function of potential. Thus, suppose the monolayer structure were as shown in Fig. 14 in the case where $\varepsilon_m = \varepsilon_w$, and the surface states are located at a

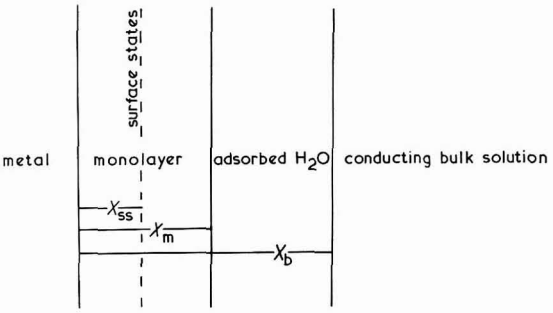

Fig. 14. Representation of surface states within the HgO monolayer.

distance, x_{ss}, from the metal, whilst the (perfectly conducting) solution is located at x_b from the metal. Then, from arguments analogous to those used in discussing the adsorptions of anions:

$$\frac{dq_m}{dE} = \left(\frac{\partial q_m}{\partial E}\right)_{q_{ss}} + \frac{x_b - x_{ss}}{x_b}\frac{dq_{ss}}{dE}$$

where

$$\left(\frac{\partial q_m}{\partial E}\right)_{q_{ss}} \approx \frac{\varepsilon_m}{4\pi x_b}$$

and q_{ss} is the charge due to surface states.

If the simplifying assumptions made above are not appropriate, then we should still expect a relationship of the form

$$\frac{dq_m}{dE} = \left(\frac{\partial q_m}{\partial E}\right)_{q_{ss}} + \frac{B dq^{ss}}{dE}$$

where B is a slowly varying function of both the solution concentration and the potential. Since C_{dl} in the monolayer region was not observed to vary significantly with potential, our results indicate that, within experimental error, dq_{ss}/dE is constant.

There is no indication from the present work whether q_{ss} is electronic or ionic in nature, since the rates of neither redox reactions nor the metal dissolution are affected measurably by the monolayer phase. It is in fact conceivable that the monolayer of HgO is a very good electronic conductor and that the surface states arise from the adsorption of hydroxyl ions on to its surface (Fig. 15). This is a possibility, since the monolayer is acted upon by the considerable pressures due to the electrical

double layer (provided that $q_m \neq 0$) and it is known that under conditions of great pressure[25] the electrical properties of many substances, *e.g.*, iodine, change drastically owing to the breakdown of covalent bonds and the subsequent delocalisation of the electrons. For a "conducting" monolayer, Fig. 15 shows a schematic representation of the system.

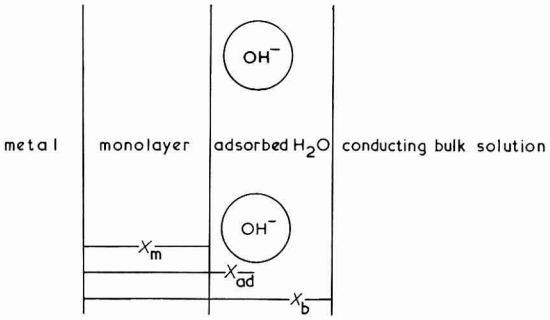

Fig. 15. Possible structure of the double layer if the monolayer were a good electronic conductor.

(iii) Comparison with the behaviour of "platinum oxide"

The properties of the anodic film on platinum electrodes have been extensively reviewed recently[6]. There is little evidence for any reversibly bound oxygen, either adsorbed as the ion OH^-, or as the radical OH, though the latter is frequently postulated as an intermediate in the oxidation of organic substances[26]. However, even on a mercury electrode, the reversible adsorption of OH^- ions is only evident over a small potential range ($\sim$60 mV) before phase formation occurs. A similar phenomenon may occur on a platinum electrode, but in this case the reduced accuracy of measurements and the polycrystalline nature of the electrode material could make positive identification difficult.

The effect of the Pt oxide film on redox reactions has been extensively investigated[7,8,27,28] and it has been found that for simple electron transfer reactions, *e.g.*,

$$Co^{3+} + e = Co^{2+} \qquad (4)$$
$$Fe^{3+} + e = Fe^{2+}$$

the oxide inhibits the rate of the reaction. In the more complex reactions, the oxide has been found to catalyse the de-dimerisation steps, whilst continuing to inhibit electron transfer steps.

Since in the case of mercury, reactions (2) and (3) are not measurably retarded by the thin anodic phase, the electrochemical properties of this phase are considerably different from those of the anodic platinum phase.

It is also of interest to note that whereas the film on platinum is formed markedly irreversibly (hysteresis greater than 200 mV) the HgO monolayer can be formed and removed with a hysteresis of less than 1 mV.

ACKNOWLEDGEMENTS

R.D.A. thanks I.C.I., Ltd., for the provision of a research fellowship, and

W.P.R. thanks the Science Research Council for the provision of a research studentship, during the tenures of which this investigation was undertaken.

NOTATION

C_b Series capacity in the absence of specific adsorption (μF cm^{-2})
C_s measured series capacity (μF cm^{-2})
C_p parallel equivalent capacity (μF cm^{-2})
C_{pf} parallel equivalent faradaic capacity (μF cm^{-2})
C_{sf} series circuit faradaic capacity (μF cm^{-2})
C_{mon} monolayer capacity (μF cm^{-2})
C_w capacity of adsorbed water layer (μF cm^{-2})
C_{ss} series circuit capacity resulting from surface states (μF cm^{-2})
C_{ad} capacity arising from the adsorption of OH^- on the HgO monolayer (μF cm^{-2})
c_0 concentration of oxidised species (M)
c_R concentration of reduced species (M)
d density of mercury (g cm^{-3})
D_O diffusion coefficient of oxidised species (cm^2 sec^{-1})
D_R diffusion coefficient of reduced species (cm^2 sec^{-1})
E potential of Hg electrode (mV or V relative to Hg/HgO in same solution)
E_r reversible mercuric oxide potential
E_z potential of electrocapillary maximum (mV relative to E_r)
F Faraday
i current density (mA cm^{-2})
i_d diffusion-limited current density (mA cm^{-2})
$\bar{i}$ mean anodic polarographic current (μA)
$\Delta\bar{i}$ mean polarographic current due to monolayer formation (μA)
i_0 exchange current density (A cm^{-2})
m mercury flow rate (g sec^{-1})
n number of electrons involved in electrode process
q_{mon} charge necessary to form the HgO monolayer (μC cm^{-2})
q_m charge on the metal (μC cm^{-2})
q'_m apparent charge on metal $= -d\gamma/dE$ (μC cm^{-2})
q_{ss} charge arising from surface states
q_1 charge of specifically adsorbed OH^- ions (μC cm^{-2})
q_{ad} charge of OH^- ions adsorbed on the monolayer
R_s measured series resistance (Ω)
R_{so} solution resistance (Ω)
R_p parallel equivalent interfacial resistance (Ω cm^2)
R_{sf} series equivalent interfacial resistance (Ω cm^2)
R_{ct} charge transfer resistance (Ω cm^2)
R_{ss} resistance associated with surface states
R_{ad} resistance associated with OH^- adsorbed on HgO monolayer
t_1 drop-time (sec)
x distance from metal surface (Å)
γ interfacial tension (dyn cm^{-1})
Γ_0 surface concentration of oxidised species (mole cm^{-2})

ε dielectric constant
θ coverage
μ_0 chemical potential of oxidised species
ω angular frequency (sec^{-1})
σ $=(1000/\sqrt{2})(RT/(n^2F^2)1/\sqrt{D_0}$ (This parameter was incorrectly reproduced in ref. 1).

SUMMARY

The anodically polarised mercury interface in hydroxide solutions has been examined at potentials at which there exists a monomolecular layer of mercuric oxide on the electrode surface. Properties of this phase have been determined from measurements of the electrode impedance and from polarography. The effects of the anodic phase on the mercury dissolution reaction and on redox reactions have been investigated. The data are analysed in terms of the structure of the double layer in the presence of the monolayer, and at potentials cathodic to that of monolayer formation. The electrical properties of the monolayer are found to be in marked contrast to those of the thin anodic phase on platinum.

REFERENCES

1 R. D. ARMSTRONG, W. P. RACE AND H. R. THIRSK, *J. Electroanal. Chem.*, 14 (1967) 143.
2 R. D. ARMSTRONG, M. FLEISCHMANN AND H. R. THIRSK, *J. Electroanal. Chem.*, 11 (1966) 208.
3 J. H. SLUYTERS AND R. DE LEEUWE, *Rec. Trav. Chim.*, 83 (1964) 657.
4 M. SLUYTERS-REHBACH AND J. H. SLUYTERS, *Rec. Trav. Chim.*, 83 (1964) 967.
5 M. SLUYTERS-REHBACH, W. J. A. WOITTIEZ AND J. H. SLUYTERS, *J. Electroanal. Chem.*, 13 (1967) 31.
6 S. GILMAN, *Electroanalytical Chemistry*, Vol. 2, edited by A. J. BARD, Marcel Dekker Inc., New York, 1967.
7 L. MÜLLER, *Electrochim. Acta*, 12 (1967) 557.
8 L. MÜLLER, *J. Electroanal. Chem.*, 13 (1967) 275.
9 R. D. ARMSTRONG, W. P. RACE AND H. R. THIRSK, *Electrochim. Acta*, 13 (1968) 215.
10 R. D. ARMSTRONG, D. F. PORTER AND H. R. THIRSK, *J. Electroanal. Chem.*, 14 (1967) 17.
11 M. FLEISCHMANN AND H. R. THIRSK, *Electrochim. Acta*, 9 (1964) 757.
12 J. E. B. RANDLES, *Discussions Faraday Soc.*, 1 (1947) 11.
13 R. DE LEVIE, *Electrochim. Acta*, 10 (1965) 395.
14 *Stability Constants of Metal Ion Complexes, Chem. Soc. London, Spec. Publ.* No. 17, 1964.
15 R. D. ARMSTRONG AND M. FLEISCHMANN, *J. Polarog. Soc.*, 11 (1965) 31.
16 R. D. ARMSTRONG, M. FLEISCHMANN AND J. W. OLDFIELD, *J. Electroanal. Chem.*, 14 (1967) 235.
17 J. W. OLDFIELD, Ph.D. Thesis, University of Newcastle upon Tyne, 1967.
18 B. TIMMER, M. SLUYTERS-REHBACH AND J. H. SLUYTERS, *J. Electroanal. Chem.*, 15 (1967) 343.
19 P. DELAHAY, *J. Electroanal. Chem.*, 15 (1967) 451.
20 R. D. ARMSTRONG AND M. FLEISCHMANN, *Z. Physik. Chem. Frankfurt*, 52 (1967) 131.
21 R. D. ARMSTRONG, M. FLEISCHMANN AND J. W. OLDFIELD, in the press.
22 C. A. BARLOW AND J. R. MACDONALD, *J. Chem. Phys.*, 40 (1964) 1535.
23 R. D. ARMSTRONG, D. F. PORTER AND G. R. THIRSK, *J. Electroanal. Chem.*, 16 (1968) 219.
24 K. L. AURIVILLIUS, *Acta Chem. Scand.*, 15 (1961) 393.
25 W. PAUL AND D. M. WARSCHAUER, *Solids under Pressure*, McGraw-Hill, New York, 1963.
26 B. J. PIERSMA AND E. GILEADI, *Modern Aspects of Electrochemistry*, Vol. 4, edited by J. O'M. BOCKRIS, Plenum Press, New York, 1966, p. 47.
27 L. MÜLLER AND L. N. NEKRASOV, *Zh. Fiz. Khim.*, 38 (1964) 1655.
28 L. MÜLLER AND L. N. NEKRASOV, *Electrochim. Acta*, 9 (1964) 1015.

ELECTROANALYTICAL CHEMISTRY AND INTERFACIAL ELECTROCHEMISTRY
Elsevier Sequoia S.A., Lausanne – Printed in The Netherlands

KINETICS OF ANODIC OXIDATION OF ADSORBED FILMS FORMED ON PLATINIZED PLATINUM IN METHANOL, FORMIC ACID AND CARBON DIOXIDE SOLUTIONS

V. N. KAMATH AND HIRA LAL
Department of Chemistry, Indian Institute of Technology, Bombay 76 (India)
(Received April 2nd, 1968)

It has been shown in a previous communication[1] that the adsorbed films formed on platinized platinum in methanol, formic acid and CO_2 solutions are closely similar to each other and consist essentially of a species having the composition, HCO. A small amount of COOH radicals may also be present. BREITER[2] is, however, of the view that the species adsorbed from methanol, formaldehyde and formic acid solutions has a likely net compositon, $H_2C_2O_3$, corresponding, in effect, to the presence of HCO and COOH radicals in equivalent amounts.

Irrespective of the exact nature and relative extent of the species adsorbed, it appears to be generally agreed that these adsorbed films are similar to each other and therefore the kinetics of anodic oxidation of these adsorbed films should also be closely similar. Tafel slopes of approximately 60 mV have been reported for the anodic oxidation of films adsorbed from methanol[3,4] and formic acid[5] in sulfuric acid solutions. The present communication throws further light on the electrochemical properties of films adsorbed on platinized platinum from methanol, formic acid and CO_2 solutions.

EXPERIMENTAL

Details of the platinized platinum electrodes, experimental procedure for the formation of the adsorbed films, and the reagents used, have already been given[1]. KCl, KBr and Na_2SO_4, additionally required for the present studies, were analytical-grade reagents and were recrystallized before use. All studies were made at $25 \pm 2°$; all potentials (φ_r) refer to the reversible hydrogen electrode in the same solution.

A significant feature of the studies reported in the present communication is the effect of chloride (and bromide) ions on the oxidation of the adsorbed species. Although quantitative data are not available, it is well-known that chloride and bromide ions inhibit the dissociative adsorption and oxidation of alcohols[4,6,7]. In our own experiments with methanol solutions in 1 *N* HCl, we found that, even with relatively small anodic currents, it was not possible to attain stable potentials. The electrode potential continued to shift in the anodic direction until eventually it went over to the oxygen region. A similar effect was noticed in formic acid oxidation.

It seems, therefore, that chloride ions seriously interfere with the dissociative adsorption of methanol and formic acid on platinum. In view of this, the adsorbed films were formed in 1 *N* H_2SO_4 containing the organic (0.5 *M*) under conditions of steady state polarization in the Tafel region. The cell was then freed of dissolved organ-

ic by repeated washing with 1 N H_2SO_4 or any other test solution. This procedure had the advantage that the same film, formed under conditions likely to be met in a practical fuel cell, was exposed to different environments, and their effect on the anodic oxidation of the adsorbed species could be studied.

It has been shown earlier[1] that the reductive adsorption of CO_2 is not significantly hindered by the presence of chloride ions in solution. In this case also, however, the adsorbed film was formed from 1 N H_2SO_4 saturated with CO_2 at a constant potential ($\varphi_r = 100$ mV). After the current required to maintain the potential constant had fallen to an insignificantly small value, the dissolved CO_2 was removed by bubbling nitrogen; the solution was subsequently replaced by the test solution. The charging curve for the oxidation of such a film in a chloride solution was practically identical with that for the film formed in the chloride solution itself.

Kinetic parameters for the anodic oxidation of the adsorbed species were evaluated from the anodic charging curves. The apparent current density normally used was 0.1 mA/cm^2. For evaluating Tafel slopes, charging curves were taken at different current densities in the range 0.025–0.2 mA/cm^2. From the charging curves, Tafel plots could be readily constructed for various constant coverages. The coefficient, K ($=Q_M/Q_{SH}$), was taken as a measure of coverage with the organic; it decreased in the course of the anodic oxidation of the adsorbed organic. The value of K at any point on the charging curve could be evaluated from the anodic charge density, Q_M, required for the oxidation of the adsorbed organic still present on the electrode, and the charge density, Q_{SH}, required to ionize a monolayer of adsorbed hydrogen in the absence of the adsorbed organic*. This procedure for evaluating Tafel slopes at constant coverage with the adsorbed organic is an improvement on the earlier procedure[3–5] in which Tafel plots corresponded to the initial region of the plateau in the charging curves taken in the presence of the adsorbed organic. A similar procedure was followed in studies on the effect of pH and chloride concentration on the oxidation of the adsorbed films.

RESULTS

Acid sulfate solutions

Typical Tafel plots are shown in Fig. 1 for the anodic oxidation of "reduced CO_2". The plots are linear and have a slope essentially similar for the three films studied (Table 1). Within the limits of accuracy of the measured Tafel slopes ($\pm$ 10 mV), the slopes were practically independent of coverage in the range of K-values 0.1–0.7. In general, however, the Tafel slopes were somewhat larger than the value of about 60 mV reported earlier for methanol[3,4] and formic acid[5] films in sulfuric acid solutions.

Experiments at various pH-values in the acid pH range (0.4–2.7) showed that the φ_r potential remained practically independent of pH; the charging curves obtained at various pH-values were virtually identical with each other. In other words, the electrode potential, φ, against a fixed reference electrode such as the normal hydrogen electrode, decreased by approximately 60 mV per unit increase of pH of the solution. The effect of pH is therefore analogous to that reported earlier[3,4] for the methanol film.

* The coverage with the organic should strictly be expressed by $\theta_m = K/K_{max}$. Since the maximum value of K is about 0.9, $\theta_m \approx K$. The evaluation of K as a measure of coverage with the adsorbed organic is, however, less ambiguous than that of θ_m.

TABLE 1

KINETIC PARAMETERS FOR THE ANODIC OXIDATION OF METHANOL, FORMIC ACID AND "REDUCED CO_2" FILMS ON PLATINIZED PLATINUM

	Medium	*Total concn. (N)*	*"CH_3OH" (mV)*	*"HCOOH" (mV)*	*"Reduced CO_2" (mV)*
$(\partial\varphi_r/\partial \log i)_{\theta_M}$	H_2SO_4	1.0	62–70	66–84	72–76
	H_2SO_4	0.1	68–72	—	62–70
	HCl	1.0	120–123	112–132	130
	HCl	0.1	—	—	108–116
	HCl + H_2SO_4	0.005 + 0.995	—	—	100–105 (K<0.5) 65–75 (K>0.6)
$(\partial\varphi_r/\partial \mathrm{pH})_{\theta_M,i}$	H_2SO_4 + Na_2SO_4	1.0	≃0	≃0	≃0
	HCl + KCl	1.0	≃−25	—	≃−30
$(\partial\varphi_r/\partial \log C_{Cl^-})_{\theta_M,i}$	HCl + H_2SO_4	1.0	52–57	45–62	47–55

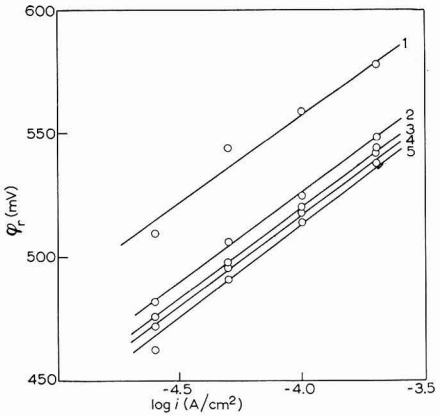

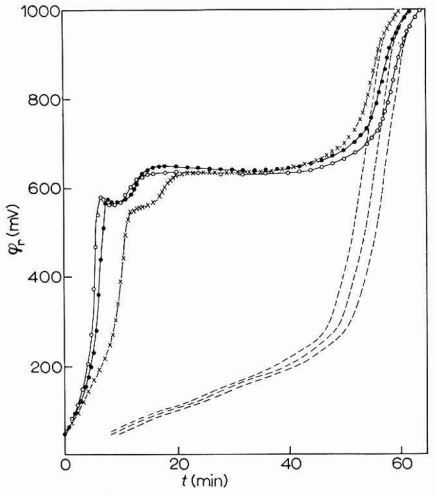

Fig. 1. Tafel plots for oxidation of "reduced CO_2" films on platinized platinum in 1 N H_2SO_4 at K-values: (1) 0.1; (2), 0.2; (3), 0.3; (4) 0.5; (5), 0.7.

Fig. 2. Charging curves for anodic oxidation of adsorbed organic in 0.1 N HCl+0.9 N H_2SO_4 (C.D. = $1 \cdot 10^{-4}$ A/cm²) (●), methanol; (○), formic acid; (×), "reduced CO_2." (- - - -) Platinum electrodes without adsorbed organic.

Acid chloride solutions

The effect of chloride ions on the anodic oxidation of the three films studied is rather complex, and is dependent on the history of the electrode used and the concentration of chloride ions. The essential features of this effect are illustrated in Figs. 2–4. Figure 2 shows the charging curves, with and without the presence of adsorbed organic, in 0.1 N HCl + 0.9 N H_2SO_4. A comparison with the corresponding charging curves in 1 N H_2SO_4 (see, for example, Fig. 1 of ref. 1) shows that chloride ions markedly increase the overpotential for the oxidation of the adsorbed organic. Furthermore, the plateau corresponding to the oxidation of the adsorbed organic is split into two in the

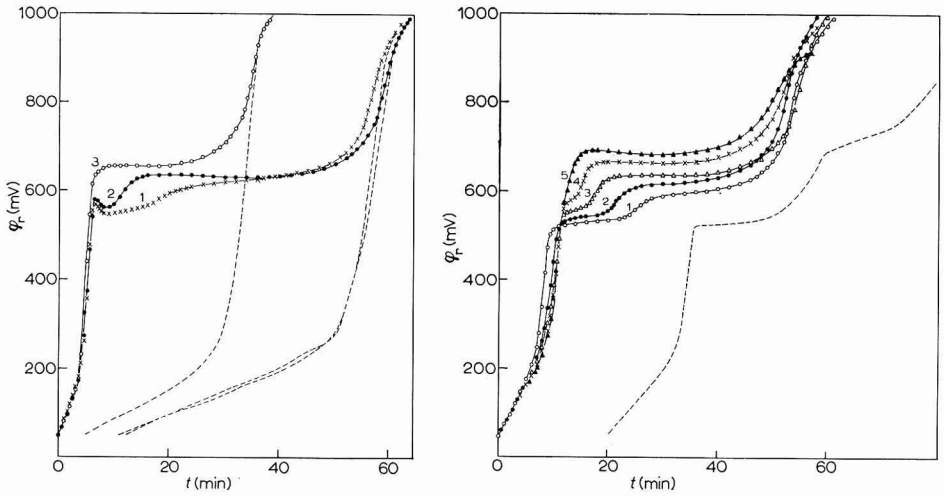

Fig. 3. Charging curves for oxidation of formic acid films in 0.1 N HCl + 0.9 N H_2SO_4 (C.D. = $1 \cdot 10^{-4}$ A/cm^2) on: (1), freshly platinized; (2), moderately aged; (3) aged platinum electrode.

Fig. 4. Effect of chloride concn. on the shape of charging curves for oxidation of "reduced CO_2" films on moderately aged platinized platinum electrode (C.D. = $1 \cdot 10^{-4}$ A/cm^2: (1) 0.01 N HCl + 0.99 N H_2SO_4; (2), 0.03 N HCl + 0.97 N H_2SO_4; (3), 0.10 N HCl + 0.90 N H_2SO_4; (4) 0.30 N HCl + 0.70 N H_2SO_4; (5), 1.0 N HCl. (----) Soln. containing 0.01 N KBr + 0.1 N H_2SO_4.

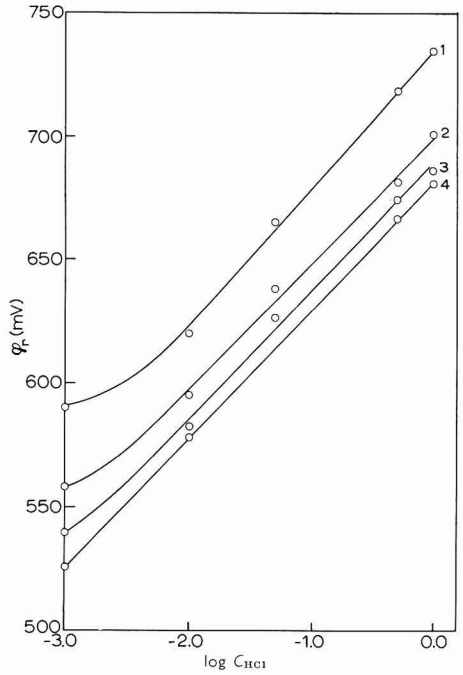

Fig. 5. Effect of chloride concn. on φ_r for oxidation of methanol film on platinized platinum at constant total acid (HCl + H_2SO_4) = 1.0 N (C.D. = $1 \cdot 10^{-4}$ A/cm^2). K-values: (1), 0.1; (2), 0.2; (3), 0.3; (4) 0.4.

presence of chloride ions. The splitting of the plateau is dependent on the history of the electrode. This is illustrated by the charging curves shown in Fig. 3 for formic acid films on freshly platinized, moderately aged, and aged electrodes. It can be seen from Fig. 3 that the splitting observed in the case of fresh, and moderately aged electrodes is absent in case of the aged electrode.

The effect of chloride concentration on the shape of the charging curves is illustrated in Fig. 4 for the adsorbed films formed in CO_2 solutions. The moderately aged electrode was used in these experiments. The inflexion corresponding to the splitting of the plateau is shifted towards the left (*i.e.*, towards higher coverages with the adsorbed organic) with increase in concentration of chloride ions until, in 1 *N* HCl, a smooth curve (No.5, Fig. 4) with a single plateau at potentials much higher than those observed in 1 *N* H_2SO_4, is again obtained. A similar behaviour is observed with the aged electrode except that the chloride concentration necessary for the disappearance of the inflexion is smaller for this electrode (compare curve 5, Fig. 4 with curve 3, Fig. 3).

These general features of the effect of chloride ions on the shape of the charging curves are closely similar for the three films studied. Whereas Fig. 4 amply testifies to the effect of chloride concentration on the overpotential for the anodic oxidation of the adsorbed species, a quantitative evaluation of this effect is difficult, particularly at higher coverages with the adsorbed organic. Consequently, quantitative data on the effect of chloride concentration on the overpotential of oxidation of the adsorbed species is restricted to *K*-values below 0.5.

The effect of chloride concentration on the electrode potential, under otherwise constant conditions of current density, pH and coverage with the adsorbed organic,

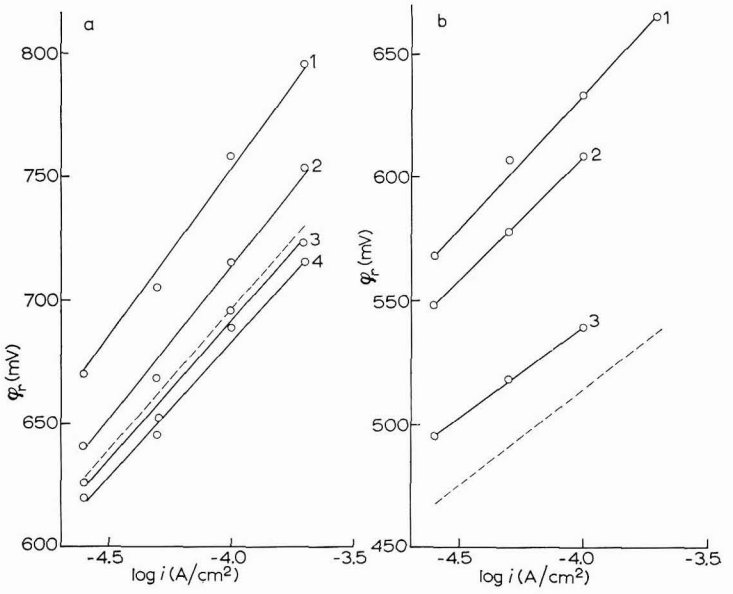

Fig. 6. (a) Tafel plots for the oxidation of formic acid film on platinized platinum in 1 *N* HCl at *K*-values: (1), 0.1; (2), 0.2; (3), 0.3; (4), 0.4. (----) $K = 0.7$.
(b) Tafel plots for oxidation of "reduced CO_2" on platinized platinum in: (1) 0.1 *N* HCl at $K = 0.3$; (2,3), 0.005 *N* HCl + 0.995 *N* H_2SO_4 at $K = 0.3$ (curve 2), and $K = 0.7$ (curve 3). (----) 1 *N* H_2SO_4 at $K = 0.7$.

is illustrated in Fig. 5 for the methanol film. φ_r *vs.* log c_{HCl} plots are linear over more than two decades of chloride concentration. The slope of these plots varies in the range 45–62 mV for the three films studied (Table 1).

Tafel plots for the anodic oxidation of the formic acid film in 1 *N* HCl are given in Fig. 6a. The plots are linear and have a slope of 112–132 mV. The corresponding data for the films formed from methanol and CO_2 solutions are closely similar (Table 1). The dashed curve in Fig. 6a, corresponding to a *K*-value of 0.7, lies a few millivolts higher than curve 4 corresponding to a *K*-value of 0.4. This effect arises from the slight hump observed in the initial region ($K = K_{max} \approx 0.9$) of the plateau corresponding to the oxidation of formic acid and methanol films.

The Tafel slope of approximately 120 mV in chloride solutions suggests that the mechanism of oxidation of the adsorbed organic in chloride medium is different from that in sulfate solutions and, therefore, it was of interest to investigate the effect of chloride concentration on the Tafel slope. Typical data for reduced CO_2 are given in Table 1. It can be seen that even in a solution containing 0.005 *N* HCl, a Tafel slope of 100–105 mV is observed for *K*-values up to 0.5 (Fig. 6b). This result suggests that there is a change in the mechanism of anodic oxidation of the adsorbed organic even when the concentration of chloride ions is as low as 0.005 *N*.

The effect of pH on the overpotential of oxidation of the adsorbed organic in chloride solution is somewhat different from that in the sulfate medium. There was a distinct tendency for the φ_r-potential to decrease with pH. In the pH- range 0.2–2.2, φ_r decreased by 25–30 mV per unit increase in pH.

Acid- bromide solutions

Only a few experiments were carried out in bromide solutions. A typical charging curve for "reduced CO_2" in 0.1 *N* H_2SO_4 containing 0.01 *N* KBr is shown by the dashed curve in Fig. 4. It is evident from this curve that bromide ions are even more effective than chloride ions in increasing the overpotential of anodic oxidation of the adsorbed organic, although the effect is not as well marked in the initial regions of the plateau where the coverage with the adsorbed organic is high. The splitting of the plateau is also more prominent than in case of chloride solutions.

DISCUSSION

The relevant kinetic data are listed in Table 1. The kinetic data are closely similar for the three films studied as is to be expected if the nature of the species adsorbed on platinum from methanol, formic acid and CO_2 solutions is the same.

The kinetic data obtained in acid sulfate solutions can be readily explained on the basis of a rate-determining step (r.d.s.) involving adsorbed hydroxyl radicals and the adsorbed organic (R).

$$H_2O \rightleftharpoons OH_{ads} + H^+ + e \qquad (1)$$

$$R_{ads} + OH_{ads} \rightarrow ROH_{ads} \qquad (2)$$

The above mechanism has been postulated by BOCKRIS *et al.*[8] and by PETRY *et al.*[3] for the anodic oxidation of acetylene and methanol, respectively. A quantitative formulation of this mechanism for methanol oxidation has also been considered by

KHAZOVA *et al.*[9]. We shall discuss this mechanism in more detail in so far as it relates to the anodic oxidation of the adsorbed organic species.

Since the end-product (CO_2) is continuously being desorbed from the electrode, and all steps following the rate-determining step (2) are fast, it may be assumed that the coverage with respect to the adsorbed species, ROH, or any other adsorbed species formed subsequent to reaction (2), is negligibly small. It may also be assumed that the coverage, θ_{OH}, with respect to the adsorbed OH is small in the potential range ($\varphi_r \approx 0.5$–0.7 V) where the oxidation of the adsorbed organic occurs. As discussed by BOCKRIS *et al.*[8], these assumptions are entirely reasonable. We shall now make the additional assumption that sulfate ions are not significantly adsorbed on platinum. Under these conditions, the total coverage $\theta_T \approx \theta_M$, and $\theta_{OH} \ll (1 - \theta_T)$. We may thus postulate Langmuir conditions for the quasi-equilibrium in reaction (1). The rate equation for the anodic oxidation of the adsorbed organic in acid sulfate solutions may then be readily formulated as follows:

$$i = k_1 g(\theta_M) \exp [F\varphi_r/RT] \tag{3}$$

where k_1 is a constant. The function, $g(\theta_M)$, has been left undefined since it is not material to the present discussion; the nature of this function has been discussed by KHAZOVA *et al.*[9].

It follows from eqn. (3) that, at constant θ_M, $(\partial\varphi_r/\partial \log i) = 2.3\ RT/F$, $(\partial\varphi_r/\partial \mathrm{pH}) = 0$, and $(\partial \log i/\partial \mathrm{pH}) = 0$. The experimental parameters (Table 1) are close to those expected from eqn. (3). The experimental Tafel slopes are, however, a little larger than the value of 60 mV expected from eqn. (3). This point is discussed further below.

The retarding effect of chloride and bromide ions on the dissociative adsorption and oxidation of alcohols has been reported earlier[4,6,7], quantitative data are, however, not yet available. KHAZOVA *et al.*[10] have reported the effect of auxiliary ions on the anodic oxidation of methanol, and have shown that the relative rate of oxidation decreases linearly with the logarithm of concentration of $H_2PO_4^-$, Cs^+ and $(CH_3)_4N^+$ ions. Of particular interest are the studies made by LU-AN *et al.*[11] on the effect of adsorption of bromide and iodide ions on the electrochemical oxidation and reduction reactions occurring in the quinone–hydroquinone system. The relative rates of these reactions were found to decrease linearly with the logarithm of halide ion concentration, the effect increasing in the order, $Cl^- < Br^- < I^-$. Direct measurements of adsorption of bromide and iodide ions on platinum showed that adsorption followed the Temkin isotherm with the result that the relative reaction rate decreased linearly with the degree of coverage with respect to these ions. It was also shown by these authors that absolute adsorption of bromide and iodide ions on platinum decreased when quinone and hydroquinone were present in the solution, indicating that the adsorption of halide ions does not occur on sites occupied by the organic. A similar effect has been reported by KAZARINOV AND MANSUROV[12].

The adsorption of chloride ions on platinum has been studied by BALASHOVA and coworkers[13], and by SHLYGIN *et al.*[14]. A systematic study on smooth platinum has been made by GILMAN[15] and although his adsorption data are much higher than those reported by the Russian workers, particularly in dilute solutions, they show that the adsorption of chloride ions follows the Temkin isotherm.

We shall now consider the effect of the adsorption of chloride ions on oxygen adsorption on the platinum electrode. In the presence of adsorbed anions, the onset

of oxygen adsorption occurs at relatively higher φ_r-potentials[13,16,17]. This is clear from a comparison of the charging curves for platinum in H_2SO_4 and HCl media[14,17]. The double-layer region of the charging curves is much steeper in chloride than in sulfate solutions, and extends towards more positive potentials. This results in a much clearer separation of the oxygen and hydrogen regions of the charging curve in chloride solutions than in sulfate or hydroxide solutions. In other words, the activation energy of the discharge of water molecules is larger for acid chloride than for acid sulfate solutions. Under these conditions, the coverage, θ_{OH}, with respect to adsorbed OH radicals in the potential region of interest ($\varphi_r = 0.4$–0.8 V) may be expected to be even smaller than for sulfate solutions.

If the adsorption of chloride ions increases the activation energy for the discharge of the water molecule, a state may be reached where the forward rate of reaction (1) becomes comparable with, or slower than, the rate of reaction (2). The rate-determining step for the oxidation of the adsorbed organic may then be expected to be the discharge of the water molecule with or without the participation of the adsorbed organic species.

$$H_2O + R_{ads} \rightarrow ROH + H^+ + e \tag{4a}$$

$$H_2O \rightarrow OH_{ads} + H^+ + e \tag{4b}$$

We propose to show that this is the case for the anodic oxidation of the adsorbed organic species studied in acid chloride solutions. The following assumptions have been made in arriving at the relevant rate equation.

(1) The adsorption of chloride ions on platinum follows the Temkin isotherm.
(2) The adsorption of chloride ions occurs only on sites unoccupied by the adsorbed organic species.
(3) Equilibrium coverage with chloride ions is attained as the adsorbed organic species are removed from the electrode during the anodic oxidation process.
(4) The coverage, θ_{OH}, is negligibly small in the potential region, 0.4–0.8 V [$\theta_{OH} \ll (1 - \theta_T)$].
(5) The activation energy for the discharge of water molecules increases linearly with chloride coverage, θ_{Cl^-}.

Assumptions 1,2,4 and 5 are reasonable in the light of the discussion above. Assumption 3 is justified in view of the slow charging technique used; it is, however, possible that equilibrium adsorption with chloride ions may not be attained in case of very dilute solutions ($< 0.005\ N$).

With the above assumptions, and, assuming reaction 4a or 4b as rate-determining, we have the following rate equation:

$$i = k_2 g'(\theta_M) \exp\left[(\beta\varphi F/RT) - \alpha f \theta_{Cl^-}\right] \tag{5}$$

Taking the Temkin isotherm for the adsorption of chloride ions into account, we thus have

$$i = k_3 g'(\theta_M)\, a_{Cl^-}{}^{\alpha} \exp\left[\beta\varphi F/RT\right] \tag{6}$$

In the above equations, k_2 and k_3 are constants, f is the surface heterogeneity factor, and α and β have a fractional value between zero and unity. The function $g'(\theta_M)$ has been left undefined as it is not of immediate interest.

The factor f has been shown to be practically independent of the nature of the

species adsorbed on platinum (see, for example, ref. 9). From our own experimental data with varying chloride concentrations (Table 1), α has a value close to 0.5. With $\alpha \approx \beta \approx 0.5$, we thus get, at constant θ_M, a Tafel slope of $4.6\,RT/F$ and $(\partial\varphi/\partial \log a_{Cl^-}) = 2.3\,RT/F$. The experimental parameters thus conform closely to those expected from eqn. 6.

Whereas eqn. 6 can account for the observed Tafel slope and the effect of chloride concentration on the rate of anodic oxidation of the adsorbed organic species, it predicts an independence of reaction rate on pH at constant φ. This is at variance with experimental observations in acid chloride solutions. WROBLOWA, PIERSMA AND BOCKRIS[18] have reported similar results for the anodic oxidation of ethylene on platinum where the water discharge mechanism has been postulated. The authors have explained the observed pH effect as arising from the fact that the potential of zero charge for platinum shifts in the same direction, and to the same extent, as the potential of the reversible hydrogen electrode[19]. Under these circumstances, φ may be replaced by φ_r in eqn. 6. We should then have $(\partial\varphi_r/\partial \mathrm{pH}) = 0$ as against the experimental value of $(\partial\varphi_r/\partial \mathrm{pH}) \approx -30$ mV (Table 1). The causes of this discrepancy are not clear at present.

The results outlined above show that the adsorption of chloride ions has a marked effect on the anodic oxidation of methanol, formic acid, and "reduced CO_2" films on platinum. Of particular interest is the effect of chloride adsorption on the Tafel slope. It should be noted that the expected Tafel slope of 60 mV (eqn. 3) in acid sulphate solutions is based on the assumption that the sulfate ion is not adsorbed. However, sulfate ion is known to adsorb on platinum to some extent[13]. It is therefore probable that Tafel slopes somewhat larger than 60 mV observed in acid sulfate solutions (Table 1) are associated with this slight adsorption of sulfate ions on platinum.

The inflexions in the plateau corresponding to the anodic oxidation of adsorbed organic (Figs. 2–4) probably arise from a lack of fulfilment of assumption 3, relating to equilibrium coverage with chloride ions at high coverages with the adsorbed organic. On an electrode surface practically completely covered with the adsorbed organic, the adsorption of chloride ions can only occur on isolated platinum sites between adjacently adsorbed organic species. Under these conditions, the adsorption of chloride ions on the bare platinum sites may well be *activated*. The effect may thus be expected to disappear at low θ_M or at high chloride concentrations as is experimentally observed. Some interesting observations have been made for solutions containing 0.005 N HCl + 0.995 N H_2SO_4 where, as already indicated, the mechanism of oxidation of the adsorbed organic changes. In this solution, a Tafel slope of 100–105 mV is observed at low coverages with the adsorbed organic ($K < 0.5$), and of about 70 mV at large coverages ($K > 0.6$). This is illustrated by curves 2 and 3 in Fig. 6b. In this solution, therefore, the kinetic behaviour of the adsorbed organic is close to that in acid chloride solutions at low coverages, and close to that in acid sulfate solutions at high coverages.

As stated above, the functions $g(\theta_M)$ (eqn. 3) and $g'(\theta_M)$ (eqn. 6) have been left undefined. It is clear, however, that these functions determine the shape of the anodic charging curves when adsorbed organic species are present on the electrode, and depend, among other things, on the rate-determining step postulated for the reaction. The nature of these functions will be discussed in a separate communication.

SUMMARY

The kinetics of anodic oxidation of the organic species adsorbed on platinized platinum from methanol, formic acid and CO_2 solutions has been investigated. The kinetic data are closely similar for the three films studied. It is shown that the mechanism of the reaction is greatly influenced by the presence of chloride ions. In acid sulfate solution, the rate-determining step involves a reaction between adsorbed organic and adsorbed hydroxyl radicals. In acid chloride solutions, however, water discharge is rate-determining. The change of mechanism has been attributed to chloride ion adsorption which increases the activation energy for the discharge of the water molecule.

REFERENCES

1 V. N. KAMATH AND HIRA LAL, *J. Electroanal. Chem.*, 18 (1968) 00.
2 M. W. BREITER, *J. Electroanal. Chem.*, 15 (1967) 221.
3 O. A. PETRY, B. I. PODLOVCHENKO, A. N. FRUMKIN AND HIRA LAL, *J. Electroanal. Chem.*, 10 (1965) 182.
4 B. I. PODLOVCHENKO, O. A. PETRY AND E. P. GORGONOVA, *Elektrokhimiya*, 1 (1965) 182.
5 B. I. PODLOVCHENKO, O. A. PETRY, A. N. FRUMKIN AND HIRA LAL, *J. Electroanal. Chem.*, 11 (1966) 12.
6 B. I. PODLOVCHENKO, O. A. PETRY AND A. N. FRUMKIN, *Dokl. Akad. Nauk SSSR*, 153 (1963) 397.
7 B. I. PODLOVCHENKO AND Z. A. IOFA, *Zh. Fiz. Khim.*, 38 (1964) 211.
8 J. W. JOHNSON, H. WROBLOWA AND J. O.'M. BOCKRIS, *J. Electrochem. Soc.*, 111 (1964) 863.
9 O. A. KHAZOVA, YU. B. VASILYEV AND V. S. BAGOTSKY, *Elektrokhimiya*, 2 (1966) 267.
10 O. A. KHAZOVA, YU. B. VASILYEV AND V. S. BAGOTSKY, *Elektrokhimiya*, 1 (1965) 439; V. S. BAGOTSKY AND YU. B. VASILYEV, *Electrochim. Acta*, 12 (1967) 1323.
11 YAO LU-AN, V. E. KAZARINOV, YU. B. VASILIEV AND V. S. BAGOTSKII, *Elektrokhimiya*, 1 (1965) 176; *Dokl. Akad. Nauk SSSR*, 151 (1963) 151.
12 V. E. KAZARINOV AND G. N. MANSUROV, *Elektrokhimiya*, 2 (1966), 1338.
13 N. A. BALASHOVA AND V. E. KAZARINOV, *Usp. Khim.*, 34 (1965) 1721; N. A. BAIASHOVA AND V. E. KAZARINOV, *Elektrokhimiya*, 1 (1965) 512; G. N. MANSUROV, V. E. KAZARINOV AND N. A. BALASHOVA, *Elektrokhimiya*, 2 (1966) 1438.
14 A. I. SHLYGIN, A. N. FRUMKIN AND W. MEDWEDOVSKY, *Acta Physicochim. URSS*, 4 (1936) 911; see also, A. N. FRUMKIN, *Advan. Electrochem. Electrochem. Eng.*, 3 (1963) 287.
15 S. GILMAN, *J. Phys. Chem.*, 68 (1964) 2112.
16 M. C. BANTA AND N. HACKERMAN, *J. Electrochem. Soc.*, 111 (1965) 114.
17 A. D. OBRUCHEVA, *Zh. Fiz. Khim.*, 31 (1958) 2155; B. ERSHLER, *Acta Physicochim. URSS*, 7 (1937) 327.
18 H. WROBLOWA, B. J. PIERSMA AND J. O.'M. BOCKRIS, *J. Electroanal. Chem.*, 6 (1963) 401.
19 E. GILEADI, S. D. ARGADE AND J. O.'M. BOCKRIS, *J. Phys. Chem.*, 70 (1966) 2044; V. L. KHEIFETS AND B. S. KRASIKOV, *Zh. Fiz. Khim.*, 31 (1957) 1992.

ELECTROANALYTICAL CHEMISTRY AND INTERFACIAL ELECTROCHEMISTRY
Elsevier Sequoia S.A., Lausanne – Printed in The Netherlands

DOUBLE-LAYER EFFECT ON THE POLAROGRAPHIC REDUCTION OF URANYL PEROXODICARBONATO ION

VERA ŽUTIĆ AND MARKO BRANICA
Department of Physical Chemistry, Institute "Ruđer Bošković", Zagreb, Croatia (Yugoslavia)
(Received April 1st, 1968)

INTRODUCTION

It has already been reported[1] that uranyl peroxodicarbonato ion gives an irreversible wave in 1 M Na_2CO_3 supporting electrolyte, with $E_{\frac{1}{2}} = -1.15$ V *vs.* SCE, corresponding to a three-electron reduction to uranium(V) tricarbonato ion. When the composition of the supporting electrolyte was changed, a significant shift of the reduction potential was observed, but the shape of the wave was unchanged. The similar behaviour of uranyl tricarbonato ion, the structure[2] and polarographic characteristics in 1 M Na_2CO_3 [1,3] of which closely resemble those of uranyl peroxodicarbonato ion (except that the electrode reaction involves only one electron), has been successfully interpreted in terms of the simple Frumkin theory[4,5] by GIERST and coworkers[6,7].

In this connection and in order to elucidate the mechanism of the electrode process, the study of the relationship between the double-layer structure and kinetics of uranyl peroxodicarbonate reduction has been undertaken.

EXPERIMENTAL

The polarographic curves were recorded with a Radelkis OH-102 polarograph in a three-electrode cell[1] at a scan rate of 50 mV/min, without damping or capacity compensating circuits. Capillary characteristics in 0.8 M $NaClO_4$ + 0.1 M Na_2CO_3 solution at -1.1 V *vs.* SCE, and at 50 cm mercury column height were: $m = 0.496$ mg/sec and $t = 11.4$ sec. The drop-time was maintained at 3.0 sec by an electromagnetic detacher. A saturated calomel reference electrode was used.

Supporting electrolytes were made from reagent-grade chemicals (previously heated at an appropriate temperature). The uranium stock solution was prepared by dissolving nuclear grade ammonium diuranate in 1 M $NaHCO_3$ solution. Reagent-grade hydrogen peroxide distilled under reduced pressure was used to prepare approximately 0.2 M stock solutions. The peroxide content was determined manganometrically just prior to measurements. All experiments were carried out at $25 \pm 0.1°$. Triply-distilled water and doubly-distilled mercury were used throughout.

RESULTS

The effect of the supporting electrolyte on the reduction of uranyl peroxo-

dicarbonato ion has been studied by adding various concentrations of sodium perchlorate to uranium peroxodicarbonato solutions (which always contained 0.1 M carbonate to stabilize the complex) or by replacing sodium ion with other alkali metal cations.

In all cases a single irreversible wave, corresponding to the three-electron reduction, was obtained. It was found to be independent of pH in the range investigated (10.5–11.2) but shifted to more positive potentials with increase in the concentration of the supporting electrolyte. The limiting current was found to be diffusion-controlled, and no adsorption of the reactant, or the product of the electrode reaction, could be detected polarographically.

The polarographic curves were analyzed according to the Weber–Koutecky method[8]:

$$\chi_1 = k_a \sqrt{12t/7D}$$

where χ_1 is a non-dimensional parameter tabulated as a function of the mean current ratio, i/i_d, k_a is the apparent formal rate constant of the electrode process, t the

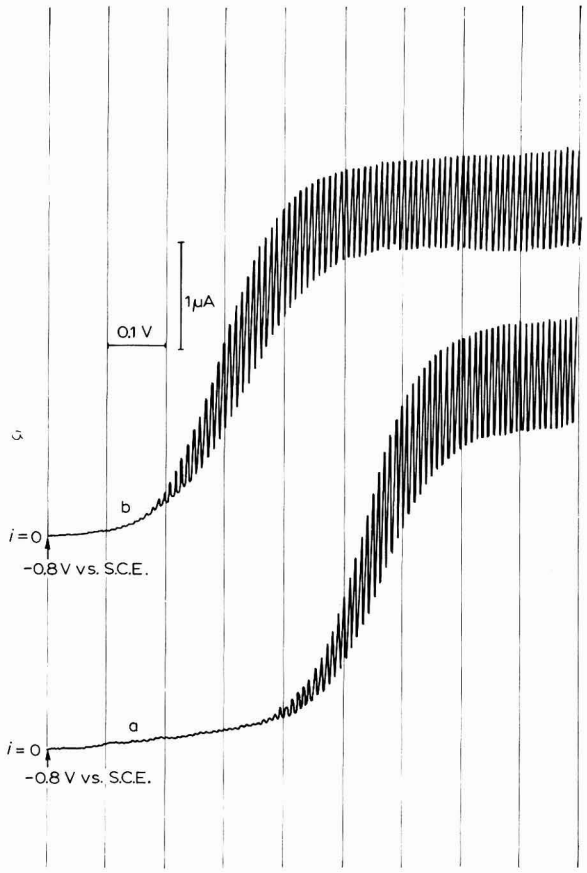

Fig. 1. Polarograms of 1 mM uranyl peroxodicarbonate in: (a), 0.1 M Na_2CO_3; (b), 0.1 M Na_2CO_3 + 1.8 M $NaClO_4$ supporting electrolyte.

drop-time, and D the diffusion coefficient. The resulting log $\chi_1 = f(E)$ plots were transferred to log k_a–E coordinates using the same value of the diffusion coefficients ($D = 5.2 \cdot 10^{-6}$ cm^2 sec^{-1} in 0.1 M Na_2CO_3 + 0.8 M $NaClO_4$ supporting electrolyte).

Figure 1 shows typical polarograms of uranyl peroxodicarbonato ion obtained without (curve a), and after (curve b) addition of 1.8 M $NaClO_4$, which caused a shift of the half-wave potential towards a more positive value of about 240 mV.

The effect of the nature of the cation of the supporting electrolyte is shown in Fig. 2. The apparent rate constants increase in the normal sequence from Li^+ to Cs^+ [9,10]. The anion of the supporting electrolyte at constant cation concentration has, however, no effect on the position of the wave (Table 1).

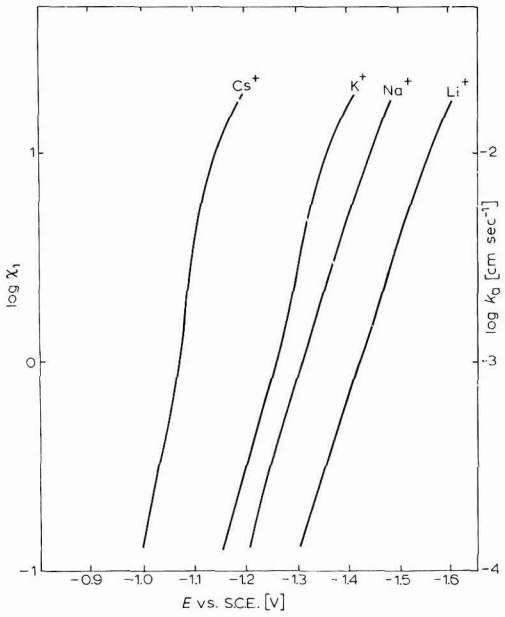

Fig. 2. Rate constant–potential curves of uranyl peroxodicarbonate (1 mM) in 0.1 M alkali carbonates.

TABLE 1

HALF-WAVE POTENTIALS OF 1 mM URANYL PEROXODICARBONATE AT VARIOUS COMPOSITIONS OF THE SUPPORTING ELECTROLYTE

Supporting electrolyte (M)			$E_{\frac{1}{2}}$ *(V vs. SCE)*
$[Na^+]$	$[CO_3^{2-}]$	$[ClO_4^-]$	
0.4	0.2	—	−1.238
	0.1	0.2	−1.240
0.75	0.375	—	−1.175
	0.1	0.55	−1.174
1.0	0.5	—	−1.152
	0.1	0.8	−1.148

This behaviour is characteristic of the reduction of a negative particle at the negatively charged mercury surface[10,11]. A quantitative analysis of the observed effects was made using the Frumkin relation[5]:

$$k_a = k_0 \exp(\alpha n_\alpha F/RT)[-(E-E_z)-(z/\alpha n_\alpha - 1)\phi_2]$$

where k_0 is the true formal rate constant at the potential of the point of zero charge (E_z)[12], α the transfer coefficient, n_α the number of electrons exchanged in the rate-determining step, z the charge of the reacting particle, and ϕ_2 the potential drop across the diffuse double layer.

The double-layer structure has been modified by a systematic variation of sodium ion concentration from 0.2 to 2 N. It is assumed that the reaction takes place at the outer Helmholtz plane and that no specific adsorption occurs. ϕ_2-values were calculated, according to Gouy–Chapman theory[13], from GRAHAME's data[14] for sodium fluoride solutions.

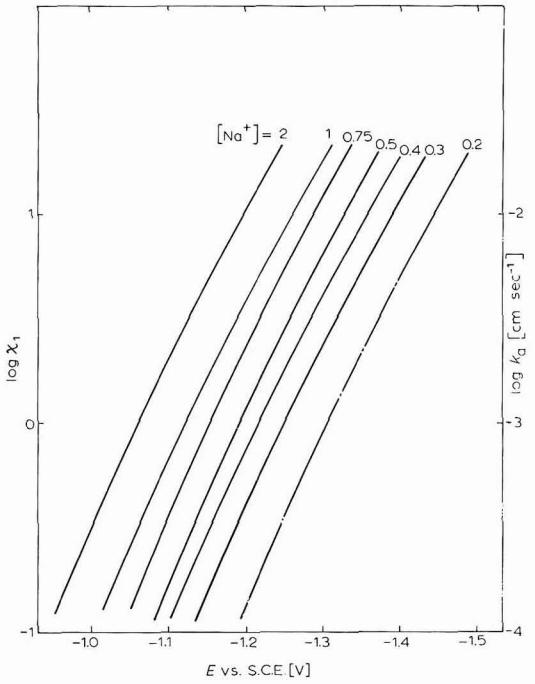

Fig. 3. Rate constant–potential diagram for 1 mM uranyl peroxodicarbonate in 0.1 M Na_2CO_3 + $[NaClO_4]_{var.}$ supporting electrolyte.

The apparent rate constant–potential dependence for different concentrations of sodium ion is represented in Fig. 3. A graphical determination of parameters, αn_α and z, using the values from Fig. 3 is shown in Figs. 4 and 5. In Fig. 4, the half-wave potentials, *i.e.*, the potentials at constant current from Fig. 3, are plotted against the corresponding ϕ_2-values. A straight line was obtained having the slope $(1-z/\alpha n_\alpha)=4.5$. The plot of the apparent rate constants at constant potential ($E=-1.2$ V *vs.* SCE) is given in Fig. 5. The slope of the straight line obtained

$(z-\alpha n_\alpha)$ is -2.55. The possible combinations of αn_α- and z-values are listed in Table 2. It is obvious that consistent values of αn_α are obtained only in the case when $z=-2$. The slope of the apparent rate constant–potential curve for $[Na^+]=0.2\ N$, for instance, gives 0.44 for the apparent value of αn_α. After correction for the effect of the double layer[5] by introducing $z=-2$, αn_α becomes 0.56, this being in excellent agreement with the values in Table 2.

The experimental and the true rate constant–potential dependence for the uranyl peroxodicarbonate electrode reaction, obtained after making the Frumkin correction using the values $\alpha n_\alpha=0.56$ and $z=-2$, are given in Fig. 6.

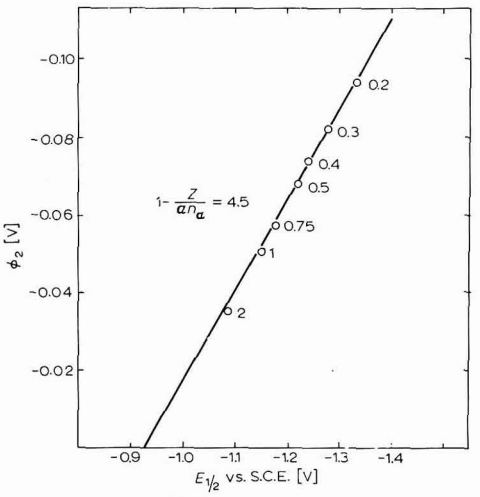

Fig. 4. Relationship between the half-wave potential of uranyl peroxodicarbonate wave and ϕ_2 for different concns. of sodium ion.

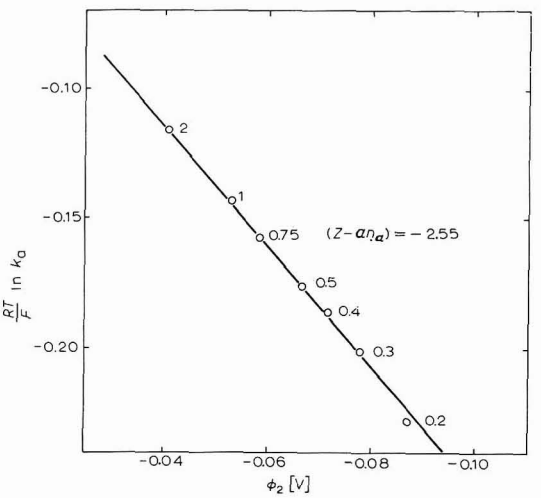

Fig. 5. Graphical determination of $(z-\alpha n_\alpha)$ value for uranyl peroxodicarbonate reduction at constant potential ($E=-1.2$ V *vs.* SCE).

TABLE 2

VALUES OF TRANSFER COEFFICIENT AND THE CHARGE OF THE REACTING PARTICLE FOR THE REDUCTION OF URANYL PEROXODICARBONATE

Method	z	αn_α
At constant rate	−1	0.29
(log χ_1 = 0.17)	−2	0.57
	−3	0.86
	−4	1.14
At constant potential	−1	1.55
(E = 1.2 V *vs.* SCE)	−2	0.55
	−3	< 0

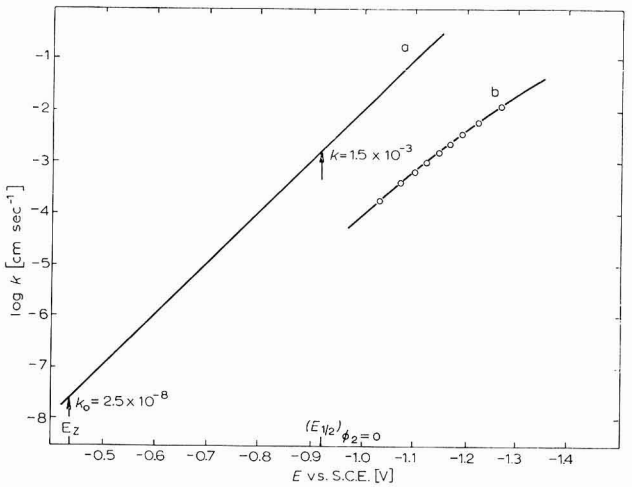

Fig. 6. (a), True rate constant–potential dependence for uranyl peroxodicarbonate reduction; (b), that obtained from the polarographic data in 0.1 M Na_2CO_3 + 0.8 M $NaClO_4$ supporting electrolyte.

DISCUSSION

It may be concluded from the analysis of the $k_a = f(E, [Na^+])$ curves that both the shift and the shape of the uranyl peroxodicarbonate wave can be quantitatively interpreted in terms of a static double-layer effect, which influences the irreversible reduction:

$$[UO_2(CO_3)_2(O_2)]^{4-} + 3e + CO_3^{2-} + 2\ H_2O \Rightarrow [UO_2(CO_3)_3]^{5-} + 4\ OH^-$$

characterized by the parameters, $\alpha n_\alpha = 0.56$, $z = -2$, $k_0 = 2.5 \cdot 10^{-8}$ and $(E_{\frac{1}{2}})_{\phi_2=0} = -0.92$ V *vs.* SCE. Since it is obviously a complex electrode process involving more than one charge transfer and, most probably, coupled chemical reactions, the values obtained correspond to the rate-determining step.

A comparison of these values with those obtained under similar conditions for uranyl tricarbonato ion reduction:

$$[UO_2(CO_3)_3]^{4-} + e \Rightarrow [UO_2(CO_3)_3]^{5-}$$

$\alpha = 0.56$[6] and 0.6[7], $n = 1$, $z = -2$, $k_0 = 4.1 \cdot 10^{-6}$, $(E_{\frac{1}{2}})_{\phi_2=0} = -0.77$ V *vs.* SCE[6,7]; indicates that in both cases the rate-determining step is the same, *i.e.*, a slow, one-electron transfer, located on the uranyl group. Accordingly, for the uranyl peroxodicarbonato ion

$$[UO_2(CO_3)_2(O_2)]^{4-} + e \Rightarrow [UO_2(CO_3)_2(O_2)]^{5-}$$

The uranium(V) peroxodicarbonato ion would then undergo faster chemical and charge-transfer reactions leading to the stable uranium(V) tricarbonato ion. Although there are no data on the uranium(V) peroxodicarbonato complex, the possibility of the formation of the peroxo complex of uranium in lower oxidation states has been considered, and some experimental evidence produced[15].

It has been proved[6,7] that the charge of the uranyl tricarbonato ion of -2 is caused by ion-pair formation with the cation of the supporting electrolyte in the bulk of the solution, and not by any chemical reaction preceding the charge transfer. This suggests that in the case of the uranyl peroxodicarbonato ion, the rate-determining step is the direct discharge of the ion-pair, $Na_2[UO_2(CO_3)_2(O_2)]^{2-}$. The accelerating action of heavier alkali metal cations is partly due to their specific adsorption at the mercury surface, as well as to the increasing tendency for ion-pair formation in the series from Li^+ to Cs^+ [7,9,16].

The negative shift of the half-wave potential of the uranyl peroxodicarbonate wave, $(E_{\frac{1}{2}})_{\phi_2=0} = -0.92$ V *vs.* SCE, compared to that of the uranyl tricarbonato ion, $(E_{\frac{1}{2}})_{\phi_2=0} = -0.77$ V *vs.* SCE, corresponds to the higher stability (already established) of the uranyl–peroxy group bond, since the standard potential of the $(UO_2^{2+})_{\text{compl.}}/(UO_2^{+})_{\text{compl.}}$ couple shifts to more negative potentials with increasing stability of the complex[6].

SUMMARY

The effect of the supporting electrolyte (alkali carbonates and perchlorates) on the polarographic reduction of uranyl peroxodicarbonato ion has been studied. In all cases, a single irreversible wave corresponding to a three-electron reduction was observed; this shifted to less negative potentials with increasing concentration and atomic number of the cation of the supporting electrolyte.

The Frumkin correction for the effect of the double layer was found to hold fairly well when the double-layer structure was varied by the addition of sodium perchlorate. The charge of the reacting particle ($z = -2$), the transfer coefficient ($\alpha = 0.56$), and the true rate constant–potential dependence were evaluated from the corresponding variation of the apparent rate constant. The difference between the formal charge of the complex ($z = -4$), and the calculated value ($z = -2$) indicates ion-pair formation. A mechanism of the electrode process involving uranium(V) peroxodicarbonato complex as an unstable intermediate is proposed.

REFERENCES

1 V. Žutić and M. Branica, *J. Polarog. Soc.*, 13 (1967) 9.
2 A. M. Gurevich, *Radiokhimiya*, 3 (1963) 321.
3 M. Branica and V. Pravdić, *Polarography 1964, Proc. Intern. Polarog. Congr. 3rd, Southampton, 1964*, Macmillan, London, 1966, p. 435.

4 A. N. FRUMKIN, *Z. Physik. Chem.*, A 164 (1933) 121.
5 A. N. FRUMKIN, V. S. BAGOTSKII, Z. A. IOFA AND B. N. KABANOV, *Kinetika elektrodnych protsesov*, Izd. Moskv. Univ., Moskva, 1952.
6 J. LEMAIRE, Thèse de doctorat, Universite Libre de Bruxelles, 1965.
7 L. GIERST, L. VANDENBERGHEN, E. NICOLAS AND A. FRABONI, *J. Electrochem. Soc.*, 113 (1966) 1025.
8 J. WEBER AND J. KOUTECKÝ, *Collection Czech. Chem. Commun.*, 20 (1955) 980.
9 A. N. FRUMKIN, *Trans. Faraday Soc.*, 55 (1959) 156.
10 P. DELAHAY, *Double Layer and Electrode Kinetics*, Interscience Publishers, New York, 1965, chap. 9.
11 G. M. FLORIANOVICH AND A. N. FRUMKIN, *Zh. Fiz. Khim.*, 29 (1955) 1827.
12 D. C. GRAHAME, *Chem. Rev.*, 41 (1947) 441.
13 C. D. RUSSELL, *J. Electroanal. Chem.*, 6 (1963) 486.
14 D. C. GRAHAME, *J. Am. Chem. Soc.*, 76 (1954) 4821.
15 F. B. BAKER AND T. W. NEWTON, *J. Phys. Chem.*, 65 (1961) 1887.
16 R. PARSONS, *Advan. Electrochem. Electrochem. Eng.*, 1 (1961) 1.

ELECTROANALYTICAL CHEMISTRY AND INTERFACIAL ELECTROCHEMISTRY
Elsevier Sequoia S.A., Lausanne – Printed in The Netherlands

THE ELECTROCHEMICAL OXIDATION OF URANIUM(IV) IN SODIUM BICARBONATE SOLUTIONS

A CHRONOPOTENTIOMETRIC STUDY

DUNJA ČUKMAN, J. ČAJA AND V. PRAVDIĆ
Department of Physical Chemistry, Institute "Rudjer Bošković", Zagreb, Croatia (Yugoslavia)
(Received April 6th, 1968)

INTRODUCTION

Nuclear technology in fuel production and reprocessing employs the reduction of uranium(IV) in, among other media, sodium carbonate or bicarbonate solutions[1-3]. The product is uranium in the +4 state, which is precipitated and processed. If uranium dioxide is the product, various considerations dictate an O/U ratio below 2.04. This requirement, if unfulfilled, will mostly be due to the reoxidation of uranium(IV) in the solution phase. Data on the oxidation of uranium(IV) in carbonate solutions are scarce. MARSHALL[4] determined the polarographic half-wave potential at −0.15 V *vs.* SCE for 1 m*M* uranium(IV) in 1 *M* $NaHCO_3$, noting that the half-wave potential is shifted towards more negative values by increased concentration of sodium carbonate, or by changing the medium to potassium bicarbonate (at same ionic strength) or to ammonium carbonate (decreasing ionic strength). Higher concentrations of uranium(IV) as reported by MARSHALL lead to "inconsistent" results. GIERST, LEMAIRE AND VANDENBERGHEN[5] have studied oxidation of uranium(IV) complexes in the presence of increasing concentrations of sulfate, fluoride and perchlorate and noted a shift towards more positive potentials. They attributed this to competition for the surface and to the deceleration of the oxidation reaction, which they found to be a two-electron transfer, and irreversible. There are no further references to the nature of the electrochemical process nor the effect of varying the concentration of the electroactive species or carbonate electrolyte.

The work of MCCLAINE and coworkers[1] and that of the Russian school, STABROVSKII[6] and CHERNYAEEV[7,8] indicates that uranium(VI) and (V) are stereochemically identical, and that only transition to the uranium(IV) state involves structural rearrangement. Therefore, it is probable that electrochemical reactions would be impeded by complex rearrangement if this is the slow step. Data on this are entirely missing in the literature.

The present paper aims at disclosing the complex mechanism of the oxidation reaction of uranium(IV) in sodium bicarbonate solutions. The approach is limited to concentrations of uranium and bicarbonate where the former is soluble[9]. In contrast to previous studies on this topic, obtained by polarographic and coulometric techniques, this study was done using the chronopotentiometric technique which is far superior in disclosing sequential kinetic processes[10].

EXPERIMENTAL

The electrical apparatus was described in detail earlier[11]. The potential–time curves were recorded on a 10-in. strip chart recorder, using a paper drive of 12 in./min, for transition times in the range of 5–approx. 60 sec. Shorter transition times were recorded by taking photographs of the screen of a Tektronix RM35A oscilloscope.

The electrolysis cell was a combination of a large mercury pool electrode for the potentiostatic reduction, and a smaller mercury cup electrode for chronopotentiometric measurements. Provisions were made for the counter electrode (which was separated from the main compartment by fritted glass), for the reference electrode (a saturated calomel electrode was used throughout) and for the inlet and outlet of gas. The cell was water-jacketted for thermostatic control. Construction details can be found elsewhere[12]. Solutions were de-aerated using purified nitrogen.

The surface area of the mercury cup electrode for chronopotentiometric measurements was determined following the recommendation of REILLEY *et al.*[13] by measuring the transition time for the reduction of Cd^{2+} in 0.1 *M* KNO_3. The value obtained was 2.84 cm^2.

Ammonium diuranate, prepared by precipitation from the highest purity grade available (Merck p.a.) uranium nitrate and ammonia, was dissolved in sodium bicarbonate in proper concentrations. The pH was measured and always found to be between 8.2 and 8.5. The solution was electrolysed at a constant potential of -1.25 V *vs.* SCE, until the current decreased below 0.5% of the initial value. Current efficiency was approximately 95%, in accordance with previous observations[14]. When reduction was complete, mercury was exchanged and potential–time curves were recorded immediately. Transition times were determined following the procedure devised by REINMUTH[15].

Analysis on uranium was made by precipitation with ammonia, heating and weighing as U_3O_8. Triple-distilled mercury and water was used throughout.

RESULTS

Figure 1a shows the oxidation wave of 1 m*M* uranium(IV) in 1 *M* $NaHCO_3$, pH $=8.5$. There is a single well-defined wave. Figure 1b shows the oxidation–re-reduction wave of uranium(IV) under the same conditions. The ratio of forward and reverse transition times τ_f/τ_r, obtained is 7.9 ± 0.2, which compares well with the theoretically expected value of 8.0[16,17].

The oxidation of uranium(IV) was studied for three different concentrations of uranium, 1.0, 2.32 and 3.85 m*M* in 1 *M* $NaHCO_3$, and for 2.32 m*M* of uranium in 0.4 *M* $NaHCO_3$.

The effect of varying concentrations of uranium on the chronopotentiometric parameter, $i\tau^{\frac{1}{2}}/C$, is shown in Fig. 2 and that of $NaHCO_3$ in Fig. 3. In both figures it is seen that the value of $i\tau^{\frac{1}{2}}/C$ decreases with increasing concentration of the respective solution component. For 1 m*M* uranium(IV), $i\tau^{\frac{1}{2}}/C$ decreases with increasing concentration of the respective solution component. For 1 m*M* uranium(IV), $i\tau^{\frac{1}{2}}/C$ does not change with current density. This means that the transition time for the oxidation of 1 m*M* uranium(IV) is determined solely by diffusion, or that the kinetic complications do not influence the rate of electron transfer.

The diffusion coefficient of uranium(IV) was calculated from the data on oxidation of its 1 m*M* solution in 1 *M* $NaHCO_3$, pH = 8.5. The result of 10 independent measurements with its standard error is:

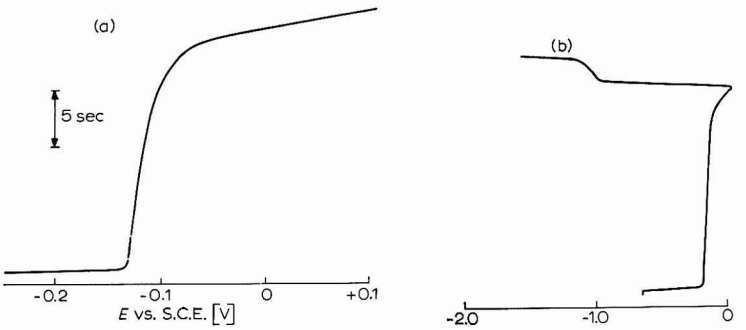

Fig. 1. Chronopotentiograms of 1 m*M* uranium(IV) in 1 *M* $NaHCO_3$, pH = 8.5 (a), current density, i = 66.9 μA/cm^2; (b), with current reversal at the transition time, i = 73.5 μA/cm^2.

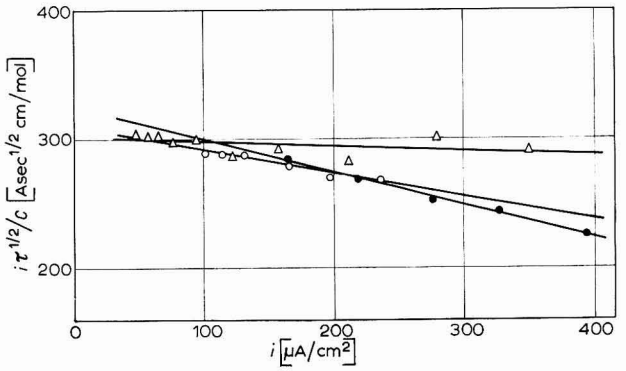

Fig. 2. Effect of varying conc. of uranium(IV) on the parameter, $i\tau^{\frac{1}{2}}/C$, at different current densities. (△)1.00, (○) 2.32, (●) 3.85 m*M* U^{4+}; at pH 8.5 and 1 *M* $NaHCO_3$.

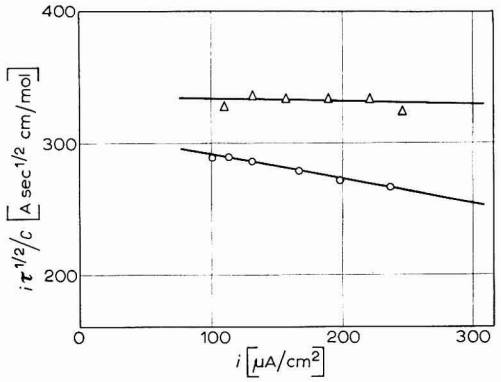

Fig. 3. Effect of varying concn. of $NaHCO_3$ on the parameter, $i\tau^{\frac{1}{2}}/C$, at different current densities: (○) 1.0, (△) 0.4 *M* $NaHCO_3$; at pH 8.5 and 2.32 m*M* U^{4+}.

$D = (3.0 \pm 0.21) \cdot 10^{-6}$ [cm²/sec].

The electrochemical reaction is an irreversible process, as shown in Fig. 4 in coordinates of log $(1-(t/\tau)^{\frac{1}{2}})$ *vs.* E for 1 mM uranium(IV). The difference in $E_{\tau/4}$ of about 0.8 V for the oxidation and re-reduction wave supports this conclusions. The

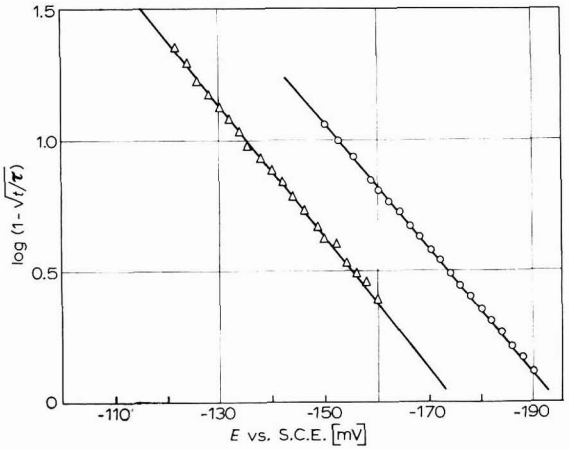

Fig. 4. Log $(1-\sqrt{t/\tau})$ *vs.* E relations for 1.0 mM uranium(IV) in 1 M $NaHCO_3$ at pH 8.5: (○) 140, (△) 160 μA.

results of measurements at different concentrations of uranium and several current densities are summarized in Table 1.

DISCUSSION

The interpretation of the results of the present study would require detailed knowledge of the structure of the carbonato-complexes of uranium(IV) at equilibrium in aqueous solution. Information available on this topic is, as shown before, limited and

TABLE 1

DATA ON OXIDATION OF URANIUM(IV) IN SODIUM BICARBONATE SOLUTIONS

Solution	i ($\mu A/cm^2$)	τ (*sec*)	$i\tau^{\frac{1}{2}}/C$ ($A sec^{\frac{1}{2}} cm/mole$)	$E_{\tau/4}$ (*mV vs. SCE*)	*Transfer coefficient*	
					calcd.	*ave.*
1.0 M $NaHCO_3$	49.3	38.2	304.7	−185	0.70	
1.0 mM U^{4+}	56.3	28.6	301.2	−165	0.73	0.71
1.0 M $NaHCO_3$	114.0	34.7	284.4	− 85	0.64	
2.32mM U^{4+}	131.5	25.4	287.0	− 80	0.67	
	166.5	15.2	279.0	− 60	0.67	0.66
1.0 M $NaHCO_3$	219.0	22.3	269.0	− 75	1.23	
3.85mM U^{4+}	276.0	12.2	250.0	− 70	1.28	
	328.0	8.2	244.0	− 75	1.33	1.28
0.4 M $NaHCO_3$	112.0	48.0	337.0	−195	1.18	
2.32mM U^{4+}	133.0	34.4	337.0	−175	0.98	
	158.0	24.0	334.0	−195	1.95	?

* These values are means of at least 10 independent measurements.

inconclusive. The reason for this is severe experimental difficulties encountered in the work with readily oxidizable species, and a large number, of apparently coexisting, partially or completely hydrolyzed carbonato complexes of uranium. The method of preparation of uranium(IV) solutions is of utmost importance[4,6,18].

A different response is obtained from solutions of uranium(IV) prepared by direct dissolution of solid salts, like UCl_4, than from solutions of uranium(V) or (VI) and subsequent electrochemical reduction.

This could be a direct evidence for slow attainment of hydrolysis equilibrium, or for the difference in structure of hydrolyzed carbonato complexes obtained in different ways.

The existence, in the solid state, of $[U(CO_3)_5]^{6-}$ as salts of alkali metals seems well established[8]. Some authors[6,19,20] use the same formula in describing the state of uranium(IV) in solutions of sodium bicarbonate. The determination of stability limits of uranium(IV) by precipitation, as reported in previous work from this laboratory[3], indicated a strong dependence on pH. This gives indirect evidence on the existence of some form of partially hydrolyzed uranium(IV) carbonato complexes in aqueous solution.

STABROVSKII[6] assumed partial hydrolysis and claimed the existence of $[U(OH)_2(CO_3)_4]^{6-}$ as the predominant, and more important, as the electroactive species undergoing direct electron transfer. A decrease in the limiting polarographic diffusion current with changing medium was attributed by STABROVSKII to complex formation giving the electro-inactive complex $[U(CO_3)_5]^{6-}$. Although this could be accepted as a possible explanation, it is still difficult to see a significant rate of a bulk reaction mechanism into which H^+ is incorporated as a reactant at pH-values between 7.2 and 10.2!

KOHMAN AND PEREC[19] simplified the interpretation of essentially the same observations by postulating the $[U(CO_3)_5]^{6-}$ complex to undergo electron transfer, and total hydrolysis of uranium(IV) into $U(OH)_4$ with incipient precipitation as the path of removal of the electroactive species. GIERST, LEMAIRE AND VANDENBERGHEN[5] did not give a plausible model to explain their results of a highly irreversible oxidation reaction and some apparent kinetic complications.

From the present work it seems well established that the charge transfer reaction is a two-electron step, preceded by some chemical transformation. KING AND REILLEY[16] have shown that, if the number of electrons involved in the forward reaction is two and in the reverse one, then the ratio of respective transition times equals eight. From the curve in Fig. 1b, a value of 7.8 was obtained.

DELAHAY[21-23] has shown that a decrease in the characteristic chronopotentiometric parameter, $i\tau^{\frac{1}{2}}$, with increasing current density indicates a chemical reaction preceding the electron transfer. Figures 2 and 3 support the assumption of a chemical step preceding the oxidation of uranium(IV). To account for the observation that these complications are becoming more pronounced with increasing concentrations of both uranium(IV) and bicarbonate, the following hypothesis of a reaction cycle, the "deactivation" model, is proposed for the mechanism of the electrochemical oxidation.

1. The most probable state of uranium(IV) in the solutions

For this we may accept the form claimed by STRABROVSKII[6], $[U(OH)_2(CO_3)_2]^{2-}$, but the treatment is equivalent if a higher complex, *e.g.* $[U(OH)_2(CO_3)_3]^{4-}$, is assumed.

Polynuclear complexes[8] although highly probable have not been described for uranium(IV). The "deactivation" hypothesis, as seen below can accommodate their existence, if proved, by only minor modifications.

2. The electrochemical reaction

Charge transfer is preceded by a chemical kinetic step which is, most probably, a dissociation reaction producing a degraded uranium(IV) complex and free carbonate ion. This complex is capable of undergoing electron exchange. Depending on whether this reactive state is a charged or uncharged species (the experimental evidence is lacking), the reaction is either one given below:

$$[U(OH)_2(CO_3)_2]^{2-} \rightleftharpoons [U(OH)_2CO_3] + CO_3^{2-} \quad (1)$$

or

$$[U(OH)_2(CO_3)_3]^{4-} \rightleftharpoons [U(OH)_2(CO_3)_2]^{2-} + CO_3^{2-} \quad (2)$$

$$[U(OH)_2CO_3] \rightarrow UO_2CO_3 + 2\ H^+ + 2e \quad (3)$$

or

$$[U(OH)_2(CO_3)_2]^{2-} \rightarrow [UO_2(CO_3)_2]^{2-} + 2H^+ + 2\ e \quad (4)$$

with subsequent reaction of the uranium(VI) species, formed in reaction (3) or (4), with carbonate to form[1,8] the known, stable form of $[UO_2(CO_3)_3]^{4-}$.

3. Complex formation in the bulk of the solution is a series of reversible reactions:

$$[U(OH)_2(CO_3)_2]^{2-} + HCO_3^- \rightleftharpoons [U(OH)_2(CO_3)_3]^{4-} + H^+ \quad (5)$$

$$[U(OH)_2(CO_3)_3]^{4-} + HCO_3^- \rightleftharpoons [U(OH)_2(CO_3)_4]^{6-} + H^+ \quad (6)$$

4. The deactivation of the reactive complex may occur by a reaction between it and a higher complex from the bulk of the solution:

$$[U(OH)_2(CO_3)_3]^{4-} + [U(OH)_2CO_3] \rightarrow 2[U(OH)_2(CO_3)_2]^{2-} \quad (7)$$

or, as an alternative,

$$[U(OH)_2(CO_3)_4]^{6-} + [U(OH)_2(CO_3)_2]^{2-} \rightarrow 2[U(OH)_2(CO_3)_3]^{4-} \quad (8)$$

thus regenerating the original form of the uranium(IV) complex.

The above mechanism described in the form of stoichiometric complex forms is certainly only a best fit. The principle, however, is that there is a complex form of highest stability, the result of an equilibrium between the free carbonate ion and uranium(IV). A check of experimental observations in terms of the above mechanism leads to full agreement: on increasing the concentration of bicarbonate in the bulk of solution the equilibrium in reactions (1) and (2) would be shifted to the left, that in reactions (5) and (6) to the right; that is, a loss of the reactive complex would occur and a gain in the "deactivator". Similar reasoning with respect to an increase in the concentration of uranium(IV) would cause the equilibrium in reactions (5) and (6) to shift to the right and, consequently, do the same in reactions (7) and (8). The effect on reactions (1) and (2) is subject to further assumptions. However, according to DELAHAY[10,21], the very evidence of kinetic complications assumes a slow step in the dissociation mechanism, little or not at all influenced by bulk activity of the electroactive ion.

In conclusion, it seems still very probable that mononuclear complexes are involved in the above sequence of reactions. Polynuclear complexes, like most of the polymers, would tend to become specifically adsorbed at the mercury–solution interface. Here, as well as in related work[12,24] no evidence for adsorption of electroactive species has been found. This work clearly calls for more studies on the hydrolytic species present in uranium(IV) carbonate solutions.

ACKNOWLEDGEMENT

The work was supported by a contract from the Yugoslav Federal Nuclear Energy Commission. The skilful assistance of Mr. F. MATIJEVAC and Mr. B. VEVEREC is gratefully acknowledged.

SUMMARY

The investigation of the mechanism of the electrochemical oxidation of uranium(IV) in sodium bicarbonate solutions is described. The investigation of the electrochemical reaction was carried out using the chronopotentiometric technique and is confined to concentrations of uranium and bicarbonate, at which the former is soluble and stable (1–4 mM of U^{4+} and 0.4–1.0 M $NaHCO_3$).

The electrochemical oxidation is an irreversible ($\beta = 0.7 \pm 0.02$), two-electron transfer reaction with an $E\tau_{/4} = -0.17 \pm 0.01$ V *vs.* SCE for 1 mM uranium(IV) in 1 M sodium bicarbonate. Evidence is given for chemical kinetic steps, preceding the electrochemical reaction, dependent both on the concentration of uranium and of carbonate.

A hypothesis of a "deactivation" mechanism, involving competing association–dissociation reactions, is advanced.

REFERENCES

1 L. A. MCCLAINE, E. P. BULLWINKEL AND J. C. HUGGINS, *Proc. Intern. Conf. Peaceful Uses At. Energy, Geneva, 1955*, 8 (1955) 26.
2 V. PRAVDIĆ, M. BRANICA AND Z. PUČAR, *Proc. III Intern. Conf. Peaceful Uses At. Energy, Geneva*, Paper 28/P/703, 1964.
3 V. PRAVDIĆ, M. BRANICA AND Z. PUČAR, *Electrochem. Techn.*, 1 (1963) 312.
4 E. D. MARSHALL, USAEC-AECD No. 3289, June 22, 1951.
5 L. GIERST, J. LEMAIRE AND L. VANDENBERGHEN, Euroatom, Report EURAEC-761, June 30, 1963.
6 A. I. STABROVSKII, *Zh. Neorgan. Khim.*, 5 (1960) 811.
7 I. I. CHERNYAEEV, V. A. GOLOVNYA AND G. V. ELLERT, *Zn. Neorgan. Khim.*, 1 (1956) 2726.
8 *Complex Compounds of Uranium* (in Russian), edited by I. I. CHERNYAEEV, Nauka, Moscow 1964, pp. 17 ff. and 437 ff.
9 M. BRANICA, V. PRAVDIĆ AND Z. PUČAR, *Croat. Chem. Acta*, 35 (1963) 281.
10 P. DELAHAY, *New Instrumental Methods in Electrochemistry*, Interscience Publishers, New York, 1954, p. 197.
11 J. ČAJA AND V. PRAVDIĆ, *J. Electroanal. Chem.*, 8 (1964) 390.
12 J. ĆAJA, Dissertation, University Zagreb, 1967.
13 C. N. REILLEY, G. W. EVERETT AND R. H. JOHNS, *Anal. Chem.*, 27 (1955) 483.
14 V. PRAVDIĆ, M. BRANICA AND Z. PUČAR, *Croat. Chem. Acta*, 33 (1961) 151.
15 W. H. REINMUTH, *Anal. Chem.*, 33 (1961) 485.
16 R. M. KING AND C. N. REILLEY, *J. Electroanal. Chem.*, 1 (1960) 434.
17 D. J. MACERO AND L. B. ANDERSON, *J. Electroanal. Chem.*, 6 (1963) 221.
18 J. LEMAIRE, Dissertation, University of Bruxelles, 1965, p. III/22.

19 L. KOHMAN AMD M. PEREC, II Yugoslav-Polish Symp. Uranium Technology and Metallurgy, Report No. 4/63, Institute of Nuclear Studies, Warsaw, 1963.
20 M. PEREC, *Nukleonika*, 5 (1961) 357.
21 P. DELAHAY AND T. BERZINS, *J. Am. Chem. Soc.*, 75 (1953) 2486.
22 J. KOUTECKÝ AND J. ČIŽEK, *Collection Czech. Chem. Commun.*, 22 (1957) 914.
23 J. W. ASHLEY JR. AND C. N. REILLEY, *J. Electroanal. Chem.*, 7 (1964) 253.
24 J. ČAJA AND V. PRAVDIĆ, to be published.

ELECTROANALYTICAL CHEMISTRY AND INTERFACIAL ELECTROCHEMISTRY
Elsevier Sequoia S.A., Lausanne – Printed in The Netherlands

AN ACIDIMETRIC CRITERION FOR EVALUATING THE RELIABILITY OF STABILITY CONSTANTS OF COMPLEXES AND THE NATURE OF THE LIGANDS

I. INTRODUCTION AND APPLICATION IN THE STUDY OF THE Ag^+–GLYCINE SYSTEM

PIETRO LANZA
Chemical Institute "G. Ciamician", Specialization School in Analytical Chemistry of the University of Bologna (Italy)
(Received March 28th, 1968)

Few scientific papers dealing with stability constants of metallic complexes with polydentate ligands having acid–base character (di- or poly-amines, polycarboxylic acids, aminoacids with two or more functional groups, etc.) define the possible acid–base forms of the ligand to which the constants refer[1]. This information would sometimes be useful. Clearly, it is not possible to deduce directly from the composition of the solution of the ligand (*i.e.*, from the concentration of the generally coexisting different acid–base forms of the ligand) the metal distribution among all the possible complexes without knowing *a priori* the value of the stepwise stability constants.

For instance, the large increase of acidity resulting from an addition of Ag^+ to a solution containing isoelectric glycine ions ($^+NH_3NH_2COO^-$) can be easily accounted for in terms of the formation of the $NH_2CH_2COO^-$ form of the complex, although the latter at the pH concerned (*ca.* 6) is certainly present at a considerably lower concentration than the amphoteric form, *i.e.*, the following displacement reaction occurs:

$$^+NH_3CH_2COO^- + Ag^+ \rightarrow [AgNH_2CH_2COO] + H^+$$

While developing a procedure for studying silver complexes with gelatine[2], we tried to establish a method that would allow us to check, (at least in not exceedingly complicated cases) whether the complex to which a certain constant is attributed is indeed formed by the supposed form of the ligand, and if complexes with different ligand forms are also present in the system. Finally, a check on the reliability of the proposed constants was also required.

The procedure is based on the following considerations. If a complexable cation is added to the solution of a ligand having acid–base properties, the ionic-strength of the system being kept constant, an increase in acidity is observed. Such an alteration in pH may be due to two factors: (1) owing to the formation of the complex, the acid/base ratio of the buffer, made up by the ligand, changes; (2) the formation of the complex can imply a displacement of protons from the protonic ligand forms.

Let us consider, for example, the Ag^+–glycine system. Generally, the following reactions of complex formation will be likely to occur:

(a) $Ag^+ + HL \rightarrow AgHL$
(b) $Ag^+ + 2HL \rightarrow Ag(HL)_2$

(c) $Ag^+ + HL \rightarrow AgL + H^+$
(d) $Ag^+ + 2HL \rightarrow AgL_2 + 2H^+$
(e) $Ag^+ + L \rightarrow AgL$
(f) $Ag^+ + 2L \rightarrow AgL_2$

where HL and L are $N^+H_3CH_2COO^-$ and $NH_2CH_2COO^-$, respectively, and the ionic charge is not indicated in the abbreviated formulae.

For the same quantity of complexed Ag^+, each of the above reactions will give rise to a different displacement of pH in a given volume of a buffer formed by the same ligand, and it will require a different quantity of base to restore the system to its initial pH-value.

After ascribing to the possible complexes the measured or computed stability constants, the correctness of these can be confirmed (or otherwise) by comparing the quantity of base used for keeping the pH constant in subsequent additions of Ag^+, with the estimated quantity.

The quantity of base needed to restore the pH to the initial value will be that required to restore the acid/base ratio, no matter how altered, to its initial value.

Let us assume that the stepwise stability constants k_1, k_2, K_1, and K_2, relevant to complexes Ag(HL), $Ag(HL)_2$, AgL and AgL_2, respectively, are known.

It will be possible to calculate the distribution of Ag^+ present as free ion, and Ag^+ bound in the various possible species when a small quantity of Ag^+ is added to excess ligand, by means of general formulae; where the total concentration of Ag in the different forms is denoted by C_{Ag}:

$$[Ag^+]/C_{Ag} = 1/\{1 + k_1[HL] + k_1k_2[HL]^2 + K_1K_2[L]^2 + \Sigma\beta_{i,j}[J]^i\} \quad (1)$$

$$[Ag(HL)]/C_{Ag} = k_1[HL]/\{1 + k_1[HL] + k_1k_2[HL]^2 + K_1[L] + K_1K_2[L]^2 + \Sigma\beta_{i,j}[J]^i\} \quad (2)$$

etc., where the term, $\Sigma\beta_{i,j}[J]^i = k_1[J] + k_1k_2[J]^2 + k_1k_2k_3[J]^3 \ldots$, takes into account the complexing action of whatever other J generic species is present in the system, besides the ligand under study. For instance, if measurements have to be carried out at a relatively high and constant ionic strength, obtained by the addition of KNO_3, the complexing action of NO_3^- upon the cation under study cannot be disregarded, and, furthermore, the interactions with OH^- in basic solution will probably have to be taken into account. In such a case, the generic term will have the value

$$\Sigma\beta_{i,j}[J]^i = \beta_{i,NO_3^-}[NO_3^-]^i + \beta_{i,OH^-}[OH^-]^j$$

In the relatively simple hypothetical case that only two of the three possible forms of the ligand are present in comparable amounts at a certain pH of the system (*e.g.*, H_2L and HL forms only, and only Ag(HL) and $Ag(HL)_2$ complexes exist) then the quantity of base (b) necessary to restore the pH to the initial value, expressed as equivalents/litre, can be calculated by the equation:

$$\{[HL]_0 - [Ag(HL)] - 2[Ag(HL)_2] + b\}/\{[H_2L]_0 - b\} = [HL]_0/[H_2L]_0 \quad (3)$$

where $[HL]_0$ and $[H_2L]_0$ are the initial concentrations before the addition of Ag^+.

In the case that complexes AgL and AgL_2 are also formed by the following reactions:

(g) $Ag^+ + HL \rightarrow AgL + H^+$
(h) $Ag^+ + 2\ HL \rightarrow AgL_2 + 2\ H^+$

eqn. (3) becomes:

$$\frac{[HL]_0 - [Ag(HL)] - 2[Ag(HL)_2] - 2[AgL] - 4[AgL_2] + b}{[H_2L]_0 - [AgL] + 2[AgL_2] - b} = \frac{[HL]_0}{[H_2L]_0} \quad (4)$$

as each mole of AgL_i produced reacts with i moles of HL and releases i H^+ ions which, with HL, form i moles of H_2L.

Equation (4) can be written in a simpler way by denoting by n, the moles/litre of HL directly and indirectly (as L) bound to the complexes and by h the equivalents/litre of H^+ released during complex formation. We have, therefore:

$$\{[HL]_0 - n - h + b\}/\{[H_2L]_0 + h - b]\} = [HL]_0/[H_2L]_0 \quad (5)$$

from which:

$$b = n/(1 + R) + h \quad (6)$$

is obtained, where

$$R = [HL]_0/[H_2L]_0 \quad (7)$$

It is obvious that $h = 0$ if the formation of the complexes, AgL and AgL_2, is negligible.

If the experiment is carried out at a pH-value at which the ligand is present only in forms HL and L, and complexes $Ag(HL)_i$ and AgL_i are formed, the following equation can be used:

$$\{[L]_0 - [AgL] - 2[AgL_2] + b\}/\{[HL]_0 - [AgHL] - 2[Ag(HL)_2] - b\} = [L]_0/[HL]_0 = R \quad (8)$$

which, by denoting by n and m, respectively, the concentration in moles/litre of L and HL bound in the complexes, is reduced to a more practical form as:

$$b = (n - mR)/(1 + R) \quad (9)$$

In the more general case in which all forms of the ligand, *i.e.*, H_2L, HL and L, are present in quantities that contribute to the buffering capacity of the solution, the formation of complexes with HL and L forms would establish a new equilibrium and also remove H_2L, owing to the reaction, $H_2L + L \rightleftarrows 2\ HL$ (i).

Let us assume that the concentrations of HL and L fixed by complexes is m and n, respectively.

The following stages can be supposed to take place successively in the course of the experiment:

(1) Before the addition of Ag^+:

$$[L]_0/[HL]_0 = 1/[H^+]_0 K_{HL} = R_1 \quad (10)$$

$$[HL]_0/[H_2L]_0 = 1/[H^+]_0 K_{H_2L} = R_2 \quad (11)$$

where K_{HL} and K_{H_2L} are the association constants of the respective acid forms, and $[H^+]_0$ is the H^+ concentration of the system.

(2) After the Ag^+ addition, the following conditions will obtain:

$$\{[L]_0 - n' - \alpha\}/\{[HL]_0 - m' + 2\alpha\} = 1/[H^+]' K_{HL} \quad (12)$$

$$\{[HL]_0 - m' + 2\alpha\}/\{[H_2L]_0 - \alpha\} = 1/[H^+]' K_{H_2L} \quad (13)$$

where m' and n' are, respectively, the concentrations of HL and L complexed at the new value of pH, α is the extent of reaction (i), and $[\overset{+}{H}]'$ the $\overset{+}{H}$ concentration at equilibrium after the addition of Ag^+.

If displacements of pH are small enough, it can be assumed that $n' = n$ and $m' = m$ within experimental error. This is clearly shown in Fig. 1b. At this point the calculation of α is possible.

(3) In order to restore the system to the initial pH, some base is added.

Let us suppose for convenience of calculation, that with regard to the total base added ($b = x + y$), the portion x is the quantity (expressed as equivalents/litre) needed for restoring H_2L to the required value, while y is the quantity reacting with HL. We have, therefore:

$$\{[L]_0 - n - \alpha + y\}/\{[HL]_0 - m + 2\alpha + x - y\} = [L]_0/[HL]_0 \quad (14)$$

$$\{[HL]_0 - m + 2\alpha + x - y\}/\{[H_2L]_0 - \alpha - x\} = [HL]_0/[H_2L]_0 \quad (15)$$

It is advisable to express the quantity of the base used in terms of mole/litre mole of added cation. In the case that solutions of the base and of the cation are of the same molar concentration, we have

$$b/C_{Ag} = V_{OH}/V_{Ag} \quad (16)$$

C_{Ag} being the concentration of the Ag^+ present in the various forms, and V_{OH} the volume of base solution needed to restore the pH altered by the addition of a volume, V_{Ag^+}, of complexable cation to a suitable volume of the ligand solution (at constant ionic strength).

This process has been applied to the Ag^+–glycine and –propylenediamine system.

Results of the Ag^+–glycine system are given in this paper.

APPARATUS AND METHODS

Measurements were carried out with a 100-ml cell in current of nitrogen and at a temperature of $25° \pm 0.1$. The mixing of solutions was carried out by magnetic agitation.

Reagents ($AgNO_3$ and NaOH) were introduced into the cell by means of capillary tubes and precision microsyringes of 1-ml capacity (checked by weighing and allowing a precision of ± 0.001 ml). During transfer, reagents were protected from carbon dioxide by connecting syringes to the reserve vessel and to the measuring cell by a three-way cock. Measurements of pH were carried out by a Knick pH-35 pH-meter. This instrument allows readings of 0.01 pH in the range 0–12.40. In order to record slight displacements of pH, the scale was further extended by connecting the instrument to a Lange Multiflex MG2 galvanometer.

A calomel electrode was connected with the solution by a bridge with sintered glass filled with IRA 400 ion-exchange resin in the nitrate form, suspended in a N KNO_3 solution. Such a resin layer has proved very effective in preventing Cl^- ion diffusion in the solution under consideration.

The pH-meter calibration was checked at the beginning as well as at the end of

every test by means of phosphate (pH = 6.86 at 25°), potassium hydrogen phthalate (pH = 4.00 at 25°) and borax (pH = 9.18 at 25°) standard buffers prepared according to the National Bureau of Standards specifications.

The substances used were chemically pure products for analysis and were not further purified.

In order to carry out measurements at constant ionic strength, 0.1 *M* glycine, $AgNO_3$ and NaOH solutions were prepared in *N* KNO_3.

After the solutions had been prepared, they were kept in vessels provided with soda lime tubes. Solutions were checked by potentiometric titration with 0.1 *N* HCl.

Determination of the dissociation constants of the ligand in N KNO_3 at 25°.

The glycine constants were determined from the pH-value at the inflection points of the potentiometric titration curves. The results, given as association constants, are as follows:

$\log K_{HL} = 9.80$ (relevant to the $H_2NCH_2COO^- + H^+ \rightleftarrows N^+H_3CH_2COO^-$ equilibrium)

$\log K_{H_2L} = 2.34$ (relevant to the $N^+H_3CH_3COO^- + H^+ \rightleftarrows N^+H_3CH_2COOH$ equilibrium)

The acid–base constants being known, the distribution of the different forms were calculated as a function of pH.

The results are presented in Fig. 1a.

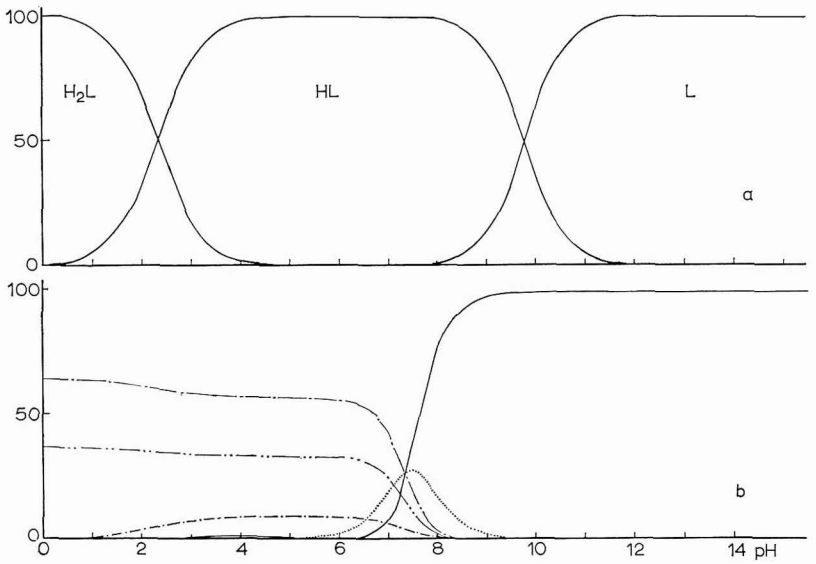

Fig. 1. (a), Distribution diagram for various glycine-forms as a function of pH; (b), distribution diagram for Ag^+–glycine system in *N* KNO_3, as a function of pH. (—.—) Ag, (—··—) $AgNO_3$, (—·—·) AgHL, (——) $Ag(HL)_2$, (·····) AgL, (——) AgL_2.

Distribution of various complex forms as a function of pH

The acid–base constants of the ligand and the stability of the complexes being known, the distribution of the different forms as a function of pH was calculated

applying the general formulae (1), (2) and analogues, with

$$\Sigma\beta_{i,j}[J]^i = \beta_{i,NO_3^-}[NO_3^-]^i + \beta_{i,OH^-}[OH^-]^i \quad (17)$$

Under the established experimental conditions there is large excess of NO_3^- ions which, according to several studies[1], have the power of associating with Ag^+ ions. MONK[3] found $K_{NO_3^-} = 0.58$ as result of $Ag^+NO_3^-$ association and associations with two or more NO_3^- ions are probably negligible ($i = 1$). The interaction with OH^- ion, though comparatively strong ($\log K_1 = 2.3$; $\log K_2 = 1.25$; $\log K_3 = 1.22$, according to JOHNSTON *et al.*[4]) has no significant effect, within the pH range explored, in the presence of ligands concerned, and the corresponding terms are negligible (as additional terms) in the denominators of eqns. (1) and (2). Therefore, eqn. (17) becomes:

$$\Sigma\beta_{i,j}[J]^i = K_{NO_3^-}[NO_3^-] = 0.58 \quad (18)$$

and eqns. (1), (2) and similar can be used directly in the special case.

Measurements of V_{OH}/V_{Ag} as function of pH (0.1 M glycine in N KNO_3)

The ligand solution (50 ml) was put into the cell and concentrated NHO_3 was added dropwise to give an acid reaction (pH 2–3). Carbon dioxide was removed by bubbling nitrogen and stirring for about 30 min; the solution was then brought to the required pH by the addition of NaOH of suitable concentration, the final addition to the exact value being made with a microsyringe. The constancy of pH was checked by allowing the solution to stand with stirring by a current of nitrogen. After the system was stabilized, 0.100 ml of $AgNO_3$ was added. A displacement of pH was observed, from some tenths to some hundredths of a pH-unit according to the buffering capacity of the system. At this point NaOH was added to restore the pH to the initial value. This operation was repeated three or four times to check the reproducibility of results and to obtain an average value.

After the V_{OH}/V_{Ag} value has been determined in this way, the solution is brought to the next pH-value by adding (if possible with the same syringe) the base required and the new value of V_{OH}/V_{Ag} is measured by the same technique.

As every single addition of $AgNO_3$ is very small, the same solution can be used for three of four values of pH.

When the pH change is exceedingly small, as is the case in the alkaline region owing to the high buffering capacity, additions of 0.200–0.300 ml of $AgNO_3$ are needed.

Results are reproducible to ± 0.001 ml at pH < 9 and $\pm$ 0.002 ml in more alkaline solutions.

The following results were obtained

pH	7.0	7.5	8.0	8.5	9.0	9.5
V_{OH}/V_{Ag}	0.34	1.01	1.66	1.81	1.70	1.32

The experimental results are also shown in Fig. 2.

Application of the acidimetric method to the study of silver complexes

Ag^+–glycine system. Investigations of the Ag^+–glycine system have been carried out by several workers and Table 1 shows the results obtained.

The procedure described in the introduction has been carried out by calculating the different values of V_{OH}/V_{Ag} from the stability constants of complexes proposed by different authors. Table 2 shows the distribution of the different complexes together with V_{OH}/V_{Ag} values. It appears from Fig. 2 that, apart from the values obtained by using the Keefer and Reiber constants, those computable from data supplied by other authors all agree with experimental values at pH > 8.0, while at lower pH-values significant deviations are observed, and the calculated NaOH consumption appears to be always a little higher than that measured. This suggested that when the pH < 8.0, Ag^+ complexes with glycine of amphoteric form are also likely *i.e.*, $[Ag(N^+H_3CH_2COO^-)]^+$ and $[Ag(N^+H_3CH_2COO^-)_2]^+$, denoted by Ag(HL) and $Ag(HL)_2$. In spite of

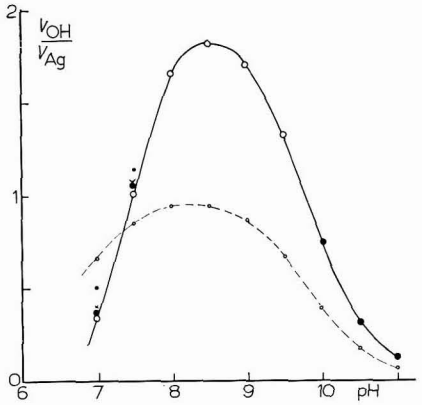

Fig. 2. Acidimetric curve for the Ag^+–glycine system. (●) DATTA; (×), MONK; (•), FLOOD; (○), KEEFER; (—), calcd.; (○), found.

TABLE 1

STABILITY CONSTANTS OF Ag^+–GLYCINE COMPLEXES ACCORDING TO VARIOUS AUTHORS

Author	*Method*	*Ionic strength*	*Temp. (°C)*	*log* K_1	*log* K_2	*log* K_1K_2	*Refs.*
MONK	glass electr. solubil.	→ 0	25	3.51	3.38	6.89	5
DUBOIS	Ag electr. spectr.	~ 0.1	19	0.59	—	7.24	6
FLOOD AND LORAS	glass electr.	0.5	20	3.7	3.3	7.0	7
KEEFER AND REIBER	solubil.	→ 0	25	4.28	—	—	8
DATTA AND GRZYBOWSKY	glass electr.	0.01	25	3.43	3.43	6.86	9

the fact that the difference between the volumes of NaOH measured and calculated in the present case is so small that it nearly falls within experimental error, we attempted to calculate constants, k_1 and k_2, of complexes with HL from the V_{OH}/V_{Ag} experimental values measured at pH 7 and 7.5. The Datta and Grzybowsky constants (*i.e.*, $K_1 = 2.70 \cdot 10^3$ and $K_1K_2 = 7.29 \cdot 10^6$) were used for complexes with $NH_2CH_2COO^-$ in the calculations.

TABLE 2

PERCENTAGE DISTRIBUTION OF Ag^+ AMONG THE VARIOUS COMPLEXED FORMS AND AMOUNT OF BASE REQUIRED AS A FUNCTION OF pH, CALCULATED FROM STABILITY CONSTANTS OF VARIOUS AUTHORS

pH		*7.0*	*7.5*	*8.0*	*8.5*	*9.0*	*9.5*	*10.0*	*10.5*	*11.0*
DATTA AND GRZYBOWSKY										
$K_1 = 2.70 \cdot 10^3$	Ag	45.60	21.04	4.25	0.55	0.07	—	—	—	—
$K_2 = 2.70 \cdot 10^3$	$AgNO_3$	26.45	12.20	2.46	0.32	0.04	—	—		—
$(K_{NO_3^-} = 0.58)$	AgL	19.57	28.40	17.90	7.12	2.63	1.10	0.61	0.45	0.40
	AgL_2	8.36	38.35	75.39	92.00	97.25	98.88	99.39	99.55	99.60
V_{OH}/V_{Ag}		0.36	1.05	1.65	1.82	1.70	1.32	0.77	0.33	0.118
MONK	Ag	43.68	19.48	3.92	0.52	0.07	0.01	—	—	—
$K_1 = 3.23 \cdot 10^3$	$AgNO_3$	25.33	11.30	2.27	0.30	0.04	—	—	—	—
$K_2 = 2.40 \cdot 10^3$	AgL	22.43	31.47	19.78	7.95	2.95	1.19	0.68	0.50	0.44
$(K_{NO_3^-} = 0.58)$	AgL_2	8.56	37.75	74.02	91.23	96.94	98.80	99.32	99.50	99.56
V_{OH}/V_{Ag}		0.40	1.06	1.65	1.81	1.70	1.32	0.77	0.33	0.118
FLOOD AND LORAS	Ag	37.99	15.15	2.95	0.39	0.05	—	—	—	—
$K_1 = 5.02 \cdot 10^3$	$AgNO_3$	22.04	8.78	1.71	0.23	0.03	—	—	—	—
$K_2 = 2.0 \cdot 10^3$	AgL	30.32	38.03	23.14	9.41	3.52	1.47	0.89	0.60	0.53
$(K_{NO_3^-} = 0.58)$	AgL_2	9.64	38.03	72.19	89.97	96.39	98.52	99.20	99.40	99.47
V_{OH}/V_{Ag}		0.50	1.14	1.65	1.80	1.70	1.32	0.77	0.33	0.118
KEEFER AND REIBER	Ag	21.66	8.98	3.19	1.07	0.38	—	—	—	—
$K_1 = 1.91 \cdot 10^4$	$AgNO_3$	12.56	5.21	1.85	0.62	0.22	—	—	—	—
$K_2 = 0$	AgL	65.78	85.80	94.96	98.30	99.40	99.75	100	100	100
$(K_{NO_3^-} = 0.58)$	AgL_2	—	—	—	—	—	—	—	—	—
V_{OH}/V_{Ag}		0.66	0.85	0.94	0.94	0.86	0.66	0.386	0.165	0.06
V_{OH}/V_{Ag} measured		0.34	1.01	1.66	1.81	1.70	1.32	—	—	—

The calculation is carried out as follows. As stated in the introductory section, the proportion of the various complexes is obtained from the equations:

$$[AgHL]/C_{Ag} = k_1[HL]/\Delta \tag{19}$$

$$[Ag(HL)_2]/C_{Ag} = k_1k_2[HL]^2/\Delta \tag{20}$$

$$[AgL]/C_{Ag} = k_1[L]/\Delta \text{ etc.} \tag{21}$$

where $\Delta = 1 + k_1[HL] + k_1k_2[HL]^2 + K_1[L] + K_1K_2[L]^2 + K_{NO_3^-}[NO_3^-]$

Since at pH 7 and 7.5, glycine is present only in the HL and L forms, the ratio V_{OH}/V_{Ag} is related to the distribution of complexes according to the equation:

$$V_{OH}/V_{Ag} = (n - mR)/(1 + R) \cdot 1/C_{Ag} \tag{22}$$

where $n = [AgL] + 2[AgL_2]$ (23)

$$m = [AgHL] + 2[Ag(HL)_2] \tag{24}$$

$$R = [L]_0/[HL]_0.$$

In the present case particularly at pH 7 and 7.5, $R \ll 1$ and $mR \ll n$, and eqn. (22) becomes

$$V_{OH}/V_{Ag} \approx n/C_{Ag} \tag{25}$$

Since K_1, K_2 and $K_{NO_3^-}$ constants and [HL] and [L] concentrations are known at the two values of pH, a system with two equations can then be formed

$$\frac{K_1[L]_i + 2K_1K_2[L]_i^2}{1 + k_1[HL]_i + k_1k_2[HL]_i^2 + K_1[L]_i + K_1K_2[L]_i^2 + K_{NO_3^-}[NO_3^-]} = \left(\frac{V_{OH}}{V_{Ag}}\right)_{pH_i} \quad (26)$$

where k_1 and k_2 are the only two unknown quantities.

If constants k_1 and k_2 are calculated directly from the system of equations (26), the results are uncertain as the least variation in the experimental parameters V_{OH}/V_{Ag} (considerably smaller than dispersion of measurements) give rise to enormous variations in the system solutions. The two equations are in fact represented by two very close and almost parallel straight lines.

However, by giving k_1 and k_2 in every equation a series of values, those values that make V_{OH}/V_{Ag} equal to the experimental value for each of the two values of pH can be found by graphic interpolation (Figs. 3a and b).

By plotting the two series of points identified in this way, two nearly linear and parallel curves appear (Fig. 4).

When allowance is made for the uncertainty range of the measurements of V_{OH} ($\pm$0.001 ml), the two curves in the k_1, k_2 diagram extend over two areas and show

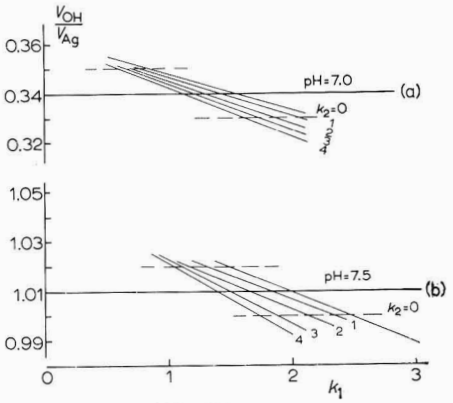

Fig. 3. Values of V_{OH}/V_{Ag} as a function of k_1 and k_2 at pH = 7.0 and pH = 7.5.

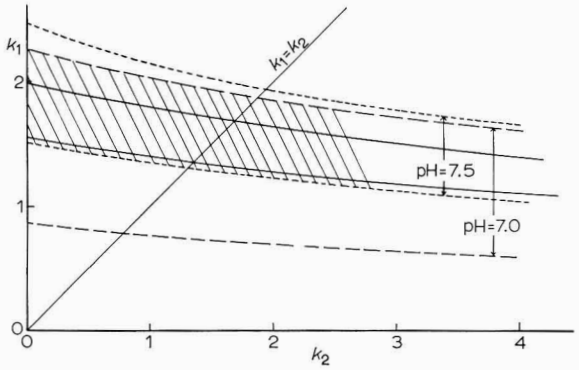

Fig. 4. Acceptable values for k_1 and k_2 for the acidimetric curve to fit the exptl. data.

an overlapping zone. All the pairs of k_1 and k_2 values included in such a zone are able, of course, to fulfil the system within the uncertainty terms of V_{OH}/V_{Ag}.

The choice of any one of the pair of values within the range determined is quite arbitrary; however, it is always such as to justify the experimental values of V_{OH}/V_{Ag}. As the overlapping area extends indefinitely towards very high values of k_2, and as a general rule the successive stepwise constants of the complexes are decreasing, and only as an exception does k_2 exceed, (though just a little) k_1 (see the system Ag^+–NH_3), it is possible to restrict the choice of the constants within the zones in the area, so that k_2 does not take an exceedingly high value compared to k_1. By way of guidance, the straight line $k_1 = k_2$ is shown on the diagram. It is obvious that k_2 can take also the value of zero; it is therefore impossible to prove, on the basis of the acidimetric criterion alone, that the $Ag(HL)_2$ complex actually exists; however, the formation of AgHL appears to be demonstrated, because $k_1 > 0$.

Conforming to the Datta and Grzybowsky values for K_1 and K_2 and assigning to k_1 and k_2 the values included within the area determined by the diagram, we calculated the curve represented on Fig. 2 by a solid line. It fits all the experimental points. The curve has been calculated for $k_1 = 1.6$ and $k_2 = 1$, or $k_1 = 2$ and $k_2 = 0$. The result does not show differences greater than those attributable to experimental accuracy.

Table 3 shows the distribution of the different complexes resulting from calculations using the following values of the constants: $k_1 = 1.6$; $k_2 = 1.0$; $K_1 = 2.7 \cdot 10^3$ and $K_2 = 2.7 \cdot 10^3$. Such a distribution (also shown in Fig. 1b) depends of course upon the arbitrary choice of k_1 and k_2, but is not conspicuously modified if k_1 and k_2 remain within the permitted zone. In the limiting case, $k_2 = 0$, the curve of the $Ag(HL)_2$ complex would disappear in favour of AgHL.

TABLE 3

PERCENTAGE DISTRIBUTION OF Ag^+ AMONG THE VARIOUS COMPLEXED FORMS AND AMOUNT OF BASE REQUIRED AS A FUNCTION OF pH, CALCULATED FROM THE FOLLOWING VALUES OF STABILITY CONSTANTS

$k_1 = 1.6$; $k_2 = 1.0$; $K_1 = 2.70 \cdot 10^3$; $K_2 = 2.70 \cdot 10^3$; $K_{NO_3^-} = 0.58$

pH	*1.0*	*2.0*	*3.0*	*4.0*	*5.0*	*6.0*	*6.5*	*7.0*
Ag^+	63.01	61.29	58.08	57.08	56.83	55.62	52.44	42.21
$AgNO_3$	36.55	35.55	33.68	33.11	32.96	32.26	30.41	24.48
Ag (HL)	0.43	3.059	7.61	8.93	0.07	8.89	8.38	6.74
Ag $(HL)_2$	—	0.09	0.62	0.87	0.90	0.89	0.84	0.67
AgL	—	—	—	—	0.24	2.25	7.00	18.12
AgL_2	—	—	—	—	—	0.09	0.92	7.78
V_{OH}/V_{Ag} calcd.								0.34
V_{OH}/V_{Ag} measured								0.34

pH	*7.5*	*8.0*	*8.5*	*9.0*	*9.5*	*10.0*	*10.5*	*11.0*
Ag^+	20.29	4.22	0.55	0.07	—	—	—	—
$AgNO_3$	11.77	2.45	0.32	0.04	—	—	—	—
Ag (HL)	3.23	0.66	0.08	—	—	—	—	—
$Ag(HL)_2$	0.32	0.06	—	—	—	—	—	—
AgL	27.40	17.77	7.12	2.63	1.09	0.60	0.44	0.40
AgL_2	36.98	74.84	92.42	97.24	98.88	99.39	95.55	99.60
V_{OH}/V_{Ag} calcd.	1.01	1.65	1.82	1.70	1.32	0.77	0.33	0.118
V_{OH}/V_{Ag} measured	1.01	1.66	1.81	1.70	1.32	—	—	—

To our knowledge, the occurrence of complexes of Ag^+ or some other cation having $N^+H_3CH_2COO^-$ ions as ligands has not so far been considered. However, at least in the case under study, the hypothesis of their formation appears suitable for interpreting the experimental picture illustrated in Fig. 3.

Further evidence for the formation of complexes with $N^+H_3CH_2COO^-$ is indicated by the slight potential shift which a silver electrode dipped into a solution of 0.1 *M* glycine in *M* KNO_3, containing 10^{-3} *M* of Ag^+ undergoes when the pH changes from 1 to 6. Within limits, the experiment supports the existence of complexes in a pH-range incompatible with forms of the AgL and AgL_2 type and favourable to the formation of AgHL and $Ag(HL)_2$.

The potential shift is so small that it is around the sensitivity limits of the equipment used, yet it is positive and measurable. Previous unpublished measurements carried out in this Laboratory during the study of the system under the same experimental conditions, by the Leden method at constant pH = 4, gave k_1 equal to 1.1, but no reliable results were obtained for k_2.

RESULTS AND CONCLUSIONS

On the basis of the results presented, it is of interest to consider again, in Table 1, the stability constants found by different workers for the Ag^+–glycine system.

MONK and FLOOD AND LORAS, as well as DATTA AND GRZYBOWSKY adopted the Bjerrum method. Their constants, in fairly good agreement, refer to the complexes $[AgNH_2CH_2COO]^+$ and $[Ag(NH_2CH_2COO)_2]^-$. MONK, in particular, also obtained the same results measuring the solubility of $AgIO_3$ and $AgBrO_3$ in glycine solutions.

KEEFER AND REIBER, however, by the same solubility method, found a somewhat high value for K_1. The greater stability assigned to the complex comes from their omitting to take into account the possibility of formation of the bicoordinate complex that must be present in significant amounts under the experimental conditions they adopted.

The low value assigned by DUBOIS to K_1 is not easy to explain. Under the experimental conditions he adopted, the lack of buffering certainly did not allow for any control of pH, and the system (owing to an indeterminate composition) was not so suitable for an investigation by the Job continuous variation method as that used here.

A comparison of the V_{OH}/V_{Ag}–pH curves calculated by the different constants, with the experimental curve (Fig. 3) shows that the above acidimetric method can supply useful criteria for evaluating the reliability of the stability constants in complexes in which ligands with acid–base properties are involved. There is an interesting possibility that the formation of some complexes in unexpected amounts in a cation–ligand system may be indicated.

It appears, for instance, that the Ag^+–glycine system is not suitably described when complexes with $N^+H_3CH_2COO^-$ are not taken into account. It is also clear that a constant calculated on the wrong assumption that there is no bicoordinate complex (AgL_2) in solution, is not confirmed experimentally by acidimetry.

The Flood and Loras K_1, definitely higher than those of DATTA and MONK, gives rise to a V_{OH}/V_{Ag}–pH curve that clearly departs from the experimental values at pH 7 and 7.5. On this account Datta and Grzybowsky constants have been preferred

for calculating approximate values of k_1 and k_2. If the Flood constants were adopted, the computation method based on acidimetric measurements, would give values of k_1 and k_2 that were too high with respect to the potentiometric measurements. On the other hand, if k_1 and k_2 are already known, the acidimetric data would emphazise their inconsistency with the Flood K_1 and K_2 constants.

The acidimetric method has been developed chiefly in order to check whether the system composition is consistent with the value assigned to certain stability constants, and to have an indirect and independent criterion for evaluating the reliability of the constants themselves.

However, under favourable conditions, the acidimetric method can be useful also for determining the value of unknown constants.

The application of the method does not involve difficult experimentation, although it is necessary to bear in mind some fundamental points in order to avoid serious error.

As with other methods for determining stability constants, the acidimetric method is not an absolute method and in order to make the calculations the acid–base constants of the ligands have to be known under the conditions of composition and temperature at which the stability constants have to be determined.

Also in the area of pH >8.5 where AgL and AgL_2 are the only forms existing, any pair of values of K_1 and K_2 (keeping the ratio, $K_1/K_2 \approx 1$) can satisfy the V_{OH}/V_{Ag}–pH curve, because the base consumption depends upon the ratio, $[AgL]/[AgL_2]$.

Therefore, the constants given by various authors, though different, could be acceptable for this area of pH. However, if measurements are extended to less basic solutions, divergences come to light. Constants below the ratio 1/1, but higher in value, would cause the V_{OH}/V_{Ag}–pH curve to deviate in the less alkaline field or would require disallowable high values of k_1 and k_2. The method can be successfully applied especially if the measurement of V_{OH}/V_{Ag} is extended to a wide range of pH.

Finally, it must be stressed that in the present paper the constants found by other workers have been compared under slighly different experimental conditions and were used mostly in a medium of comparatively higher ionic strength.

A careful study of the above mentioned papers suggests that differences in the various reported results should be ascribed more to the uncertainty of measurements and methods used than to different experimental conditions. The figures in Table 1 show no effect of ionic strength or of temperature.

The acidimetric method avoids errors due to unexpected complexed forms or to arbitrary limitation of the coordination number (KEEFER).

Obviously, the use of the acidimetric method for calculating constants or for checking them rigorously within the uncertainty limits implied in the procedure, requires uniformity of experimental conditions. Another application will be the subject of a future report.

ACKNOWLEDGEMENT

I wish to express my grateful appreciation to Dr. BRUNELLA DALL'OCA for her kind collaboration in performing both experimental measurements and calculations.

The present work has been carried out with the help of contributions from the National Research Council of Italy.

SUMMARY

An acidimetric method is described that allows the nature of the ligand species in complexes of metals with ligands having acid–base character, to be defined. The basis of the procedure is the measurement of the quantity of H^+ displaced by the cation owing to complex formation. A comparison of the quantity of effectively displaced H^+ with the quantity that can be calculated on the basis of known values of stability constants is a useful criterion for evaluating the reliability of these constants. The method has found application in a study of the Ag^+–glycine system and has enabled the stability constant of the complex, $[Ag^+(N^+H_3CH_2COO^-)]$, to be calculated.

REFERENCES

1 Edited by L. G. SILLÉN AND A. E. MARTELL, *Stability Constants, Chem. Soc., London, Spec. Publ. No. 17*, 1964.
2 P. LANZA AND I. MAZZEI, *J. Electroanal. Chem.*, 12 (1966) 320.
3 C. B. MONK, *Electrolytic Dissociation*, Academic Press, New York, 1961, p. 140.
4 H. L. JOHNSTON, F. CUTA AND A. B. GARRETT, *J. Am. Chem. Soc.*, 55 (1933) 2311.
5 C. B. MONK, *Trans. Faraday Soc.*, 47 (1961) 292.
6 S. DUBOIS, *Compt. Rend.*, 224 (1947) 113.
7 H. V. FLOOD AND V. LORAS, *Tidsskr. Kjemi Bergvesen, Met.* 5 (1945) 83, cited by F. R. N. GURD AND P. E. WILCOX in: *Advan. Protein Chem.*, 11 (1956) 311.
8 R. M. KEEFER AND H. G. REIBER, *J. Am. Chem. Soc.*, 63 (1941) 689.
9 V. DATTA AND H. K. GRZYBOWSKY, *J. Chem. Soc.*, (1959) 1091.

ELECTROANALYTICAL CHEMISTRY AND INTERFACIAL ELECTROCHEMISTRY
Elsevier Sequoia S.A., Lausanne – Printed in The Netherlands

AN ACIDIMETRIC CRITERION FOR EVALUATING THE RELIABILITY OF STABILITY CONSTANTS OF COMPLEXES AND THE NATURE OF THE LIGANDS

II. APPLICATIONS TO THE STUDY OF THE Ag^+–1,3-DIAMINOPROPANE SYSTEM

P. LANZA

Chemical Institute "G. Ciamician", Specialization School in Analytical Chemistry of the University of Bologna (Italy)

(Received March 28th, 1968)

INTRODUCTION

An acidimetric method for checking the reliability of stability constants of complexes with ligands having acid–base properties has been described in the previous paper[1]. It is based on the observation that the addition of a complexable cation to an acid–base ligand solution is always followed by a decrease in the pH. As the change of pH is the result (among other factors) of the quality and quantity of the complexes forming, there is a relation between this change and the stability constants of complexes in the system.

The method is therefore based on the measurement of the quantity of base required to restore a ligand solution to the initial pH-value, in the case that the pH had been altered by the addition of a certain quantity of complexable cation.

If the quantity of base used under standard experimental conditions is computable in terms of the constants of the complexes, a comparison between the quantity of base used and that calculated can be a useful criterion for establishing the accuracy of the constants used in the calculation.

The previous paper[1] describes the calculation procedure and the methods adopted and reference should be made to it for details.

The procedure has been successfully applied in the study of the Ag^+–glycine system because it has enabled the most reliable stability constants to be selected from those available in the literature. Also it was possible to point out the existence of the Ag^+ complex with glycine in the $\overset{+}{N}H_3CH_2COO^-$ form and approximately evaluate its stability.

The present paper deals with the Ag^+–1,3-diaminopropane system. This subject has been treated by SCHWARZENBACH, *et al.*[2] and BERTSCH *et al.*[3]. SCHWARZENBACH found the following constants for this system ($t=20°$, $\mu=0.1$ KNO_3):

$\log k_1 = 2.60$ (relevant to AgHL complex)

$\log K_1 = 5.85$ (relevant to AgL complex)

$\log K_1K_2 = 7.65$ (relevant to AgL_2 complex)

($HL=NH_2(CH_2)_3\overset{+}{N}H_3$; $L=NH_2(CH_2)_3NH_2$).

Constants k_1 and K_1 were obtained experimentally while K_2 was obtained from theoretical considerations[4].

However, since the Schwarzenbach method is based on a study of the neutralization curves of the ligand alone or in the presence of a considerable excess of complexable cation, it is not suitable for determinating k_2 and K_2 successive constants.

BERTSCH *et al.*, applying the Bjerrum method, found log $K_1=5.92$ ($\mu=0.1$; 20°) in agreement with SCHWARZENBACH's result.

None of these workers was able to determine the constant, k_2, relevant to the $Ag(HL)_2$ complex. Owing to the difficulty involved in measuring this constant by the usual methods, the acidimetric procedure was tried.

In order to test the practical possibilities of the new method and to establish a comparison with results obtained by standard methods, constants K_1 and K_2 relevant to the AgL and AgL_2 complexes and also the acid dissociation constants of 1,3-diaminopropane at 25° in N KNO_3 have been determined.

In order to determine K_1 and K_2 experimentally, the potentiometric method of LEDEN has been applied[5]; this seems to suit the problem particularly well, provided that the measurements are carried out at constant and high pH as, under these conditions, only AgL and AgL_2 complexes are formed; there is no formation of Ag(HL) and $Ag(HL)_2$. This simplifies the problem because the complexes in the L-form are much more stable than those in HL-form. On the other hand, and for the same reason, it is impossible to apply this method when measuring k_2 for $Ag(HL)_2$, because the data would be altered owing to the presence of AgL.

EXPERIMENTAL

For a description of the general methods of measurement and calculation, reference should be made to the previous paper[1], the account in this paper being limited to those experiments concerning the system under study.

Determination of the acid dissociation constants of 1,3-diaminopropane

As there are no published data for the propylenediamine acid dissociation constants under the conditions used in the present investigation, the constants were determined at 25° in 1 M KNO_3 solution by means of a potentiometric titration curve. As the constants have very nearly the same value, calculations were carried out, using the method of Noyes[6]. The values obtained, expressed as association constants,

TABLE 1

AVAILABLE STABILITY CONSTANTS FOR THE Ag^+–1,3-DIAMINOPROPANE SYSTEM

Author	*log* k_1	*log* k_2	*log* K_1	*log* K_1K_2	*Exptl. conditions*
SCHWARZENBACH *et al.*	2.60	—	5.85	7.65	20° μ = 0.1
BERTSCH *et al.*	—	—	5.92	—	20° μ = →0
This work, Leden method	—	—	6.20	7.60	25° μ = 1
This work, acidimetric method	3.18	2.80	6.72	7.85	25° μ = 1

were: $\log K_{HL} = 10.80$ and $\log K_{H_2L} = 9.19$ (during the titration, the ionic strength varied from 1.0 to 1.3).

The acid–base constants being known, the distributions of the different forms as a function of pH have been calculated. The results are plotted in Fig. 1.

Determination of the stability constants of Ag^+ complexes with $H_2N(CH_2)_3NH_2$

For the measurements of constants $K_1 = [AgL]/[Ag^+][L]$ and $K_2 = [AgL_2]/[L][AgL]$ in 1 *M* KNO_3 at 25° ,the Leden method was adopted[5]. Increasing quantities of a solution of 0.05 *M* propylenediamine in 1 *M* KNO_3 at pH 12.2, containing 10^{-3} *M* $AgNO_3$ to keep the total Ag^+ concentration and the ionic strength constant, were added to a solution of 10^{-3} *M* $AgNO_3$ in 1 *M* KNO_3. After the addition, the pH was restored by adding 1 *N* NaOH and the variations of potential, as indicated by a silver electrode, were noted.

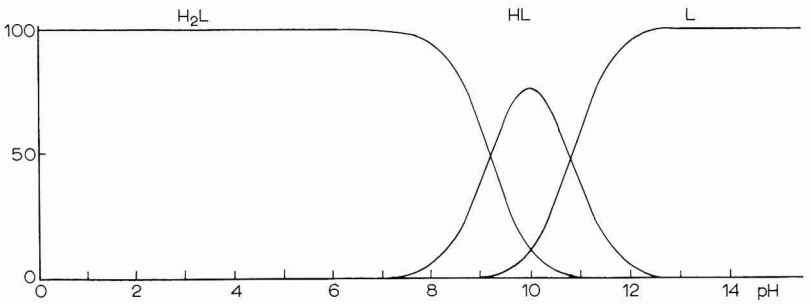

Fig. 1. Distribution diagram for various forms of 1,3-diaminopropane in 1 *N* KNO_3 at 25° as a function of pH.

The potentiometric measurement and a knowledge of the concentration of free and complexed ligand enable the successive partial constants of complexes present in the system to be calculated. For the calculation details, reference should be made to the original publication by LEDEN or to the two fundamental treatises on this subject by SCHLÄFER[7] and ROSSOTTI AND ROSSOTTI[8].

Our results were as follows:

$\log K_1 = 6.20$; $\log K_2 = 1.40$ (at 25° in 1 *M* KNO_3).

Application of the acidimetric method for evaluating the accuracy of the constants available

An important application is a check on whether the available stability constants justify the composition of the system based on the acidimetric data. First, the distribution of different complexes is determined by using the available constants: $\log k_1 = 2.60$; $\log K_1 = 6.20$ and $\log K_2 = 1.40$. For this exploration calculation, the Schwarzenbach k_1 constant has been accepted although it should not be suitable for our experimental conditions because it is valid at 20° and $\mu = 0.1$.

The distribution being known, the V_{OH}/V_{Ag}–pH curve is then calculated by applying the methods described in the previous paper[1].

By comparing the values obtained in this way with those obtained experimentally (Fig. 2), notable differences, for the pH-range considered, have been observed;

these cannot be explained solely by the fact that k_1, obtained under different experimental conditions, is probably too low for the system under study.

Also, if the value is doubled, results are no longer in agreement, and the points approach to and depart from the experimental value according to the pH-value considered.

The results obtained by acidimetric measurements indicate that the three constants used are insufficient for an accurate description of the system under study.

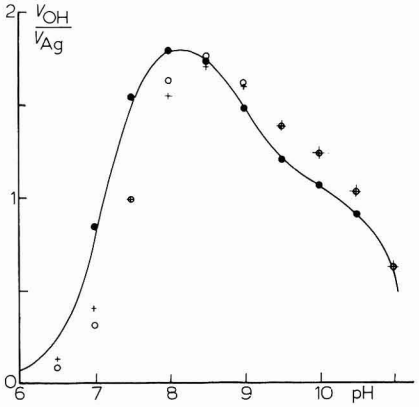

Fig. 2. Acidimetric curve for the Ag^+–1,3-diaminopropane system. Calcd. points for various values of stability constants.

log k_1	*log* k_2	*log* K_1	*log* K_2
(○), 2.70	—	6.20	1.40
(+), 3.00	—	6.20	1.40
(—), 3.19	2.74	6.71	1.14
(●), exptl. points			

Calculation of the stability constants from acidimetric data

The considerable difference between the experimental and calculated values as shown in Fig. 2 cannot be ascribed to inaccurate values of the three constants, k_1, K_1 and K_2, indeed the values given to them by different workers are in fairly good agreement.

It seems advisable to take into consideration the possible presence of the $Ag(HL)_2$ complex. This form was admitted by SCHWARZENBACH, although the technique he adopted was not suitable for calculating its stability constants.

Owing to the difficulty of using the usual methods, the acidimetric procedure was tried in order to obtain an independent calculation of all four constants, k_1, k_2, K_1 and K_2.

If the distribution of the complexes obtained in this preliminary way using the above constants is considered, it can be deduced that at $pH < 9$, the complex AgL_2 is practically absent. In this case, the system composition can be determined by the constants k_1, k_2 and K_1, of the AgHL, $Ag(HL)_2$ and AgL complexes.

The calculation is carried out in the following way: as stated in the previous paper, the fraction of the various complexed forms is given by the equations:

$$[AgHL]/C_{Ag}=k_1[HL]/\Delta \quad (1)$$

$$[Ag(HL)_2]/C_{Ag}=k_1k_2[HL]^2/\Delta \quad (2)$$

$$[AgL]/C_{Ag}=K_1[L]/\Delta \quad (3)$$

where $\Delta=1+K_{NO_3^-}[NO_3^-]+k_1[HL]+k_1k_2[HL]^2+K_1[L]$

As has been demonstrated in the introduction, since HL and H_2L are practically the only forms present in the range of pH investigated, the ratio, V_{OH}/V_{A_g}, is related to the distribution of the complexes according to the equation:

$$V_{OH}/V_{Ag}=\{n/(1+R)+h\}1/C_{Ag} \quad (4)$$

where

$$n=[AgHL]+2[Ag(HL)_2]+[AgL] \quad (5)$$

$$h=[AgL] \quad (6)$$

$$R=[HL]_0/[H_2L]_0 \quad (7)$$

By introducing expressions (5), (6) and (7) into (4) and using eqns. (1), (2) and (3) for the various fractions of the complexes as functions of the constants, the following equation is obtained:

$$\frac{[HL]k_1+2[HL]^2k_1k_2+[L]K_1+[L]K_1(1+R)}{1+[NO_3^-]K_{NO_3^-}+[HL]k_1+[HL]^2k_1k_2+[L]K_1}=\frac{V_{OH}}{V_{Ag}}(1+R) \quad (8)$$

As $K_{NO_3^-}=0.58^9$, by using the experimental values of V_{OH}/V_{Ag} at pH 7.0, 7.5, 8.0, 8.5 and 9.0, the following five equations result, where the unknown quantities are the constants k_1, k_2 and K_1:

$$\begin{aligned}
&0.1193\cdot 10^{-3}\,k_1+0.4859\cdot 10^{-6}\,k_1k_2+0.12053\cdot 10^{-6}\,K_1=1.3272 && (pH=7.0)\\
&-1.1367\cdot 10^{-3}\,k_1+1.6981\cdot 10^{-6}\,k_1k_2+0.4491\cdot 10^{-6}\,K_1=2.4825 && (pH=7.5)\\
&-5.4867\cdot 10^{-3}\,k_1+3.4741\cdot 10^{-6}\,k_1k_2+1.5247\cdot 10^{-6}\,K_1=3.0106 && (pH=8.0)\\
&-18.3176\cdot 10^{-3}\,k_1-23.6472\cdot 10^{-6}\,k_1k_2+10.302\cdot 10^{-6}\,K_1=3.2905 && (pH=8.5)\\
&-55.910\cdot 10^{-3}\,k_1-660.16\cdot 10^{-6}\,k_1k_2+129.80\cdot 10^{-6}\,K_1=3.8469 && (pH=9.0)
\end{aligned} \quad (9)$$

If $10^{-3}\,k_1=x$, $10^{-6}\,k_1k_2=y$ and $10^{-6}\,K_1=z$, a system of five linear non-homogeneous equations containing three unknowns is obtained. The empirical character of these equations does not allow the system to have exact roots, but the best solution is obtained by applying the least-squares method. By using standard procedures of numerical calculus[10] system (9) is transformed into the following normal three-equations system with three unknown quantities:

$$\begin{aligned}
&3.4928\,x+37.3217\,y-7.4547\,z+0.2945=0\\
&37.3217\,x+436.3856\,y-85.9262\,z+2.6021=0\\
&-7.4547\,x+85.9262\,y+16.9567\,z-0.5391=0
\end{aligned} \quad (10)$$

From which, with suitable substitutions, is obtained:

$$k_1=1.57\cdot 10^3;\ k_2=5.57\cdot 10^2;\ K_1=5.16\cdot 10^6$$

In order to find the value of K_2, it is advisable to consider the field at the highest pH-values where, presumably contributions from AgHL and $Ag(HL)_2$ are negligible. In this case, however, it is not easy to state a system of equations to three or more

points of the V_{OH}/V_{Ag}–pH curve; on this account and since for pH-values 9.5–10.5 all three acid–base forms of the buffer are present in comparable quantities and (according to the previous paper) equations of the general case should be applied (see eqns. (10)–(15), ref. 1).

A start can be made to the approximate calculation of K_2 by introducing some simplifications.

For instance, if the system is considered at pH 10.5 (where 3.16% of the H_2L-form is present and its contribution can be assumed to be negligible for the purpose of an approximate calculation) the following equation can be used:

$$V_{OH}/V_{Ag} = \{(n - mR)/(1 + R)\}1/C_{Ag} \tag{11}$$

as in ref. 1, where

$$n = [AgL] + 2[AgL_2]\,;\; m = [AgHL] + 2[Ag(HL)_2]\,;\; R = [L]_0/[HL]_0$$

This equation relates the base consumption (V_{OH}/V_{Ag}) with the quantity and quality of the complexes formed (n and m) and the buffering conditions of the ligand (R), and is strictly true for $[H_2L] = 0$. At pH = 10.5, $R = 0.5$, $V_{OH}/V_{Ag} = 0.90$, and, to a good approximation, the concentrations of AgHL and $Ag(HL)_2$ can be considered as negligible ($mR \ll n$). We have therefore:

$$V_{OH}/V_{Ag} = \{(n - mR)/(1 + R)\}1/C_{Ag} \approx \{n/(1 + R)\}1/C_{Ag} = 0.90 \tag{12}$$

which gives:

$$n = [AgL] + 2[AgL_2] = 1.35 \cdot C_{Ag} \tag{13}$$

If complex forms other than AgL and AgL_2 do not exist,

$$\{[AgL] + [AgL_2]\}/C_{Ag} = 1 \tag{14}$$

Equations (13) and (14) are verified for one value of the ratio:

$$[AgL_2]/[AgL] = 0.538$$

We have, therefore, the first approximate value of K_2:

$$K_2 = \{[AgL_2]/[AgL][L]\} = 0.538/[L] = 0.538/32.34 \cdot 10^{-3} = 16.6$$

The constants, k_1, k_2 and K_1, being known, the exact value of K_2 can be found by assigning subsequent values to it in (1), (2) and similarly to find the distribution of complexes such as to verify at pH = 10.5 the experimental datum, $V_{OH}/V_{Ag} = 0.90$. According to this procedure the following distributions values and V_{OH}/V_{Ag} were obtained:

K_2	*16*	*14*	*12*
Ag^+	—	—	—
$AgNO_3$	—	—	—
AgHL	0.039	0.041	0.043
$Ag(HL)_2$	1.41	1.48	1.54
AgL	64.93	67.80	70.90
AgL_2	33.61	30.68	27.31
V_{OH}/V_{Ag}	0.9241	0.9026	0.8791

Bearing in mind that V_{OH}/V_{Ag} is accurate to ± 0.01, we get by graphical interpolation:

$$K_2 = 13.8 \pm 0.85$$

The four constants, k_1, k_2, K_1 and K_2, being known, the distribution of the complexes and the real V_{OH}/V_{Ag}-values can be calculated (Fig. 3); the latter agree with the experimental data over the pH-range considered (Fig. 2).

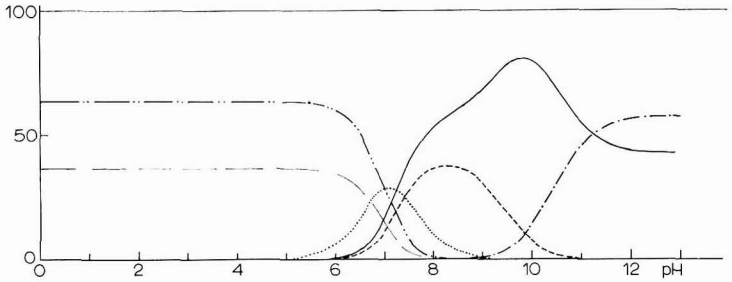

Fig. 3. Distribution diagram for the Ag^+–1,3-diaminopropane system in 1 N KNO_3 at 25° as a function of pH, calcd. with the constants: $k_1 = 1.57 \cdot 10^3$; $k_2 = 5.57 \cdot 10^2$; $K_1 = 5.16 \cdot 10^6$; $K_2 = 13.8$. (—..—)Ag^+,(——)$AgNO_3$, (.....)AgHL, (—)AgL, (—.—)AgL_2, (----)Ag $(HL)_2$.

RESULTS AND DISCUSSION

The chemical literature is lacking in data relevant to the system under study. The only works that have been found to apply are those of SCHWARZENBACH and BERTSCH. Constants available at present are listed in Table 1. First, it can be seen that the calculated V_{OH}/V_{Ag}–pH curve does not pass through the experimental points over the pH range considered if the four constants are not introduced in the calculations. This proves that the system cannot be composed of the AgL- and AgL_2-forms alone and that AgHL and $Ag(HL)_2$ are also abundantly present in wide pH-ranges. On the other hand, the above statement also agrees with the interpretation of SCHWARZENBACH although his method of measurement does not permit the determination of K_2. The presence of other forms, such as Ag_2L or Ag_2L_2, that are likely to exist in a system with excess Ag^+, could not even be indicated by the acidimetric method, because the former, owing to its stability constant being about 10^5 times smaller than AgL_2, would be present in negligible quantities under experimental conditions similar to those of the present research; the Ag_2L_2 complex would not behave differently from AgL for acidimetric purposes. On the other hand, BERTSCH *et al.* did not succeed in detecting the AgL_2 form because (the ratio K_1/K_2 being as high as $3.74 \cdot 10^4$) they should have extended their measurements to a much higher concentration of free diamine (inflexion point of the formation curve at $p[L] = 1.14$.) It is not clear why BERTSCH *et al.* disregarded the presence of AgHL and $Ag(HL)_2$. Under their experimental conditions, p[L] varies from 5.2 to 6.2 (see the formation curve in Fig. 1 of their paper[3]). As a result of the total concentration of 1,3-diaminopropane that they used, the concentrations of the HL-and H_2L-forms should be high and allow the formation of AgHL and $Ag(HL)_2$ in significant quantities. However, it must be emphasized that the Bjerrum method is essentially based on the presupposition that in any system, no matter how complex, these is only one ligand

species; otherwise, the fact that the formation curve has the shape of the theoretical formation curve does not guarantee the reliability of the results, as n would lose its exact meaning.

The experiments described above show that the presence in the system of forms other than the AgL and AgL_2 complexes seems clearly proved by the acidimetric method.

The extent of the deviations shown in Fig. 2 indicate that complexes other than AgL and AgL_2 are certainly present in significant quantities at $pH < 9$. The acidimetric method can be directly applied for the calculation of k_1 and k_2 under far less critical conditions than those implied when adopting the Ag^+–glycine system studied in the previous paper.

ACKNOWLEDGEMENT

I wish to express my grateful appreciation to Dr. BRUNELLA DALL'OCA, for her kind collaboration in performing both experimental measurements and calculations.

The present work has been carried out with the contribution of the National Research Council of Italy.

SUMMARY

The Ag^+–1,3-diaminopropane system has been studied by the application of a new acidimetric method, which allows the nature of the ligand species in complexes with ligands having acid–base properties to be defined.

The existence of complexes involving protonated ligands has been proved. The stability constants of the complexes, $Ag^+NH_2(CH_2)_3\overset{+}{N}H_3$ and $Ag^+(NH_2(CH_2)_3\overset{+}{N}H_3)_2$, have been measured.

REFERENCES

1 P. LANZA, *J. Electroanal. Chem.*, 19 (1968) 275.
2 G. SCHWARZENBACH, B. MAISSEN AND H. ACKERMANN, *Helv. Chim. Acta*, 35 (1952) 2333.
3 C. R. BERTSCH, W. C. FERNELIUS AND P. B. BLOCK, *J. Phys. Chem.*, 62 (1958) 444.
4 G. SCHWARZENBACH, *Helv. Chim. Acta*, 36 (1953) 23.
5 J. LEDEN, *Z. Phys. Chem. A*, 188 (1941) 160.
6 A. A. NOYES, *Z. Phys. Chem.*, 11 (1893) 495; A. ALBERT AND E. P. SERJEANT, *Ionization Constants of Acid and Bases*, Methuen and Co. Ltd, London, 1962.
7 H. L. SCHLÄFER, *Komplexbildung in Lösung*, Springer Verlag, Berlin-Göttinger-Heidelberg, 1961.
8 F. J. C. ROSSOTTI AND M. ROSSOTTI, *The Determination of Stability Constants*, McGraw-Hill, New York-London, 1961.
9 G. B. MONK, *Electrolytic Dissociation*, Academic Press, New York, London, 1961, p. 140.
10 G. BOAGA, *Calcolo Numerico*, Fasano, Milano, 1949, p. 280.

ELECTROANALYTICAL CHEMISTRY AND INTERFACIAL ELECTROCHEMISTRY
Elsevier Sequoia S.A., Lausanne – Printed in The Netherlands

POLAROGRAPHIC REDUCTION OF SOME ACETOPHENONES

J. R. JONES
Department of Chemistry, University of Surrey, London (England)
J. A. ROWLINSON
May and Baker Ltd., Dagenham, Essex (England)
(Received January 31st, 1968; in revised form, April 10th, 1968)

Although a great deal of information on various aspects of homogeneous chemical reactions has been arrived at assuming that the effect that a particular substituent has on the rate of reaction is related to a substituent factor, the same cannot be said for heterogeneous reactions. This is partly because even if we restrict our considerations to a series of structurally related compounds and assume that the mechanism of the electrode process is the same for all, and that the half-wave potentials are measured under identical conditions, it would still seem likely that a satisfactory structure–rate relationship would have to take into account the properties of the electrode–solution interface. Unfortunately, details of such interfaces are known for relatively few systems. However, a considerable amount of polarographic work[1] has been done on the basis that the rates of heterogeneous electrode processes are principally influenced by the same structural changes that would bring about similar changes in the rates of homogeneous chemical reactions. Therefore, the value of the reaction constant (ϱ) is not considered in terms of the composition of the solvent and supporting electrolyte, and the results available frequently refer to widely different solvents, and there is little basis for a quantitative consideration of individual ϱ-values.

The equation relating the half-wave potential ($E_{\frac{1}{2}}$) and the rate of an irreversible electrode process (k_f) at 25° is:

$$E_{\frac{1}{2}} = -0.2142 + (0.05915/\alpha n_a)\log(1.349\, k_f\, t^{\frac{1}{2}}/(D_0^{\frac{1}{2}}) \quad (1)$$

Then in the case of structurally similar compounds,

$$\Delta E_{\frac{1}{2}} = (0.05915/\alpha n_a)\log(k_1/k_2) \quad (2)$$

provided D_0 and t are constant.
As the equation relating rate and structure is of the form

$$k_1/k_2 = \varrho\sigma \quad (3)$$

it follows that

$$d\Delta E_{\frac{1}{2}}/d\sigma = 0.05915\varrho/\alpha n_a = \varrho' \quad (4)$$

and it is ϱ-values which should thus be compared when comparisons with different homogeneous reactions are made. But in order that this be justified it is necessary to show that:

(1) both D and t either remain constant for a series of compounds, or the variation can be allowed for;

(2) αn_a, the product of the transfer coefficient and the number of electrons transferred in the rate-determining process, is constant;

(3) the contribution made by the electrode double layer is taken into account.

EXPERIMENTAL

The polarograms were obtained using an Atlas-Tast polarograph, with the cell thermostatically controlled at $25 \pm 0.05°$. The potentials were measured with reference to an Ag/AgCl electrode which was standardised against a saturated calomel electrode using a Cambridge potentiometer and a Weston standard cell.

All the ketones, which were either purchased commercially or prepared by methods described in the literature, were either distilled or recrystallised prior to use and subjected to gas–liquid chromatography and infrared analysis. The ketone solutions were at a concentration of 10^{-3} M and 10^{-1} M with respect to KCl which was used as the supporting electrolyte.

The drop-time (t) of the electrode was determined at intervals of 0.02 V of applied potential over the whole range employed, and values of αn_a were obtained as outlined in the discussion.

RESULTS

Table 1 contains the values of drop-times as a function of the applied potential. Table 2 contains the values of $E_{\frac{1}{2}}$ as measured, as well as those corrected for different droptimes and also for the structure of the electrode double layer. The values of the ionisation rate coefficients, $k^{H}_{OH^-}/3$, are taken from the work of JONES *et al.*[2,3].

TABLE 1

DROP-TIMES AS A FUNCTION OF APPLIED POTENTIAL

Potential (V)	*Drop-time (sec)*	*Potential (V)*	*Drop-time (sec)*	*Potential (V)*	*Drop-time (sec)*
(a) Meta- and para-substituted acetophenones					
−1.48	2.53	−1.60	2.45	−1.72	2.20
−1.50	2.52	−1.62	2.40	−1.74	2.20
−1.52	2.52	−1.64	2.42	−1.76	2.18
−1.54	2.50	−1.66	2.40	−1.78	2.18
−1.56	2.46	−1.68	2.38	−1.80	2.16
−1.58	2.46	−1.70	2.28		
(b) Ortho-substituted acetophenones					
−1.44	3.58	−1.54	3.38	−1.61	3.21
−1.46	3.52	−1.56	3.33	−1.63	3.16
−1.48	3.48	−1.58	3.34	−1.65	3.12
−1.50	3.46	−1.60	3.24	−1.67	3.16
−1.52	3.41				

TABLE 2

HALF-WAVE POTENTIALS FOR A SERIES OF ACETOPHENONES AND IONISATION RATE COEFFICIENTS ($k^{H}_{OH^-}/3$) AT 25°

Ketone	αn_a(*av.*)	$-E_{\frac{1}{2}}$			$10^3 k^{H}_{OH^-}/3$	
		measured	*Corrected for t*	*Corrected for t and ψ*	($l\,m^{-1}\,sec^{-1}$)	σ
1. *p*-methylacetophenone	0.84	1.745	1.940	1.800	159	−0.17
2. *m*-methylacetophenone	1.0	1.682	1.846	1.712	216	−0.069
3. acetophenone	0.96	1.671	1.843	1.709	244	0.0
4. *p*-fluoroacetophenone	1.0	1.668	1.824	1.691	290	+0.062
5. *m*-methoxyacetophenone	1.2	1.663	1.802	1.670	340	+0.115
6. *p*-bromoacetophenone	0.67	1.622	1.786	1.654	410	+0.232
7. *m*-fluoroacetophenone	1.0	1.593	1.752	1.622	450	+0.337
8. *m*-bromoacetophenone	1.0	1.571	1.733	1.604	470	+0.391
9. *o*-methylacetophenone	0.96	1.642	1.818	1.686	487	
10. *o*-bromoacetophenone	0.48	1.505	1.859	1.724	2350	
11. *o*-fluoroacetophenone	0.94	1.516	1.696	1.578	420	
12. *o*-methoxyacetophenone	0.76	1.566	1.788	1.656	225	
13. *o*-chloroacetophenone	0.86	1.645	1.845	1.711	2200	

DISCUSSION

In order that the half-wave potential obtained takes into account the variation in drop-time as a function of applied potential, the individual values of diffusion coefficients, and the term αn_a, it is necessary to specify a corrected value given by

$$E_{\frac{1}{2}}(\text{corrected}) = E_{\frac{1}{2}} - (0.02957/\alpha n_a)/\log t/D \tag{5}$$

The appropriate values of t and αn_a are given in Tables 1 and 2. It can be seen that the drop-time decreases in an almost linear manner with applied potential and that except for *ortho*-bromoacetophenone the values of αn_a are close to unity. As far as the other factors are concerned, no data are available for the diffusion coefficient of any of the acetophenones, either in water or 0.1 *M* KCl solutions. Although the variation in the diffusion coefficient of an ion at low salt concentrations can be predicted theoretically, no such solution exists in the case of a non-electrolyte. However, accurate measurements[4] of the self-diffusion coefficient of water in water and in a number of salt solutions have been made and the results found to obey the equation:

$$D_{\text{soln.}} = D_{H_2O}(1 - hm) \tag{6}$$

where h is a parameter related to the average hydration number of the cation. Thus for a 0.1 *M* KCl solution, the diffusion coefficient of water is $2.15 \cdot 10^{-5} cm^2 sec^{-1}$ compared to $2.25 \cdot 10^{-5} cm^2 sec^{-1}$ in pure water. Therefore, the effect of supporting electrolyte on the diffusion coefficient, assuming it to be the same for other molecules, can be neglected.

As no experimental data exist for the diffusion coefficients of the acetophenones in aqueous media, we have assumed that these can be given, to a good approximation, by the equation of Stokes:

$$D = (2.96/\eta)\ (d/M)^{1/3} \tag{7}$$

where d and M are the density and molecular weight of the compound, respectively,

and η, the viscosity of the medium, is effectively that of 0.1 M KCl solution. By taking the average value of d/M for the 13 acetophenones studied, an average diffusion coefficient of $6.3 \cdot 10^{-6}$cm^{2}sec^{-1} is obtained.

There is one further factor that, although not represented in eqn. (5), may affect the reproducibility of the $E_{\frac{1}{2}}$-values. This arises from the fact that as hydrogen ions are being consumed in the reduction process, the pH at the electrode surface will increase as the cathodic current increases. This can be avoided by the use of buffered solutions, but unfortunately, electrode double-layer characteristics for such media are not readily obtainable. We have therefore used an aqueous medium and find the half-wave potentials to be highly reproducible (± 0.003 V) and unaffected by changes in ketone concentration. We have then assumed that such a contribution is not important in the present work.

The value of αn_a given for each compound is the mean of two separate values. These were obtained[5] as a result of measurements of the currents at various potentials near the foot of the wave, and, as the cathodic current resulting from reduction at any potential is given by

$$i_c = nFAC^\circ k' \exp[-\alpha n_a F(E-E')/RT] \tag{8}$$

where k' is the value of the rate constant for the electrode process when the electrode potential, E, is equal to the reference value, E', a plot of log i *vs.* $E_{d.e.}$ will be a straight line with a slope at 25° of $-\alpha n_a/0.05915$ V. A further value of αn_a can be obtained from the slope of a plot of $E_{d.e.}$ *vs.* log $[(i/(i_d-i)] - 0.546$ log t, the latter being $0.054/\alpha n_a$ V. Of the 13 compounds studied, 10 give αn_a-values within 20% of unity, and in the further case of *o*-bromoacetophenone an extra factor (steric) seems to be important. Consequently, the near constancy of the values suggest their accuracy so that the point mentioned by ZUMAN[1], namely that a good $E_{\frac{1}{2}}$ *vs.* σ correlation becomes poor when $\Delta\alpha n_a$ is inserted, is not valid. Our findings are also at variance with those of SCHWABE[6] who found αn_a to vary with structure. In this way, the constant values are able to contribute towards the elucidation of the stoichiometry of the rate-determining step associated with a totally irreversible wave.

The electrode potential (E) is composed of two contributions:

(a) the potential difference between the reaction surface and the bulk of solution (ψ), which will influence the concentration of any charged species in such a way that,

$$C_s = C_b \exp(-z'F\psi/RT) \tag{9}$$

where C_s and C_b are the concentrations at the reaction surface and in the bulk of solution, and z' is the charge on the electroactive species;

(b) the potential difference between the electrode and reaction surface ($E-\psi$), influences the rate constant of the electron-transfer step so that eqn. (8) becomes:

$$i_c = nFA\, C_b k_f^* \exp\{-F[(\alpha n_a E) + (z' - \alpha n_a)\psi]/RT\} \tag{10}$$

where k_f^* is the heterogeneous rate constant when $\psi = 0$. ψ is a function of the electrolyte and, for a z–z valent electrolyte, its value can be computed from the Gouy–Chapman theory using the equation

$$\psi = (2RT/zF) \sinh^{-1}(\pi q^2/2\varepsilon KTc)^{\frac{1}{2}} \tag{11}$$

Values of the surface charge density (q) and its variation with applied potential have

been determined for a number of media[7] including 0.1 M aqueous KCl solution. On this basis, values of ψ were determined and a plot of $\{(E_{\frac{1}{2}})+[(z-\alpha n_a)/\alpha n_a]\psi\}$ *vs.* σ (Fig. 1) and *vs.* log $k^{H}{}_{OH^-}/3$ (Fig. 2) were made, the $E_{\frac{1}{2}}$ value having been previously corrected for different drop-times.

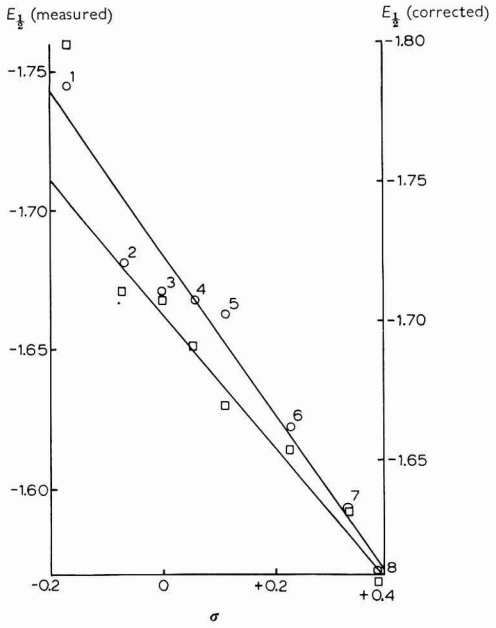

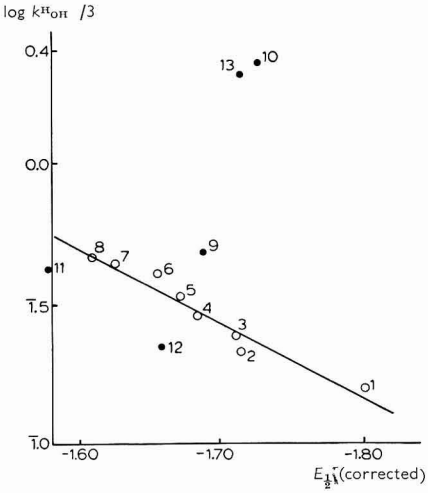

Fig. 1. Plot of $E_{\frac{1}{2}}$ (measured) and $E_{\frac{1}{2}}$ (corrected) (for t and ψ) *vs.* σ. Numbers correspond to those given in Table 2 and □ to right-hand side axis.

Fig. 2. Plot of $E_{\frac{1}{2}}$ (corrected) (for t and ψ) *vs.* log ionisation rate coefficient; (●) refers to *ortho*-substituents.

When half-wave potentials that take into account all relevant physical factors have been obtained, variations in $E_{\frac{1}{2}}$ caused by substituents in the aromatic ring can then be discussed. First, it is necessary to know the mechanism of the reduction, as there are two possibilities. In one case, one electron would be transferred, giving pinacol as product:

$$C_6H_5COCH_3 + e^- + H^+ = C_6H_5\dot{C}OHCH_3$$

or two electrons can be involved giving carbinol:

$$C_6H_5COCH_3 + 2e^- + 2H^+ = C_6H_5CHOHCH_3$$

The near constancy of αn_a, except in the case of *o*-bromoacetophenone, together with the value of near unity suggest that it is the latter mechanism that is involved. Furthermore, the much lower value of αn_a for *o*-bromoacetophenone can be attributed to the fact that the large *ortho*-substituent hinders the approach of the second hydrogen. This is in keeping with the fact that the bromo-group is the largest *ortho*-substituent employed. We have also calculated some values of n from the height of the polarographic wave using eqn. (11).

$$I = 607\, nD^{\frac{1}{2}} \qquad (11)$$

where I, the diffusion current constant, is defined by $I = i_d/Cm^{\frac{2}{3}}t^{\frac{1}{6}}$. In each case, the values obtained (1.7 acetophenone, 2.1 *m*-fluoro, 1.9 *m*-methyl, 2.2 *m*-methoxy, 1.8 p-methoxy and 2.1 *p*-fluoro) are consistent with the above, although in view of the theoretical limitations involved, no great significance can be attached to the absolute values.

Reduction of substituted acetophenones at a dropping mercury electrode will be facilitated by electron-withdrawing groups, and the influence of inductive and mesomeric factors will operate in the opposite direction to those present in the ionisation of acetophenones in alkaline media[2]:

$$XC_6H_4COCH_3 + OH^- \rightarrow XC_6H_4COCH_2^- + H_2O$$

Consequently, the slope of the $E_{\frac{1}{2}}$ (corrected) *vs.* log $k^{H}_{OH^-}/3$ for *meta*- and *para*-substituted acetophenones will reflect the different extent to which mesomeric and inductive forces can influence reaction at the carbonyl and methyl groups.

In the case of *ortho*-substituted acetophenones it is necessary to consider the importance of steric factors. Although it is sometimes suggested that polarographic reductions of compounds should be less sensitive to steric factors than most chemical reactions involving the same compound, there is as yet little direct evidence relating to the polarographic behaviour of densely sterically-hindered compounds. Where evidence is available, it concerns the electrochemical reduction of aromatic compounds containing an *ortho*-substituent and shows that these compounds are much easier to reduce than predicted. In other words, the half-wave potential becomes less negative than for the corresponding *meta- and para*-substituted compounds, in agreement with the present findings, with the exception of *o*-bromoacetophenone. This is the largest *ortho*-substituent employed and the importance of steric hindrance is indicated by the fact that the αn_a-value is approximately half the other values and therefore only one electron is transferred in the reduction.

The results of Fig. 2 show that in those cases where steric hindrance should be most significant (*o*-bromo, -chloro and -methyl) the effect is more important in the reduction process than the ionisation, whereas for *o*-fluoro (small) and *o*-methoxy (flexible) the opposite is true. Allowing for the fact that two different reactions are being studied, one of which involves an attack on the carbonyl group and the other the removal of a proton from an acetyl group, and that the detailed mechanism of the electrode process is not as well defined as the homogenous reaction, the results do seem to indicate that rather than obtain specfic σ_0-values analogous to σ_p and σ_m, it would be preferable to make a detailed analysis of the steric forces in operation.

Finally, the reaction constant from the $E_{\frac{1}{2}}$ *vs.* σ plot is +0.029 V compared to +0.024 V from the $E_{\frac{1}{2}}$ (corrected) *vs.* σ plot. Therefore, in this particular work the correction for the double-layer effect does not appreciably alter the slope. Nevertheless, this should not be taken as an argument in favour of neglecting this factor, as its insertion is aimed at ensuring that the half-wave potentials measured in very different media can be compared. In order that the value of ϱ be comparable to those obtained in homogeneous chemical reactions, it should be multiplied by $\alpha n_a/0.05915$. Taking the value of $\alpha n_a \sim 1$, this results in a slope of + 0.4 in the case where the half-wave potential has been corrected.

SUMMARY

Measurements are reported on the reduction of a series of ring-substituted acetophenones at a dropping mercury cathode at 25°. An attempt has been made to place the halfwave potentials on a more absolute basis than hitherto, by taking into account the structure of the electrode double layer. The effect of this is to change the slope of the Hammett plot. In addition, a relationship between the reduction process and the ionisation of acetophenones in alkaline media is indicated. The effect of *ortho*-substituents on the half-wave potential can be interpreted on the different steric requirements of the electrode and ionisation processes, and in the case of the *ortho*-bromo substituent, the effect becomes sufficiently important to prevent the approach of the second hydrogen in the reduction process.

REFERENCES

1 P. ZUMAN, *Collection Czech. Chem. Commun.*, 25 (1960) 3225.
2 J. R. JONES, R. E. MARKS AND S. C. SUBBA RAO, *Trans. Faraday Soc.*, 63 (1967) 111.
3 J. R. JONES, R. E. MARKS AND S. C. SUBBA RAO. *Trans. Faraday Soc.*, 63 (1967) 993.
4 J. R. JONES, D. L. G. ROWLANDS AND C. B. MONK, *Trans. Faraday Soc.*, 61 (1965) 1384.
5 L. MEITES, *Polarographic Techniques*, Wiley and Sons, New York, 1965, p. 236.
6 K. SCHWABE, *Progr. Polarog.* 2 (1962) 333.
7 D. C. GRAHAME, *J. Am. Chem. Soc.*, 71 (1949) 2977.

Elsevier Sequoia S.A., Lausanne – Printed in The Netherlands

SHORT COMMUNICATIONS

Comment on the paper "Adsorption et impedance faradique" by A. M. Baticle and F. Perdu

The study of electrode processes with specific adsorption of reactants is at present of special interest, especially with regard to the interpretation of impedances of galvanic cells. Recently, DELAHAY[1] has given a theory for the most general case, taking into account charge transfer, diffusion and adsorption of the reactants; this unfortunately, turns out to be very complicated, so that interpretation of cell impedances in terms of an equivalent circuit seems hardly feasible. Until some way round this has been found, it is certainly worthwhile to fit experimental data to a less rigorous circuit derived on the basis of some approximations. For example we showed that at frequencies between 0.2 and 8 kHz, the $Tl^+/Tl(Hg)$ electrode in 1 M KNO_3 and 1 M KNO_3 + 0.1 M KCl appears to behave like a normal Randles' circuit with only an additional capacitance, ΔC, parallel to the double-layer capacitance[2]. On the other hand, BATICLE AND PERDU[3] communicated in this journal that the same electrode in 0.5 M H_2SO_4 does not meet the Randles' circuit and that the more elaborate circuit proposed by SENDA AND DELAHAY[4] is to be preferred. However, we have some comments on BATICLES' paper, which in our opinion are of sufficient interest to justify this Note.

1. *Calculation of the impedance* $R_r - j/\omega C_r$

For their analysis, BATICLE AND PERDU have to correct the measured impedance, $R_s - j/\omega C_s$, for the attributions of the ohmic resistance, R_E, and the double-layer capacitance, C_E (see their Fig. 1). The evaluation of R_E by extrapolation of R_s to infinite frequency is known to be without objections, except that subtraction of the "high frequency", R_E, leaves, at the lower frequencies, a minor frequency-dependent attribution of the solution resistance introduced by cell geometry (capillary response[5]). Therefore, $R_s - R_{s,\omega=0}$ should not be too small, say not below 10% of R_E.

However, from Fig. 1 (ref. 3) it follows immediately that, when $R_t = 0$, C_s at $\omega \to \infty$ does not reduce to C_E, but to

$$\underset{\omega \to \infty}{C_s \to} C_E + C_{aO} C_{aR}/(C_{aO} + C_{aR}) \qquad (1)$$

Therefore, theoretically C_E can be found by extrapolation of C_s to infinite frequency only if $R_t > 0$. *In practice* the value obtained must be definitily wrong when the extrapolation is made from a frequency range where R_t is negligibly small. This may be illustrated by the following example. We infer that, after subtraction of $C_{s(\omega \to \infty)}$ and $R_{s(\omega \to \infty)}$, there remains an impedance, $R_r - j/\omega C_r$, that has no capacitive component at $\omega = \infty$. In other words, C_r must become zero on extrapolation to infinite frequency. Unfortunately, values of C_r were not reported in ref. 3 but we may use the values recalculated from the reported parameters which, according to the authors, are in good agreement with the experimental values (see also point 5). We recalculated, therefore, C_s for case II[3] at various frequencies and found that a plot of

C_r *vs.* ω^{-1} approximates a straight line with a slight bending at the highest frequencies (40 kHz). A plot of C_r *vs.* $\omega^{-\frac{1}{2}}$ yields a perfect straight line (Fig. 1) with, however, an intercept of *ca.* 40 μF cm^{-2}. To check, we also calculated the capacity, C_s, of the total electrode impedance, arbitrarily taking C_E = 100 μF cm^{-2}. A plot of this C_s *vs.* $\omega^{-\frac{1}{2}}$ gives a similar straight line with intercept 140 μF cm^{-2}.

That BATICLE AND PERDU also did not find this extra capacitance of 40 μF cm^{-2}, is somewhat puzzling.

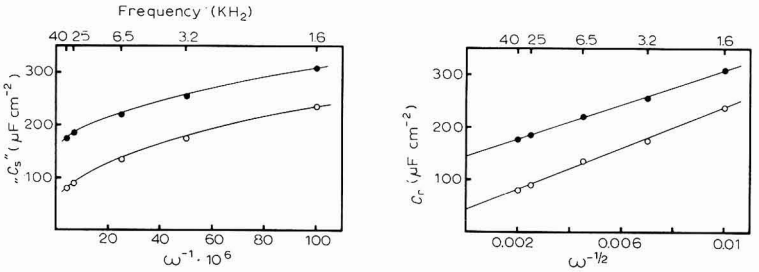

Fig. 1. Apparent electrode capacity, C_r (○) and measured capacity, "C_s" (●), as a function of frequency, calcd. from the data reported for case II in ref. 3, taking C_E = 100 μF cm^{-2}. See also text.

This example clearly demonstrates the *practical* invalidity of obtaining C_E by extrapolation to infinite frequency in the case of the $Tl^+/Tl(Hg)$ electrode. The limit for R_t that should be exceeded depends on the other variables and is not easily calculated. Since, however, BATICLE AND PERDU report in their Table 2 that R_t is either zero or very small, we believe that their evaluation of C_E is incorrect also in the other cases (see also point 5). Clearly, such a doubtful start to the analysis must have considerable influence on the parameters calculated later.

2. *Frequency-dependence of cotg* θ, R_r *and* $1/\omega C_r$

The plot of cotg θ *vs.* $\omega^{\frac{1}{2}}$, proposed in an earlier paper by BATICLE AND PERDU[6], as a basis for a qualitative decision about the equivalent circuit, appears to be of less value in the present case. In our paper[2] on the Tl reaction we stated that for the Randles' circuit with additional capacitance and negligible R_t

$$\text{cotg}\,\theta = \omega C_r R_r = 1/(1 + 2\sigma\omega^{\frac{1}{2}}\Delta C) \qquad (2)$$

Plots of 1/cotg θ (taken from Fig. 2, ref. 3) *vs.* $\omega^{\frac{1}{2}}$ appear to be straight lines, in accordance with (2), up to 25 kHz, in some cases even up to 40 kHz. Deviations at higher frequencies, attributed by BATICLE AND PERDU to the existence of a finite adsorption resistance, R_{ao} (see also their reply), might well fall within the experimental error due to subtraction of the ohmic resistance. This error is reported (ref. 3, p. 370) to exceed 10%. The frequency-dependence of cotg θ is therefore suggestive of a Randles' circuit, as with the plots of R_r and $1/\omega C_r$ *vs.* $\omega^{-\frac{1}{2}}$. In this connection it should be noted that it is useless to confirm the parallelism of these plots at low frequencies by a plot of $1/\omega C_r$ *vs.* R_r as in Fig. 8. The intercept in the latter is naturally identical with the distance obtained in the first.

3. *Determination of the charge transfer resistance* R_t

The exact equation for R_r in the circuit of SENDA AND DELAHAY[4] (see Fig. 1,

ref. 3) may be written in the form:

$$R_r = R_t + \omega^{-2} \Sigma \frac{1}{R_{ai} C_{ai}^2} \frac{1}{1 + 1/p_i + [1 + 1/\sigma_i \omega^{\frac{1}{2}} C_{ai}]^2 / p_i (p_i + 1)} \quad (3)$$

in which $p_i = R_{ai}/\sigma_i \omega^{-\frac{1}{2}}$. This equation reduces to eqn. (3) given by BATICLE AND PERDU at such high frequencies that the denominator of the second fraction reduces to $1 + (1/p_i)$ while, in addition, $1/p_i < 0.3$. From the values reported in their Tables 2 and 3 it can be calculated that in none of cases I – IV are these conditions fulfilled. For example, for case IV we calculated (at $\omega = 25 \cdot 10^4$ (40 kHz)) the summation term to be $2.3 \cdot 10^{-9}$ with the exact equation, and $-4 \cdot 10^{-9}$ with BATICLE's eqn. (3). Clearly, the approximation is by no means valid and consequently the values for R_t in Table 2 (ref. 3) have no meaning. Moreover, even if R_t had been determined without an approximation, the results would have been in error because of the doubtful evaluation of C_E. The accordance with literature values is in this case a rather doubtful argument, since in the quoted works of RANDLES[7] and BARKER[8], the adsorption of reactants could not be accounted for.

To get some idea of the feasibility of the extrapolation of R_r *vs.* ω^{-2}, we made such a plot (Fig. 2) for case II (reported $R_t \sim 0$) and case IV (reported $R_t = 0.060$), again with the values recalculated from the reported parameters. We cannot see how such a precise result ($R_t = 0.060$ in case IV) can be obtained, even from the highest frequencies, when the error due to the ohmic resistance must be extremely large.

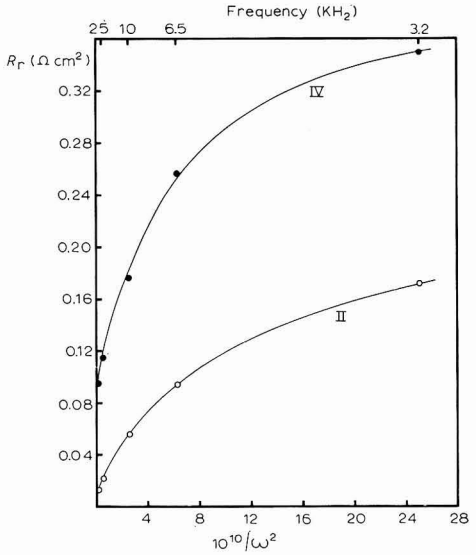

Fig. 2. Apparent resistive component as a function of frequency, calcd. from the data reported for cases II and IV in ref. 3.

4. *Calculation of the adsorption capacitance and resistance*

The error in the evaluation of C_E and R_t throws suspicion on the values of C_{ai} and R_{ai} reported by BATICLE AND PERDU in their Table 3, because the quantities A and B needed for the calculations are obtained from C_E and R_t. Serious errors are

possible; *e.g.*, in case VI, R_t amounts to *ca.* 25% of $R_r - \sigma_0\omega^{-\frac{1}{2}}$ at 1.6 kHz and even 80% of $R_r - \sigma_0\omega^{-\frac{1}{2}}$ at 40 kHz.

Too much importance should not be attached to the coincidence of the measured impedance components and those recalculated from the evaluated parameters. This only shows that it is possible for the equivalent circuit considered to describe the experimental facts within the applied frequency range, but it does not prove that other equivalent circuits, or even the same circuit with another set of parameters, would not fit (*cf.* our analysis of the Pb^{2+}/Pb(Hg) electrode[9]). In this connection it would have been useful to report the precision of the results.

5. *The possibility of the Randles' circuit with additional capacitance*

In the discussion of their paper, BATICLE AND PERDU comment upon our interpretation of the impedance of the Tl^+/Tl(Hg) electrode. They state, incorrectly, that we *supposed* the transfer resistance to be negligible and that we applied a graphical analysis. Actually, we considered just the same overall impedance as represented in eqn. (19) of BATICLE AND PERDU; therefore the latter is by no means original. Furthermore, we feel that our method of evaluating the parameters is much simpler than their method: eqns. (20) and (21) contain in principle three unknowns and have to be solved with at least two different frequencies. However, we understand (see also their reply) that BATICLE AND PERDU consider σ as a known quantity obtained from R_r and $1/\omega C_r$ (*after subtraction of* C_E, which is a rather doubtful quantity, see point 1) at low frequencies. In our opinion, it is illogical to solve the unknown $C = C_E + \Delta C_E$ from eqn. (20) in ref. 3 after such a procedure. As BATICLE AND PERDU have said that insertion of their experimental data into those equations did not lead to consistent results, we tried to check this with our own method.

As the data on the total cell impedance were not reported, we recalculated the components, R_r and $1/\omega C_r$, from the tabulated values of R_t, D_O, D_R, C_{aO}, C_{aR}, R_{aO} and R_{aR} using the expressions pertaining to SENDA's circuit. The calculations were performed for cases I–VI at some frequencies in order to check whether the results could fit the equation for the Randles' circuit:

$$1/(R_r - j/\omega C_r) = j\omega\Delta C_E + 1/\{R_t + \sigma\omega^{-\frac{1}{2}}(1-j)\} \qquad (4)$$

Obviously, if this is the case, the components, R_s and $1/\omega C_s$, of the total impedance must fit the analogous eqn. (19) of ref. 3, since C_E is a capacitance parallel to ΔC_E. The first step in our method is the calculation of:

$$\{R_r^2 + (1/\omega C_r)^2\}/R_r = q = R_t + \sigma\omega^{-\frac{1}{2}} + \sigma^2\omega^{-1}/(R_t + \sigma\omega^{-\frac{1}{2}}) \qquad (5)$$

From the frequency dispersion of q, the values of R_t and σ may be obtained, but for all cases I–VI we found q/ω to be virtually constant up to 25 kHz, and we conclude therefore that R_t is negligibly small, as we found for the Tl reaction in KNO_3 solutions. Again, the existence of a finite R_t or R_a is assumed by BATICLE AND PERDU on the basis of measurements at very high frequencies where the error due to the ohmic resistance is large.

The values of $\frac{1}{2}\, q/\omega = \sigma$ agree with those obtained by BATICLE AND PERDU from the low-frequency data (see their eqn. (4) and Table 2). Introduction of these values, together with $R_t = 0$, into eqn. (4) leads to ΔC_E-values constant, within experimental error, up to 25 kHz. As measurements at higher frequencies, are valueless

in our opinion, because of their inaccuracy, it can be concluded that the impedance of the $Tl^+/Tl(Hg)$ electrode in 0.5 M H_2SO_4 fits the Randles' circuit, in contrast with the statements of BATICLE AND PERDU. Actually, in cases I, II and VI (high amalgam concentrations) the attribution of the Red-component to the impedance appears to be negligible up to 40 kHz, and R_t is reported to be zero or negligibly small, so that in these cases SENDA'S circuit automatically becomes identical with Randles' circuit, with $C_{aO} = \Delta C_E$.

Of course, C_s is still frequency-dependent (*cf.* Fig. 1) but this does not mean that the Randles' circuit is invalid as stated by BATICLE AND PERDU[1] in their introduction. We think that they misunderstand the method for checking the validity of Randles' circuit, because their argument on this point, and also in section 5, is confused.

The question arises, how can real values for ΔC_E be found, when, in fact, ΔC_E should have been incorporated into the apparent C_E obtained at $\omega \to \infty$. This may be due to experimental deviations which are likely to occur at frequencies as high as 50 kHz. This is supported by the negative ΔC_E calculated by us in case VI.

In conclusion, we wish to stress that care should be taken in fitting experimental data to an equivalent circuit that rationalizes specific adsorption of reactants. Consistency of the calculated parameters with the approximations used should be checked, taking into account the accuracy of the measurements.

Finally, since all redox systems with adsorption of reactants so far studied[2,3,9-12] appear to proceed with an immeasurable rate of charge transfer, a causal connection between reversibility and presence of specific adsorption might exist. If so, simultaneous control by adsorption and charge transfer would not occur in practice. This would be of great value to electrochemistry as relatively simple expressions for the electrode impedance could then be used[10]; these, in the case of weak adsorption, become identical with those of the Randles' circuit with an additional concentration-dependent capacitance.

Laboratory of Analytical Chemistry,
State University, Utrecht
(The Netherlands)

M. SLUYTERS-REHBACH
B. TIMMER
J. H. SLUYTERS

1 (a) K. HOLUB, G. TESSARI AND P. DELAHAY, *J. Phys. Chem.*, submitted. Manuscript kindly supplied by P.D.
(b) P. DELAHAY AND G. G. SUSBIELLES, *J. Phys. Chem.*, 70 (1966) 3150.
2 M. SLUYTERS-REHBACH, B. TIMMER AND J. H. SLUYTERS, *Rec. Trav. Chim.*, 82 (1963) 553.
3 A. M. BATICLE AND F. PERDU, *J. Electroanal. Chem.*, 13 (1967) 364.
4 M. SENDA AND P. DELAHAY, *J. Phys. Chem.*, 65 (1961) 1580.
5 R. DE LEVIE, *J. Electroanal. Chem.*, 9 (1965) 117.
6 A. M. BATICLE AND F. PERDU, *J. Electroanal. Chem.*, 12 (1966) 15.
7 J. E. B. RANDLES, *Electrode Processes*, edited by E. YEAGER, John Wiley and Sons, New York, 1961, p. 209.
8 G. C. BARKER, *Electrode Processes*, edited by E. YEAGER, John Wiley and Sons, New York, 1961, p. 325.
9 M. SLUYTERS-REHBACH, B. TIMMER AND J. H. SLUYTERS, *J. Electroanal. Chem.*, 15 (1967) 151.
10 B. TIMMER, M. SLUYTERS-REHBACH AND J. H. SLUYTERS, *J. Electroanal. Chem.*, 15 (1967) 343; 18 (1968) 93.
11 M. SLUYTERS-REHBACH AND J. H. SLUYTERS, *Rec. Trav. Chim.*, 83 (1964) 217, 967.
12 J. R. GALLI AND R. PARSONS, *J. Electroanal. Chem.*, 10 (1965) 245.

Received May 4th, 1967; in revised form, October 27th, 1967

Possibilités d'interprétation des données expérimentales de la réaction Tl(Hg)/Tl^+ a partir de deux représentations électriques différentes

Les remarques de SLUYTERS et ses collaborateurs[1] concernant notre étude[2] de l'impédance faradique du système Tl(Hg)/Tl^+ nous amènent à apporter quelques précisions sur l'interprétation de nos résultats expérimentaux. Rappelons que les conditions expérimentales, dans notre étude, sont assez différentes de celles utilisées par SLUYTERS et ses collaborateurs dans une étude antérieure du même système[3]. Dans notre travail, les ions de l'électrolyte support, H_2SO_4, 0.5 M, sont peu adsorbés sur le mercure et n'interviennent probablement pas dans le mécanisme d'adsorption du thallium. Par contre, dans l'étude de SLUYTERS[3] les anions de l'électrolyte support (KCl, 0.1 M + HNO_3, 1 M) fortement adsorbés sur le mercure peuvent modifier l'adsorption des cations[4,7]. D'autre part nos expériences en courant sinusoïdal seul, sur électrodes à goutte d'amalgame, font appel à des concentrations plus élevées en Tl^0 et Tl^+ que l'étude de SLUYTERS[3] en courants continu et sinusoïdal surimposés, sur électrodes à gouttes de mercure, dans des solutions de Tl^+. Enfin notre dispositif expérimental nous a permis d'explorer un domaine de fréquences assez étendu. Dans ces conditions, la représentation de l'impédance de la cellule à l'aide du schéma simple (dit "de Randles") est possible pour les expériences I, II et III. Par contre, son emploi conduit à une dispersion anormale en fonction de la fréquence des termes de résistance de transfert, R_t, et de capacité de double couche pour les expériences IV, V et VI. D'autre part, la valeur anormale de la capacité globale[3] observée lorsqu'on extrapole C_s à fréquence infinie, comparée à celle qui apparaît en basses fréquences, ne nous a pas permis de retenir l'hypothèse approximative d'un "schéma simple de Randles", même dans nos trois premières expériences où le rôle de la diffusion des espèces Ox est si important qu'elle seule existe pratiquement dans le circuit auquel nous aboutissons, dans le domaine des fréquences accessibles aux calculs.

Sur le plan théorique il nous a semblé logique pour rendre compte de l'adsorption des espèces réagissantes de nous appuyer sur la littérature[5-11]. Celle-ci propose des mécanismes réactionnels qui aboutissent tous à l'existence d'une partie réelle de l'impédance d'adsorption, distincte de la résistance de transfert, et à des expressions d'impédance faradique plus élaborées que celles des réactions simples, sans adsorption. Dans nos expériences I et II, nos conditions expérimentales ne nous ont pas permis de mettre en évidence R_t et σ_k qui ont des valeurs trop faibles. Aussi les impédances faradiques correspondantes peuvent être représentées à l'aide d'un schéma semblable à celui proposé par Randles. Mais dans ces cas limites, l'interprétation des termes constitutifs de cette impédance est toute différente.

Nous avons voulu faire le moins possible d'approximations et rendre compte au mieux des faits expérimentaux en utilisant le schéma de l'étude de SENDA ET DELAHAY[9] qui, en faisant appel à un minimum d'hypothèses, restait exploitable sur le plan des calculs. L'interprétation physique à laquelle nous avons été conduits, passage progressif de la prédominance cinétique des ions à celle des atomes, nous semblait satisfaisante.

Sur le plan expérimental nous avons essayé de mettre en évidence dans une impédance globale le plus grand nombre de paramètres en utilisant un domaine de

fréquences le plus étendu possible et nous avons cherché objectivement à tenir compte de toutes les variations de l'impédance globale mesurée.

(1) *Calcul de l'impédance, $R_r - j/\omega C_r$*

Nous avons corrigé l'impédance globale mesurée, $R_s - j/\omega C_s$, des valeurs de résistance de l'électrolyte, R_E, et de capacité de double couche, C_E, ces valeurs étant choisies comme celles obtenues par extrapolation de R_s et C_s à fréquence inifinie.

Nous avons une incertitude de l'ordre de 1% sur l'extrapolation de R_E que nous avons signalée, dans notre publication[2], et qui amène une erreur sur les points aux fréquences élevées, points dont nous n'avons pu tenir compte dans nos calculs de R_{ao} et C_{ao}. La limite exploitable, pour les calculs, était de 10–20 kHz suivant les expériences sauf pour l'expérience V que nous avions mise à part.

Cette erreur systématique n'intervient pas sur les valeurs mesurées de C_s qui ont servi aux extrapolations destinées à atteindre C_E. Il n'est pas étonnant que la valeur de C_E à laquelle nous a conduit l'extrapolation de la courbe expérimentale représentative des variations de C_s soit différente de celle à laquelle aboutit SLUYTERS dans la Fig. 1 de l'article[1] à partir de valeurs recalculées.

En effet, pour calculer les capacités d'adsorption, il nous a fallu raisonner sur des capacitances qui font intervenir un coefficient en ω^{-1}. Cette nécessité amène une incertitude dans la détermination de C_{ao} qui, dans l'expérience II est de 18% (Figs. 6 et 7 de réf. 2), les valeurs proposées dans le Tableau 1 de réf. 2 ne constituant que des moyennes. Recalculer les valeurs de C_s à partir d'une telle moyenne revient à obtenir sur ces valeurs une incertitude qui atteint 25% à 50 kHz et à définir, non pas une courbe, mais un domaine dans la Fig. 1 de réf. 1. A l'intérieur de ce domaine se trouve la courbe expérimentale. L'extrapolation de la courbe recalculée dans la Fig. 1 de réf. 1 ne peut donc avoir de signification. On ne voit pas d'ailleurs comment physiquement et donc expérimentalement, l'extrapolation de C_s pourrait nous conduire à la valeur proposée dans l'éqn. (1) de réf. 1. Avec le schéma réactionnel que nous avons choisi[9], les valeurs de C_s aux plus hautes fréquences nous conduisent toujours à C_E lorsque ω est infini car il n'est pas possible alors de négliger R_t si petit soit-il. En effet on a:

Dans le cas de l'adsorption d'une seule espèce O:

$$C_{s\omega \to \infty} \sim C_E + (\sigma_R/R_t^2)\omega^{-3/2} \to C_E \qquad (1)$$

Dans le cas de l'adsorption des deux espèces:

$$C_{s\omega \to \infty} \sim C_E + (1/C_E + 1/C_{aO} + 1/C_{aR})\ (\omega^{-1}/R_t^2) \to C_E \qquad (2)$$

(2) *Variations de cotg θ, R_r et $1/\omega C_r$ avec la fréquence*

La limitation du domaine des fréquences expérimentales ne permet pas toujours d'atteindre le domaine des variations caractéristiques de cotg θ et l'allure de la courbe expérimentale, cotg $\theta/\omega^{\frac{1}{2}}$, ne peut pas toujours apporter les critères de différenciation qualitative des processus partiels d'une réaction que nous proposions théoriquement[13].

Cependant les courbes tg θ_r que nous avons obtenues ne sont pas des droites. Dans notre interprétation des trois premières expériences pour lesquelles le "schéma simple de Randles" peut rendre compte des résultats expérimentaux, le calcul nous conduit à introduire une résistance, R_{ao}, non nulle et une capacité, C_{ao}. L'expression de tg θ_r s'écrit alors:

$$\text{tg}\,\theta_r = 1 + 2\,\sigma C_{aO}\omega^{\frac{1}{2}} + (R_{aO}C_{aO}\omega - 1)/(1 + \sigma\omega^{-\frac{1}{2}}/R_{aO}) \quad (3)$$

La forme des courbes expérimentales prouve que la valeur de R_{aO} ne peut être négligée et que tg θ ne présente pas de variation linéaire en $\omega^{\frac{1}{2}}$. Aux basses fréquences, lorsque $\omega \ll \sigma^2/R_{aO}$, la courbe tg θ coincide effectivement avec une droite du type, $1 + 2\sigma\Delta C\omega^{\frac{1}{2}}$. Mais lorsque ω croît, tant que $\omega < 1/R_{aO}C_{aO}$, la présence de R_{aO}, valeur toujours petite dans nos expériences, a pour effet d'abaisser les valeurs de tg θ par rapport à la droite définie ci-dessus. Cet effet disparait pratiquement dans l'expérience I, mais est plus sensible dans les expériences II et III où les courbures s'accentuent.

Les valeurs de tg θ pour l'expérience IV, très proches de 1, et celles de l'expérience VI, inférieures à 1, ne sont pas interprétables avec un modèle analogue à celui de Randles.

(3) *Détermination de la résistance de transfert de charges, R_t*

Comme nous l'avons fait remarquer dans notre publication[2], il ne nous a pas été possible d'utiliser l'approximation proposée dans le calcul théorique[13], les domaines de fréquences où ces approximations seraient valables n'étant pas atteints dans nos expériences. Nous avons donc été amenés à extrapoler des courbes, ce qui est moins précis. Cependant, lorsque $\omega \to \infty$, le terme R_r décroit constamment et tend vers R_t (eqn. (10) de réf. 13 ou eqn. (3) de réf. 1) et les courbes n'ont pas de point d'inflexion dans le domaine de fréquences servant à l'extrapolation, ce qui limite le domaine d'erreur possible.

Nos extrapolations pour obtenir R_t aussi bien que celles pour obtenir C_E ne sont pas fausses à priori même si elles ne sont pas précises. Nous avons tenu compte de cette imprécision dans la plupart de nos expériences en considérant que la valeur de R_t était simplement voisine de zéro, sans pour cela atteindre cette valeur qui ne correspond pas à une réalité physique. Nous n'avons d'ailleurs attaché que peu d'importance à la vitesse de transfert de charges, déterminée avec trop peu de précision, et n'avons voulu que signaler l'accord de l'ordre de grandeur obtenu avec les valeurs données comme approximatives par Barker[7] et Randles[12]. Car ces auteurs, bien qu'ayant constaté l'existence de l'adsorption ont utilisé des schémas de réactions simples, mais tous deux sont amenés à des courants d'échange apparents finis, c'est-à-dire à l'existence d'une partie réelle de l'impédance faradique ajoutée à l'impédance de Warburg. Signalons que l'éqn. (3) de l'article 1 et l'éqn. (3) de l'article 2 ne sont pas applicables lorsqu'il n'y a adsorption que d'une seule espèce réagissante, c'est-à-dire dans la plupart de nos expériences.

(4) *Calcul des capacités et résistances d'adsorption*

La dispersion des valeurs de R_a et C_a calculées pour chaque fréquence est représentée sur les Figs. 6 et 7 de notre publication[2]. Les incertitudes, liées aux évaluations de R_t, R_E et C_E, conduisent à une augmentation de cette dispersion dans le domaine des plus hautes fréquences et, pour cette raison, les valeurs de R_a et C_a correspondantes n'ont pas été mentionnées sur les Figs. 6 et 7. La diffusion, prépondérante vers les basses fréquences, limite dans ce domaine la précision du calcul de R_a et C_a.

Il a été possible, dans le domaine des fréquences intermédiaires, de déterminer des valeurs probables de R_a et C_a. Ces valeurs permettent d'obtenir des courbes calcu-

lées qui coincident bien avec les valeurs expérimentales et qui tiennent compte de la variation de l'impédance, en fonction de ω, dans nos domaines expérimentaux. Il est possible que l'utilisation d'un domaine de fréquences plus étendu mène à un schéma représentatif de l'impédance qui soit plus élaboré que celui que nous avons utilisé, de la même manière qu'un domaine plus restreint conduit à un schéma représentatif simplifié.

(5) *Etude de la possibilité d'un circuit de Randles avec une capacité additionnelle*

Il apparaît que nous avions mal interprété la publication réf. 3 (calcul et non construction graphique), mais celle-ci étant antérieure à la nôtre[2], il nous a paru nécessaire, préalablement à toute interprétation sur le mécanisme réactionnel du système Tl(Hg)/Tl^+, d'examiner si l'impédance de la cellule pouvait être représentée à l'aide d'un "schéma simple de Randles".

Dans une telle représentation l'impédance globale de la cellule en fonction de ses composants est donnée[2] par l'éqn. (19) dont nous ne revendiquons en aucune façon l'originalité. Les équations originales (20) et (21) de réf. 2 permettent de déterminer directement à partir des données expérimentales et pour *chaque* fréquence les valeurs de R_t et de $C_E + \Delta C_E$ à condition toutefois de connaître les valeurs de R_E et de σ.

La prédominance du contrôle de la réaction par la diffusion dans une grande partie du domaine des fréquences expérimentales, permet l'obtention de σ avec une bonne précision, soit à partir de la pente en basses fréquences des droites R_r et $1/\omega C_r$ en fonction de $\omega^{-\frac{1}{2}}$, soit pour ces mêmes fréquences à partir de R_s et $1/\omega C_s$[16] qui ne nécessitent pas une connaissance préalable de C_E. Signalons à ce propos que l'étalement des abscisses en $\omega^{-\frac{1}{2}}$ peut quelquefois amener à considérer des pentes erronées. L'avantage de la représentation dans le plan semi-complexe des impédances est de permettre la détermination, sans ambiguité, par la pente à 45°, du domaine de fréquences où l'impédance de diffusion assure à elle seule l'évolution en fonction de la fréquence. C'est là l'utilité de l'emploi des deux représentations graphiques.

Dans nos expériences les σ étaient connus à 1% près et suivaient la loi de variation des concentrations des espèces réagissantes au sein des phases.

σ étant ainsi déterminé et R_E étant connue avec l'imprécision notée plus haut, occassionnant par là même dans le domaine des hautes fréquences une incertitude plus grande sur les valeurs calculées, il ne reste comme inconnue que $C_E + \Delta C_E$ dans l'éqn. (20) qui peut être résolue pour chaque fréquence. L'équation (21) permet de calculer R_t pour chaque fréquence. Ces deux équations sont d'ailleurs utilisables même si C_E et R_t ne sont pas constants dans le domaine de fréquences étudié.

La méthode de détermination proposée dans la publication réf. 1 nous parait peu sensible et moins rigoureuse. En effet, la nullité de R_t y est déduite de la constance, en fonction de la fréquence, de l'expression:

$$q/\omega = \sigma(1 + R_t/\sigma\omega^{-\frac{1}{2}} + 1/(1 + R_t/\sigma\omega^{-\frac{1}{2}})) \qquad (4)$$

Cependant, la constance de q/ω, dans un grand domaine de fréquences, n'implique pas forcément que $R_t = 0$ mais que R_t^2 est petit devant $(\sigma\omega^{-\frac{1}{2}})^2$. Dans nos expériences, la constance de q/ω ne révèle simplement qu'un contrôle prépondérant de la réaction par la diffusion, à l'intérieur du domaine de fréquences où elle intervient.

D'ailleurs il semble énigmatique que les valeurs de R_r et $1/\omega C_r$ recalculées en

s'appuyant sur le circuit de SENDA ET DELAHAY conviennent également à une représentation conforme au circuit de RANDLES.

L'utilisation de notre méthode a confirmé que pour les expériences I, II, III et dans le domaine de fréquences accessible aux calculs, le "schéma de Randles" est une approximation valable puisque l'impédance due aux espèces Red est négligeable. Pour l'expérience V, pour toutes les fréquences, l'hypothèse $R_t = 0$ conduit à des valeurs de capacités négatives alors que le fait d'admettre une résistance non nulle permet d'obtenir des valeurs de capacités positives (éqn. (20) de réf. 2).

Pour cette expérience cependant, comme nous l'avions signalé[2], l'influence du R_t est très grande et pour des fréquences supérieures à 5 kHz le schéma approximatif que nous avons donné ne peut être contrôlé par suite de l'incertitude sur R_E. Pour les fréquences inférieures, la capacité extrapolée, C_s, que nous avons retirée, se trouve simplement ajoutée si l'on fait le calcul sans l'enlever à priori.

Pour les expériences IV et VI l'approximation n'est pas possible. Les valeurs que nous avons obtenues en utilisant le schéma de l'étude 9 concordent bien avec les valeurs expérimentales dans le domaine des fréquences utilisables.

En conclusion, dans le domaine de fréquences où nous avons travaillé, apparaissent des écarts des valeurs expérimentales, par rapport à un circuit de réaction simple, que nous n'avons pas voulu négliger.

Il est certain que les valeurs des termes d'impédances obtenues manquent de précision car les écarts dont nous avons cherché à rendre compte sont faibles. Il se peut que le schéma choisi ne soit qu'un des schémas possibles, qu'il faille chercher une autre interprétation dans le sens des publications 14 et 15. Mais dans ces expériences sur le système $Tl^+/Tl(Hg)$ il reste très délicat de faire des essais de calculs, si l'on considère le faible domaine de fréquences utilisables dans lequel la diffusion n'est pas prépondérante. Nous étudions actuellement deux autres systèmes, à vitesses de réactions plus lentes et pensons pouvoir en tirer des conclusions sans ambiguité en utilisant une méthode de calcul différente et ne comportant pas d'hypothèse sur la double couche.

Laboratoire d'Electrolyse du C.N.R.S., A. M. BATICLE
92-Bellevue, France. F. PERDU

1 M. SLUYTERS-REHBACH, B. TIMMER ET J. H. SLUYTERS, *J. Electroanal. Chem.*, 19 (1968) 305.
2 A. M. BATICLE ET F. PERDU, *J. Electroanal. Chem.*, 13 (1967) 364.
3 M. SLUYTERS-REHBACH, B. TIMMER ET J. H. SLUYTERS, *Rec. Trav. Chim.*, 82 (1963) 553.
4 G. G. SUSBIELLES, P. DELAHAY ET E. SOLON, *J. Phys. Chem.*, 70 (1966) 2601.
5 H. A. LAITINEN ET J. E. B. RANDLES, *Trans. Faraday Soc.*, 51 (1955) 54.
6 H. GERISCHER, *Z. Elektrochem.*, 55 (1951) 98.
7 G. C. BARKER, *Transactions of the Symposium on Electrode Processes*, edited by E. YEAGER, John Wiley and Sons, New York, 1961, p. 325.
8 J. LLOPIS, J. FERNANDEZ-BIARGE ET M. PEREZ FERNANDEZ, *Transactions of the Symposium on Electrode Processes*, edited by E. YEAGER, John Wiley and Sons, New York, 1961, p. 221.
9 M. SENDA ET P. DELAHAY, *J. Phys. Chem.*, 65 (1961) 1580.
10 W. LORENZ ET G. SALIE, *Z. Physik. Chem., Leipzig*, 218 (1961) 259.
11 B. KASTENING, H. GARTMANN ET L. HOLLECK, *Electrochim. Acta*, 9 (1964) 741.
12 J. E. B. RANDLES, *Transactions of the Symposium on Electrode Processes*, edited by E .YEAGER, John Wiley and Sons, New York, 1961, p. 209.
13 A. M. BATICLE ET F. PERDU, *J. Electroanal. Chem.*, 12 (1966) 15.
14 P. DELAHAY, *J. Phys. Chem.*, 70 (1966) 2373.
15 K. HOLUB, G. TESSARI ET P. DELAHAY, *J. Phys. Chem.*, 71 (1967) 2612.
16 A. M. BATICLE, F. PERDU ET P. VENNEREAU, *Compt. Rend.*, séance du 8 juillet 1968.

Reçu le 18 septembre 1967, en forme revisée le 25 mars, 1968

The potential-dependence and the upper limits of electrochemical rate constants

Recently, OLDHAM[1] drew attention to the fact that an electrochemical rate constant, $\vec{k}$, should vary with potential, E, in a sigmoidal fashion, in contrast to the widely accepted dependence

$$\vec{k} = k_s \exp\left[-(E - E_c^0)\,(\alpha F/RT)\right]$$

which increases without limit as E is made negative of the formal potential E_c^0 (the symbols have their usual meaning). He pointed out that an infinite variety of mathematical forms for the functional dependence of $\vec{k}$ upon E would yield such behaviour, but implied that an additional criterion to be satisfied would be that the dependence becomes quadratic near E_c^0 in accordance with the electron transfer theories of HUSH[3] and MARCUS[4]. The limiting case of "non-activated" behaviour of an electrode process, when $\vec{k}$ tends to a limit, $\vec{k}_m$, at high overpotential, was discussed in a similar way by KRISHTALIK[2]. In this Note it is demonstrated that, for reactions involving only electron transfer, a particular form of sigmoidal dependence is predicted by the electron transfer theories, provided that proper account is taken of all the electronic levels in the electrode.

The upper limit to the rate has been ascribed by various authors either to the frequency of collision between the reactant and the electrode, or to the frequency of tunnelling of the electron. It is suggested here, that one effect of the manifold of energy states of electrons in metal electrodes is to make the collision limit more likely than it is in the case of a homogeneous oxidation–reduction reaction.

The correct means of accounting for the many equally probable parallel paths for a "redox" electrode reaction, arising from the closely spaced energy levels of the electron gas in a metal, has been indicated in most detail by LEVICH, DOGONADZE and their coworkers[5-7]. The calculated contributions to the rate from each individual path are summed by first multiplying by the density of energy levels in unit energy range, and then integrating over energy. In the following, the work of assembly of the reactants and products from their equilibrium configurations into the pre- and post-electron transfer states, respectively, has been neglected for simplicity. One obtains:

$$\vec{k} = \frac{\vec{k}_m}{\sqrt{\pi}} \int_{-\infty}^{\infty} \frac{\exp\{-[(\varepsilon_f - \varepsilon_p)^2/4\lambda RT]\}}{1 + \exp\left[(\varepsilon_f - \varepsilon_F)/RT\right]}\, \mathrm{d}\left(\frac{\varepsilon_f}{2\sqrt{\lambda RT}}\right)$$

Here, ε_f is the energy of an individual level, and ε_F that of the fermi level, of the electrode; ε_p, given by

$$\varepsilon_p = \varepsilon_F \pm \lambda + nF(E - E_c^0)$$

is the energy level of the electrode *most favourably situated* to donate an electron to an oxidised species or to accept an electron from a reduced species (the positive sign is taken in the former case, and the negative sign in the latter); λ is the energy required to change the positions of molecules and ligands in the environment of the reactant in solution, until they take up the equilibrium configuration adopted about the product,

whilst maintaining constant the charge on the central species; $\vec{k}_m$, the upper limit for the rate constant, will be discussed later; n is the number of electrons transferred. Although one should integrate only over the conduction band, the limits may be extended to $-\infty$ and $+\infty$ since the integrand is only finite in the region near ε_p and ε_F.

The numerator of the integrand is proportional to the probability that an individual energy level is involved in the reaction and the Fermi factor $\{1+\exp[(\varepsilon_f-\varepsilon_F)/RT]\}^{-1}$ is the probability that this level contains an electron. If λ is large, ε_p is widely separated from the Fermi level at $E=E_e^0$, that is in the region of energy where the electron density is low for a reduction reaction, and high for an oxidation reaction. Then the standard rate constant of the electrode process is small.

Notice that the use of a Boltzmann distribution of energies of the reactants is equivalent to an assumption that the cross-section through the potential energy surface for the system, made by the reaction coordinate, is parabolic at all overpotentials. This is a common postulate, but its validity is uncertain.

Usually, λ is considerably larger than RT. In such a situation, the Fermi factor varies from unity to zero in an energy range narrow in comparison with the width of the peak of $\exp\{-[(\varepsilon_f-\varepsilon_p)^2/4\lambda RT]\}$. A good approximation to the integral may be found, therefore, by replacing the Fermi function by a unit step function, or equivalently, by removing the Fermi function from the integrand and integrating only over the states above or below ε_F, whichever is appropriate. This procedure yields

$$\vec{k}=0.5\,\vec{k}_m\,[1-\mathrm{erf}\,(a)]$$

where

$$a=[\lambda\pm nF(E-E_e^0)]/(2\sqrt{\lambda RT})$$

erf represents the error function. The positive sign is to be taken for a reduction process and the negative sign for an oxidation process. Although this approximation is inferior to that obtained from Laplace's method of evaluation (used by LEVICH AND DOGONADZE[7]) in the range of $\vec{k}\ll\vec{k}_m$, yet it has the advantage of reproducing two required properties of the integral, namely that it tends to the limit $\vec{k}_m$ for large negative values of a, and that $\vec{k}(a)=\vec{k}_m-\vec{k}(-a)$; $\vec{k}/\vec{k}_m$ is plotted against the argument, a, in Fig. 1. *The sigmoidal shape of the plot of an electrochemical rate constant against electrode potential is made evident.*

Physically, the limit of $\vec{k}$ arrives when the electrode overpotential is made so large, that ε_p is to be found far from ε_F, where virtually all of the electron states are either occupied or empty. The Figure shows that a must be less than -2 for this condition to obtain, that is:

$$E<E_e^0\mp(\lambda+4\sqrt{\lambda RT})/(nF)$$

It is predicted, therefore, that the forward rate constant for an "outer sphere" redox electrode reaction becomes independent of potential when the electrode overpotential is greater than $(\lambda+4\sqrt{\lambda RT})/nF$ V. This limit is at 1.63 V when $\lambda=1$ eV and at 0.48 V

when $\lambda = 0.2$ eV. Similarly, it can be shown that $\vec{k} = 0.5\vec{k}_m$ when the overpotential is λ/F V.

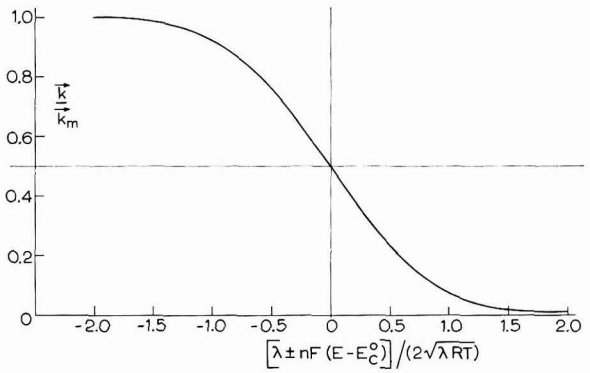

Fig. 1. The sigmoidal dependence upon potential of an electrochemical rate constant.

Of the authors who have formulated theories of electron transfer at electrodes the Russian school[6,7] and DE HEMPTINNE[8] have employed a non-adiabatic approach and essentially ascribe the magnitude of $\vec{k}_m$ to the rate of tunnelling of electrons, whilst MARCUS[4] and HUSH[3], employing an adiabatic approach, ascribe its magnitude to the rate of collision between the reactant and the electrode. Thus:

$\vec{k}_m = 4\pi^2\delta|V|^2\varrho/h$ Non-adiabatic reaction

$\vec{k}_m = (kT/2\pi m)^{\frac{1}{2}}$ Adiabatic reaction

Formally, the two approaches may be made equivalent by inclusion of a transmission coefficient in the adiabatic expressions. In the formulae, δ represents the distance of the reactant from the electrode in the transition state, ϱ the density of states in the electrode per unit range of energy, and m the mass of the reacting molecule or ion; $|V|$ is the expectation value for the energy of interaction between the reactant and the electrode—its magnitude allows a choice to be made between the expressions for $\vec{k}_m$. It should be compared with the quantity, $|V_{cr}|$, given by:

$$|V_{cr}| = [h/(4\pi^2\delta\varrho)]^{\frac{1}{2}}\,[kT/(2\pi m)]^{\frac{1}{4}}$$

If $|V| > |V_{cr}|$, the collisional formulae should be employed; otherwise the reaction is non-adiabatic.

Owing to the large magnitude of ϱ ($\sim 10^{20}$ eV^{-1}), $|V_{cr}|$ is made very small for an electrode process, *viz.*, $\sim 10^{-13}$ eV. This contrasts with its magnitude for homogeneous reations (a formula for $|V_{cr}|$ in this case is given by DOGONADZE, KUZNETSOV AND CHERNENKO[6]), *viz.*, $\sim 10^{-3}$ eV. Since there is no particular reason why the interaction energy between an oxidant and an electrode should be small in comparison with its interaction with a reductant in homogeneous solution, it is suggested that the propor-

tion of reactions that are adiabatic should be much higher when one reactant is an electrode, than when both reactants are species in solution.

Cyanamid European Research Institute, J. M. HALE
Cologny, Geneva (Switzerland)

1 K. B. OLDHAM, *J. Electroanal. Chem.*, 16 (1968) 125.
2 L. I. KRISHTALIK, *Russ. J. Phys. Chem.*, 33 (1959) 125; 34 (1960) 43; *Electrochim. Acta*, in press.
3 N. S. HUSH, *J. Chem. Phys.*, 28 (1958) 962
4 R. A. MARCUS. *Ann. Rev. Phys. Chem.*, 15 (1964) 155.
5 R. R. DOGONADZE AND Y. A. CHIZMADZHEV, *Proc. Russ. Acad. Sci.*, 145 (1962) 563.
6 R. R. DOGONADZE, A. M. KUZNETSOV AND A. A. CHERNENKO, *Russ. Chem. Rev.*, 34 (1965) 759.
7 V. G. LEVICH, *Advan. Electrochem. Electrochem. Eng.*, 4 (1960) chap. 4.
8 X. DE HEMPTINNE, *Bull. Soc. Chim. France*, (1964) 2328; *Bull. Soc. Chim. Belges*, 77 (1968) 21.

Received March 12th, 1968

J. Electroanal. Chem., 19 (1968) 315–318

Chemical softness and specific adsorption at electrodes

The principle of soft and hard acids and bases (SHAB) has been shown to be useful in rationalizing a wide variety of chemical phenomena[1]. No unequivocal definition of hardness and softness has been given but it is generally true that hardness is associated with low polarizability and isolated electronic ground states, and that softness implies high polarizability and low-lying electronic states[2]. The SHAB principle states that hard acids prefer to coordinate with hard bases, and soft acids coordinate preferentially with soft bases. Various tabulations of soft and hard acids and bases have been given[3–6]. Hard interactions are normally ionic. Soft interactions tend to be covalent.

A chemical phenomenon which is not well understood is the specific adsorption of ions at the electrode–electrolyte interface[7]. In terms of Grahame's model of the double-layer at this interface, ions which are contained in the inner layer are said to be specifically adsorbed (see ref. 8 for a more complete definition of specific adsorption). GRAHAME assumed that specific adsorption involved covalent bonding between the adsorbed anion and the (mercury) electrode[9]. This interpretation was rejected by LEVINE *et al.*[10] who proposed image energy as the origin of specific adsorption, and by BOCKRIS *et al.*[11] who suggested that the degree and type of ionic solvation were predominant in determining whether an ion would be specifically adsorbed. The latter authors demonstrated that image energy was insufficient to explain the magnitude of adsorption of most ions.

As specific adsorption resembles to some extent adsorption in heterogeneous catalysis (for example, similar isotherms are used in discussing both types of adsorption) and as the latter phenomenon has been examined in terms of the SHAB principle[3], it seemed possible that specific adsorption may be amenable to explanation, or at least rationalization, using this principle.

PEARSON[3] has shown that the adsorptive characteristics of the surface of a bulk metal are consistent with the metal surface having the properties of a soft acid

(metals in the zero-valent state are soft) and of a soft base ("conduction electrons are non-innocent ligands *par excellence*"[2]). That is, soft acids and bases are adsorbed from the gaseous phase whereas hard species are not. It does not seem unreasonable to consider a metallic electrode in the same manner.

If an electrode at the point of zero charge (p.z.c., *i.e.*, when the electronic charge on the electrode surface is zero) can be considered to be soft then, if specific adsorption is a soft interaction, it would be predicted that soft anions and soft cations would be adsorbed.

Anions are more strongly adsorbed than cations on mercury (at which electrode most adsorption studies have been made). While there is no quantitative relationship between the potential at the p.z.c. (E_{pzc}) and the amount of adsorbed anion, it is found in solutions of simple salts, and in the absence of specific adsorption of cations (Li^+, Na^+ and K^+ are negligibly adsorbed), that E_{pzc} shifts cathodic with increasing specific adsorption of the anion. E_{pzc} for 0.1 *M* solutions of numerous salts is given in Table 1, and applying PEARSON's classification of softness of anions it can

TABLE 1

RELATIONSHIP BETWEEN E_{pzc} AND SOFTNESS OF ANIONS

Anion	$-E_{pzc}$ *(mV vs. SCE)*	*PEARSON's classification of anion*	*Anion*	$-E_{pzc}$ *(mV vs. SCE)*	*PEARSON's classification of anion*
S^{2-}	880	Soft	Cl^-	461	Hard
I^-	693	Soft	OAc^-	456	Hard
CN^-	645	Soft	NO_2^-	450	Intermediate*
CNS^-	589	Soft	HCO_3^-	440	Hard
Br^-	535	Intermediate	CO_3^{2-}	440	Hard
N_3^-	509	Intermediate	SO_4^{2-}	438	Hard
NO_3^-	478	Hard	F^-	437	Hard
ClO_4^-	470	Hard			

These results were obtained in the presence of a non-specifically adsorbed cation. Salt concns. were 0.1 *M* except in the case of sulfide (0.5 *M*). This concn. difference would not affect the given order.

The data on N_3^- and NO_2^- were obtained by J. LAWRENCE, E. GONZALEZ AND R. PARSONS (private communication). Other E_{pzc} were taken from *Handbook of Analytical Chemistry*, edited by L. MEITES, McGraw-Hill, Inc., New York, 1963, chap. 5.

* Another classification by F. BASOLO AND R. G. PEARSON (*Mechanisms of Inorganic Reactions* J. Wiley and Sons, Inc., New York 1967, p. 140) suggests that NO_2^- is hard.

be seen that strongly adsorbed anions are soft, and that weakly adsorbed anions are hard. This table also reproduces very closely the order of softness given by PEARSON[3].

There has been much debate on the existence or non-existence of specific adsorption of cations but it is now generally accepted that the ions, NR_4^+ (where R is an alkyl radical), Tl^+ and Cs^+, are specifically adsorbed on mercury. These are soft cations. The softest metal ions (Hg^{2+}, Au^+, Tl^{3+} and Ag^+ according to a recent classification[6]) are reduced at potentials more anodic than that at which they might be expected to adsorb. Hard cations are not detectably adsorbed.

On the basis of this apparent correlation between softness and adsorbability we suggest that specific adsorption is a soft interaction (at least in the region of the p.z.c.) and therefore involves the formation of a covalent bond between the electrode and the adsorbed ion. BOCKRIS *et al.*[11] criticized GRAHAME's concept of covalency

on, principally, the grounds that in the halide series the order of specific adsorption on mercury was the reverse of the Hg–halide bond energy in the gaseous phase. This reversal can be brought about by solvation effects. In covalent interactions, desolvation of the reacting species, prior to bond formation, often presents a substantial energy barrier and it is therefore not valid to compare gaseous bond energies and stability in solution without consideration of desolvation energies.

KLOPMAN[6] has recently suggested that a scale of ionic softness in solution can be developed by taking, for a given ion, the sum of its desolvation energy and orbital energy. Softness in a base is characterized by low desolvation and high orbital energy, and in an acid by low desolvation and low orbital energy. On the basis of this description, soft interactions are essentially covalent bonding between empty and filled orbitals of comparative energies. In the halide series, the orbital energy *increases* in the order $F^- < Cl^- < Br^- < I^-$, while the desolvation energy *decreases* in the same order, predicting the softness of the halides (and on the present hypothesis, their adsorbability) to decrease in the order, $I^- > Br^- > Cl^- > F^-$, in agreement with experiment.

BOCKRIS *et al.*[11] indicated that a relationship existed between the extent of hydration of an ion and its adsorbability, (the less hydrated ions were strongly adsorbed) which agrees with what is being said here inasmuch as soft ions are often, though not invariably, weakly hydrated. However, these authors go further and propose that low hydration is a *necessary* condition for the specific adsorption of an ion. More recently, DEVANATHAN AND TILAK[12] have augmented this and suggested that for specific adsorption, "ease of hydration of the ion is a necessary condition, and a covalent ion–metal bond is the sufficient condition."

In direct contradiction to this view of low hydration being a necessary condition for specific adsorption to occur, ARMSTRONG *et al.*[13] have recently reported very strong specific adsorption of the sulfide ion on mercury (see *Note**). The sulfide ion, which is strongly hydrated[14], is very soft which supports the suggestion that the factor that determines the adsorbability of an ion is not its degree of solvation but its softness.

The anion PF_6^- though weakly hydrated[15], would be expected to be hard, as the coordination number of fluorine seldom exceeds 1. Recent measurements in aqueous[16] and non-aqueous[16,17] solvents have shown this ion to be only slightly adsorbed, again suggesting a softness criteria for specific adsorption. It seems reasonable to predict that the smaller BF_4^- would be even less adsorbed than PF_6^-.

It is to be expected that the extent (and possibly the order) of adsorbability of ions will vary with the solvent, as an increase in the interaction between the electrode and the solvent will tend to decrease ion adsorption, and the softness of an ion is determined in part by the interaction of the ion with the solvent. KLOPMAN[6] has indicated that the order of softness can change radically with decreasing dielectric constant of the solvent.

When the electrode is positively charged it would be predicted that its acidic character would be enhanced and its basic character reduced. Anion adsorption should then increase, and cation adsorption decrease with increasing positive charge, as is

Note: The adsorption data for sulfide ion was obtained in a medium of 0.5 *M* Na_2S + 1 *M* $NaHCO_3$ where the concentration of free sulfide ion is only $1.5 \cdot 10^{-5}$ *M*. In view of this, and of the large concentration of the soft bisulfide ion, it is probable that this ion is co-adsorbed with sulfide.

observed (the converse behavior would of course occur when the electrode is negatively charged). At the extremes of positive polarization, the electrode would become increasingly harder (as an acid) and it is then feasible that soft anions could be desorbed and hard anions be adsorbed. In fact, PAYNE[18] has proposed that extrapolation of his data for the adsorption of the nitrate ion on mercury from nitrate–fluoride mixtures indicates that at high positive charges nitrate desorbs, and that either water or fluoride is adsorbed. As this does not appear to occur in the absence of fluoride, it is probable that fluoride is adsorbed at high positive charges. This, on the present hypothesis, is reasonable as fluoride (or water) is much harder than nitrate and the SHAB principle predicts that hard interactions are to be preferred to hard–soft interactions.

Acknowledgement

This work was supported by the National Science Foundation.

*Gates and Crellin Laboratories of Chemistry** DONALD J. BARCLAY
California Institute of Technology
Pasadena, Calif. 91109 (U.S.A.)

1 (a) 1st Symposium on *Hard and Soft Acids and Bases*, Cologny, Geneva, 1965; (b) 2nd Symposium on *Hard and Soft Acids and Bases*, Northern Polytechnic, London, 1967.
2 C. F. K. JØRGENSEN. *Structure and Bonding*, 1 (1966) 234.
3 (a) R. G. PEARSON, *J. Am. Chem. Soc.*, 85 (1963) 3533.
(b) R. G. PEARSON, *Chem. in Britain*, 2 (1967) 103.
4 R. S. DRAGO AND B. B. WAYLAND, *J. Am. Chem. Soc.*, 87 (1965) 3571.
5 A. YINGST AND D. H. MCDANIEL, *Inorg. Chem.*, 6 (1967) 1067.
6 G. KLOPMAN, *J. Am. Chem. Soc.*, 90 (1968) 223.
7 P. DELAHAY, *Double Layer and Electrode Kinetics*, Interscience Publishers, New York, 1965.
8 D. M. MOHILNER, *Electroanalytical Chemistry*, Vol. I, Marcel Dekker, New York, 1966.
9 D. C. GRAHAME, *Chem. Rev.*, 41 (1947) 441.
10 S. LEVINE, G. M. BELL AND D. CALVERT, *Can. J. Chem.*, 40 (1962) 518.
11 J. O'M. BOCKRIS, M. A. V. DEVANATHAN AND K. MULLER, *Proc. Roy. Soc., London*, 274A (1963) 55.
12 M. A. V. DEVANATHAN AND B. V. K. S. R. A. TILAK, *Chem. Rev.*, 65 (1965) 635.
13 R. D. ARMSTRONG, D. F. PORTER AND H. R. THIRSK, *J. Electroanal. Chem.*, 16 (1968) 219.
14 B. E. CONWAY AND J. O'M. BOCKRIS, *Modern Aspects of Electrochemistry*, No. 1., Butterworths, London, 1954, p. 85.
15 E. R. NIGHTINGALE JR., *Chemical Physics of Ionic Solutions*, John Wiley and Sons, Inc., New York, 1966, chap. 7, p. 90 *et seq.*
16 R. PAYNE, *J. Am. Chem. Soc.*, 89 (1967) 489.
17 J. LAWRENCE AND R. PARSONS, *Trans. Faraday Soc.*, 64 (1968) 751.
18 R. PAYNE, *J. Electrochem. Soc.*, 113 (1966) 999.

Received May 23rd, 1968

* Contribution No. 3695.

Elsevier Sequoia S.A., Lausanne – Printed in The Netherlands

BOOK REVIEWS

Ion Exchange, Vol. 1, edited by J. A. MARINSKY, Marcel Dekker, Inc., New York, 1966, 424 pages, $16.75.

This collaborative work, the first in a projected "Advances" series, is indispensable for anyone working on the basic physical chemistry of ion-exchange resins. There have been no spectacular advances in this field during the last 10 years, but the total activity is now too great for any one author to cover.

The topics dealt with are as follows: 1. Transport processes in membranes (S. R. CAPLAN AND D. C. MIKULECKY). 2. Ion-exchange kinetics (F. HELFFERICH). 3. Ion-exchange studies of complex formation (Y. MARCUS). 4. Liquid ion exchangers (E. HÖGFELDT). 5. Precise studies of ion-exchange systems using microscopy (D. H. FREEMAN). 6. Heterogeneity and the physical chemical properties of ion-exchange resins (L. S. GOLDRING). 7. Ion-exchange selectivity (D. REICHENBERG). 8. Resin selectivity in dilute to concentrated solutions (R. M. DIAMOND AND D. C. WHITNEY). 9. Interpretation of ion-exchange phenomena (J. A. MARINSKY).

These very competent articles by leading specialists will impress the reader with the severe theoretical problems that now face research workers in this field. Had this volume included an article on the available thermochemical data, the futility of any *simple* theories of ion-exchange equilibria would have been even more apparent.

J. A. KITCHENER, Imperial College, London

Polarographie, by J. PROZST, V. CIELESZKY und K. GYÖRBIRÓ, Akadémiai Kiadó, Budapest, 1967; 587 pages, £7.

This book, published in German, has three sections. A general section deals mainly with a basic introduction to classical d.c. polarography, and the applications to inorganic and organic chemistry are treated in the other two sections. The style is comprehensible and good from the didactic viewpoint. The book offers an easy, elementary approach to many fundamentals of classical d.c. polarography, and its applications, for the beginner in polarography. However, for a 1967 publication the treatise remains unsatisfactory, even for an elementary treatment, in view of the present state of the fundamental aspects of electrochemical kinetics.

Nothing is said about the evaluation of the kinetic parameters of the charge transfer reaction, the influence of double-layer effects on electrode kinetics, and inhibition. Adsorption is treated only very incompletely, while the discussion of the kinetics of chemical reactions coupled to the charge transfer step and of the catalysis of hydrogen evolution can only be regarded as satisfactory within the frame work of this book. There are two basic problems with this book. The title sounds too ambitious. It cannot be regarded as a textbook of polarography in the modern sense, and a title such as "Introduction to Classical d.c. Polarography" would have been much

more adequate. No serious account is given of the most important developments in theory and techniques of modern polarography and the resulting substantial increase in potentialities of this electrochemical discipline for applications to trace analysis and physical chemistry. Even with restriction to classical d.c. polarography, the treatise has a somewhat antique flavour. This book has appeared at least 8 years too late, to be recommended generally as a textbook of polarography. Judging from the literature cited, of which 90% belongs to the fifties and forties, it was written at the beginning of this decade. In 1964 the Hungarian issue appeared, and it has taken nearly a further four years to publish the German translation, obviously without any significant alterations or supplements.

The translation is fairly satisfactory although the German is not always very elegant or exact (*viz.* the use of the expression "Diffusionsschicht" instead of "Diffuse Doppelschicht" on page 76 or the expression "Übertrittsreaktion" instead of "Durchtrittsreaktion" for the charge transfer step) and it sometimes has a curious flavour (*viz.* the expressions used for single- and multi-sweep techniques). As in most books, some errors or inconsistencies can be found. The explanation for the large overvoltage of the hydrogen evolution from mercury in terms of the strong adsorption of H-atoms on mercury (p. 66) is unsound. For the two polarographic steps obtained with the pyruvic acid system, two different explanations are given on pages 157 and 402; the latter, in terms of keto–enol-tautomerism, is the wrong one. On page 388 a mesomeric effect is called a tautomeric effect.

Despite the reservations and criticisms mentioned, the reviewer is inclined to recommend the book for laboratories using polarography for two reasons:

(1) The book could serve as an easily digestible introduction to classical d.c. polarography for beginners, provided their attention was also drawn to the modern aspects of the subject.

(2) The sections on inorganic and organic applications form a valuable and, generally, well selected collection and review of the work and results in these fields for the last two decades.

H. W. NÜRNBERG,
Zentrallabor für chemische Analyse
der Kernforschungsanlage Jülich GmbH

Molten Salts Handbook, par G. J. JANZ, Academic Press, Inc., New York, London, 1967, 558 pp. $25.00/200 s.

Les sels fondus intéressent les chercheurs et techniciens dans des domaines très divers de la chimie et de la physico-chimie: structure des liquides ionisés, thermochimie, cinétique et catalyse, électrochimie, chimie en solution non-aqueuse (chimie de coordination), processus préparatifs, technologie nucléaire, piles et batteries, séparations par extraction et chromatographie, etc. Les données numériques expérimentales dont on peut avoir besoin pour l'utilisation des sels fondus dans tel ou tel de ces domaines sont également extrêmement variées et posent souvent un difficile problème de documentation lorsqu'elles sont afférentes à un domaine très différent

de celui auquel on s'intéresse plus particulièrement. L'abondance de ces données qui s'accumulent depuis environ 25 ans est devenue telle que leur rassemblement en un ouvrage unique correspond à un réel besoin ressenti par tous les expérimentateurs; un rassemblement intégral, car les seules données thermodynamiques, ou électrochimiques, ou spectroscopiques sont insuffisantes; on a besoin également, conjointement, par exemple des points de fusion des eutectiques ou des viscosités pour la réalisation d'opérations électrochimiques, etc.

L'ouvrage proposé par le Professeur JANZ, spécialiste réputé des sels fondus, tente pour la première fois de répondre à ce besoin par une compilation d'un nombre considérable de valeurs numériques publiées sur les sels fondus. Ces valeurs ont été classées en cinq grands chapitres, comme suit:

I. Propriétés physiques: rayons ioniques et atomiques, points de fusion et d'ébullition des sels purs et des eutectiques (avec leur composition), densités, viscosités, pressions de vapeur, tensions superficielles, indices de réfraction, données critiques.

II. Propriétés thermodynamiques: immiscibilité liquide–liquide, systèmes sel fondu–métal, sel fondu–oxyde, sel fondu–sel d'argent; études sur la règle des phases; solubilités des gaz, d'oxydes, de métaux; données thermiques, données cryométriques; compressibilités et études sous haute pression.

III. Propriétés électrochimiques: électrodes de référence, séries de f.e.m., conductivités électriques; données polarographiques, chronopotentiométriques et double couche; nombres de transport et coefficients de diffusion; propriétés diélectriques et thermoélectriques.

IV. Spectroscopie et structure: spectres de vibration, spectroscopie u.v. et visible, NMR et RPE, diffraction neutronique et de rayons X.

V. Considérations pratiques: préparations et purifications; les récipients et leur corrosion; chromatographie, électrolyse, processus chimiques, piles et batteries, technologie nucléaire, mettant en oeuvre des sels fondus.

Ce chapitre est suivi d'un certain nombre d'illustrations de dispositifs expérimentaux et d'une bibliographie annotée sur les techniques expérimentales.

Les données sont présentées sous forme de tableaux, suivis chacun d'une liste des références bibliographiques correspondantes. La diversité des tableaux nuit un peu à la clarté de l'ensemble, mais la présentation est tout de même très satisfaisante. Il n'y a pratiquement aucun texte d'accompagnement, sinon au dernier chapitre.

Un tel ouvrage comporte immanquablement de nombreuses lacunes et ne peut être entièrement satisfaisant. Nous aurions aimé trouver les diagrammes de phases, par exemple: bien des données que nous connaissons et avons extraites d'une littérature qui n'est pas absolument récente n'y figurent pas. Mais ce qu'on peut y trouver est déjà si abondant que ce manuel est nécessaire à tous les utilisateurs des sels fondus et que nous le leur recommandons très fortement.

B. TREMILLON, Faculté des Sciences de Paris

VOL. 19 NO. 3 JOURNAL OF ELECTROANALYTICAL CHEMISTRY NOVEMBER 1968
AND INTERFACIAL ELECTROCHEMISTRY

CONTENTS

Photoluminescence of Solutions

With Applications to Photochemistry and Analytical Chemistry

by C. A. Parker, Royal Naval Scientific Service, Head of Chemistry Division of the Admiralty Materials Laboratory, Holton Heath, Poole, Dorset, England

6 × 9″, xvi + 544 pages, 53 tables, 188 illus., 443 lit. refs., 1968, Dfl. 85.00, £11.10.0.

Contents: 1. Basic principles and definitions. 2. Kinetics of photoluminescence. 3. Apparatus and experimental methods. 4. Special topics and applications. 5. Application to analytical chemistry. Indexes.

Comprehensive Analytical Chemistry

edited by C. L. Wilson, Professor of Inorganic and Analytical Chemistry, University of Belfast (Northern Ireland)
and D. W. Wilson, Head of the Chemistry Department, Sir John Cass College, London (England)

VOLUME IIB: Physical Separation Methods

6 × 9″, xvi + 445 pages, 30 tables, 116 illus., 897 lit.refs., 1968, Dfl. 70.00, £8.10.0.

Volume Two, Part B is devoted to physical separation methods. After an account of the theory and practise of liquid chromatography in columns, the volume continues with a lengthy treatment of gas chromatography.
The next chapter, on ion exchangers, is notable for the account it gives of analytical applications, while distillation (theory and technique) is the last topic to be treated in the present volume.

Contents: I. *Liquid Chromatography in Columns.* 1. Introduction. 2. Theory. 3. Apparatus and operation. II. *Gas Chromatography.* 1. Introduction and general principles. 2. Theoretical aspects. 3. Apparatus. 4. The partitioning phases. 5. Absorbents and gas-solid chromatography. 6. Gas-liquid chromatography. 7. Analytical methods. 8. Applications. III. *Ion Exchangers.* 1. Foreword. 2. Introduction. 3. The constitution of ion exchangers. 4. The mechanism of ion exchange. 5. Technique. 6. Analytical applications. Appendix 1: Ion-exchanger data. Appendix 2: Methods of testing ion exchangers. Appendix 3: Bibliography. IV. *Distillation.* 1. Introduction. 2. Theoretical background. 3. Experimental techniques.

Atomic-Absorption Spectroscopy

and Analysis by Atomic-Absorption Flame Photometry

by J. Ramírez-Muñoz, Principal Applications Chemist at Beckman Instruments Inc. and Scientific Research Collaborator of the C.S.I.C., Spain

6 × 9″, xii + 493 pages, 23 tables, 156 illus., 950 lit. refs., 1968, Dfl. 80.00, £9.15.0.

Contents: *Part I: Fundamentals.* 1. Origins of the method and nomenclature. 2. General principles and characteristics. 3. Absorption and emission. 4. The literature of atomic-absorption spectroscopy. 5. Theory. *Part II: Instrumental Systems.* 6. Instrumental systems. 7. Emission systems. 8. Absorption system. 9. Selection system. 10. Photometric system. 11. Instruments. *Part III: Range and Limitations of Atomic Absorption Methods.* 12. Determinable elements. Choice of lines. 13. Sensitivity. 14. Limitations in atomic absorption. *Part IV: Experimental Methods.* 15. Experimental process. 16. Standard solutions. 17. Preparation of the sample. 18. Experimental measurements and calibration. *Part V: Applications.* 19. Applications. Appendix. Bibliography.

Elsevier Publishing Company Amsterdam London New York